

TECHNISCHE UNIVERSITÄT MÜNCHEN
WISSENSCHAFTSZENTRUM WEIHENSTEPHAN FÜR
ERNÄHRUNG, LANDNUTZUNG UND UMWELT
PROFESSUR FÜR BIOTHERMODYNAMIK

**ADVANCES IN SEPARATION METHOD DEVELOPMENT IN
LIQUID-LIQUID CHROMATOGRAPHY**

Simon Karl Ludwig Röhrer

Vollständiger Abdruck der von der Fakultät Wissenschaftszentrum Weihenstephan für Ernährung, Landnutzung und Umwelt der Technischen Universität München zur Erlangung des akademischen Grades eines

DOKTOR-INGENIEURS (Dr.-Ing.)

genehmigten Dissertation.

Vorsitzender: Prof. Dr. Michael Rychlik

Prüfende der Dissertation: 1. Prof. Dr. Mirjana Minceva
2. Prof. Dr. Sonja Berensmeier

Die Dissertation wurde am 04.06.2019 bei der Technischen Universität München eingereicht und durch die Fakultät Wissenschaftszentrum Weihenstephan für Ernährung, Landnutzung und Umwelt am 05.11.2019 angenommen.

Acknowledgements

My deepest gratitude goes to Prof. Dr.-Ing. Mirjana Minceva for supervising this thesis as well as for her insightful guidance and mentoring over the years. I am very grateful to Prof. Dr. Sonja Berensmeier for reading and examining this dissertation. Furthermore, I would like to thank Prof. Dr. Michael Rychlik for chairing my thesis committee.

Special thanks goes to Dr. Jürgen Behr, who introduced me to the world of hops and inspired me with his enthusiasm for the separation of hop components. Thank you for your strong encouragement, support, and many fruitful discussions during our great collaboration. Many thanks also to Prof. Vogel and the team of Technical Microbiology for giving me the opportunity to carry out the microbial tests, the team of BayBioMS for their help during the mass spectrometry experiments, Dr. Guillaume Médard (Chair of Proteomics and Bioanalytics) for his support during the xanthohumol C semi-syntheses, Dr. Oliver Frank (Chair of Food Chemistry and Molecular Sensory Science) for his help during the NMR structure analysis, Dr. Thomas Goudoulas (Chair of Fluid Dynamics of Complex Biosystems) for assistance in the viscosity measurements, Prof. Hauner and Manuela Hubersberger (Chair of Nutritional Medicine) for giving me the opportunity to carry out the cell culture experiments in their lab and for their great support during the experiments. I would like to thank Petra Kiefer (Chair of Separation Science and Technology, FAU Erlangen-Nuremberg), who always had an open ear for my analytical questions. Dr. Thomas Pfeiffer is gratefully acknowledged for kindly loaning me his lab equipment.

I thank the publishing houses Elsevier, Wiley, PLOS ONE, and MDPI for the kind permission to include already published work to this thesis. All helpful comments on my publications, provided by various anonymous reviewers, are acknowledged.

I thank all of my supervised students who contributed to this thesis, namely Lukas Weber, Barbara Pfeiffer, Katja Malec, Mara Ramires, Asafe de Araujo, Dominic Andre, Verena Stork, and Lukas Braumann. I really enjoyed it working with all of you!

For a great shared time in the office, I thank Franziska Bezold. Equally, I am grateful to all other former and current members of BTX for many fruitful discussions and for creating such a pleasant working atmosphere. It was an honor for me to work in this group. Additionally, I would like to thank the colleagues from SVT for the warm welcome in Freising and the great time we had together. My thanks goes further to Dr. Anja Glanz for her mentoring.

Most important I would like to thank my family and friends who often had to do without me when my biphasic systems and CPC's needed a little more attention. I deeply thank my parents and sister for their unconditional support and encouragements during my education and whole life. Finally, I would like to thank my girlfriend Tijana for her incredible and not self-evident support including proof-reading. Without her love, patience and understanding I would not have been able to finish this work.

This page is intentionally left blank.

Abstract

In recent years, solid support-free liquid-liquid chromatography (LLC), comprising countercurrent chromatography (CCC) and centrifugal partition chromatography (CPC), has become a powerful technique with increasing popularity for the separation of bioactive compounds from natural resources, such as plant extracts and biotechnological products. A tremendous number of applications has been established in literature with a wide variety of different columns. In LLC, both stationary and mobile phase are liquid, corresponding to the two phases of a chosen biphasic liquid solvent system. The two phases are in equilibrium and hence, their compositions cannot be selected successively and independently of each other. The liquid nature of the stationary phase brings several advantages, but also some particularities such as the column design and the application of a centrifugal field that have to be considered during separation method development, its transfer between different columns, and scale-up. This makes separation method development rather complex. Hence, the aim of this thesis is to gain better understanding and improve LLC separation method development.

The first part of the thesis focuses on factors that influence the separation performance. Apart from column design and operating conditions (flow rate, centrifugal field), this involves external factors such as temperature changes, the type of the biphasic solvent system, as well as the physical properties of the liquid phases. For this purpose, a systematic procedure for an extensive characterization of a CPC column for varying operating conditions was established based on a novel column prototype with spherical cells. In addition, the impact of temperature fluctuations on the physical properties of the phases and thus the separation performance was systematically investigated. Here, non-aqueous biphasic liquid systems were focused, as they are considered to be particularly susceptible to temperature. Further, a promising new biphasic solvent system class based on so-called deep eutectic solvents (DES) was evaluated for the applicability in CPC. DES could be used as a water substitute in new tailor-made non-aqueous systems and thus could fill the current lack of biphasic solvent systems for the separation of highly hydrophobic or nonpolar natural compounds.

Factors that impact the separation performance must be also taken into account for the development of separation method transfer and scale-up. Given a wide variety of LLC column designs and sizes, intra- and inter-apparatus method transfer is often very time consuming, requiring substantial user experience and experimental effort. Thus, a systematic short-cut method for a fast prediction of separation method transferability and a subsequent model-based separation method transfer was established. This method considers comprehensive column characteristics and operating conditions.

The second part of the thesis focuses on the application of LLC for the separation of bioactive minor compounds from natural resources. In this context, the purification of the promising compound xanthohumol C is established. Two approaches were investigated: a capture and enrichment of xanthohumol C directly from the natural extract, and semi-synthesis steps followed by an LLC purification. It is shown that sufficient amounts of the minor target compound can be provided in high purity without the need for additional purification. Further, the treatment of human breast cancer cells in combination with quantitative proteomics and comprehensive statistical analysis was demonstrated as a powerful and quick method for the evaluation of the bioactivity of minor hop compounds.

Kurzzusammenfassung

Die Flüssig-Flüssig-Chromatographie (FFC) hat sich in den vergangenen Jahren zu einer leistungsstarken und vielseitigen Trenntechnologie mit zunehmender Popularität für die Gewinnung verschiedenster bioaktiver Naturstoffe aus natürlichen Ressourcen wie Pflanzenextrakten oder biotechnologischen Produkten entwickelt. FFC umfasst allgemein sowohl die sogenannte Gegenstromverteilungschromatographie (engl. countercurrent chromatography, CCC) als auch die zentrifugale Verteilungschromatographie (engl. centrifugal partition chromatography, CPC). Eine Besonderheit der FFC ist die Verwendung einer sowohl flüssigen mobilen als auch einer flüssigen stationären Phase. Zusammen bilden diese ein flüssiges Zweiphasensystem und stehen miteinander im Gleichgewicht. Die Zusammensetzung der Phasen ist dadurch festgelegt und eine schrittweise bzw. unabhängige Auswahl ist nicht möglich. Eine flüssige stationäre Phase ist zwar in vielerlei Hinsicht vorteilhaft, erfordert jedoch v.a. bei der Entwicklung von Trennmethode, ihrem Transfer zwischen verschiedenen Säulen und dem Scale-up die Berücksichtigung einiger Besonderheiten wie Säulendesign und Zentrifugalkraft. Dies macht die Entwicklung von FFC – Trennmethode komplex. Ziel dieser Arbeit ist es deshalb, zu einem verbesserten Verständnis bei der Entwicklung und Auslegung von Trennmethode in der FFC beizutragen und diese dadurch verbessern zu können.

Der erste Teil der Arbeit befasst sich mit möglichen Einflussfaktoren auf die Trennleistung in der FFC. Neben Säulendesign/-geometrie und Betriebsbedingungen (Volumenstrom, Zentrifugalfeld) sind dies v.a. äußere Einflussfaktoren wie Temperaturänderungen, die Art des Zweiphasensystems, sowie physikalische Eigenschaften der flüssigen Phasen. Anhand eines neuartigen CPC-Prototyps mit sphärischen Zellen wurde zu diesem Zweck eine systematische und umfassende Charakterisierung von Säulen bei unterschiedlichen Betriebsbedingungen etabliert. Darüber hinaus wurde der Einfluss von Temperaturschwankungen auf die physikalischen Eigenschaften der Phasen und der damit verbundenen Auswirkung auf die Trennleistung untersucht. Ein Fokus lag hierbei v.a. auf wasserfreien Systemen, die als potenziell temperatursensitiv gelten. Außerdem wurden stark eutektische Lösungsmittel (engl. deep eutectic solvents, DES) als Teil neuer flüssiger Zweiphasensysteme auf ihre Anwendbarkeit in der CPC untersucht. DES kann dabei potentiell als Wasserersatz in maßgeschneiderten wasserfreien Systemen eingesetzt werden und dadurch einen Beitrag zum gegenwärtigen Bedarf an Lösungsmittelsystemen zur Trennung stark hydrophober bzw. unpolarer Naturstoffe leisten.

Auch der Transfer und Scale-up von Trennmethode ist von Einflussfaktoren, die sich auf die Trennleistung auswirken können, abhängig. Angesichts der Vielzahl verwendeter LLC-Säulendesigns und -größen ist die Übertragung zwischen verschiedenen Säulen oft zeitlich und experimentell sehr aufwendig, und erfordert erhebliche Erfahrung. So wurde eine systematische Short-cut Methode etabliert, die eine schnelle Vorhersage der Übertragbarkeit von Trennmethode unter Berücksichtigung umfassender Säulencharakteristika und Betriebsbedingungen mit anschließender modellbasierter Übertragung ermöglicht.

Der zweite Teil der Arbeit fokussiert sich auf die Anwendung von FFC zur Trennung von bioaktiven Minorkomponenten aus natürlichen Quellen. In diesem Zusammenhang wird die Gewinnung der vielversprechenden Komponente Xanthohumol C (XNC) etabliert. Zwei verschiedene Ansätze wurden dabei verfolgt: eine Konzentrierung von XNC mit direkter Isolierung aus dem Naturextrakt sowie halbsynthetische Schritte mit anschließender Aufreinigung von XNC ausschließlich mittels FFC. In beiden Fällen können ausreichende

Mengen der gewünschten Minorkomponente XNC in hoher Reinheit ohne zusätzliche Reinigungsschritte gewonnen werden. Dazu konnte gezeigt werden, dass eine Kombination aus Zellkulturversuchen mit humanen Brustkrebszellen und quantitativer Proteomik mit umfassenden statistischen Analysen dafür geeignet ist, die Bioaktivität von Hopfenminorkomponenten schnell und effektiv zu evaluieren.

Table of Contents

Acknowledgements	2
Abstract.....	4
Kurzzusammenfassung	5
Table of Contents	7
1. Introduction and motivation	9
2. Theoretical background.....	15
2.1. Fundamentals of liquid-liquid chromatography	15
2.2. Thermodynamics of liquid-liquid phase equilibria.....	24
2.3. Solvent system selection in liquid-liquid chromatography.....	27
2.3.1. Biphasic solvent systems	27
2.3.2. Screening methods for solvent system selection	29
2.4. Column design in LLC.....	32
2.5. Hydrodynamic characteristics of LLC Columns	37
2.6. Operating modes	39
2.7. Chromatographic models	43
2.7.1. Introduction to chromatographic models.....	43
2.7.2. Chromatographic models in LLC	43
2.8. Separation method development in LLC.....	47
2.8.1. Current challenges in separation method development	47
2.8.2. Separation method transfer and scale-up in LLC.....	47
3. Results.....	51
3.1. Paper I: Characterization of a centrifugal partition chromatographic column with spherical cell design.....	51
3.1.1. Summary.....	51
3.1.2. Manuscript	53
3.2. Paper II: Deep eutectic solvents in countercurrent and centrifugal partition chromatography	63
3.2.1. Summary.....	63
3.2.2. Manuscript	65
3.3. Paper III: Influence of temperature on the separation performance in solid support-free liquid-liquid chromatography	74
3.3.1. Summary.....	74
3.3.2. Manuscript	76

3.4. Paper IV: Evaluation of inter-apparatus separation method transferability in countercurrent chromatography and centrifugal partition chromatography.....	87
3.4.1. Summary.....	87
3.4.2. Manuscript	88
3.5. Strategies for the isolation and purification of bioactive minor components from plant extracts using LLC.....	104
3.5.1. Process concept for solute capture and enrichment with LLC	104
3.5.2. Paper V: Xanthohumol C, a minor bioactive hop compound: Production, purification strategies and antimicrobial test	111
3.5.2.1. Summary	111
3.5.2.2. Manuscript.....	113
3.5.3. Paper VI: Analyzing Bioactive Effects of the Minor Hop Compound Xanthohumol C on Human Breast Cancer Cells using Quantitative Proteomics	124
3.5.3.1. Summary	124
3.5.3.2. Manuscript.....	125
4. Discussion and Conclusion	147
5. Outlook.....	153
6. List of other published manuscripts	155
7. Abbreviations and Symbols	156
8. List of Figures and Tables	161
9. References.....	164
10. Appendix.....	174
10.1. Supplementary information for Paper I.....	174
10.2. Supplementary information for Paper III	177
10.3. Supplementary information for Paper V	184
10.4. Supplementary information for Paper VI.....	187
10.5. Curriculum Vitae	194

1. Introduction and motivation

Solid support-free liquid-liquid chromatography (LLC), better known as countercurrent chromatography (CCC) and centrifugal partition chromatography (CPC), is a chromatographic separation technique that uses a liquid stationary and mobile phase. The separation principle is based on the different solubility of the solutes in the two liquid phases of a biphasic liquid solvent system and consequently a different distribution of the solutes between the phases. The two liquid phases are usually formed by mixing and subsequently equilibrating portions of two to five solvents such as heptane, ethyl acetate, methanol and water. Theoretically, an unlimited number of possible solvent combinations exists to create biphasic liquid systems. In this context, LLC combines characteristics from two other separation techniques: liquid-liquid extraction and conventional liquid chromatography. One of the two liquid phases is kept stationary with the help of a centrifugal field in a specially designed column, while the other phase is used as mobile phase. In comparison to conventional liquid chromatography (LC), where the separation is based on a solute interaction with the surface of the solid stationary phase, in LLC the whole volume of the stationary phase is accessible to the solutes. The fact that the stationary phase is of liquid nature is beneficial especially for the separation of sensitive natural compounds, due to the absence of a solid phase, where adsorption/desorption processes and irreversible adsorption take place, and can result in product or activity loss. In addition, a (catalytic) reaction or degradation of the solutes in the presence of a solid stationary phase can be prevented. While in LC the user selects the column from a limited number of commercially available stationary phases, in LLC the user prepares both phases. This is especially advantageous for the purification of complex natural products, as it enables the user to individually tailor the stationary and mobile phase for the respective target component. In addition, natural crude extracts can be introduced to the column without extensive sample pre-processing, since no blocking of the interparticle volume and porous particles like in LC can occur with a liquid stationary phase. Moreover, in contrast to LC, the stationary phase can be easily renewed and replaced.

This thesis represents a contribution towards a better understanding and improvement of LLC separation method development. The first part focuses on column characteristics and influencing parameters for LLC separations, while the second part addresses the application of LLC for the separation of natural compounds. So far, LLC is mostly used at lab-scale for the purification and separation of high value-added natural products. Since its invention by Ito in the 1960s [1, 2], its popularity has been steadily increasing. The technology has probably made its decisive industrial breakthrough by being one of the key purification methods for the separation of cannabinoids as part of the global trend towards legalizing cannabis for medical applications [3-5]. Continuously, more and more applications with new biphasic solvent systems are being developed [6, 7]. At the same time, new columns are constantly being designed and improved for a wide variety of specific applications from small lab-scale up to industrial-scale [8-12]. As a result, many separation methods have been developed on a variety of columns [6, 9]. However, a successful separation in LLC depends not only on the different distribution of the compounds in the biphasic system (thermodynamics), but also on the influence of hydrodynamics and mass transfer kinetics. Hence, many parameters can affect the separation. First, the separation depends on the geometry and size of the CCC and CPC columns, as well as on the different operating conditions such as applicable flow rates and centrifugal fields. In this sense, the separation performance of a new CPC column design with spherical cells was systematically evaluated in this thesis and compared to conventional CPC

columns with twin-cell design. In combination with a theoretical simulation study, a set of operating conditions where the column is most suited to achieve high productivities and low solvent consumptions was identified for the studied system. In addition, it was possible to investigate for which kinds of applications or separation difficulty, i.e. separation factor range, such a column type is reasonable. The obtained results were published in **Paper I**.

In addition to column design, the choice of a biphasic solvent system represents another key factor influencing the separation performance. The vast majority of the solvent systems in LLC are aqueous-organic biphasic solvent systems, which are applicable for the separation of medium-polar compounds [6, 7]. However, for the separation of highly nonpolar or hydrophobic compounds, new non-aqueous biphasic solvent systems are needed. Continuous developments of column and cell designs enable the application of unconventional systems. In this thesis, the applicability of a new class of biphasic systems based on so-called deep eutectic solvents was studied in CPC. The results of this work are presented in **Paper II**.

As mentioned above, the mobile and the stationary phases are two liquid phases of a biphasic solvent system in equilibrium. The compositions of the phases, as well as their physical properties (density, viscosity, interfacial tension) may change during the separation process. This can occur e.g. due to temperature fluctuations, which may be caused by insufficient temperature control or by friction, leading to energy dissipation during the operation of the plant. Therefore, a systematic procedure for the evaluation of temperature susceptibility of biphasic solvent systems for the use in LLC was established in the current thesis. The impact of temperature fluctuations on the separation performance was then systematically explored with a representative non-aqueous biphasic solvent system composed of *n*-hexane/ethyl acetate/acetonitrile. The results of this study can be found in **Paper III**.

In LLC, separation methods are mostly developed at lab-scale. Subsequently, they are often scaled-up to a larger column or transferred to other columns, e.g. between research groups of different labs. Currently, there is a trend to use LLC also for preparative and industrial-scale separations of natural products. However, such intra- and inter-apparatus method transfers are still strongly based on experience and trial-and-error, which is laborious and time consuming even for experienced users. In order to perform a successful method transfer, it is important to carefully consider all factors that can influence the separation performance. In the framework of this thesis, a systematic short-cut approach for the estimation of separation method transferability was established. It is based on characterizing the separation performance of both chromatographic columns at various operating conditions. The results of this study were submitted for publication in **Paper IV**.

The second part of this thesis focuses on the application of LLC for an improved preparative isolation of minor bioactive compounds from natural resources. The increasing demand for natural bioactive ingredients as additives in functional foods, pharmaceutical drugs, cosmetics, and other products proposing health claims is a general global trend. Studies show that the bioactivity of many plants can be assigned to minor components whose effects often exceed those of the main constituents [13-15]. Probably one of the best known medicinal plants worldwide is hops (*Humulus lupulus L.*). Apart from giving beer its distinctive taste, hops contains a tremendous variety of bioactive ingredients with health promoting effects [16]. Many of these bioactive effects are particularly associated with flavonoids, such as xanthohumol [17] and its minor analogue xanthohumol C [18, 19], whose antiproliferative, cytotoxic [20], neuro-protective [21] and antioxidative [22, 23] activities were recently shown. Hence, there is an

increasing interest in making such natural minor plant compounds available in sufficient amounts. In this work, xanthohumol C was recovered in a high purity from a xanthohumol-enriched raw hop extract, where the target compound xanthohumol C is present only in very small amounts (0.2-2.2%). Production and separation strategies involving capture and enrichment steps as well as one-step semi-syntheses with LLC as the sole separation technique were investigated for the preparative isolation of xanthohumol C. Subsequent extensive analytical as well as microbiological and cell culture experiments emphasize the potential of LLC as a highly selective and at the same time gentle separation technique for the purification of promising natural minor compounds. This work was published in **Paper V**.

As mentioned above, previous studies demonstrated the chemopreventive and anticarcinogenic potential of xanthohumol and other hop minor components in various human cancer cell lines. However, it is difficult and time consuming to attribute the antiproliferative and cytotoxic effects observed in cell culture experiments to specific intracellular and molecular modes of action. Up to now, many individual detection reactions needed to be performed for this purpose on specific mechanisms, e.g. using Western blots. A quick alternative and possibly future standard procedure for the bioactivity screening of natural compounds could be the use of state-of-the-art quantitative proteomics in combination with statistical analysis, where the entire proteome of the treated cells is explored. In this thesis, such a mass spectrometry-based quantitative proteomics approach was investigated for the in-vitro treatment of a human MCF-7 breast cancer cell line with xanthohumol and xanthohumol C. The results can be found in **Paper VI**.

Objective and structure of the thesis

The aim of this thesis is to study and improve current separation method development in LLC for the preparative separation of high value-added compounds. The work focuses on the investigation of influencing factors and their impact on the separation performance, which needs to be considered for separation method development and both intra- and inter-apparatus method transfer. In this sense, especially alternative biphasic solvent systems, novel column designs, operating modes, temperature fluctuations, and column characteristics are explored. In parallel, the thesis focuses on new strategies for the preparative isolation of bioactive minor components from hops involving LLC as a key technology.

The thesis is cumulative, includes six papers, and is structured into a theoretical background (Chapter 2), results (Chapter 3), a general discussion and conclusion (Chapter 4), and an outlook (Chapter 5).

In Chapter 2, relevant theory and methods are summarized. Additional subject-specific literature, state of the art, and detailed material and method descriptions are provided in each paper. For each of the six papers, short summaries are given in Sections 3.1. to 3.5., followed by copies of the original manuscripts, respectively. In Chapter 4, a general discussion and conclusion of the results of Papers I-VI is provided. Chapter 5 contains an outlook for future work.

Publication list

Parts of this thesis have been published in the following peer-reviewed journals:

Paper I:

S. Roehrer, M. Minceva, (2019). Characterization of a centrifugal partition chromatographic column with spherical cell design. *Chemical Engineering Research and Design*, 143, 180-189.

Paper II:

S. Roehrer, F. Bezold, E.M. García, M. Minceva, (2016). Deep eutectic solvents in countercurrent and centrifugal partition chromatography. *Journal of Chromatography A*, 1434, 102-110.

Paper III:

S. Roehrer, M. Minceva, (2019). Influence of temperature on the separation performance in solid support-free liquid-liquid chromatography. *Journal of Chromatography A*, 1594, 129-139.

Paper IV:

S. Roehrer, M. Minceva, (2019). Evaluation of inter-apparatus separation method transferability in countercurrent chromatography and centrifugal partition chromatography, *Separations*, 6(3), 36.

Paper V:

S. Roehrer, J. Behr, V. Stork, M. Ramires, G. Médard, O. Frank, K. Kleigrewe, T. Hofmann, M. Minceva, (2018). Xanthohumol C, a minor bioactive hop compound: production, purification strategies and antimicrobial test. *Journal of Chromatography B*, 1095, 39-49.

Paper VI:

S. Roehrer, V. Stork, C. Ludwig, M. Minceva, J. Behr, (2019). Analyzing Bioactive Effects of the Minor Hop Compound Xanthohumol C on Human Breast Cancer Cells using Quantitative Proteomics. *PLoS ONE*, 14(3), e0213469.

Parts of this thesis have been presented to the scientific community:

Talks:

S. Roehrer, M. Minceva, (2018), Separation Method Transfer in Liquid-Liquid Chromatography, CCC2018, Braunschweig, Germany.

S. Roehrer, J. Behr, V. Stork, M. Ramires, M. Minceva, (2018), Liquid-Liquid Chromatography: A promising unit operation for the purification of bioactive minor hop compounds, 52. DGQ Vortragstagung und ProcessNet Phytoextrakte, Gießen, Germany.

S. Roehrer, M. Minceva, (2017). Separation of bioactive hop compounds from hop extract by liquid-liquid chromatography, Bavarian Center for Biomolecular Mass Spectrometry (BayBioMS), "Advanced Mass Spectrometry"-Seminar, Technical University of Munich, Germany.

S. Roehrer, M. Minceva, (2017). Inter-apparatus separation method transfer in liquid-liquid chromatography, 13th International PhD Seminar on Chromatographic Separation Science (SoCSS), Karlsruhe, Germany.

S. Roehrer, F. Bezold, E.M. García, M. Minceva, (2015). Application of Deep Eutectic Solvents in Centrifugal Partition Chromatography, AIChE Annual Meeting, Salt Lake City, USA.

S. Roehrer, F. Bezold, E.M. García, M. Minceva, (2015). Application of Deep Eutectic Solvents in Liquid-Liquid Chromatography, Processnet Annual Meeting, Bamberg, Germany.

Posters:

S. Roehrer, M. Minceva, (2018), Influence of Column and Solvent Temperature on Separation Performance in Liquid-Liquid Chromatography, CCC2018, Braunschweig, Germany.

S. Roehrer, J. Behr, V. Stork, M. Ramires, M. Minceva, (2018), Purification Strategies for Bioactive Minor Hop Compounds, CCC 2018, Braunschweig, Germany.

S. Roehrer, J. Behr, V. Stork, M. Ramires, M. Minceva, (2018), Liquid-Liquid Chromatography: A promising unit operation for the purification of bioactive minor hop compounds, IBF, Garching, Germany.

S. Roehrer, F. Bezold, M. Minceva, (2016), Novel non-aqueous biphasic solvent systems in centrifugal partition chromatography, CCC, Chicago, USA.

The following supervised student theses contributed to this work:

Lukas Braumann, Temperatureinfluss auf die Trennung von Naturstoffen in der Flüssig-Flüssig-Chromatographie, Bachelor thesis, TU Munich, 2018.

Verena Stork, Purification of Xanthohumol C by liquid-liquid chromatography and its bioactivity screening in microorganisms and cell cultures, Master thesis, TU Munich, 2017.

Dominic Andre, Einfluss der Säulentemperatur auf die Trennung von Natur- und Wirkstoffen mittels Flüssig-Flüssig Chromatographie, Bachelor thesis, TU Munich, 2017.

Mara Alexandra Batista Ramires, Synthesis and Purification of Xanthohumol C from Xanthohumol Hop Extract, Master thesis, Técnico Lisboa (in collaboration with TU Munich, experimental implementation at the chair of Biothermodynamics), 2016.

Barbara Pfeiffer, Modellbasierte Konzentrierung von Wertstoffen mittels Flüssig-Flüssig-Chromatographie, Master thesis, TU Munich, 2016.

Lukas Weber, Verteilung von Naturstoffen in zweiphasigen Systemen mit stark eutektischen Lösungsmitteln, Bachelor thesis, TU Munich, 2015.

2. Theoretical background

2.1. Fundamentals of liquid-liquid chromatography

In solid support-free liquid-liquid chromatography (LLC), comprising countercurrent chromatography (CCC) and centrifugal partition chromatography (CPC), two phases of an equilibrated biphasic liquid solvent system provide the mobile and the stationary phase. The two liquid phases are usually formed by mixing certain portions of two to five solvents. With the help of a centrifugal field, one of the two liquid phases is kept in place as the stationary phase in a specially designed column. The other liquid phase is used as the mobile phase and pumped through the column [1, 2, 9, 24-26].

As shown in Figure 1, a LLC setup is similar to a conventional HPLC setup. It includes a solvent and sample delivery system before the LLC column and a detection and fractionating system placed after the column. Depending on the compounds and solvents used for the particular separation, various detector types can be applied and an (automated) fraction collector can be used. The only difference is that the HPLC column is replaced by a specially designed column mounted on a centrifugal axis, as described later in Section 2.5.

For each separation, the biphasic system is prepared by mixing the respective solvents and equilibrating the phases. Then, the phases are split into two reservoirs and the column is filled with one phase selected as the stationary phase. Subsequently, a certain rotational speed is set at the column and mobile phase is pumped through the column with a constant flow rate until no more stationary phase is displaced from the column. As a result, a constant ratio of mobile and stationary phase is present in the column (= hydrodynamic equilibrium) and the separation run can be started by introducing a sample dissolved in mobile and/or stationary phase. The components of the mixture distribute differently between the phases. Consequently, they move with a different velocity along the column and by this can be separated.

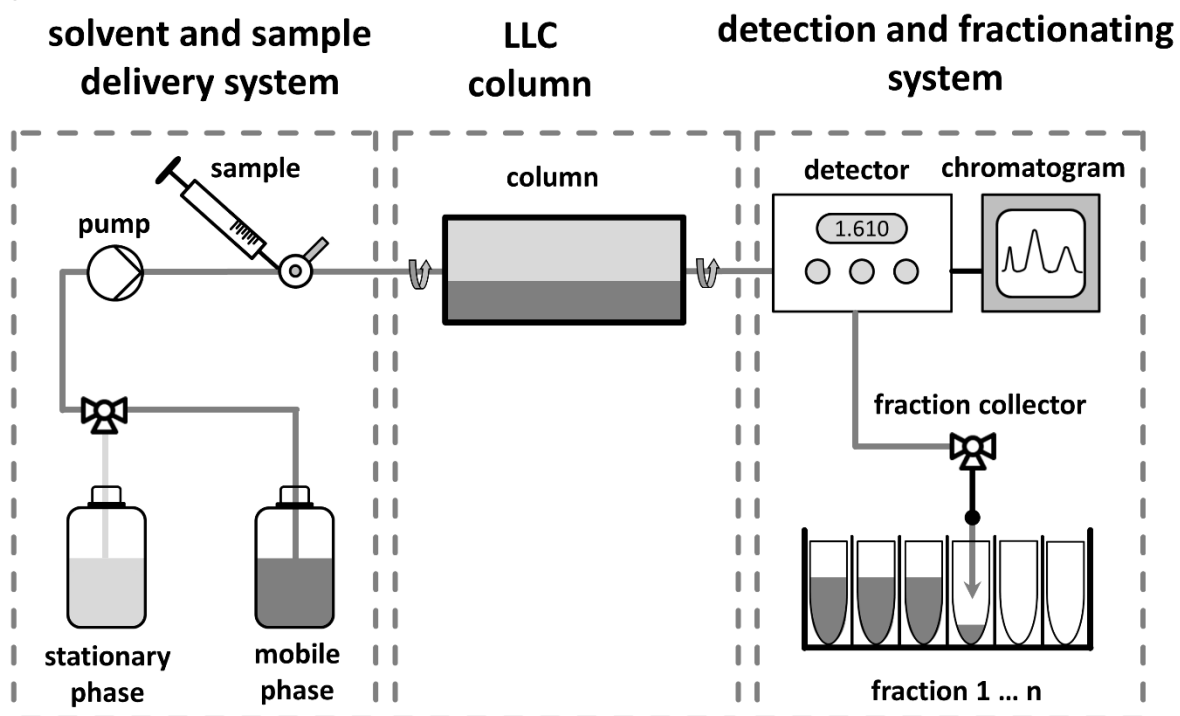


Figure 1: Schematic presentation of a liquid-liquid chromatographic (LLC) setup.

Due to the liquid nature of the stationary phase, the chromatographic separation in LLC differs from conventional liquid chromatography with a column packed with a (porous) solid stationary phase. A comparison of important key features of both technologies is given in Table 1.

Table 1: Difference between conventional liquid chromatography (LC), e.g. HPLC, and solid support-free liquid-liquid chromatography (LLC) (partly adapted from [9, 27]).

Liquid Chromatography (LC)	Liquid-Liquid Chromatography (LLC)
<p><u>General differences:</u></p> <ul style="list-style-type: none"> • solid stationary phase • fixed ratio of stationary and mobile phase inside the column (<10% stationary phase volume) • laborious and expensive column packing • mostly pre-defined commercial stationary phases <p><u>Separation principles:</u></p> <ul style="list-style-type: none"> • solute interaction with groups (e.g. alkyl chains) on the surface of the stationary phase (e.g. silica) • various separation mechanisms possible: adsorption, ion-exchanges, pore size exclusion • irreversible adsorption possible <p><u>Operation and method design:</u></p> <ul style="list-style-type: none"> • sequential selection of stationary and mobile phase • change of mobile phase composition (e.g. gradient) • sample injection with mobile phase • no change of phase role possible, i.e. stationary phase not pumpable • low column loadability • usually no affection of the stationary phase composition and volume due to sample overload or surfactants 	<p><u>General differences:</u></p> <ul style="list-style-type: none"> • liquid stationary phase • variable ratio of stationary and mobile phase inside the column (50-90% stationary phase volume) • fast and simple column preparation by filling the column • tailor-made mobile and stationary phase prepared by the user <p><u>Separation principles:</u></p> <ul style="list-style-type: none"> • solute interaction with a solvent mixture (i.e. whole volume of the stationary phase accessible to the solute) • solute separation based on different solubility in mobile and stationary phase, i.e. different distribution between the phases • no irreversible adsorption, i.e. full recovery of solutes possible <p><u>Operation and method design:</u></p> <ul style="list-style-type: none"> • simultaneous selection of stationary and mobile phase (biphasic solvent systems) • mostly isocratic separations, but gradients possible • sample injection with mobile and/or stationary phase • change of the phase role possible, i.e. both phases pumpable • high column loadability • affection of the hydrodynamic equilibrium possible due to sample overload or surfactants (volume of the phases or volume of stationary phase)

The LLC system and separation can be characterized by the following parameters: stationary phase retention, partition coefficient, separation factor, column efficiency, and resolution. The stationary phase retention (S_F) is defined as the fraction of the column volume occupied by the stationary phase:

$$S_F = \frac{V_{SP}}{V_C} \quad (\text{Equation 1})$$

where V_{SP} is the volume of the stationary phase and V_C is the volume of the column. For a given biphasic solvent system and column, S_F is a function of the operating conditions, e.g. flow rate and centrifugal field.

The separation in LLC depends on the different distribution or partitioning of the solutes to be separated between the stationary and the mobile phase. The partition coefficient of a solute i (P_i) is defined as the concentration ratio of a solute i in the stationary and mobile phase at equilibrium (Eq. 2):

$$P_i = \frac{c_i^{SP}}{c_i^{MP}} \quad (\text{Equation 2})$$

where c_i^{SP} is the concentration of solute i in the stationary phase and c_i^{MP} is its concentration in the mobile phase. The partition coefficient is a function of the solute concentration in the system. Its value is constant in the linear range of the partition equilibrium and defined as $c_i^{SP} = f(c_i^{MP})$.

The separation factor (Eq. 3) for a binary mixture of two compounds is defined as the ratio of their partition coefficients:

$$\alpha_{ij} = \frac{P_j}{P_i} \quad (\text{Equation 3})$$

where P_j corresponds to the solute with the larger partition coefficient and P_i to the solute with lower partition coefficient. Consequently, the higher the separation factor the easier is the separation.

In the linear range of the partition equilibria, the retention volume (V_R) of a compound i can be calculated according to Eq. 4 based on the partition coefficient and the volumes of stationary phase (V_{SP}) and mobile phase (V_{MP}) in the column. Furthermore, the retention volume can be calculated from the retention time by considering the mobile phase flow rate ($V_R = F \cdot t_R$).

$$V_{R,i} = V_{MP} + P_i V_{SP} = V_C [(1 - S_F) + S_F P_i] \quad (\text{Equation 4})$$

Consequently, the partition coefficient of a solute (P_i) can be determined according to Eq. 5., once the retention volume of the solute and the volume of the phases in the column are known.

$$P_i = \frac{V_{R,i} - (1 - S_F) \cdot V_C}{S_F \cdot V_C} \quad (\text{Equation 5})$$

The chromatographic key parameters in LLC, in analogy to LC, are usually derived from measured concentration profiles, e.g. UV-signal chromatograms. Pulse injection experiments are performed with a tracer and the solutes of interest. As a tracer, a compound that is not retained by the stationary phase ($P_i = 0$) is used. Preferably a low solute concentration is chosen in order to stay in the linear range of the partition equilibria and the linear range of the concentration-dependent detector response, so that the detector signal can be directly used

for analysis. As described in Fig. 1, a typical setup for batch separations consists of pumps and an injection valve, followed by the column where the separation takes place, and the detector and fraction collector. In addition, all parts of the setup are connected by a tubing and valves. In order to characterize the whole system and determine the influence of the different setup parts on the solute residence time distribution, i.e. the elution profile of the peaks, two experiments are necessary: one pulse injection without and one pulse injection with column. A schematic chromatogram including both experiments is illustrated in Fig. 2. The sample injection is assumed as a rectangular pulse with a duration t_{inj} . The influence of the off-column volume is characterized by carrying out a pulse injection experiment with the tracer (or the solute) while the column is replaced by a zero-volume connector or bypass. The corresponding retention time is $t_{R,plant}$ (Peak 1) in Fig. 2. In a second experiment, i.e. pulse injection with the column being connected, the tracer and at least one target solute are injected. The corresponding retention times are $t_{R,0}$ (tracer, Peak 2, solute with $P_i = 0$) and $t_{R,i}$ (solute, Peak 3, solute with $P_i > 0$).

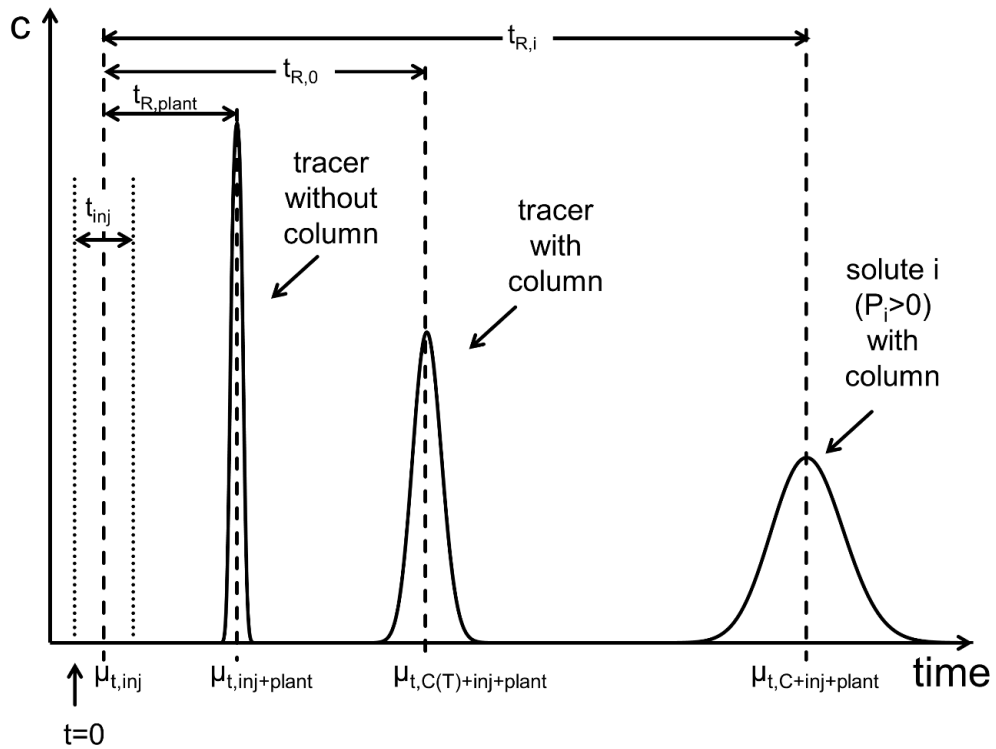


Figure 2: Representation of the elution peaks of pulse injection experiments of a tracer and a solute, with and without column connected to the system (modified figure adapted from [28]).

The peaks are analyzed by calculating the first and second moment through integration of the elution profiles [28]. The first moment (Eq. 6) represents the retention time $t_{R,i}$ of the compound. In the case of symmetrical peak shapes (Gaussian peaks), the first moment is equal to the retention time of the peak maximum. The peak variance σ_i^2 is determined with the second moment (Eq. 7).

$$t_{R,i} = \mu_t = \frac{\int_0^{\infty} t \cdot c(t) \cdot dt}{\int_0^{\infty} c(t) \cdot dt} \quad (\text{Equation 6})$$

$$\sigma_{t,i}^2 = \frac{\int_0^{\infty} (t-\mu_t)^2 \cdot c(t) \cdot dt}{\int_0^{\infty} c(t) \cdot dt} \quad (\text{Equation 7})$$

Both moments additively consist of several contributions [29] and according to Fig. 2 can be summarized in three sections: the sample injection unit; the plant including the tubing and connecting parts such as fittings and valves between the injector and detector as well as the detector itself; and the actual column.

The sample injection is assumed to be a rectangular pulse and hence, the first and second moments resulting from the injection are described in Eq. 8 [28]:

$$\mu_{t,\text{inj}} = \frac{t_{\text{inj}}}{2}, \quad \sigma_{t,\text{inj}}^2 = \frac{t_{\text{inj}}^2}{12}, \quad (\text{Equation 8})$$

Subsequently, the “plant” can be characterized independently from the used injection volume and the column (Eqs. 9 and 10). The parameter t_{plant} is the time a tracer needs from the point of sample introduction to the point of detection.

$$t_{\text{plant}} = \mu_{t,\text{plant}} = \mu_{t,\text{inj+plant}} - \mu_{t,\text{inj}} = \mu_{t,\text{inj+plant}} - \frac{t_{\text{inj}}}{2} \quad (\text{Equation 9})$$

$$\sigma_{t,\text{plant}}^2 = \sigma_{t,\text{inj+plant}}^2 - \sigma_{t,\text{inj}}^2 = \sigma_{t,\text{inj+plant}}^2 - \frac{t_{\text{inj}}^2}{12} \quad (\text{Equation 10})$$

Finally, the first and second moments of the column can be described by Eqs. 11 and 12 [28]:

$$t_{\text{C}} = \mu_{t,\text{C}} = \mu_{t,\text{C+inj+plant}} - \mu_{t,\text{inj+plant}} = \mu_{t,\text{C+inj+plant}} - \mu_{t,\text{plant}} - \frac{t_{\text{inj}}}{2} \quad (\text{Equation 11})$$

$$\sigma_{t,\text{C}}^2 = \sigma_{t,\text{C+inj+plant}}^2 - \sigma_{t,\text{inj+plant}}^2 = \sigma_{t,\text{C+inj+plant}}^2 - \sigma_{t,\text{plant}}^2 - \frac{t_{\text{inj}}^2}{12} \quad (\text{Equation 12})$$

In addition to a column characterization with pulse injections of small injection volumes, the characteristic parameters can also be determined by applying large injection volumes resulting in breakthrough curves (Fig. 3). With the help of frontal analysis, the first and second moment can be calculated from the concentration profile (or directly from the detector signal when working in the linear range of the concentration-dependent detector response). At the beginning of the experiment ($t = 0$), a feed concentration $c_{\text{feed},i}$ is introduced into the column. The introduced feed volume has to be large enough in order to reach a plateau, which means that the concentration at the column outlet is equal to $c_{\text{feed},i}$. The resulting elution profile is called a “breakthrough curve”. The first derivative of the breakthrough curve, between breakthrough time t_{B} and plateau describes an elution peak equivalent to a pulse injection with the same retention time $t_{\text{R},i}$. With the help of the moment analysis, the first and second moment can be calculated.

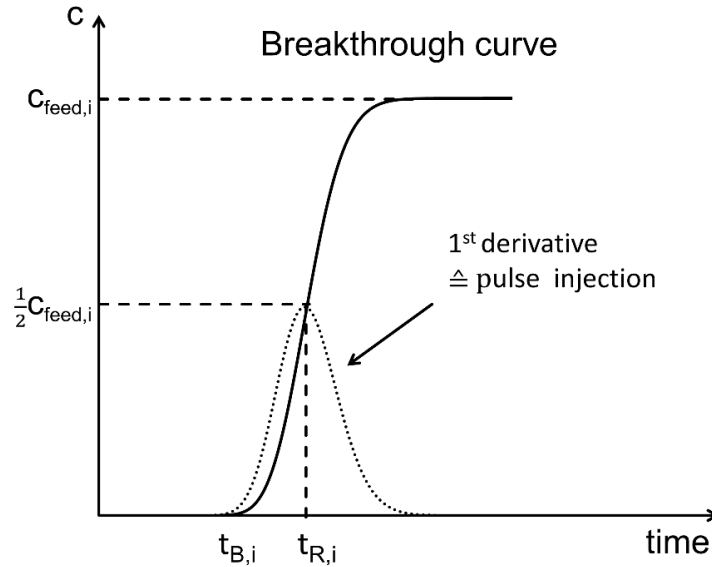


Figure 3: Representation of a breakthrough curve and a corresponding pulse injection elution profile

In the case of a symmetric peak, the retention time can also be read directly from the breakthrough curve. It corresponds to the time at the half feed concentration $\frac{1}{2} C_{\text{feed},i}$. Furthermore, the breakthrough time t_B can be defined as [30]:

$$t_{B,i} = t_{R,i} - 2\sigma_i \quad (\text{Equation 13})$$

Mass transfer effects and axial dispersion are characterized and quantified by the column efficiency, also called number of theoretical plates (N_i), according to Eq. 14:

$$N_i = \frac{\mu^2 t_i}{\sigma^2 t_i} = \frac{t_{R,i}^2}{\sigma_i^2} \quad (\text{Equation 14})$$

where $t_{R,i}$ is the retention time of component i and σ_i the corresponding standard deviation of the peak.

The column efficiency characterizes chromatographic systems and captures deviations from ideal behavior. The higher the theoretical plate number, the narrower is the peak width and consequently, the closer the peak shape approaches the ideal function of the assumed injection profile with a rectangular concentration profile of the solute injected at the entrance of the column.

The resolution R_S of two peaks is defined according to Eq. 15. For a Gaussian peak shape ($w = 4\sigma$), the resolution can also be calculated according to Eq. 16.

$$R_S = \frac{2(t_{R,j} - t_{R,i})}{w_j + w_i} \quad (\text{Equation 15})$$

$$R_S = \frac{t_{R,j} - t_{R,i}}{2(\sigma_j + \sigma_i)} \quad (\text{Equation 16})$$

Here, $t_{R,i}$ and $t_{R,j}$ are the retention times of a first and a second eluting component, respectively; w_i and w_j are their peak widths at base line; σ_j and σ_i are the peak standard deviations.

In Eq. 17, the resolution between compound i and compound j is derived from Eq. 16, assuming the generally valid solution for $N_j \neq N_i$. Often, an approximation of an equal number of theoretical plates for compounds that elute directly one after the other is done (Eq. 18), presuming $N_j = N_i = N$ [9, 24, 31]. Alternatively, N is often also calculated by simply taking the mean value of the number of the theoretical plates of both compounds ($N = (N_i + N_j)/2$) [9]. The resolution of the peaks can be expressed as a function of the parameters S_F , N_i , and P_i .

For $N_j \neq N_i$:

$$R_S = \frac{t_{Rj} - t_{Ri}}{2 \left(\frac{t_{Rj}}{\sqrt{N_j}} + \frac{t_{Ri}}{\sqrt{N_i}} \right)} = \frac{0.5 \cdot \sqrt{N_i N_j} \cdot (P_j - P_i)}{\left[\sqrt{N_i} \left(\frac{1 - S_F}{S_F} + P_j \right) + \sqrt{N_j} \left(\frac{1 - S_F}{S_F} + P_i \right) \right]} \quad (\text{Equation 17})$$

For $N_j = N_i = N$:

$$R_S = S_F \frac{1}{4} \sqrt{N} \frac{(P_j - P_i)}{1 - S_F \left[1 - \frac{P_j + P_i}{2} \right]} \quad (\text{Equation 18})$$

In LLC, the whole volume of the stationary phase is accessible to the solutes. As mentioned before, S_F of each biphasic solvent system is column dependent and influenced by the operating conditions, such as mobile phase flow rate, centrifugal field, and temperature. In general, a higher stationary phase retention is advantageous for a LLC separation. As demonstrated in Fig. 4 with the elution profile as a function of (a) retention volume and (b) partition coefficient, an increase in stationary phase retention results in an increase in peak resolution.

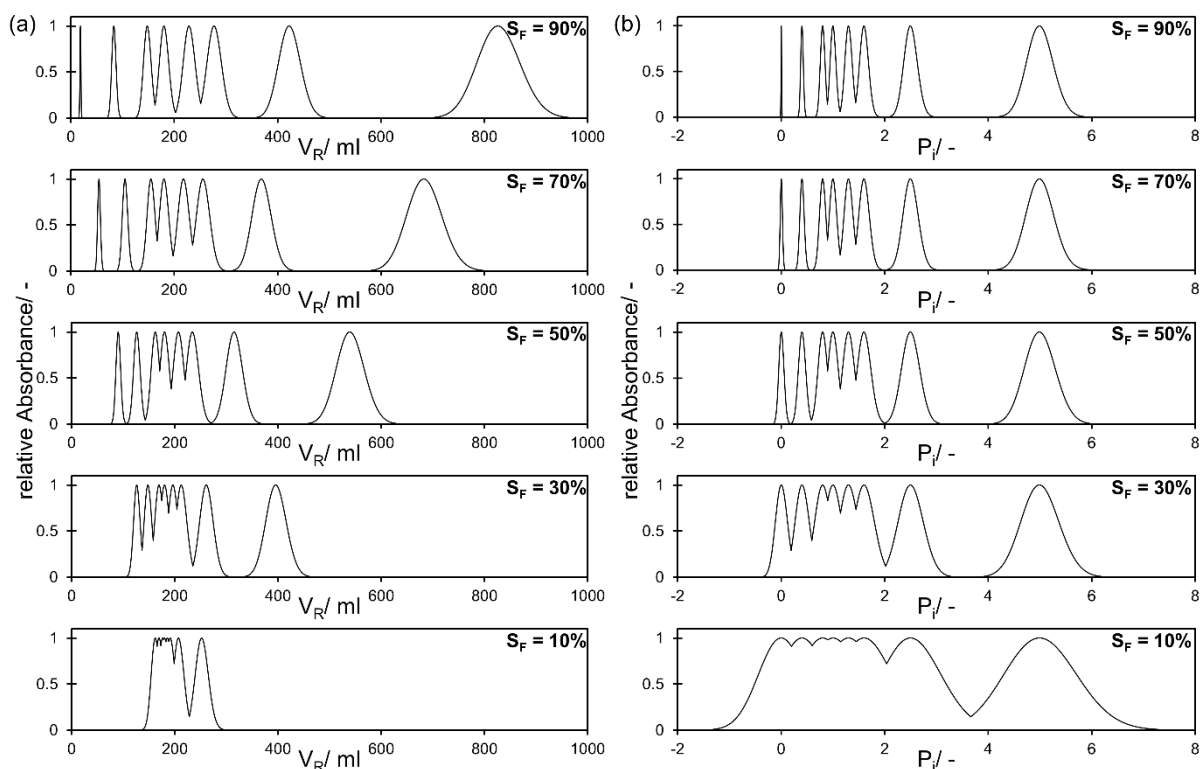


Figure 4: Influence of stationary phase retention (S_F) on the separation of a multicomponent mixture. Simulated chromatograms for S_F between 0.1 and 0.9 in (a) as a function of the retention volume V_R and (b) as a function of the partition coefficient P_i : $V_C = 180$ ml, $N = 400$, $V_{inj} = 1$ ml, $c_{inj} = 1$ mg ml $^{-1}$, $F = 12$ ml min $^{-1}$, $P_{1-8} = 0/0.4/0.8/1/1.3/1.6/2.5/5$.

Fig. 5 visualizes the dependence between the resolution R_S and the parameters S_F , P_i , α , and N according to Eq. 18. In general, and as apparent from Fig. 5a-d, the resolution increases significantly with an increase in stationary phase retention. For a constant separation factor and efficiency, the resolution increases (Fig. 5a-b) towards higher partition coefficients, especially when lower stationary phase retention is present. Assuming a constant efficiency and a constant partition coefficient of the first eluting compound P_i , the resolution increases with both an increase in S_F and α . As expected, the increase is even more pronounced for both higher stationary phase retention and higher separation factors (Fig. 5c-d). Similarly, an increase in column efficiency is more advantageous for an increase in resolution at higher stationary phase retention (Fig. 5e). Correspondingly, this effect is even stronger for higher separation factors (Fig. 5f).

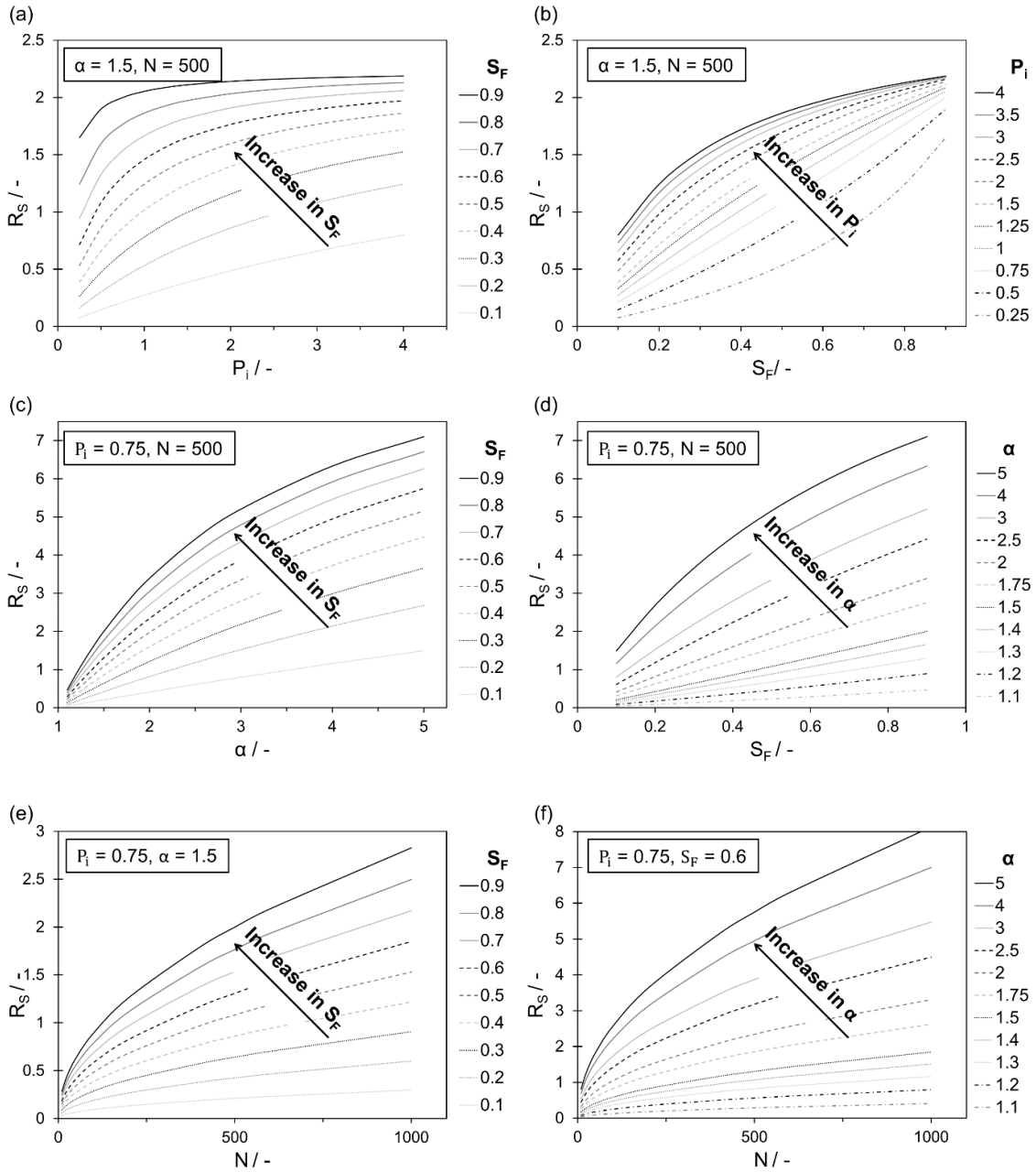


Figure 5: Graphical representation of the dependence of R_S on the characteristic parameters S_F , N , and P . The resolution R_S is shown (a) as a function of P_1 at different S_F from 0.1 to 0.9. (b) as a function of S_F at different P_1 from 0.25 to 4. (c) as a function of α at different S_F from 0.1 to 0.9. (d) as a function of S_F at different α from 1.1 to 5. (e) as a function of N at different S_F from 0.1 to 0.9. (f) as a function of N at different α from 1.1 to 5.

2.2. Thermodynamics of liquid-liquid phase equilibria

The equilibrium conditions of a heterogeneous closed system consisting of π phases and m components at thermodynamic equilibrium are defined in Eqs. 19 to 21 [32, 33]:

$$\text{thermal equilibrium: } T^\alpha = T^\beta = \dots = T^\pi \quad (\text{Equation 19})$$

$$\text{mechanical equilibrium: } p^\alpha = p^\beta = \dots = p^\pi \quad (\text{Equation 20})$$

$$\text{chemical equilibrium: } \mu_i^\alpha = \mu_i^\beta = \dots = \mu_i^\pi \quad (\text{Equation 21})$$

for $i = 1, 2, \dots, m$

where T is the temperature, p is the pressure, and μ_i is the chemical potential of compound i .

In order to express the chemical potential in a more physical way, the concept of fugacity was introduced by G.N. Lewis [32, 33] to describe the phase equilibrium between phase α and phase β . In this sense, Eq. 22 defines the relationship between the fugacity and the chemical potential for component i in any phase, i.e. solid, liquid, or gas.

$$\mu_i^\pi = \mu_i^{0\pi} + RT \ln\left(\frac{f_i^\pi}{f_i^{0\pi}}\right) \quad (\text{Equation 22})$$

Here, f_i corresponds to the fugacity of phase π , f_i^0 to an arbitrary reference state which is commonly called standard fugacity, and μ_i^0 is the chemical potential at the selected reference state. However, when μ_i^0 or f_i^0 is chosen, the other quantity is fixed.

The fugacity can be used to transform the fundamental equation of the phase equilibrium (Eq. 21) to a more practical description. Assuming that the reference states of the two phases are the same ($f_i^{0\alpha} = f_i^{0\beta}$ and $\mu_i^{0\alpha} = \mu_i^{0\beta}$) and according to Eq. 22, the fugacity of compound i in both phases is the same (Eq. 23).

$$f_i^\alpha = f_i^\beta \quad (\text{Equation 23})$$

Using the so-called iso-fugacity criterion, the liquid-liquid equilibrium between the phases can also be defined with the activity coefficient. The ratio between fugacity and standard fugacity is introduced as activity a_i ($a_i = f_i/f_i^0$), while the activity coefficient γ_i represents the ratio between the activity and the concentration of compound i ($\gamma_i = a_i/x_i$). In this context, the fugacity of compound i in a liquid solution can be expressed as follows:

$$x_i^\alpha \gamma_i^\alpha f_i^{0\alpha} = x_i^\beta \gamma_i^\beta f_i^{0\beta} \quad (\text{Equation 24})$$

where x_i is the molar fraction, γ_i the activity coefficient, and f_i^0 the standard fugacity.

For the same standard fugacity f_i^0 in both phases, where a pure component usually is selected as a reference state, the iso-fugacity criterion from Eq. 24 can be simplified. Thus, the fugacity can be simply described with the mole fraction and the activity coefficient as the activity of the phase:

$$x_i^\alpha \gamma_i^\alpha = x_i^\beta \gamma_i^\beta \quad (\text{Equation 25})$$

The distribution of the compounds between the phases is defined by the distribution coefficient K_i (Eq. 26). At infinite dilution, the distribution coefficient of a particular compound between two phases is constant at:

$$K_i^{\alpha\beta} = \frac{x_i^\alpha}{x_i^\beta} = \frac{\gamma_i^\beta}{\gamma_i^\alpha} \quad (\text{Equation 26})$$

In liquid-liquid extraction and liquid-liquid chromatography, concentration ratios are usually used instead of molar fractions to calculate the distribution coefficient. The resulting concentration-based distribution coefficient is commonly called partition coefficient P_i [34] and is defined according to Eq. 27. In LLC, α refers to the stationary phase and β to the mobile phase:

$$P_i^{\alpha\beta} = \frac{c_i^\alpha}{c_i^\beta} = \frac{x_i^\alpha v^\alpha}{x_i^\beta v^\beta} = K_i^{\alpha\beta} \frac{v^\alpha}{v^\beta} \quad (\text{Equation 27})$$

where c_i is the concentration of compound i in one of the phases and v is the molar volume of the phases.

The molar volumes of the phases can be derived from the composition of the phases and the molar volume of the pure solvents v_{i0} , considering the excess volume of mixing v^E .

$$v = \sum x_i v_{i0} + v^E \quad (\text{Equation 28})$$

A schematic representation of the liquid-liquid equilibrium of a ternary solvent system is illustrated in the phase diagram in Fig. 6. The shown ternary system with pure solvents in the corners of the diagram forms a miscibility gap. The miscibility gap is defined by the border between the monophasic and the biphasic region, the so-called binodal curve, which is temperature- and pressure-dependent. For many ternary systems used in LLC, the miscibility gap shrinks with an increase in temperature ($T_2 > T_1$). In practice, the influence of pressure on the phase equilibrium can be neglected, since the LLC separations are carried out in a pressure range below 100 bar (mostly ambient pressure). For the preparation of the biphasic system, a composition in the biphasic region is selected, the corresponding portions of the solvents are mixed, and subsequently equilibrated at constant temperature and pressure. The intercepts of a tie-line with the binodal curve represent the compositions of the two phases (phase α and phase β) that are formed in thermodynamic equilibrium. Towards the plait point, the compositions of the phases approach each other, leading to a single-phase region.

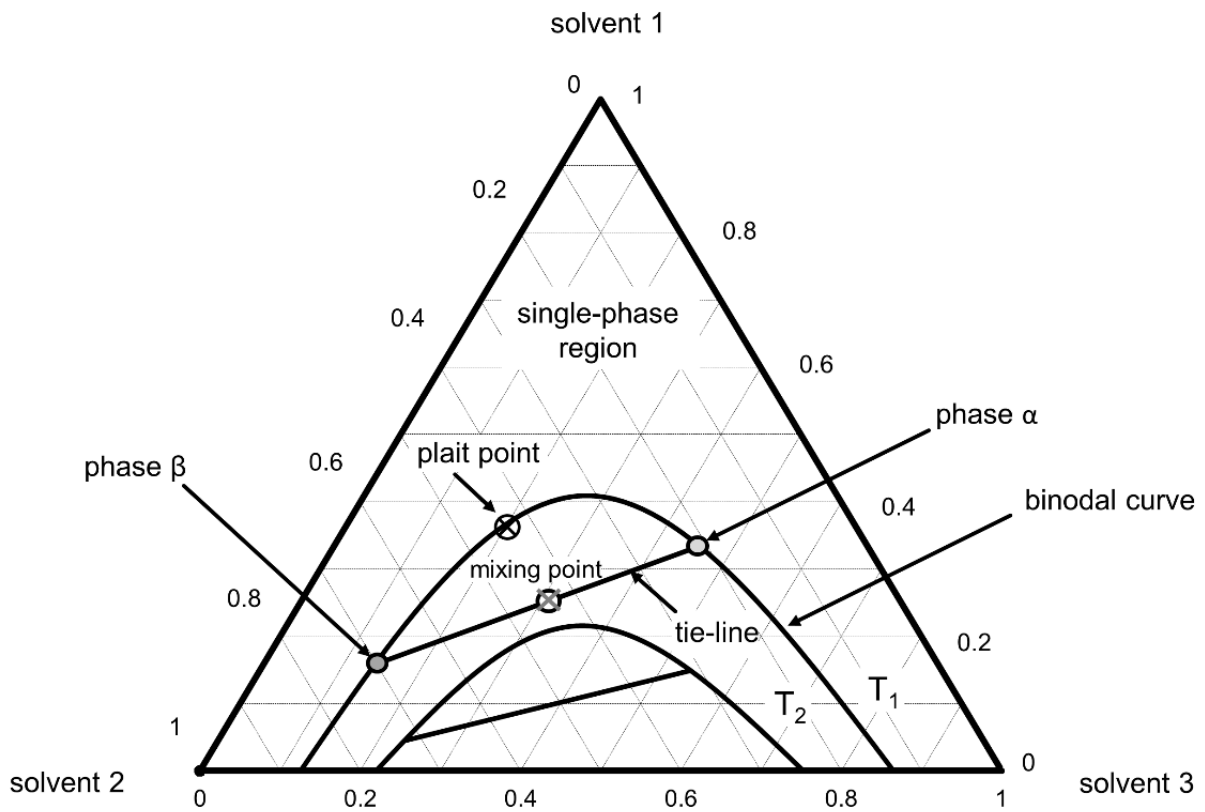


Figure 6: Schematic representation of a type 1 ternary phase diagram including a miscibility gap at two different temperatures (adapted from [35]).

2.3. Solvent system selection in liquid-liquid chromatography

2.3.1. Biphasic solvent systems

The stationary and mobile phase used in LLC to perform the separation are two phases of a biphasic liquid system in equilibrium. In comparison to LC where the stationary phase is selected first and the composition of the mobile phase is then selected and tuned until the desired separation is achieved, in LLC the phases cannot be selected successively and independently from each other. Hence, the phases are selected simultaneously by selecting the solvents and their mixtures composition from the biphasic liquid region. The simplest possible two-phase system would be a binary mixture of e.g. ethyl acetate and water, or hexane and water. In such binary systems, the composition of the phases is fixed at a given temperature according to the thermodynamic equilibrium and cannot be tuned. Consequently, the partition coefficient of a certain target compound and its impurities are fixed as well and cannot be further modified in case of an unsatisfactory separation. Therefore, multi-solvent biphasic systems composed of three or four solvents are mostly used in LLC [6, 9, 24, 36-39]. Such systems are advantageous, since the composition of both phases can be tuned by varying the ratio of the solvents. Preferably, biphasic solvent systems are selected where the partition coefficients of the target compounds are in the so-called *sweet spot* range between 0.4 and 2.5. As illustrated in Fig. 7, this provides a good compromise between separation resolution and solvent consumption [37, 40]. For partition coefficients $P_i < 0.4$, a strong peak overlap is observed, while separations with $P_i > 2.5$ tend to be inefficient due to broad peaks, i.e. highly diluted products, and long separation times (high solvent consumption). In order to completely separate two components, the separation factor α should also be sufficiently large. The necessary value of α for a successful separation can vary greatly depending on the selected columns, differing in column efficiency and stationary phase retention, and the selected separation mode. For simple batch separations, a separation factor of $\alpha > 1.5$ is usually targeted [41].

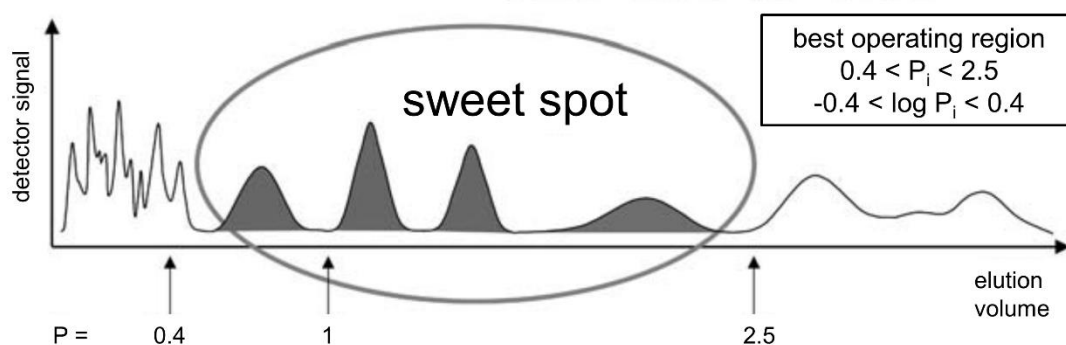


Figure 7: Schematic representation of the *sweet spot* range in LLC (adapted from [37]).

Theoretically, an unlimited number of various biphasic solvent systems can be created. This enables tailor-made systems for specific applications. Rapid developments in this field have already established a wide variety of solvent systems in LLC [6]. Aqueous-organic solvent-based systems are mostly used [42], but also non-aqueous systems as well as nonconventional aqueous two-phase systems (ATPS) and the recently upcoming deep eutectic solvent (DES)-based systems. The probably best-known solvent systems are

n-hexane/ethyl acetate/methanol/water (called HEMWat), and *n*-heptane/ethyl acetate/methanol/water (called Arizona) with *n*-heptane instead of *n*-hexane [24, 38]. These systems have been used for the separation of a wide range of medium polar substances. Their advantage is that the polarity of the phases can be easily adjusted by simply varying the ratio of the individual solvents.

Especially for the separation of highly hydrophobic (nonpolar) and highly hydrophilic (polar) compounds, there is still a huge demand for suitable biphasic solvent systems in LLC [6, 42, 43]. For the separation of rather hydrophilic compounds, such as proteins, the use of organic solvents is rather unsuitable because denaturation of the proteins can occur. Hence, for the separation of such polar and sensitive molecules, either butanol/water-based solvent systems [44] or ATPS are currently used [35, 45-49].

In aqueous two-phase systems, both phases are mainly composed of water. In addition, they generally contain either two polymers such as polyethylene glycol (PEG) and dextran, or a polymer and a salt (e.g. phosphate salt). As an alternative to polymers as a phase forming component, ionic liquid (IL)-based ATPS have been successfully applied for the separation of proteins with LLC [45, 50]. The phase properties can be tuned by varying the chain length of the polymers (PEG 500 – 4000) [51], the combination of IL cation and anion [52], or by changing the salts along the Hofmeister series for anions and cations [53-57].

In terms of non-aqueous biphasic solvent systems for the separation of hydrophobic compounds, only few systems such as *n*-heptane/toluene/acetonitrile or *n*-hexane/ethyl acetate/acetonitrile are available. Recently, a new class of solvent systems based on deep eutectic solvents (DES) has been established as candidates for non-aqueous systems. DES are mixtures of at least two compounds that form a eutectic mixture. A hydrogen-bond donor (HBD) and a hydrogen-bond acceptor (HBA) are combined in a certain molar ratio to form a mixture with a melting point substantially lower than that of the individual compounds, as illustrated in Fig. 8a [58]. In literature, DES are highlighted as a new generation of designer solvents, since the physical properties, in analogy to the ionic liquids, can be tailored by an almost limitless number of possible combinations of different HBDs and HBAs [59-66] and to some extent also by varying the molar ratios in which they are prepared [67-71]. DES can be produced from cheap bulk materials such as carboxylic acids (e.g. levulinic acid), alcohols (e.g. glycerol), sugars (e.g. glucose), terpenes (e.g. menthol), amino acids (e.g. proline), carbamide (e.g. urea), and ammonium salts (e.g. choline chloride). Advantageous is their easy preparation, as DES are commonly prepared by heating the mixture of their constituents as shown in Fig.8b for choline chloride and levulinic acid. The probably best-known DES composition is the combination of choline chloride (HBA) and urea (HBD).

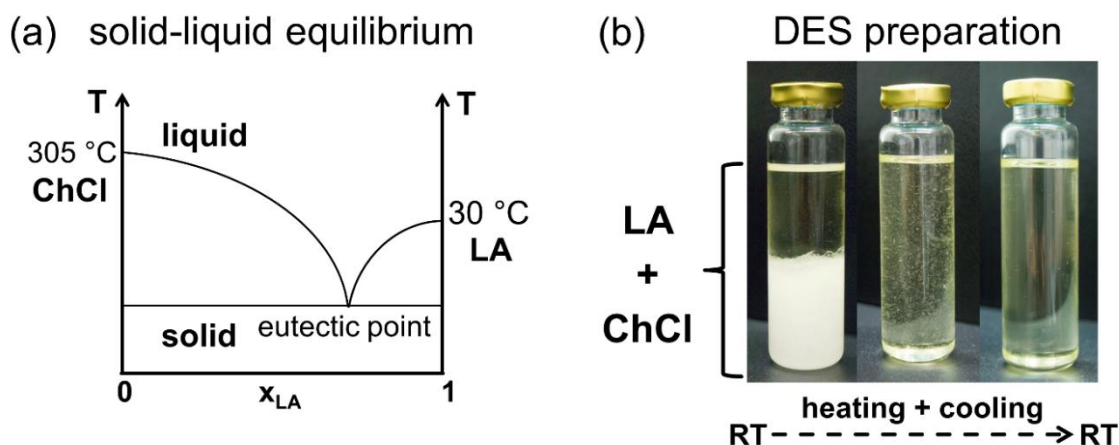


Figure 8: (a) Schematic solid-liquid equilibrium phase diagram for the binary eutectic mixture of choline chloride (ChCl) and levulinic acid (LA). Note: The given melting points of ChCl and LA are estimated melting points. ChCl decomposes before melting. (b) Illustration of the preparation of a binary DES in a crimped flask by mixing LA and ChCl in a molar ratio of 1:2 at room temperature (RT), followed by a heating to 80 °C resulting in a clear and homogeneous liquid phase that stays liquid after cooling back to room temperature.

DES based on natural primary metabolites such as sugars, amino acids, and organic acids are referred to as natural deep eutectic solvents (NADES), since they are considered biocompatible, renewable, and biodegradable [66]. In this context, DES-based solvents are also often referred to as promising non-toxic or “green” solvents. Nevertheless, liquid-liquid equilibrium data of DES-based biphasic systems is still limited, but the number of publications in this field is rising [72-77]. The use of DES-based biphasic solvent systems has steadily increased especially in the field of solid-liquid and liquid-liquid extraction, e.g. for the extraction of flavonoids and phenolic compounds from plants [64, 78-80]. However, an application of DES-based biphasic liquid systems in LLC has not yet been explored.

2.3.2. Screening methods for solvent system selection

Due to the huge variety of possible biphasic systems, the selection of a suitable solvent system in LLC is the most laborious and time-consuming step in the separation method development [41]. Often, extensive trial-and-error experiments are performed in order to find a suitable biphasic solvent system for the separation of a particular target compound from a mixture. In literature, few approaches are proposed in order to search for an appropriate solvent system in a more systematic way:

- “Best solvent” approach [9, 24, 36]:

First, a solvent where the sample is well soluble is selected (“best solvent”). Then, two other solvents that are almost immiscible or poorly miscible with each other, but both miscible with the first solvent, are selected. Usually, one of the two other solvents is “less-polar” and the other one is a “more-polar” solvent compared to the “best solvent”. Hence, a ternary system with a so-called *type 1* miscibility gap is formed, where the “best solvent” partitions between

the two phases. Consequently, the compounds with a good solubility in the “best solvent” also distribute between the phases in dependence of their different polarity [9, 24].

- “Multisolvent system” approach:

Predefined solvent system families composed of four or five solvents in different ratios are used along a scale of stepwise changing system polarity. Oka et al. [38] for the first time defined different mixtures of *n*-hexane, ethyl acetate, *n*-butanol, methanol, and water. Without the *n*-butanol, this solvent system family is now widely known as the HEMWat series. With *n*-heptane instead of *n*-hexane, Margraff established the so-called Arizona family [36]. In this approach, the predefined systems are then screened with the target mixture in order to find a system, where the compounds show appropriate partition coefficients and separation factors.

- “GUESSmix” approach [37]:

In the “Generally Useful Estimate of Solvent Systems” (“GUESSmix”) approach [37], solvent system families such as HEMWat are characterized with a model mixture of 20 commercially available compounds that cover a wide range of polarities, i.e. an octanol-water partition coefficient range $\log P_{O/W}$ between -5.1 (new coccine red) to 15.2 (carotene) compounds [40]. Subsequently, the target compounds are compared with these GUESSmix compounds in terms of polarity, i.e. $\log P_{O/W}$, and molecular structure, and a potential suitable biphasic solvent system is selected. Furthermore, Friesen et al. proposed the comparison of R_F -values from thin layer chromatography (TLC) between GUESSmix compounds and the target compounds to estimate a possibly suitable system from the HEMWat series [37]. By this, components “equivalent” to the GUESSmix compounds are searched. More recently, Friesen et al. [81] modified this approach by considering the polarity and selectivity of solvent systems by means of the GUESSmix compounds. There, the polarities and selectivities of solvent system pairs are visually compared in so-called 2-dimensional reciprocal shifted symmetry plots (ReSS²). This can be used to find orthogonal solvent systems, i.e. systems with similar polarity but different selectivity [81].

- “Thermodynamic model-based prediction” approach:

In this approach, biphasic solvent systems are screened using thermodynamic models [50, 82-86]. The partition coefficients of the target compounds P_i are calculated according to Eq. 25 using predicted activity coefficients and molar concentrations of the compounds in the two liquid phases. First, a pool of suitable solvents are selected according to given requirements (e.g. toxicity, reactivity, price, vapor pressure, boiling point etc.) for the particular application. Then, following the idea of the “best solvent” approach of Foucault et al. [24], the solubility of the particular target compound in the selected solvents is assessed by the predicted values of the solvent capacity, which is the reciprocal value of the activity coefficient of a solute in the solvent at infinite dilution. In this sense, the activity coefficient at infinite dilution is calculated with a thermodynamic model. In general, the higher the capacity, the higher is the solubility of a particular solute in the solvent. After that, a list of possible biphasic liquid systems containing at least one solvent with high solute solubility and two other solvents from the pool of solvents is composed. The LLE data of potential biphasic solvent systems at different global compositions is either predicted or taken from literature. A broad screening is performed by calculating the partition coefficient of the target compounds in each listed biphasic system composition. Finally, a small number of most promising systems where the partition coefficient of the target compounds was predicted in or close to the *sweet spot range* is selected for

experimental evaluation. In this context, different thermodynamic models can be used: the quantum mechanics based Conductor like Screening Model for Realistic Solvation (COSMO-RS) [87], the group-contribution model Universal Quasichemical Functional-Group Activity Coefficients (UNIFAC) [88-91], the two of the local composition concept based models, Non-Random-Two-Liquid (NRTL) model [92] and the Universal Quasichemical (UNIQUAC) model [93], and the Perturbed-Chain Statistical Associating Fluid Theory (PC-SAFT) [94].

Independent of the specific solvent system screening method, experiment-based or predictive, the partition coefficients of the target compounds in the selected biphasic solvent system are usually determined by shake-flask experiments before performing the LLC separation. A small amount of the biphasic solvent system (10-20 ml) is prepared and equilibrated. Then, equal volumetric portions of upper and lower phase are taken, 2-5 ml respectively, and transferred to a suitable flask and a small amount of the sample mixture is added. It must be noted, that the partition coefficient is concentration-dependent. Hence, a low sample concentration is selected, usually 1-5 mmol l⁻¹ dissolved in the biphasic system, in order to not exceed the linear range of the partition equilibria. Finally, a sample of the upper and the lower phase is taken, e.g. with a syringe connected to a cannula, and the concentration of the relevant components in both phases is determined with an applicable analytical method, for example HPLC, LC-MS, or GC-MS. The partition coefficient is then calculated according to Eq.2. In this context, Garrard [95] suggested a semi-automatic solvent system screening with a liquid-handling robot in combination with HPLC.

2.4. Column design in LLC

In addition to the selection of a suitable biphasic solvent system, the choice of a suitable column, and appropriate operating conditions play an important role in the design of a separation method. In LLC, the general separation principle is based on the difference in the partition coefficient of the compounds. However, the column geometry and operating conditions have a significant influence on the stationary phase retention (Eq. 1) and the column efficiency (Eq. 14), which are essential factors for a successful separation (see also the definition of resolution in Eq. 18). LLC is categorized based on two different types of column principles, hydrodynamic and hydrostatic columns.

Hydrodynamic Columns

Hydrodynamic columns, better known as countercurrent chromatography (CCC), were invented by Ito et al. in 1966 [1]. They consist of a tubing (coil) that is wound on a bobbin. The bobbin rotates around two axis with planetary motion, its own axis (axis of rotation) and around another centrifugal axis (axis of revolution) with the same angular velocity (ω). The resulting centrifugal field keeps one of the two liquid phases stationary, while the other phase is pumped through the column as mobile phase [41]. The rotation of the two axis can be carried out in counter rotation direction (I-type CCC) or the same direction (J-type CCC) [8]. Many different varieties and continuous developments have been made [2, 8, 25]. However, the most widely used type is the J-Type CCC as illustrated in Fig. 9. The planetary motion results in a periodic change of centrifugal field intensity and direction, which generates mixing and settling zones along the coil [41]. Mixing zones, where the mass transfer between the phases takes place and settling zones, where phase separation occurs, are shown in Fig. 9b.

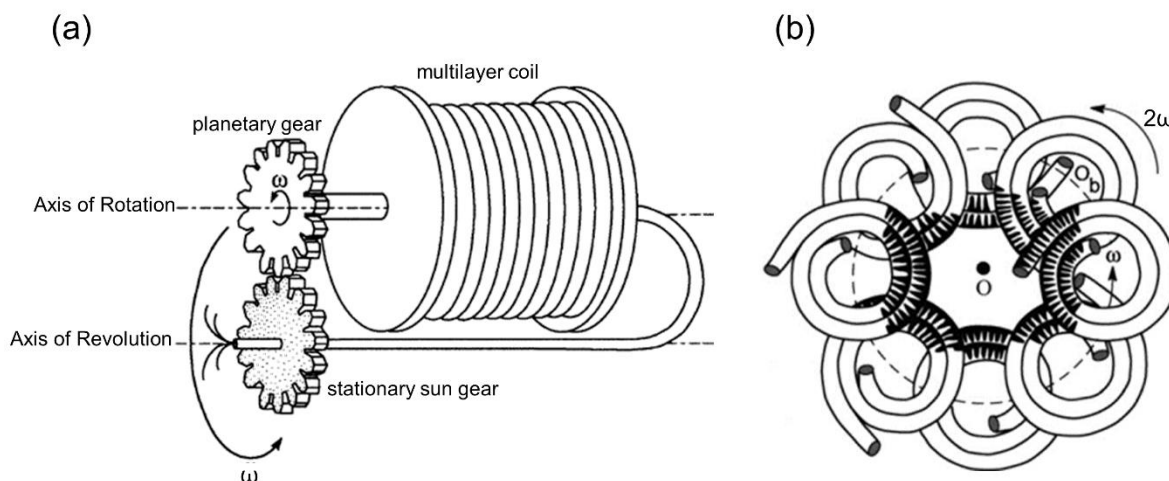


Figure 9: Design of a J-type CCC column (a) and illustrated mixing (black) and settling (white) zones inside the coil (b) [41].

In addition to different developments in the setup of the column, the coil geometry itself was continuously improved. On the one hand, different tubing diameters or rectangular tubings with different aspect ratios can be used [96]. On the other hand, the tubing can be modified by e.g. crimping the tubing with different geometries [97]. Both influences the hydrodynamics in the mixing and settling zones. It was shown that this can improve the stationary phase retention, efficiency, and consequently the peak resolution of a separation [96, 97].

Hydrostatic Columns

Hydrostatic columns, also called centrifugal partition chromatography (CPC), in comparison to CCC have only one axis of rotation that generates a centrifugal field that keeps one of the liquid phases stationary [9, 24, 26]. Currently available conventional CPC columns consist of several identical annular disks that are connected in series, with PTFE plates in between acting as seals (see Fig. 10). This modular construction allows for a flexible selection of the column lengths [9, 24, 26]. A certain number of cells interconnected by narrow short channels, referred to as ducts, are engraved circumferentially in each annular disk. The ducts are filled with mobile phase only and therefore behave as dead volume that does not contribute to the separation. A higher proportion of the duct volume reduces the effective column volume that participates in the separation and results in a decrease in column efficiency. In addition, ducts cause pressure drop and hence, limit the applicable mobile phase flow rate [98]. In the history of CPC, a wide variety of column designs, i.e. cell or chamber designs, has been developed. The most significant developments in CPC cell designs are described and illustrated in Table 2.

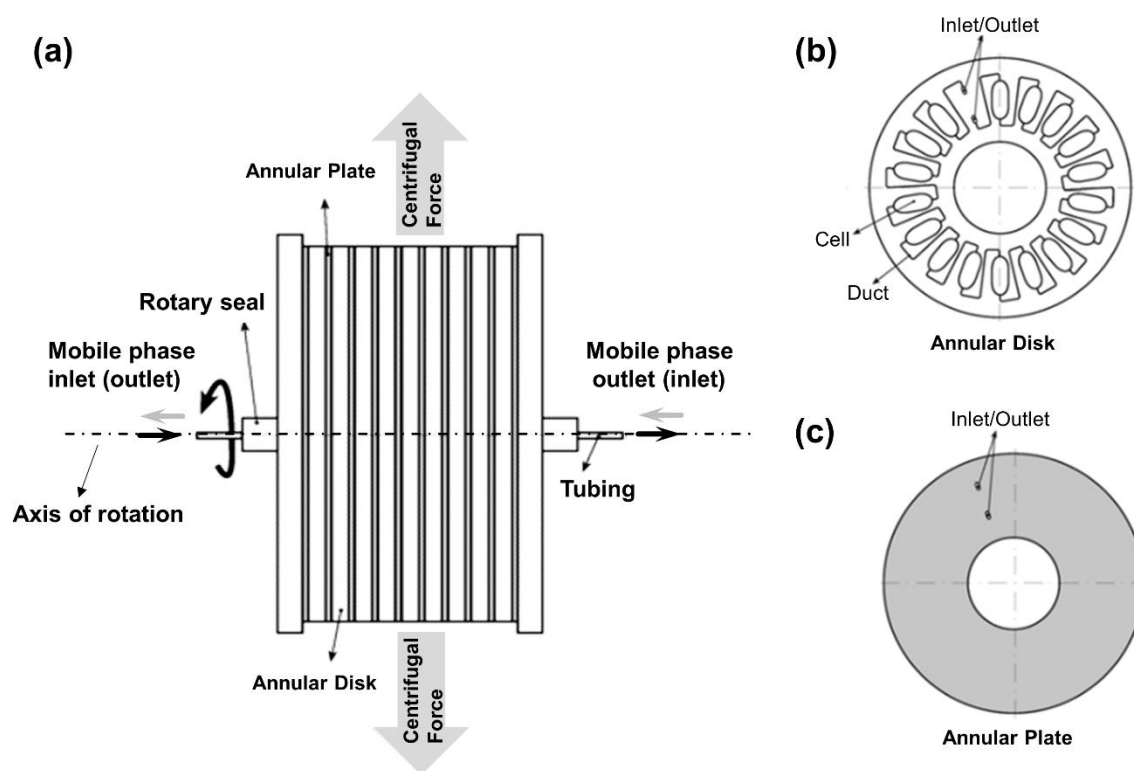


Figure 10: Schematic illustration of (a) the design of a conventional CPC column with one axis of rotation consisting of several stacked disks and sealing plates in between, (b) an annular disk with cells interconnected by ducts, and (c) an annular plate for sealing (adapted from [86]).

Murayama et al. developed the first cell design in 1982 [99], which had the form of interconnected column cartridges mounted on a rotor of a centrifuge. Subsequently, other cell designs optimized in terms of flow patterns were developed in order to improve stationary phase retention and to enhance the mass transfer between the phases. Nunogaki et al. [100] (Sanki Engineering Ltd.) introduced the concept of an annular disk with interconnected cells (chambers) and annular plates in between the disks as illustrated in Fig. 10, which is still used

in modified form and with different cell designs in currently available conventional CPC systems. The Nunogaki chambers have a radial and conical cell shape. The disk plate is made of synthetic resin and consists of multiple slots or chambers, which are placed circumferentially and radially in the annular disk. The chambers are interconnected by ducts [100]. De la Poype et al. invented the first so-called FCPC®-chambers [101] also named as radial cells, consisting of interconnected cells of quadrangular shape. A further development of FCPC®-chambers are the so-called Z-cells, which are slightly tilted [101]. This has the advantage that the effect of the apparent Coriolis force on the flow regime is reduced. A new cell geometry concept were the twin-cells [12, 102] and asymmetric twin-cells [11, 103], where circular or elliptical cells are paired two by two in series, so that cell pairs are in direct contact. Neighboring cell pairs are connected by ducts. The new cell geometry and arrangement of the cells enabled for a larger number of cells per disk while reducing the total duct volume of the column. This increases the effective column volume available for the separation and thus also allows for higher separation efficiency. Currently, the cell design of most of the commercial CPCs is based on different cell shapes of the twin-cell geometry. Another rather new development in this context are the spherical cells [12, 104]. The column is made in the form of a monobloc that contains a series of spherical twin-cells. Analogous to the previous cell designs, the twin-cells are placed circumferentially in a layer of the monobloc around the rotational axis and interconnected by small ducts. In this case, the duct volume is significantly reduced, which leads to a higher effective column volume that is available for the separation. In addition, no sealing PTFE plates are needed, which allows the operation at a higher pressure drop and subsequently the use of higher flow rates.

An alternative cell design is that of interconnected cylindrically-shaped RotaChrom®-cells [10, 105, 106] with packing material for flow distribution. The cells are interconnected with tubings and mounted on a centrifugal plate. The cells are much larger than other existing CPC cells and thus, allow the operation at industrial-scale with higher flow rates. Another column design is the so-called spiral disk CCC assembly, where multiple disks are interconnected in series and stacked together to form one column. The disks consist of inert plastic plates with spiral grooves and rotate around one axis of rotation [44, 107].

Table 2: Overview of different column and cell geometries of available CPC column designs.

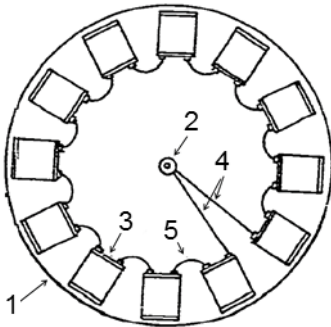
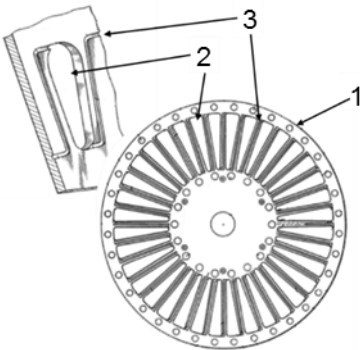
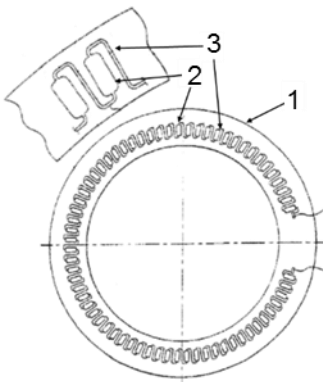
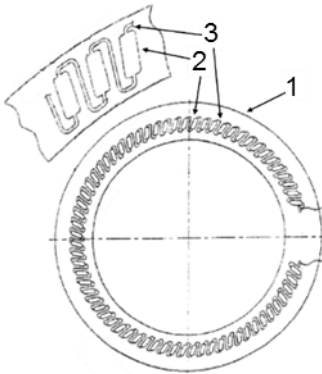
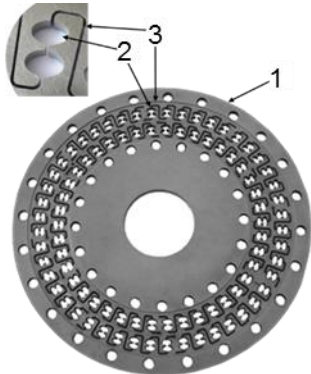
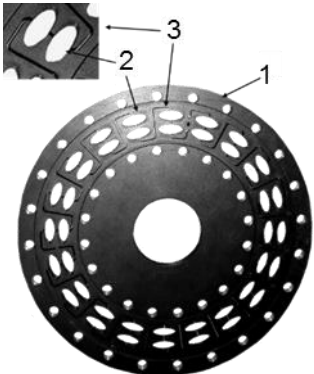
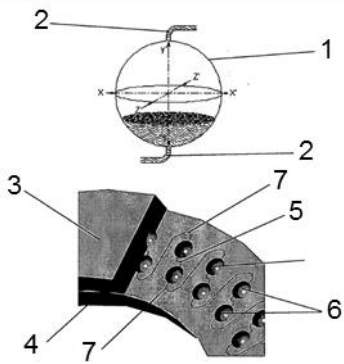
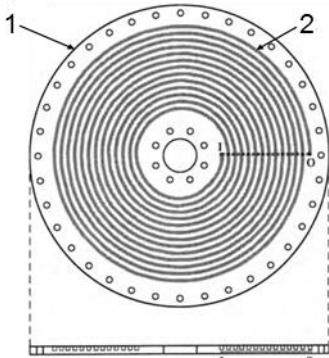
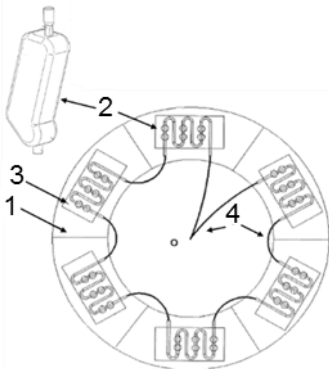
Column cartridges	Nunogaki chambers	FCPC®-chambers - Radial cells	FCPC®-chambers - Z-cells	Twin-Cells
				
<p>Interconnected column cartridges:</p> <p>1: rotor of the centrifuge 2: rotary seal joint 3: column cartridge 4: connecting tubes between rotary seal joint and column cartridges 5: connecting tubes between column cartridges</p>	<p>Interconnected radial and conical cells:</p> <p>1: annular disk 2: cells of radial and conical shape 3: duct (interconnecting channels)</p>	<p>Interconnected cells of quadrangular shape:</p> <p>1: annular disk 2: cells of quadrangular shape 3: duct (interconnecting channels)</p>	<p>Interconnected tilted radial cells:</p> <p>1: annular disk 2: tilted cells of quadrangular shape 3: duct (interconnecting channels)</p>	<p>Interconnected circular cell shape:</p> <p>1: annular disk 2: symmetric twin-cells with circular shape 3: duct (interconnecting channels)</p>
[99]	[100]	[101]	[101]	[12, 102]

Table 2: Overview of different column and cell geometries of available CPC column designs.

Asymmetric Twin-Cells	Spherical cells	Spiral disk assembly	RotaChrom®-cells
			
<p>Interconnected elliptical cell shape:</p> <p>1: annular disk 2: asymmetric twin-cells with elliptical shape 3: duct (interconnecting channels)</p>	<p>Interconnected three-dimensional spherical cells:</p> <p>1: spherical cell 2: duct (cell inlet/outlet) 3: annular disk (upper part) 4: annular disk (bottom part) 5: duct (interconnecting channels) 6: spherical twin-cells 7: duct (interconnecting channels)</p>	<p>Spiral grooves in interconnected disks:</p> <p>1: disk 2: interwoven spiral channels</p>	<p>Cylindrically-shaped cells with packing material:</p> <p>1: rotating plate, on which the cells are mounted 2: cylindrical cell 3: module with several interconnected cells 4: tubes that interconnect cells</p>
[11, 103]	[12, 104]	[44]	[10, 105, 106]

2.5. Hydrodynamic characteristics of LLC Columns

LLC column hydrodynamics influence the retention of the stationary phase and the mass transfer between the two liquid phases. Different column operating principles, e.g. hydrostatic or hydrodynamic columns, as well as their different geometries result in different flow regimes. The flow pattern is fundamentally different between the hydrodynamic and the hydrostatic columns. In CCC, the whole column volume participates in the separation, since mixing and settling zones line up alternately without interconnecting channels or ducts that reduce the effective column volume (see Fig. 9b). Hence, there is no additional pressure drop in the column as it is caused by ducts in CPC. Thus, the pressure drop in CCC is lower in comparison to CPC. Therefore, the pressure drop in a CCC column is usually assumed independent of the mobile phase flow rate and constant for a given solvent system and rotational speed [108, 109]. The repetitive mixing and settling zones move through the CCC coil and the hydrodynamic motion is similar to the so-called Archimedean screw effect [41]. Such continuous contact between the two liquid phases results in a higher column efficiency (N_i) of CCC compared to CPC [26]. Different column and tubing modifications such as tubing geometries and aspect ratios can improve both the stationary phase retention and the efficiency [96, 97, 110].

In conventional hydrostatic columns, different flow regimes have been observed by visualization with transparent disks, dyed mobile phases, and a stroboscopic camera system [31, 98, 111-113]. The flow pattern in CPC is usually assigned to three general categories as shown in Fig. 11 for FCPC chambers [112]: (a) stuck film or unbroken sheet, (b) oscillating sheet or broken jet, and (c) atomization. In addition, van Buel et al. [111] described a droplet regime for very low flow rates and rotational speeds, which is rather suboptimal for a good mass transfer between the two phases. Such droplet regime can result in dead zones in the cell, which causes additional peak broadening due to an increased residence time distribution of the solutes [112].

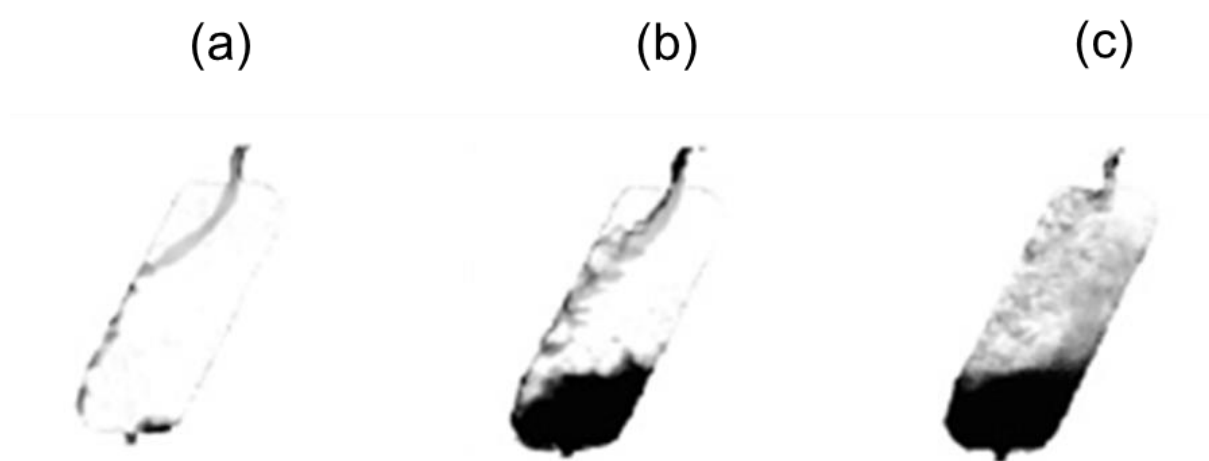


Figure 11: Three different flow regimes in CPC cells, namely (a) stuck film, (b) oscillating sheet, and (c) atomization, with white representing the stationary phase, grey representing the two phases in contact, and black representing the mobile phase in descending mode (adapted from [112]).

The dispersion of the phases changes from a stuck film towards atomization with an increase in flow rate and rotational speed. A higher dispersion of the mobile phase in the stationary phase is associated with an increase in efficiency (N_i) [31]. However, this increase in the contact area, which is also dependent on the interfacial tension between the phases, increases the settling time of the biphasic system. This can cause a loss in stationary phase (column bleeding) and leads to a lower stationary phase retention. In hydrodynamic equilibrium, the residence time of the mobile phase, which can be calculated as volume of the mobile phase inside one CPC cell divided by the mobile phase flow rate ($\frac{V_{MP,cell}}{F}$) and the settling time of the two phases are equal [98]. Therefore, at a certain flow rate the stationary phase retention is higher in larger CPC cells. In this context, an optimal cell would include both a region where atomization takes place for a high mass transfer and a region where coalescence with a good phase separation occurs, in order to achieve a high stationary phase retention [31].

The flow regimes vary between the different cell geometries (i.e. cell shape, size, volume, material), physical properties of the liquid phases (i.e. density difference, viscosity, interfacial tension) and operating conditions (i.e. operating mode, flow rate, rotational speed) [31, 111, 112]. Schwienheer et al. [98] compared the flow regimes of FCPC cells (Z-cells) with different horizontal elliptical twin-cells, one with a broader and the other one with a higher elliptic geometry, and a tailor-made (TU-Dortmund) cell design, which resembles a more tilted Z-cell with a cell inlet and outlet position on the sides of the cell (see also Fig. 12d). In Fig. 12, the flow pattern of mobile phase (black) and stationary phase (white) is visualized in different cell types. It was shown that the stationary phase retention was comparable between the FCPC and the two twin-cell designs. In contrast to these cell designs, the TU-Dortmund chamber showed a higher stationary phase retention, but lower dispersion [98].

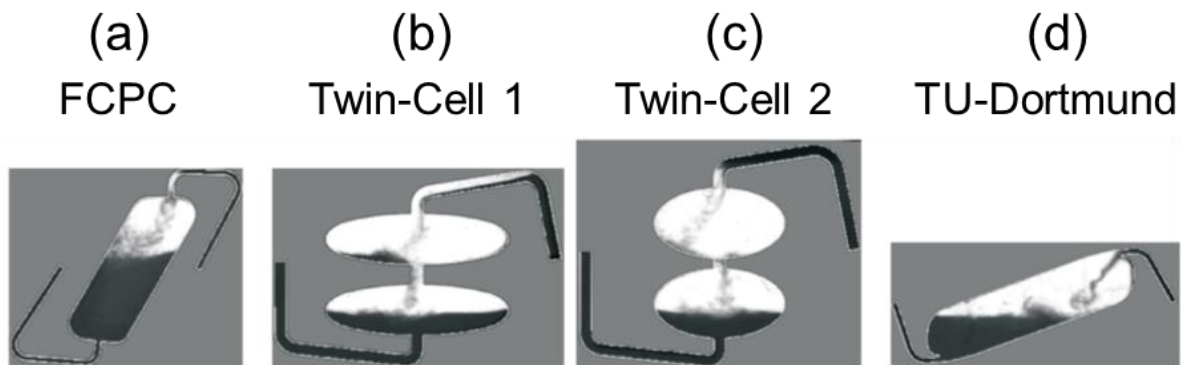


Figure 12: Visualization of the flow regime in different CPC cell designs with black representing the mobile phase and white representing the stationary phase in a (a) modified FCPC cell, (b) Twin-Cell 1, (c) Twin-Cell 2, (d) tailor-made TU-Dortmund cell (adapted from [98]).

2.6. Operating modes

With respect to conventional liquid chromatography, the fact that the stationary phase has a liquid nature in LLC offers opportunities in terms of new operating modes. In LLC, not only the pumping direction of the mobile phase can be switched during the separation run, but also the role of the phases. Hence, the phase being the stationary phase can be used as the mobile phase and vice versa. The switch of the role of the phases can be performed once or several times during the process. This can be used in setups consisting of one or two columns. In this work, operating modes where only one column is necessary are focused. Their operating principles are described in the following paragraphs. A detailed description of alternative operating modes requiring two columns, such as sequential CPC (sCPC) or trapping multiple dual mode (trapping MDM) are presented in [114-129]. A comprehensive overview about batch and continuous operating modes in LLC and the selection of operating parameters for the different modes can be found in [130].

Batch separation mode

The most common separation mode in LLC is the classical batch separation mode or elution mode, involving a pulse injection with a particular injection volume in either ascending or descending mode. In descending mode (Dsc), in CCC also called head-to-tail, the denser lower phase is used as the mobile phase and the lighter upper phase is used as the stationary phase. In ascending mode (Asc), in CCC also called tail-to-head, the role of the phases is reversed [9, 24]. It must be noted that also the value of the partition coefficient of a component i becomes reciprocal in ascending mode ($P_{i,Asc} = P_{i,Dsc}^{-1}$).

In batch separations, a feed composed of a solute mixture dissolved in either mobile phase, stationary phase, or a mixture of stationary and mobile phase is injected via an injection loop. Consequently, the retention volume (or time) of each compound can be calculated according to Eq. 4. Such pulse injections can also be performed in so-called stacked injection mode (Fig. 13), where pulse injections are introduced in regular intervals so that the last peak of the previous injection does not overlap with the target peak of the current injection [28]. This increases productivity, saves operating time, and reduces solvent consumption.

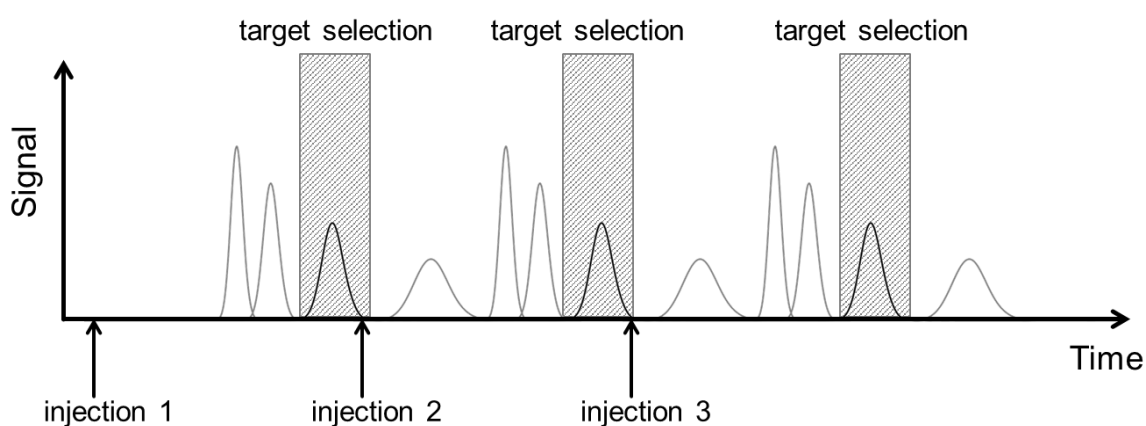


Figure 13: Schematic illustration of three stacked injections with a complete separation between the compounds (adapted from [28]).

Dual mode

In dual mode (DM), the role of the two phases is reversed during the separation run. First, the separation is started in a normal elution mode. Consequently, compounds with high partition coefficients are retained more strongly and move only slowly through the column. In order to quickly elute highly retained compounds from the column, the role and the flow direction of the two phases is changed after a certain time, e.g. by switching from descending to ascending mode or vice versa. Therefore, the value of the partition coefficients becomes reciprocal and compounds with an initially high partition coefficient elute first from the column at the opposite end of the column [131, 132]. Nevertheless, the separation factor remains the same in both modes, ascending and descending. In literature, dual mode is mostly applied to shorten the separation run time, when compounds with very different partition coefficients are present [133, 134]. It must be noted that the switching of the modes can also influence the hydrodynamic equilibrium in the column. This can lead to stationary phase loss. Hence, this needs to be taken into account when selecting the flow rate for the second step. In Fig. 14, the dual mode is schematically illustrated.

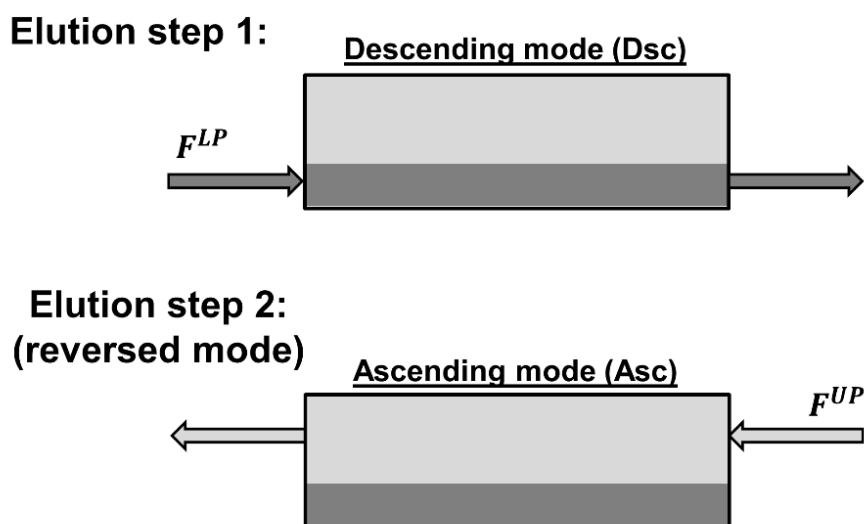


Figure 14: Schematic illustration of the dual mode separation in LLC here starting in descending mode and switching to ascending mode with light grey representing the upper phase and dark grey representing the lower phase of the biphasic solvent system (adapted from [9]).

Furthermore, switching from one mode to the other can be repeated several times during a separation. This is also known as multiple dual mode (MDM) [119, 124-129]. In this sense, MDM is used to improve the peak resolution by “simulating” a longer column (artificial prolongation of the column). The switching time can be selected so that certain compounds can be selectively retained in the column while others elute totally or partially from the opposite ends of the column.

Back-extrusion mode

Two alternative methods to reduce the elution time of highly retained compounds are the so-called back-extrusion mode and the elution-extrusion mode. In the back-extrusion mode, first a classical elution mode is performed, followed by an extrusion step. As illustrated in Fig. 15a, the back-extrusion is realized by changing the pumping direction of the mobile phase. This change of the flow direction causes a rapid collapse of the hydrodynamic equilibrium inside the column. Consequently, no retention of the stationary phase can be achieved any longer and a so-called extrusion step follows. In CCC columns, the phases completely split inside the column, i.e. the lower phase moves to the “tail” end of the column and the upper phase moves to the “head” end [135]. As a result, first the stationary phase elutes from the column on the opposite end of the column (former inlet) including the retained compounds. Then, only mobile phase elutes from the column at the same end of the column including compounds (“echo peak elution”), which were present in the mobile phase at the end of the classical elution mode. During the extrusion, theoretically no mixing and interaction between the phases occurs, neglecting possibly occurring back-mixing between the phases at the phase front during the extrusion. In this sense, no further separation of the compounds takes place and the compounds are eluted according to the concentration profile inside the column as present at the time of the switching. Remarkably, the elution profile of the compounds becomes narrower, since they move closer to the column outlet when stationary and mobile phase split before the extrusion. In the extrusion step, the elution order of the components is reversed, since the pumping direction is switched. Like in dual mode, the compounds with higher partition coefficients elute first from the column at the opposite end of the column [135, 136]. So far, the described mechanisms of back-extrusion mode have only been reported in literature for CCC columns. In CPC columns, a different hydrodynamic phase behavior in the extrusion step might occur, since physical cells that retain the stationary phase are present instead of a tubing in CCC. Therefore, it can be assumed that the phases do not split completely before the extrusion and the mobile phase displaces the stationary phase in each cell successively [130]. Consequently, this might lead to a co-elution of the compounds in a mixture of both phases. Latest after pumping of one entire column volume of mobile phase, all solutes are completely eluted from the column.

Elution-extrusion mode

In elution-extrusion mode, a classical elution mode is followed by an extrusion step. In contrast to the back-extrusion mode, there is no change of the pumping direction. After the first separation step, performed in classical elution mode, stationary phase is pumped instead of mobile phase in the same direction. As illustrated in Fig. 15b, consequently, the hydrodynamic equilibrium in the column collapses. Subsequently, first mobile phase elutes from the column in the so-called sweep elution. Then, stationary phase elutes in the extrusion step [137, 138]. It is worth mentioning that during the gradual displacement of the mobile phase, some compounds still undergo a separation in the part of the column where both phases are present (sweep elution), while others are already overtaken by the stationary phase front (extrusion step). As soon as the stationary phase front has surpassed a certain compound, no further separation occurs and the solute band just moves towards the column outlet. Theoretically, when neglecting dispersive effects during the extrusion step, the compounds elute from the column while maintaining the resolution achieved inside the column [137, 138]. Latest after

pumping of one entire column volume of stationary phase, all solutes are completely eluted from the column. In this context, the elution-extrusion mode extends the suitable range of partition coefficients of the sweet-spot range in LLC, which is recommended for an optimal solute resolution. Thus, Friesen et al. suggested a range of the partition coefficient between 0.25 and 16 [40]. A further benefit of elution-extrusion compared to back-extrusion is the fact that at the end, the column is completely filled with stationary phase. Consequently, the equilibrating of the column for a new separation run by pumping mobile phase can directly start without any re-flushing of the column.

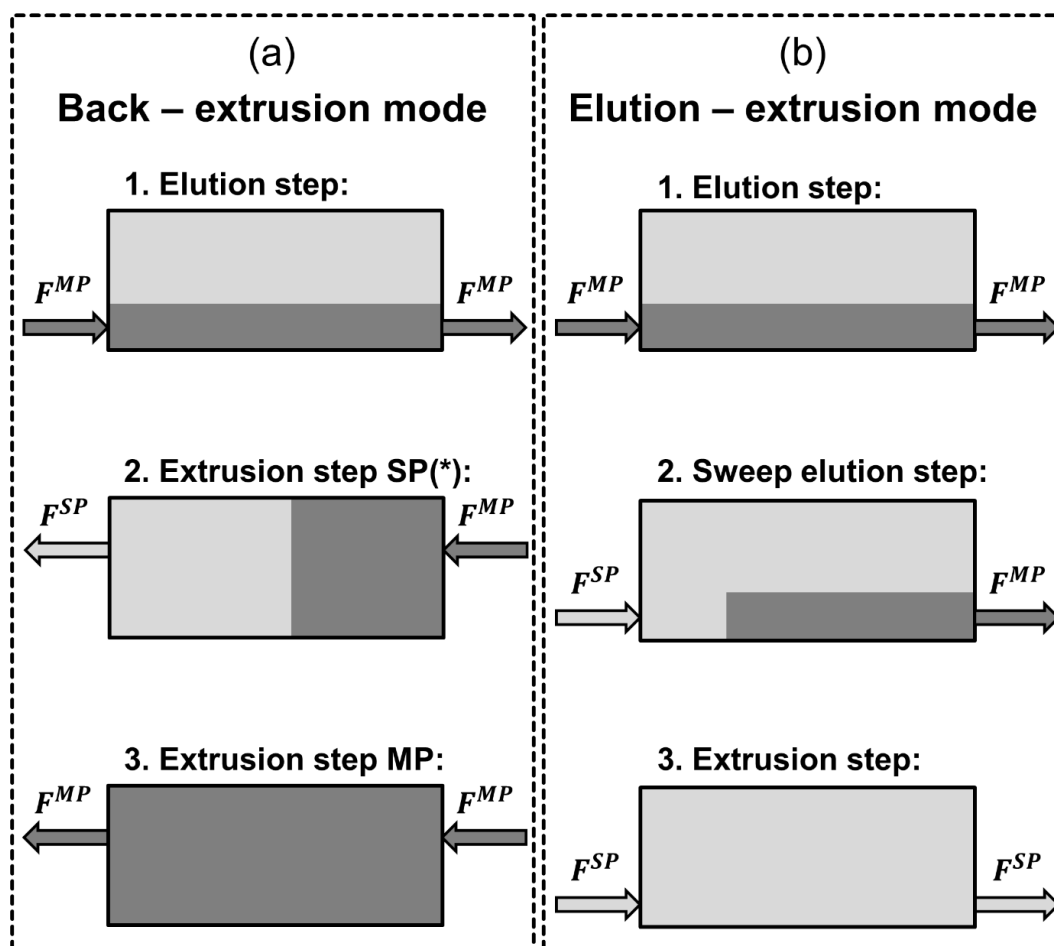


Figure 15: Schematic illustration of (a) the back-extrusion mode and (b) the elution-extrusion mode in LLC indicating the different steps and pumping directions of mobile phase (MP) and stationary phase (SP) (adapted from BECCC [132] and EECCC [137, 138]). (Note: The split of the phases before the extrusion in back-extrusion mode (*) has only been reported for CCC columns.)

2.7. Chromatographic models

2.7.1. Introduction to chromatographic models

Chromatographic separations are dynamic and complex processes, governed by the thermodynamics, hydrodynamics, and mass transfer phenomena. Hence, experimental design and optimization involves many trial-and-error steps, is time and cost intensive, and might not lead to optimal operating parameters [28]. This can be overcome by the use of mathematical models. Chromatographic processes are described with dynamic models, which are based on microscopic material, momentum and energy balances in addition to equations that describe the thermodynamic equilibria of the distribution of the solutes between the two phases. [28, 139, 140]. In literature, various models have been described and are comprehensively summarized in monographs by [139, 141, 142]. Commonly made assumptions in most of the models are that the process is isothermal, the mobile phase density and viscosity are constant, and radial distributions are negligible. Consequently, standard models consist typically of one-dimensional mass balances. The models differ in the assumptions used in the description of the mass transfer of the solute from the bulk mobile phase to the adsorption site in the pores of the stationary phases and the kinetics adsorption itself. They range between the simplest model, the so-called "ideal" equilibrium model to the most detailed models, the so-called general rate models. The "ideal" equilibrium model, assumes permanent local equilibria between the phases and consequently considers only convective mass transport and thermodynamics. Such a model can be useful for a rapid process development with satisfactory accuracy for highly efficient columns ($N \gg 1000$ in LC) [28]. In contrast, the general rate models [28, 139, 143-145] consider all relevant contributions to mass transfer kinetics in the mass balances, such as axial dispersion as a sum of axial and eddy diffusion, external film mass transfer, intra-particle diffusion, surface diffusion and adsorption kinetics [28, 139, 143-145].

Another group of models are the stage models [146, 147]. In these models, the column is considered as a series of connected equilibrium stages, so-called theoretical plates, and equilibrium is assumed in each stage. Instead of formulating dynamic microscopic balances, the column is modeled as a sequence of a finite number N of stages. Two models have been reported. The Martin and Synge plate model [146], also referred to as cell model, assumes a continuous mobile phase flow and the Craig's countercurrent distribution model [147] which considers discrete transfer of the mobile phase from stage to stage, so that the residence time in each stage is sufficient to achieve equilibrium. The Martin and Synge model is actually equivalent to the concept of cascades of stirred tank from reaction engineering. The predicted peak dispersion in both models becomes insignificant for $N > 100$ [148].

2.7.2. Chromatographic models in LLC

For the modelling of LLC separations, up to now only the linear range of the partition equilibria is considered, which is comparable to the linear range of the adsorption isotherm in LC. The slope of the linear range of the partition equilibria is equal to the partition coefficient of the solute infinitively diluted in the biphasic solvents system. Hence, the partition coefficient in LLC is equivalent to the Henry coefficient in LC. In linear chromatography, the thermodynamic influence on the shape of the elution profile can be neglected and attributed to hydrodynamics

and kinetic effects [139]. In addition, for many models such as the stage models, analytical solutions are available in literature.

In recent years, different chromatographic models have been applied to LLC [149]. One of the most widely used models in LLC are the stage models, since they provide fast and accurate results of the residence time distribution of the solutes. Initially, Kostanyan et al. [150, 151] introduced the cell model to LLC and showed a good agreement between simulated and experimental elution profiles. Furthermore, the cell model has been also used to simulate the sequential CPC model [152] and the trapping multiple dual mode [124, 125]. Wei et al. [153] used the cell model to simulate the influence of the temperature on the separation. They added an experimentally determined individual term for the partition coefficient of each solute as a function of the temperature to describe the elution profile when the temperature increases during the separation. It was assumed that the stationary phase retention is not influenced by the change of the temperature. Guzlek et al. [154] used the cell model of Martin and Syngé to calculate the chromatogram in a CCC column. They proposed a correlation for the calculation of the column efficiency N_i based on geometric column characteristics (coil dimensions, β -value, number of coil loops) and operating parameters. In addition, experimental values of the stationary phase retention and the partition coefficients of the solutes are needed calculation of the elution profiles of the solutes. However, in this approach physical properties of the phases are not considered in the calculation of the column efficiency, which is different for different solvent systems and compounds.

The mass transfer kinetics approach of van Deemter et al. [155] and Villermaux et al. [156] has been introduced to LLC by van Buel et al. [157] with an transport-dispersive model, also called “plug flow” model. The model considers axial dispersion and mass transfer with an overall volumetric mass transfer coefficient (k_{0a}). This can be calculated from dimensionless model parameters that need to be fitted to experimental effluent concentration profiles at different flow rates (and rotational speeds). In addition, the partition coefficient of the solutes are needed, which can also be calculated from the elution profiles. Furthermore, off-column volume (connecting tubes and channels) can be considered by adding an additional term assuming a plug flow with only axial dispersion [31]. This model was also used to study the influence of flow regimes on the mass transfer in CPC columns [31], i.e. the correlation between the different flow regimes and the mass transfer coefficient. Chollet et al. [158] used this methodology to calculate and design the optimal volume of CPC columns as a series of cells in order to make tailor-made columns for particular applications. He derived a correlation for the calculation of the overall mass transfer coefficient with respect to the dimensionless Sherwood number. Based on experimental data at different operating conditions, several dimensionless numbers are determined by fitting the data to evaluate the flow regime and to calculate the Sherwood number, which describes the ratio of convective and diffusive mass transfer.

Schwienheer et al. [159] modified the mass transfer dispersion model of van Buel et al. to account for the effect of dead zones in the cells. As van Buel et al. [157], an overall mass transfer coefficient was assumed and the channels were considered as tubes only filled with mobile phase contributing to axial dispersion. An important difference is that the column is considered as a number of physical cells. There the amount of stationary phase is split into two zones, a certain portion of the stationary phase volume that actively participates in the separation, i.e. mass transfer with the mobile phase, and another portion that is considered as a dead zone but with a constant volume exchange with the “active” part of the stationary phase.

An example of a statistical model has been implemented by Folter et al. [160] based on a probability mass function as the so-called Probabilistic model for immiscible separations and extractions (ProMISE). In comparison to the models mentioned above, the column is subdivided in probabilistic units and no discrete stages. Here, an injected sample compound is split in many small portions, which are represented by so-called compound units. Based on a probability mass function, derived from the Bayes' theorem, the probability of solute location in one phase and the relative movement to the other phase is predicted. In addition, the partition coefficient, stationary phase retention, and the rotational speed are considered as input parameters. A density function including a Gaussian filter is used to create a chromatogram resulting from output data of the compound units. It was shown that the model predicts the elution profile accurately with little deviations in the peak shape.

All implemented models predicted the retention time sufficiently well and, to a certain extent, the peak broadening of a solute eluting from an LLC column. In this context, the fact that the stationary phase is liquid simplified the models in comparison to LC in terms of the number of involved mass transfer steps, i.e. absence of a mass transfer in the pores of solid particles. Nevertheless, this fact makes the models more complex in comparison to the presence of a solid stationary phase, since a change in the mass transfer area between the phases as a function of operating conditions needs to be considered.

In this thesis, the cell model of Martin and Synge is used [146] and referred to as "cell model". In the following, the model is explained in more detail. As illustrated in Fig. 16, the column is regarded as a series of connected cells, i.e. theoretical plates. It should be noted that in CPC, the number of theoretical plates N is not equal to the number of physical cells in the column. N_i can be determined according to Eq. 14 from the elution profile of a pulse injection performed with a very small injection volume (often $V_{inj} < 1\% V_C$).

The following assumptions are made:

1. The volume of the liquid stationary and mobile phase is constant and the same in each cell for a particular flow rate and centrifugal field.
2. The mixing and equilibration of the phases in each cell occurs instantaneously (ideal mixing).
3. The solute retention is only based on partitioning between the two liquid phases and no sorption mechanisms are present.
4. The partition coefficients of the compounds are constant and independent of the solute concentration or the presence of other solutes in the mixture.
5. The number of theoretical plates is solute dependent, but constant and independent of the solute concentration and injection volume.

The mass balance of a compound i can be described by Eq. 29 [150].

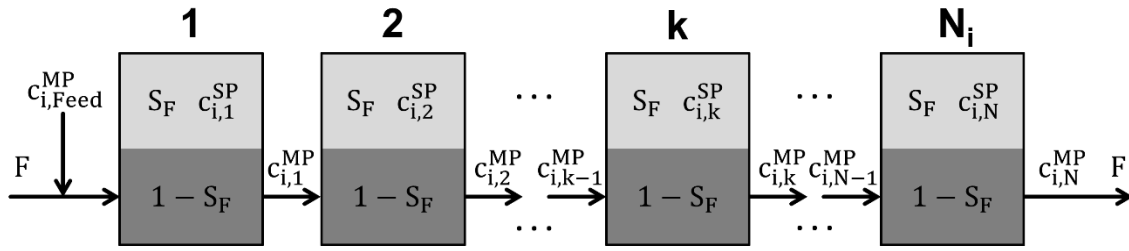


Figure 16: Schematic illustration of the cell model with N_i ideally mixed cells (adapted from [150]).

$$\frac{V_C(1-S_F)}{N_i} \frac{dc_{i,k}^{MP}}{dt} + \frac{V_C S_F}{N_i} \frac{dc_{i,k}^{SP}}{dt} = F (c_{i,k-1}^{MP} - c_{i,k}^{MP}) \quad (\text{Equation 29})$$

Here, cell $k = 1, 2, \dots, N_i$ refers to the number of the cell, S_F is the stationary phase retention, V_C is the total column volume, $c_{i,k}^{MP}$ is the concentration of compound i in the mobile phase in cell k , $c_{i,k}^{SP}$ is the concentration of compound i in the stationary phase of cell k , and F is the total mobile phase flow rate. The concentration of compound i in the stationary phase is calculated from its concentration in the mobile phase at each stage (Eq. 30):

$$c_{i,k}^{SP} = P_i \cdot c_{i,k}^{MP} \quad (\text{Equation 30})$$

For the simulation of a pulse injection in batch mode, e.g. in descending mode, the mass balance equation of the cell model (Eq. 29) should be solved using the following initial and boundary conditions.

Initial conditions ($t = 0$):

$$c_{i,1}^{MP} = c_{i,2}^{MP} = \dots = c_{i,N}^{MP} = 0 \quad (\text{Equation 31})$$

Boundary conditions at the column inlet (first cell):

$$c_{i,1}^{MP}(t) = \begin{cases} c_{i,feed}^{MP}, & t \leq t_{inj} \\ 0, & t > t_{inj} \end{cases} \quad (\text{Equation 32})$$

2.8. Separation method development in LLC

2.8.1. Current challenges in separation method development

In LLC separation method development, many different factors have to be considered. Therefore, process requirements such as production volumes, product purities, and solvent requirements should be clarified in advance in order to narrow the number of possibilities. When developing a separation method, the most important task is the selection of a suitable biphasic solvent system, but also an appropriate column type and design, and corresponding operating parameters need to be chosen. Often, the separation method development is reduced to the selection of a biphasic solvent system, where the partition coefficient of the target compound is in the *sweet spot range*, i.e. $0.4 < P_1 < 2.5$. However, the selected biphasic solvent system should also possess a good stationary phase retention in the desired column, which is in general beneficial for a good separation. This is important especially if the method needs to be scaled-up or transferred to another column after the development at lab-scale. This prevents the method from having to be laboriously altered or completely redeveloped on another column.

After selecting a biphasic solvent system with the target compound in or close to the *sweet spot range* and where the separation factor α between the target compound and major impurities is preferably greater than 1.5, operating modes and conditions need to be evaluated and selected. Here, Dsc or Asc, batch vs. (quasi-) continuous modes, and column load strategies need to be optimized. In this context, the design criteria may be different when the method is developed for the characterization or analysis of a complex matrix, or for the isolation of a single target compound at preparative scale for production purposes. In both cases, a model-based method development can be applied, e.g. by making use of the cell model (Section 2.7.2), to save time and costs for process optimization [117, 130].

2.8.2. Separation method transfer and scale-up in LLC

Separation methods are mostly developed and optimized using lab-scale columns with a volume between 10 ml and 300 ml. For various reasons, the methods often need to be transferred to another column of different size and/or design, e.g. due to a transfer to production scale. Another common scenario is that different labs with varying equipment want to exchange the developed methods or establish an application from literature in their own lab. As commonly known and shown in Fig. 2, a good separation performance is related to a high stationary phase retention [9]. This is probably the reason why the separation method transfer in LLC is commonly done by adjusting operating parameters, i.e. rotational speed and flow rate, in order to keep the stationary phase retention in both columns the same ($S_{F,1} = S_{F,2}$). Then, mostly linear scale-up factors (SUF) are used for calculating the injection volume or mass load, e.g. the ratio of column volumes in CPC and CCC, or coil lengths in CCC columns [120, 161-164]. Wood et al. [162] showed that a similar peak resolution can be achieved in CCC when applying a “volumetric SUF”. There, the ratio of the column volumes of column 1 and column 2 is set equal to the ratio of the mobile phase flow rates (Eq. 33).

$$\text{Volumetric SUF} = \frac{V_{C2}}{V_{C1}} = \frac{F_2}{F_1} \quad (\text{Equation 33})$$

where V_C is the total column volume and F is the mobile phase flow rate.

In addition, the introduced sample volume is scaled-up according to the same volumetric factor. However, this includes some assumptions. The column length and the rotor radius including the same rotating angle are kept constant, while the inner coil diameter is adjusted in order to create the same centrifugal field and to operate at a similar flow regime during the separation [162].

Later, das Neves Costa et al. [163] proposed two other linear scale-up factors in CCC:

- the “cross-sectional area SUF” for columns with different lengths and inner coil diameters (Eq. 34).

$$\text{Cross – sectional area SUF} = \frac{A_2}{A_1} \quad (\text{Equation 34})$$

- the “column length SUF” for columns of different column length but same inner coil diameter (Eq. 35).

$$\text{Length SUF} = \frac{L_2}{L_1} \quad (\text{Equation 35})$$

Here, A is the cross-sectional coil area and L is the total column (coil) length.

Although linear SUFs have often been used as a fast and relatively satisfactory strategy in CCC, this is not a generally valid separation method transfer approach for both CCC and CPC. Hence, such linear scale-up rules might lead to good results only in columns with similar length. As discussed in Section 2.3.1, LLC columns differ in size and design (i.e. different coils and cell geometries), and are used at different operating conditions. As a result, different flow regimes occur, and the columns may behave differently as a function of flow rate and rotational speed (g-field) [47, 98, 165-167]. Differences in stationary phase retention and column efficiency have a clear influence on the separation resolution and process performance, including product purity, recovery, achievable productivity, and solvent consumption [31, 98, 111, 112, 168-170]. Hence, a reliable and universal approach for the separation method transfer between columns independent of their size and type is needed.

An alternative strategy for the separation method transfer between CCC and CPC columns is the approach of constant mobile phase velocity, commonly used in conventional liquid chromatography. In this approach, the same mobile phase linear velocity is used in both columns when transferring the separation method between columns of the same height and packed with the same solid stationary phase [164]. However, the applicability of this approach to LLC is difficult, since the cross-sectional area of the CPC cells is not constant and changes inside the cell due to e.g. asymmetric cell geometries. In addition, the stationary phase retention (equivalent to column porosity in LC) and the mass transfer area change with both column design and operating conditions. In this context, the linear velocity of the mobile phase in CCC (u_{CCC}) is calculated according to Eq. 36 [164]. In terms of CPC, an equivalent to the inner cross section has been introduced, the so-called average cross section (\overline{CS}) (Eq. 37). Then, an average mobile phase velocity (u_{CPC}) can be calculated also with respect to CPC (Eq. 38) [164].

$$u_{CCC} = \frac{4F}{\pi d^2(1-S_F)} \quad (\text{Equation 36})$$

$$\overline{CS} = \frac{V_{cell}}{h_{cell}} \quad (\text{Equation 37})$$

$$u_{\text{CPC}} = \frac{F}{\overline{CS}(1-S_F)} \quad (\text{Equation 38})$$

Here, F is the mobile phase flow rate, S_F is the stationary phase retention, d is the inner CCC coil diameter, V_{cell} is the CPC cell volume, and h_{cell} is the CPC cell height.

This approach enabled an inter-apparatus transfer from a small lab-scale CCC to a semi-preparative CPC column with small cell volumes. However, it was demonstrated that an average theoretical cross-sectional area \overline{CS} does not give satisfactory results when cells clearly differ in design and/or size [164]. Consequently, this approach cannot be applied as a general strategy for LLC separation method transfer.

Another separation method transfer approach between different CPC columns is the model-based methodology for optimizing a CPC column size for a particular separation, introduced by Chollet et al. [158]. Varying hydrodynamics and mass transfer efficiency in different columns are considered, enabling the calculation of an optimal column volume defined by the number of discs and corresponding number of cells. This approach uses a transport-dispersive model (see Section 2.7.2.) for the design of an optimal tailor-made column size for a particular application. In this context, preliminary tests for the determination of the model parameters and experience in modelling are required. Several dimensionless numbers need to be determined by fitting experimental data. As input parameters for the model, physical properties of the biphasic solvent system (i.e. densities, viscosities), partition coefficients of the solutes, cell design and operating conditions must be known in order to predict a chromatogram. Then, the column length can be adjusted in order to fulfil the desired requirements in terms of separation resolution [158]. However, commercial columns are usually standardized and have a fixed size. Consequently, this approach is not suitable as a routine for separation method transfer in standardized and non-adjustable columns.

Bouju et al. [171] proposed the “free-space between the peaks” method for the intra-apparatus method transfer between differently sized CPC columns with same cell geometry. With this strategy, a separation method developed at lab-scale can be easily transferred to large-scale columns using the relation of the space between the peaks determined by pulse injections on the two columns. In this context, a separation method is developed and optimized on a lab-scale column, e.g. by increasing the injection volume, so that a baseline separation ($R_S = 1.5$) is achieved. Then, one pulse injection is performed on a second column within a suitable operating range. Subsequently, the difference in elution volume (ΔV) between the end of the first elution and the start of the second eluting compound, also called “free-space between peak”, is determined based on the pulse injections for the two columns, respectively. The ratio of these different space between the peaks volumes of the two columns represents the scale-up factor (F_{SU}). As illustrated in Fig.17, the sample load on the second column can then simply be calculated by multiplying the maximum injection volume of column 1 ($V_{\text{inj-max,C1}}$) with this scale-up factor. This strategy represents a rather easy and quick method to transfer a separation method previously maximized in sample load from lab-scale to semi-preparative or preparative-scale. However, this method assumes in advance that the transfer of the separation method between the two columns is possible. In addition, this approach does not consider the selection of operating parameters. Hence, this approach cannot be directly applied when a lower separation resolution occurs on the column to which the method is intended to be transferred.

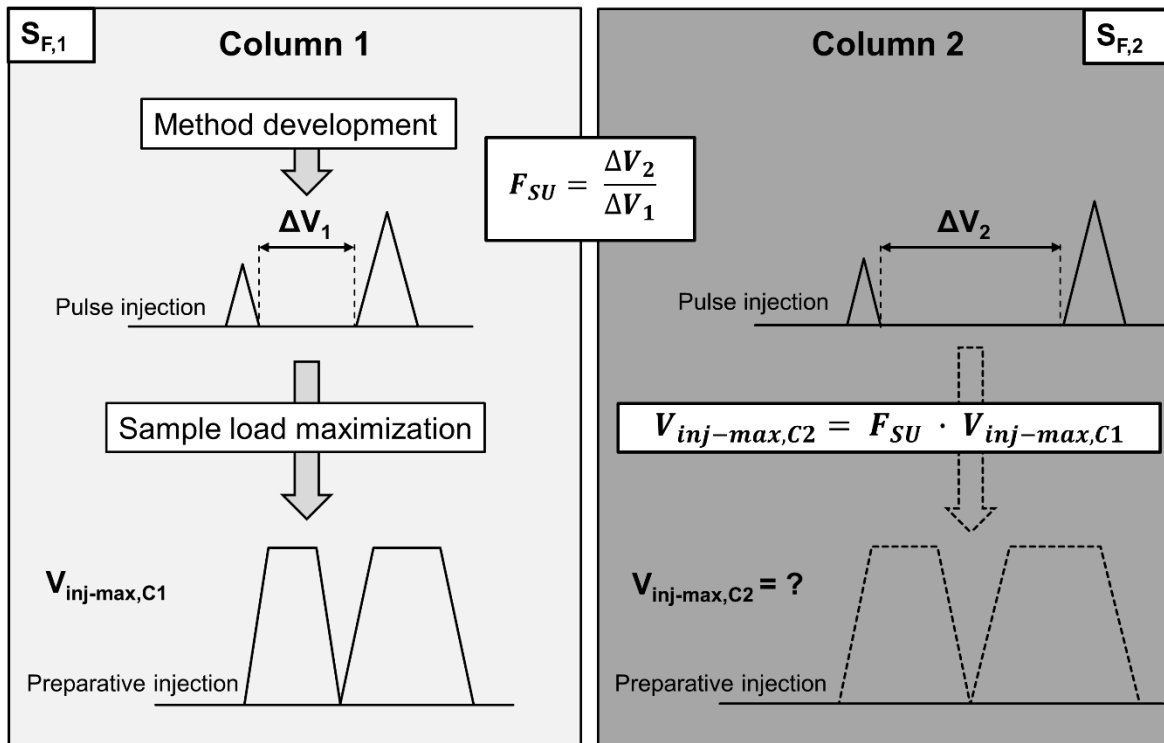


Figure 17: Illustration of the “free-space between the peak” method for scaling-up a sample load maximized separation method to another column of different size and design (adapted from [171]).

3. Results

3.1. Paper I: Characterization of a centrifugal partition chromatographic column with spherical cell design

3.1.1. Summary

Citation

S. Roehrer, M. Minceva, (2019). Characterization of a centrifugal partition chromatographic column with spherical cell design. *Chemical Engineering Research and Design*, 143, 180-189
<https://doi.org/10.1016/j.cherd.2019.01.011>

Summary

The development of new columns and cell designs is one of the most innovative fields in centrifugal partition chromatography. In conventional CPC columns the cells are connected by ducts. Depending on the column type, the ducts occupy a different proportion of the total column volume, which manifests as “dead” volume in the column. Thus, the duct volume is not involved in the separation, but contributes to peak dispersion and pressure drop. The objective of this work was to systematically characterize a prototype of a new semi-preparative column with spherical cell design and negligible interconnecting duct volume. The investigated new column with a special monobloc design can be operated at a higher maximal pressure drop (200 bar instead of 100 bar in conventional CPC) and rotational speed (4000 rpm instead of 3000 rpm in conventional CPC). In the study, the cell volume of the new spherical cells (1.23 ml) is larger than that of a conventional CPC twin-cells (0.1 ml) and is similar to twin-cells of centrifugal partition extractors (CPE, 0.93 ml). All three columns have the same total column volume. Hence, they differ in the number of physical cells (CPC: 1800 twin-cells, CPE: 240 twin-cells, CPE spherical cells: 196 spherical cells). The separation performance of the prototype was systematically characterized in terms of stationary phase retention, column efficiency, and separation resolution. In this sense, pulse injections performed at different flow rates and rotational speeds, were compared with a conventional CPC and CPE column. Subsequently, it was shown that the new cell design leads to a much higher stationary phase retention and can be operated at much higher flow rates in comparison to conventional CPC columns with twin-cells. Even though the single cell efficiency of the new spherical cells was highest, its total column efficiency was similar to the CPE column and much lower than of the CPC column. This was due to the different numbers of cells in each column. Thus, the separation resolution achieved with the new spherical cells column was only slightly better than in the CPE, while being much lower in comparison with CPC. An extensive simulation study was used to further compare the columns in terms of achievable productivity and solvent consumption at maximized injection volume and baseline separation. In addition, it was evaluated for which separation factor range the different columns are more favorable. Finally, it could be concluded that columns with larger cells are beneficial for preparative separations where higher separations factors or lower purity requirements are present. However, in the case of more challenging separations (separation factor $\alpha < 2.5$), columns with higher numbers of small cells are crucial in order to enable a sufficient separation.

Contributions

The author of this dissertation had a leading role in this work. The author did the conceptual design of the work and performed all experiments as well as the simulations. The author selected the system compositions, model substances, and operating parameters for the CPC separations. The author wrote the manuscript and discussed the results with M. Minceva.



Contents lists available at ScienceDirect

Chemical Engineering Research and Design

journal homepage: www.elsevier.com/locate/cherdiChemE
ADVANCING
CHEMICAL
ENGINEERING
WORLDWIDE

Characterization of a centrifugal partition chromatographic column with spherical cell design



Simon Roehrer, Mirjana Minceva*

Biothermodynamics, TUM School of Life Sciences Weihenstephan, Technische Universität München, Maximus-von-Imhof-Forum 2, Freising, D-85354, Germany

ARTICLE INFO

Article history:

Received 21 June 2018

Received in revised form 29

November 2018

Accepted 8 January 2019

Available online 16 January 2019

Keywords:

Centrifugal partition

chromatography

Cell design

Spherical cells

Stationary phase retention

Column efficiency

Productivity

ABSTRACT

A new centrifugal partition chromatography (CPC) column with spherical cells, insignificant duct (channel) volume, and without PTFE plates between the disks was evaluated. Due to the reduced duct volume, almost the entire column volume is available for the separation. This allows operation at higher pressure drop and thus increased rotational speed and flow rates. The new column was characterized in terms of stationary phase retention, column efficiency and resolution as a function of flow rate and rotational speed. The separation performance was compared to that of two conventional twin-cell CPC columns of the same total volume. The new column leads to an increased productivity especially at higher flow rates and outperforms columns with smaller cells in terms of higher separation factors and reduced purity or recovery requirements.

© 2019 Institution of Chemical Engineers. Published by Elsevier B.V. All rights reserved.

1. Introduction

In solid support-free liquid–liquid chromatography, a multi-solvent biphasic liquid system is used to separate a mixture of compounds based on the difference in the partitioning between the two liquid phases. One of the two phases is kept stationary with the help of a centrifugal field, while the other phase is pumped through the column (Foucault, 1995). The separation can be performed by using two main types of liquid–liquid chromatographic columns: hydrodynamic and hydrostatic columns. Hydrodynamic columns, better known as countercurrent chromatography (CCC) columns, consist of tubing that is wound on a bobbin that rotates around its own axis and revolves around the axis of a centrifuge. In contrast, hydrostatic columns, also called centrifugal partition chromatography (CPC) columns, have only one axis of rotation (Foucault, 1995; Berthod, 2002; Berthod and Faure, 2015). A conventional CPC column consists of several identical annular disks that are connected in series, with PTFE plates in between acting as seals. This modular construction allows for flexible selection of the column length (Foucault, 1995; Berthod, 2002;

Berthod and Faure, 2015). In each annular disk a certain number of cells interconnected by narrow short channels, referred to as ducts, are engraved circumferentially. During a separation, the ducts are filled with mobile phase only and therefore behave as dead volume that does not contribute to the separation and consequently reduces the effective column volume. In addition, this dead volume leads to a broadening of the peaks which decreases the column efficiency (Schwienheer et al., 2015).

In CPC, the column efficiency and separation resolution are dependent on the partition coefficients of the solutes, the amount of stationary phase in the column and its distribution in the cells. The stationary phase retention and the contact area between the two phases are influenced by several factors, including the physical properties of the two liquid phases, cell geometry, mobile phase flow rate and rotational speed (Foucault, 1995; Adelmann and Schembecker, 2011; Marchal et al., 2000; Foucault et al., 1994; Van Buel et al., 1998; Foucault et al., 1992).

In the history of solid support-free liquid–liquid chromatography, a wide variety of biphasic solvent systems has been established

* Corresponding author.

E-mail address: mirjana.minceva@tum.de (M. Minceva).<https://doi.org/10.1016/j.cherd.2019.01.011>

0263-8762/© 2019 Institution of Chemical Engineers. Published by Elsevier B.V. All rights reserved.

(Foucault, 1995; Berthod, 2002; Berthod and Faure, 2015; Skalicka-Woźniak and Garrard, 2015). Each system has different physical properties and not all of them can be applied in CPC at high flow rates due to pressure drop limitations or low stationary phase retention. This is relevant especially for preparative applications. Therefore, there is a strong need for the development of new cell designs, especially for unstable biphasic systems but also for very stable systems that could not be used in CPC columns due to low stationary phase retention or pressure limitations at high flow rates (Adelmann and Schembecker, 2011). Thus, besides the development of new biphasic systems and operating modes, one of the most innovative fields has been the design of different cell geometries for CPC columns. Murayama et al. developed the first cell design in 1982 (Murayama et al., 1982), which had the form of interconnected column cartridges mounted on a rotor of a centrifuge. Subsequently, other cell designs optimized in terms of flow patterns were developed in order to enhance mass transfer between the phases and improve stationary phase retention: FCPC[®]-chambers (de La Poype et al., 2003), also known as Radial Cells, consisting of interconnected cells of quadrangular shape. Z-cells, where the cells are slightly tilted. Twin-cells (Foucault et al., 2008; Couillard, 2010) and asymmetric twin-cells (Foucault et al., 2010), where circular or elliptical cells are paired two by two in series, so that cell pairs are in direct contact. Neighboring cell pairs are connected by ducts. An alternative cell design is that of interconnected cylindrically-shaped RotaChrom[®]-cells (Lorantfy et al., 2015; Lórántfy and Németh, 2016) with packing material for flow distribution and mounted on a centrifugal plate. Another column design is the so-called spiral disk CCC assembly, where multiple disks are interconnected in series and stacked together to form one column. The disks consist of inert plastic plates with spiral grooves and rotate around one axis of rotation (Ito et al., 2013).

Currently the cell design of commercial CPC is mostly based on the twin-cell geometry patented by Foucault et al. (2008). Goll et al. (2015) showed a higher stationary phase retention in the centrifugal partition extractor (CPE), which has bigger but a lower number of cells per column volume. He observed no significant change of the separation resolution with increasing flow rate in the studied range. The CPE column could be operated at higher flow rates compared to the CPC. Hence, a higher productivity could be achieved. Nevertheless, it was shown that the CPE column is appropriate for less stable biphasic systems, such as aqueous two-phase systems. Schwieneher et al. (2015) compared twin-cells with different elliptical shape, a FCPC[®]-chamber and a more tilted modified FCPC[®]-chamber with different inlet and outlet position of the cell. Higher stationary phase retention was achieved for twin-cells as a function of flow rate.

In this work, a column with a new cell design is characterized in terms of stationary phase retention, column efficiency and resolution as a function of flow rate and rotational speed. The column is in the form of a monobloc that contains a series of spherical cells that are connected with small ducts. Consequently, duct volume is significantly reduced, leading to higher effective column volume per total column volume. Since no sealing PTFE plates are needed due to the monobloc design, the column can be operated at a pressure drop of up to 200 bar, which allows using higher mobile phase flow rates. Mandova et al. (2017) evaluated the column for the purification of swertiamarin and pointed out its high potential for industrial scale applications.

The separation performance of the new column with spherical cells was compared to two conventional columns with twin-cell design. All three columns have the same total column volume, but differ in cell size, cell geometry and total number of cells. The experiments were performed with a model mixture of hydroquinone and pyrocatechol and one of the most commonly used biphasic systems in solid support-free liquid-liquid chromatography (heptane/ethyl acetate/methanol/water). Besides the experimental study, an extensive simulation study was carried out in order to identify the application range of the new column.

2. Materials and methods

2.1. Materials

2.1.1. Chemicals

The solvents heptane, ethyl acetate and methanol of the biphasic system were all of analytical grade (EMSURE, purity 99%) from Merck KGaA (Darmstadt, Germany). Deionized water was used from the existing house supply. Pyrocatechol and hydroquinone with a purity of $\geq 99\%$ were purchased from Sigma-Aldrich, USA.

2.1.2. Equipment

Experiments were performed with two CPC columns, both with a total column volume of 250 ml, from Gilson Purifications SAS (formerly Armen Instruments, France):

- CPC 250 PRO SC prototype column with spherical cells, in the following text referred to as a CPE spherical cells column.
- CPC 250 PRO SPECIAL BIO VERSION column with twin cells, in the following text referred to as a CPE column.

The prototype of the CPE spherical cells column has a monobloc design made of stainless steel and contains 196 cells in total. The cells are connected to each other with small ducts with a total volume of only 5 ml. Due to the different column design, no sealing PTFE plates between the column disks are necessary, allowing an operation of the column with a maximal pressure drop of 200 bar and a rotational speed of 4000 rpm (2450 g). A detailed description of the design and production process can be found in the corresponding patent (Couillard, 2009).

The CPE column has 12 disks, where each disk contains 20 engraved twin-cells; in total 240 cells. The disks are made of stainless steel and are additionally coated with PTFE for applications with biomolecules. The disks are sealed by PTFE plates. The column can be operated at a pressure drop of up to 100 bar and a maximal rotational speed of 3000 rpm.



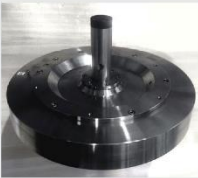
As a result from the different diameters of the disks, with a bigger diameter of the CPE spherical cells compared to the CPE, the achievable relative centrifugal acceleration, i.e. g-force (for the definition, see Section 3.3), at the same rotational speed is higher in the CPE spherical cells than in the CPE.

Both columns (CPE spherical cells and CPE) were connected to an isocratic preparative HPLC pump (PrepStar 218 Solvent Delivery Module, Varian, USA), which could deliver flow rates of up to 200 ml min⁻¹. The effluent was monitored with a UV-vis detector (ProStar 325 UV-vis Detector, Varian, USA) and a SUPER PREP 4 × 0.15 mm detector cell at a wavelength of 280 nm for pyrocatechol and hydroquinone. The sample was introduced through a six port manual injection valve. An injection loop of 1 ml was used.

In this work, the separation performances of the two columns were compared with the SCPC 250 column from Armen Instrument, described by Hopmann et al. (2012). The relevant data regarding the characterization of the SCPC 250 are taken from Goll et al. (2015). For the sake of clarity, in the following text the SCPC 250 column is referred to as a CPC column. The specifications of the column geometry and range of operating parameters of all three columns are summarized in Table 1.

Table 1 – Specifications of SCPC-250 (Armen Instrument, Saint-Avé, France), CPC 250 PRO SPECIAL BIO VERSION and CPC 250 PRO SC PROTOTYPE (Gilson Purification, Saint-Avé, France).

Parameter	SCPC 250 (CPC)	CPC 250 PRO SPECIAL BIO VERSION (CPE)	CPC 250 PRO SC prototype (CPE spherical cells)
Total column volume/ml	250 (247) ^a	250 (244) ^a	250 (244) ^a
Total cell volume/ml	181.8	211.4	244.0
Total connecting duct volume/ml	68.2	38.6	5.2
Number of disks/-	20	12	Monobloc design with 2 sets of cells
Number of twin cells per disk/-	90	20	98 cells per set
Total number of twin cells/-	1800	240	196
Average column radius R/m	0.07	0.07	0.137
Volume of one twin cell without ducts/ml	0.10	0.96	1.23
Material	Stainless steel	PTFE coating (bio compatible)	Stainless steel
Rotational speed/rpm	3000	3000	4000
RCF/g	715	715	2450
Maximal pressure drop/bar	100	100	200

^a Experimentally determined total column volume.

2.2. Methods

2.2.1. Preparation of the biphasic liquid systems

The biphasic liquid system heptane/ethyl acetate/methanol/water 1/2/1/2 (v/v/v/v), ARIZONA K, was prepared by mixing the corresponding volume portions of the solvents. The mixture was vigorously shaken and equilibrated for at least two hours. For the experiments the phases were split and placed in two separate containers. Feed solutions were prepared by adding certain amounts of the solutes pyrocatechol and hydroquinone to the mobile phase used for the pulse injections, upper phase in ascending mode or lower phase in descending mode. A sample concentration of 5 mg ml^{-1} of each component dissolved in mobile phase was used for the pulse injection experiments.

2.2.2. Measurement of stationary phase retention

The stationary phase retention in the CPE spherical cells and CPE column was measured in ascending and descending mode. With the CPE spherical cells, the mobile phase flow rate was varied between 20 and 80 ml min^{-1} and the rotational speed was set at 2000 rpm. In CPE, the mobile phase flow rate was varied between 12 and 80 ml min^{-1} and the rotational speed was set at 1700 rpm. In addition, the influence of the rotational speed on the stationary phase retention was studied in CPE spherical cells at a constant flow rate of 60 ml min^{-1} . The rotational speed was varied between 1000 and 4000 rpm.

For all measurements, the columns were first filled with the intended stationary phase without rotation. After that, the rotational speed was set to the desired value. Mobile phase was then pumped through the column at the desired flow rate until stationary phase was no longer observed at the column outlet, at least for one column volume. Subsequently, the remaining stationary phase inside the column at hydrodynamic equilibrium was determined by displacing it by pumping mobile phase in the other mode (changing from ascending mode to descending mode or vice versa). The

stationary phase retention was calculated by dividing the displaced stationary phase volume by the total column volume. For each flow rate, a new experiment was performed following the procedure described before. The experiments are carried out only once due to a good reproducibility with a standard deviation below 5%, determined with a similar solvent system Arizona N (heptane/ethyl acetate/methanol/water 1/1/1/1 v/v/v/v).

2.2.3. Pulse injection experiments

Pulse injections of pyrocatechol and hydroquinone were performed with the CPE spherical cells and CPE with the heptane/ethyl acetate/methanol/water system 1/2/1/2 (v/v/v/v), in ascending and descending mode. With the CPE spherical cells, the mobile phase flow rate was varied between 20 and 80 ml min^{-1} and the rotational speed was set at 2000 rpm. In CPE, the mobile phase flow rate was varied between 12 and 80 ml min^{-1} and the rotational speed was set at 1700 rpm. The sample mixture, 5 mg ml^{-1} of each compound dissolved in the mobile phase, was injected via a 1 ml sample loop with the manual injection valve. Before injecting the sample, the columns were filled completely with stationary phase and mobile phase was pumped at the selected mobile phase flow rate until hydrodynamic equilibrium was reached.

2.2.4. Simulations

Simulation of the pulse injections for the theoretical feasibility study in Section 3.4 was completed by numerical solution of the equilibrium cell model equations using gPROMS Model Builder v4.2 software from Process Systems Enterprise (London, UK). The assumptions and equations of the equilibrium cell model (Martin and Synge, 1941), also known as the plate model, were already implemented in previous work (Völkl et al., 2013; Hopmann and Minceva, 2012; Goll et al., 2013).

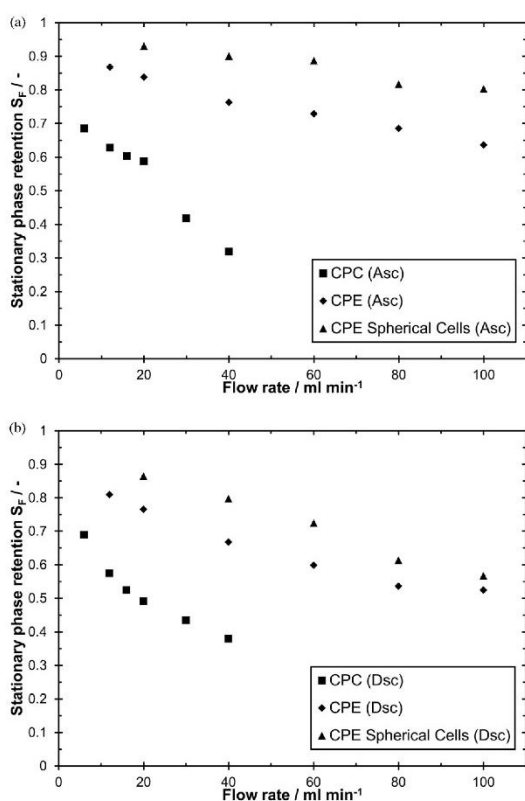


Fig. 1 – Stationary phase retention at different mobile phase flow rates for the solvent system heptane/ethyl acetate/methanol/water 1/2/1/2 (v/v/v/v) at a rotational speed of 1700 rpm in CPC and CPE, and 2000 rpm in CPE spherical cells in: (a) ascending mode (Asc) and (b) descending mode (Dsc).

3. Results and discussion

3.1. Stationary phase retention

The stationary phase retention (S_F) is the fraction of the column volume occupied by the stationary phase:

$$S_F = \frac{V_{SP}}{V_C} \quad (1)$$

where V_{SP} is the volume of the stationary phase and V_C is the volume of the column.

In Fig. 1a and b the stationary phase retention as a function of the mobile phase flow rate obtained with the CPE spherical cells column (2000 rpm, 613 g) and CPE (1700 rpm, 230 g) is presented and compared to the stationary phase retention of the CPC (1700 rpm, 230 g) column determined by Goll et al. (2015) for the system heptane/ethyl acetate/methanol/water 1/2/1/2 (v/v/v/v), Arizona K, in ascending mode (upper phase as mobile phase) and descending mode (lower phase as mobile phase). The rotational speed of 1700 rpm in CPC was selected in order to achieve a compromise between the mobile phase flow rate and pressure drop limitations of the column. In CPE, the same rotational speed was selected to compare the results at the same relative centrifugal acceleration. The radius of 0.137 m in the CPE spherical cells column is bigger than the radius of in the CPC and CPE column. For the purpose of approximately the same relative centrifugal acceleration of 230 g as in the CPC

and CPE column, a rotational speed of 1225 rpm would have had to be selected in CPE spherical cells. This is a suboptimal for such a column in terms of S_F and phase distribution (i.e. column efficiency), as shown later in Section 3.3 with different selected rotational speeds. Hence, a slightly higher rotational speed of 2000 rpm was selected in CPE spherical cells.

In both ascending and descending mode, the stationary phase retention decreases linearly with the increasing flow rate within the studied flow rate range for the three different columns. This was expected based on similar studies from literature. Foucault et al. (1992), Adelmann and Schembecker, (2011), Adelmann et al. (2013), Kotland et al. (2015), Schwienheer et al. (2015) and Fumat et al. (2016) observed a linear decrease of stationary phase retention as a function of flow rate in descending and ascending mode for different solvent systems in different geometries of CPC columns up to a certain flow rate. Above this flow rate, the slope of the decrease of stationary phase retention becomes steeper. The highest stationary phase retention in the current study was achieved in the CPE spherical cells column but still in the same range as in the CPE column. Compared to that, the stationary phase retention achieved in the CPC column is significantly lower and its decrease with increasing flow rate has a sharper decline than in the other two columns. The stationary phase retention in ascending mode is slightly higher than in descending mode due to the higher density and viscosity of the stationary phase (lower phase) in ascending mode and the resulting lower drag force, as presumed by Fumat et al. (2016) and Adelmann et al. (2013). Additionally, in descending mode the decline in stationary phase retention with increasing flow rate is sharper than in ascending mode for both CPE and CPE spherical cells due to the more viscous lower phase being the mobile phase.

Due to the different diameters of the disks and therefore the different average distance of the cells from the axis of rotation, the achievable relative centrifugal acceleration (for the definition, see Section 3.3) in the CPE spherical cells (613 g at 2000 rpm) column at the same rotational speed is higher than in CPC (230 g at 1700 rpm) and CPE (230 g at 1700 rpm). In addition to the different cell design, this is one of the reasons for the higher stationary phase retention in this column.

Due to the significantly reduced duct volume in CPE spherical cells, the total cell volume in CPE spherical cells (244 ml) is approximately equal to the total column volume. This means that almost the complete mobile phase volume is present in the cells and theoretically involved in the separation. In hydrostatic columns with connecting ducts, e.g. the CPC and CPE column in this study, the effective column volume, i.e. the column volume used for the separation, is equal to the column volume reduced by the ducts volume. This is also reflected by the parameter $S_{F,0}$, the stationary phase retention at a mobile phase flow rate of 0 ml min^{-1} , which was introduced by Foucault (1995). $S_{F,0}$ represents the volume fraction of the cells in the column and is the maximal theoretically achievable stationary phase retention of the column. The experimental data of the stationary phase retention as a function of flow rate was fitted linearly and correlates to the function:

$$S_F = S_{F,0} - BF \quad (2)$$

where S_F is the stationary phase retention at a certain flow rate, F the mobile phase flow rate and B the slope of the linear correlation. With 0.97 (Asc) and 0.95 (Dsc) at the CPE spherical cells column, the $S_{F,0}$ is clearly higher than in the CPC

(Asc: 0.77, Dsc: 0.67) and even in the CPE column (Asc: 0.89, Dsc: 0.83) for the solvent system Arizona K. Theoretically, $S_{F,0}$ should be the same in both modes and equal to the value that could be calculated directly from the cell and duct volumes provided by the manufacturer (Table 1). Possible reasons for the observed deviations could be a non-complete wetting of the ducts by the mobile phase, penetration of the stationary phase into the ducts and the fitting of the experimental data with linear regression.

In conclusion, even though the relative centrifugal acceleration is different in all three columns, the selected rotational speeds are in the range where the rotational speed has minor influence on the stationary phase retention (see Fig. 4a for CPE spherical cells). Therefore, one of the possible reasons for the observed difference in S_F are the differences in $S_{F,0}$. Furthermore, it seems that in columns with larger cells and higher $S_{F,0}$ the decrease of stationary phase with an increase in flow rate is less pronounced. In particular, a visual evaluation of the flow regimes in CPE and CPE spherical cells would be helpful to elucidate the influence of the cell geometry and operating conditions on the stationary phase retention.

3.2. Column efficiency and resolution

Pulse injection experiments of pyrocatechol and hydroquinone were performed at the CPE spherical cells and CPE column at different mobile phase flow rates in ascending and descending mode (see representative chromatograms in Supplementary Fig. S3 and S4). The column efficiency, i.e. the number of theoretical plates (N_i) was calculated from the recorded UV-vis signal with Eq. (3).

$$N_i = \left(\frac{t_{R,i}}{\sigma_i} \right)^2 \quad (3)$$

where $t_{R,i}$ is the retention time of component i and σ_i^2 the corresponding peak variance. For the calculation of the number of theoretical plates (N_i), the measured retention time in both modes was corrected by a dead volume of the system setup of 3 ml.

In Fig. 2a and b, the efficiency of the CPE spherical cells and CPE in ascending and descending mode, calculated from the hydroquinone peak, is presented as a function of flow rate and compared to the efficiency of the CPC unit determined by Goll et al. (2015).

The efficiency of all three CPC columns increases in both modes with the increase of the mobile phase flow rate. The number of theoretical plates for CPE spherical cells and CPE is in the same range and increases slightly with the increase of the flow rate. The number of theoretical plates of the CPC column is significantly higher than in CPE spherical cells and CPE, and increases considerably with the increase of the flow rate. This is in line with previous results, since CPE spherical cells and CPE have a similar number of cells with a similar single cell volume (see Table 1), while the number of twin-cells in the CPC column (1800) is by far the highest compared to the number of cells in CPE (240) and CPE spherical cells (196). Compared to the CPC column, the maximal achievable pressure drop was not reached in the experiments at the CPE spherical cells and CPE columns. Hence, even higher flow rates and rotational speeds than used within this study could be selected in these two columns.

The resolution of pyrocatechol and hydroquinone as a function of mobile phase flow rate for all three columns is pre-

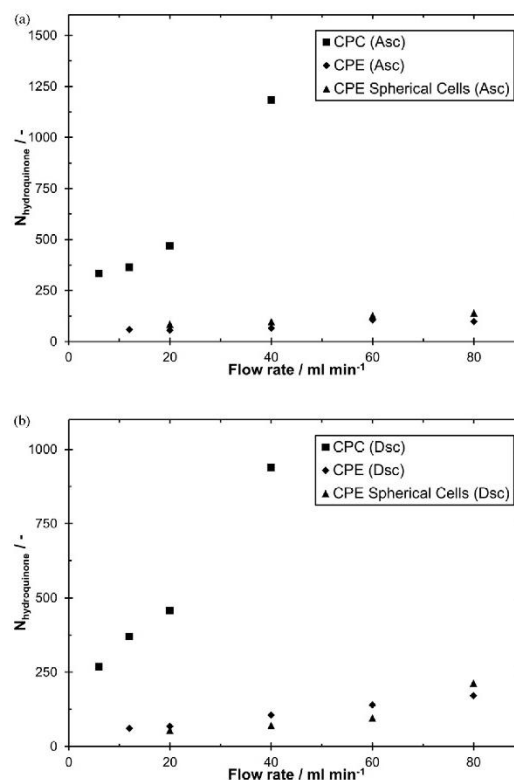


Fig. 2 – Column efficiency determined from pulse injections of hydroquinone at different mobile phase flow rates in (a) ascending mode (Asc) and (b) descending mode, in CPC, CPE and CPE spherical cells with the system heptane/ethyl acetate/methanol/water 1/2/1/2 (v/v/v/v), an injection volume of 1 ml, feed concentration of 5 mg ml⁻¹ per compound and a rotational speed of 1700 rpm (CPC and CPE) and 2000 rpm (CPE spherical cells).

sented in Fig. 3a and b for ascending and descending mode, respectively.

The resolution was calculated from the chromatograms according to Eq. (4) (Foucault, 1995).

$$R_s = S_F \frac{1}{4} \sqrt{N} \frac{(P_2 - P_1)}{1 - S_F \left[1 - \frac{P_2 + P_1}{2} \right]} \quad (4)$$

where P_1 and P_2 are the partition coefficients of the first and second eluting component (In descending mode: 1 = hydroquinone, 2 = pyrocatechol); S_F is the stationary phase retention at a certain flow rate, N is the mean value of the number of theoretical plates of both components ($N = (N_1 + N_2)/2$) (Berthod, 2002).

From Eq. (4) it becomes apparent that both column dependent parameters that are analyzed in this study, stationary phase retention S_F and column efficiency N , influence the resolution of the peaks. As shown in Fig. 2a and b, the column efficiency in CPC is much higher than in CPE and CPE spherical cells. At the same time, the column efficiency of CPE and CPE spherical cells is very similar. In contrast to this tendency, the peak resolution in ascending mode at CPE spherical cells is higher than in CPE but still much lower than in CPC (Fig. 3a). This difference between CPE spherical cells and CPE is due to the higher stationary phase retention at CPE spherical cells

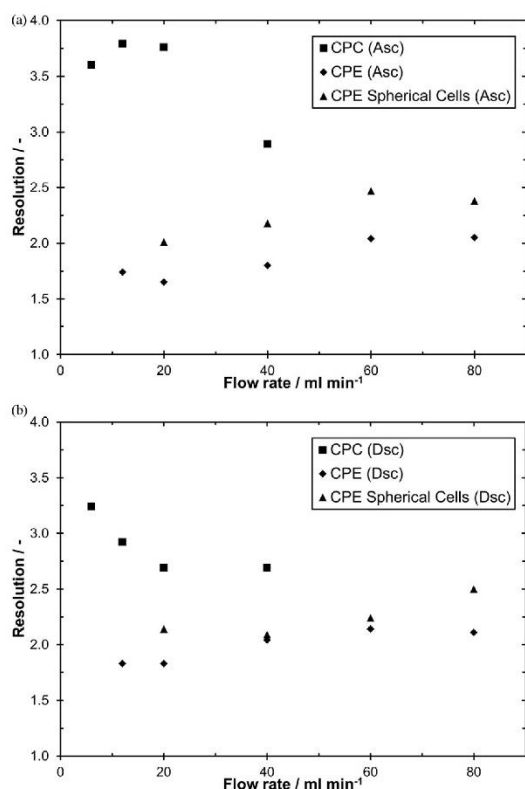


Fig. 3 – Separation resolution determined from pulse injections of hydroquinone and pyrocatechol at different mobile phase flow rates in (a) ascending mode (Asc) and (b) descending mode, in CPC, CPE and CPE spherical cells at different mobile phase flow rates with the system heptane/ethyl acetate/methanol/water 1/2/1/2 (v/v/v/v), an injection volume of 1 ml, feed concentration of 5 mg ml⁻¹ per compound and a rotational speed of 1700 rpm (CPC and CPE) and 2000 rpm (CPE spherical cells).

than in CPE, while the column efficiency is approximately the same in both columns. In descending mode (Fig. 3b), the peak resolution of CPE spherical cells and CPE is in a comparable range for the studied flow rates. Due to the higher stationary phase retention of CPE spherical cells, but higher efficiency of CPE in descending mode, there is no big difference in resolution as could be observed in ascending mode. Interesting to mention is, that resolution decreases with an increase of flow rate in CPC while resolution slightly increases in CPE and CPE spherical cells in both modes. However, the CPC could not be operated at higher flow rates due to pressure drop limitations.

3.3. Influence of centrifugal acceleration on stationary phase retention, column efficiency and resolution

Stationary phase retention, column efficiency and resolution as a function of the relative centrifugal acceleration (RCF), also called g-force, were determined in CPE spherical cells for the solvent system Arizona K in ascending and descending mode at a constant flow rate of 60 ml min⁻¹ and are presented in Fig. 4.

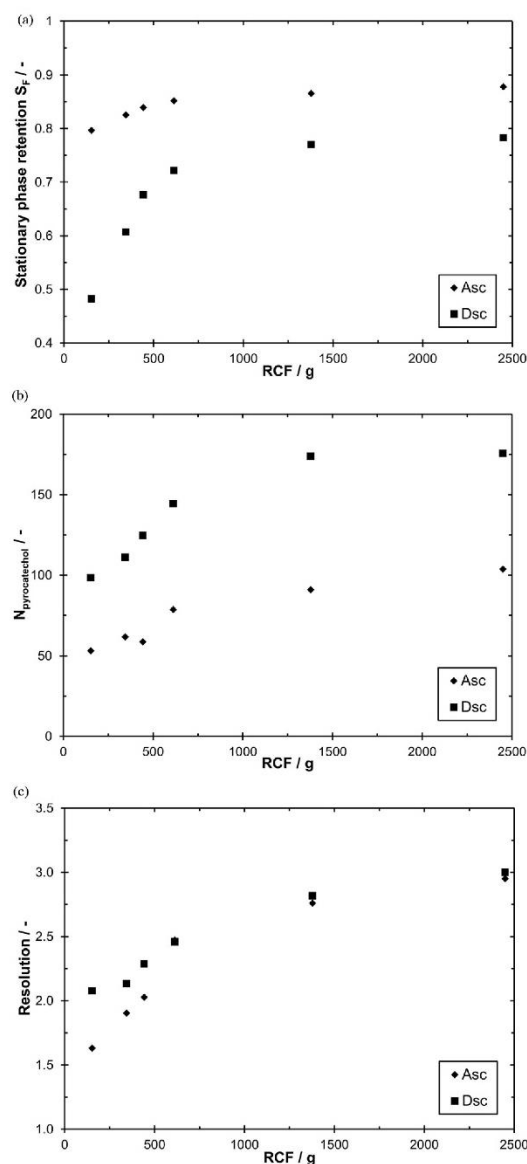


Fig. 4 – Stationary phase retention at 60 ml min⁻¹ of mobile phase flow rates for the solvent system heptane/ethyl acetate/methanol/water 1/2/1/2 (v/v/v/v) in ascending (Asc) and descending mode (Dsc) as a function of relative centrifugal acceleration (RCF) (a). Column efficiency of pyrocatechol (b) and separation resolution (c) determined from pulse injections of hydroquinone and pyrocatechol as a function of RCF at a mobile phase flow rate of 60 ml min⁻¹ in ascending (Asc) and descending mode (Dsc) in CPE spherical cells with an injection volume of 1 ml and a feed concentration of 5 mg ml⁻¹ per compound.

Centrifugal acceleration was normalized by the Earth's gravitational constant as follows:

$$RCF = \frac{RC\omega^2}{g} = \frac{RC4C\pi^2Cn^2}{g} \quad (5)$$

where g is the Earth's gravitational acceleration equal to 9.81 ms⁻², R the rotational radius as the average distance of the cells from the axis of rotation, ω the angular velocity in

radians per second and n the rotational speed of the column in revolutions per second.

As shown in Eq. (5), RCF correlates with the square of the angular velocity. The selected range in this study was from 153 g ($\omega = 105 \text{ rd s}^{-1}$, 1000 rpm) to 2450 g ($\omega = 419 \text{ rd s}^{-1}$, 4000 rpm). According to Fig. 4a, the influence of rotational speed on the stationary phase retention is much higher in descending mode where the lower phase, which has a higher density and viscosity, is the mobile phase. In this case, S_F increases from 153 g to 2450 g by about 30%. In comparison, the increase in stationary phase retention in ascending mode is just 8%.

This is in good agreement with similar studies from literature using different CPC columns and solvent systems, where an increase in stationary phase retention (equivalent to a decrease in mobile phase fraction) with increasing rotational speed was also observed (Adelmann et al., 2013; Kotland et al., 2015; Fumat et al., 2016; Marchal et al., 2002; Chollet et al., 2015). The flow inside the cells is more dispersed at a higher rotational speed (Schwienheer et al., 2015; Van Buel et al., 1998; Marchal et al., 2002, 2003). Furthermore, the different physical properties (interfacial tension, density difference and viscosity) influence the significance of rotational speed on the flow regime change. This also explains why the influence of rotational speed on the stationary phase retention is more significant in descending mode, where the more dense and viscous lower phase is used as mobile phase.

In addition to the stationary phase retention, the number of theoretical plates and therefore cell efficiency, which is the column efficiency divided by the number of actual cells, also increases with rotational speed in both modes, which is consistent with literature (Foucault et al., 1994; Fumat et al., 2016). Column efficiency N is presented as a function of RCF in Fig. 4b and increases clearly in both ascending and descending mode within the investigated range of RCF (153 g–2450 g). Foucault et al. (1994) observed a linear increase of N with rotational speed in descending mode within a certain range of rotational speed at low flow rates, which was explained by a linear correlation of efficiency to the interfacial area inside the cells. This is in accordance with the results from visual observations of the flow regime inside the cells where smaller droplets (higher dispersion) and consequently a higher interfacial area between the phases occur at higher rotational speed (Schwienheer et al., 2015; Van Buel et al., 1998).

Since stationary phase retention and the number of theoretical plates increase as a function of rotational speed, the resolution increases as well, as evident from Eq. (4) and Fig. 4c. Due to the fact that the CPE spherical cells column has a higher pressure drop limitation, both a higher rotational speed and a higher flow rate can be used at the same time. As shown in Figs. 2 and 4b, column efficiency increases with both an increase in flow rate and rotational speed. Consequently, cell efficiency increases as well.

3.4. Productivity and solvent consumption

3.4.1. Comparison of productivity and solvent consumption at equal column load

First, productivity and solvent consumption of the three columns at different mobile phase flow rates are compared for the separation of hydroquinone and pyrocatechol with small injection volume (1 ml) and low concentration (5 mg ml^{-1} per compound). In this study, the separation runtime is defined as the time between the sample injection and complete elu-

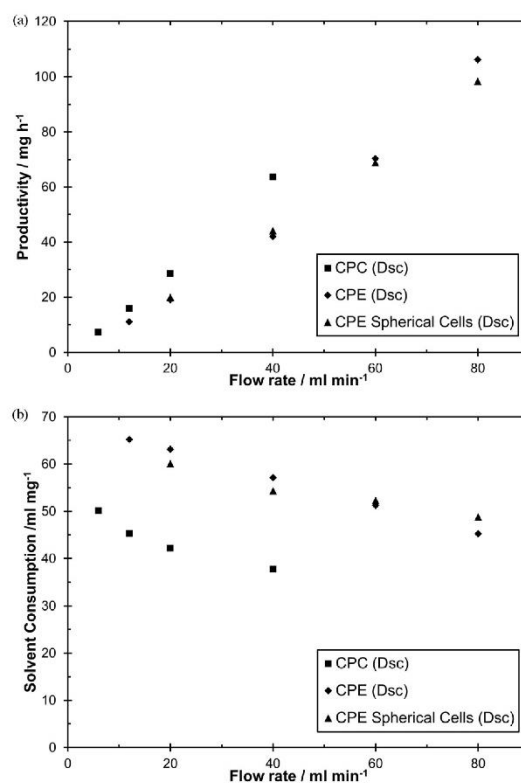


Fig. 5 – Productivity (a) and solvent consumption (b) calculated based on the pulse injections (injection volume of 1 ml) and the injected feed mass load in descending mode of hydroquinone and pyrocatechol in CPC, CPE and CPE spherical cells as a function of flow rate.

tion of the second component, i.e. pyrocatechol in descending mode and hydroquinone in ascending mode. Productivity is defined as the mass load of the feed mixture per runtime of the separation. The solvent consumption is calculated by dividing the mobile phase volume necessary to completely elute both components with the injected total mass.

Similar productivities, increasing with an increase in flow rate, were observed on all three columns (Fig. 5a). The highest productivity was achieved at the highest studied flow rate, e.g. 40 ml min⁻¹ for CPC and 80 ml min⁻¹ for CPE spherical cells and CPE. In terms of solvent consumption, the opposite tendency can be observed in Fig. 5b. The solvent consumption decreases as a function of flow rate for all three columns. The solvent consumption of CPE and CPE spherical cells are in the same range, but both about 10 ml per mg mass load higher than in CPC up to the maximal possible flow rate of 40 ml min⁻¹ in CPC. The lower solvent consumption observed in the CPC column is due to the lower stationary phase retention and at the same time higher column efficiency, which leads to a lower retention volume and faster elution time within the studied flow rate range. The results regarding ascending mode are similar and can be found in the Supplementary information.

However, the injection volume of 1 ml is not the maximal possible injection volume that could be used in each column, since peak resolution is above 1.5 for all three columns within the analyzed flow rate range. Consequently, a theoretical feasibility study was performed in order to maximize a possible injection volume for the separation in descending mode at

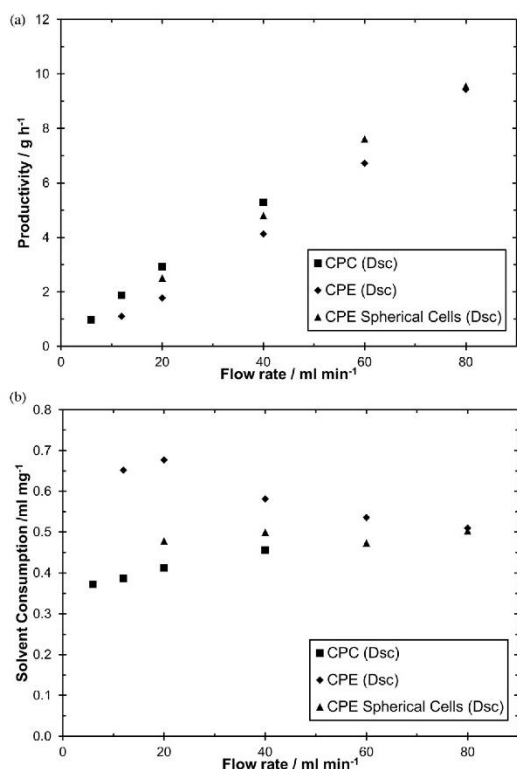


Fig. 6 – Productivity (a) and solvent consumption (b) based on optimized injection volume as a function of flow rate in CPC, CPE and CPE spherical cells.

different flow rates. This enables the comparison of the three columns regarding both their maximal possible productivity and minimal possible solvent consumption at a certain flow rate. Within the linear range of the partition equilibrium, the observed tendencies are not dependent from the absolute value of the feed concentration.

3.4.2. Comparison of productivity and solvent consumption for maximal injection volume

The maximal injection volume was determined by simulations as the highest volume at which baseline separation of the two model components was still achieved ($R_S = 1.5$). The simulation studies were performed for different mobile phase flow rates by changing the injection volume while keeping feed concentration (5 mg ml^{-1} per compound) and partition coefficients ($P_1 = 0.6$, $P_2 = 2.2$, 1-Hydroquinone, 2-Pyrocatechol) constant. For each flow rate, the corresponding experimentally determined stationary phase retention and column efficiency was used. Under the described assumptions, separation simulations based on the equilibrium cell model equations were performed with the commercial software gPROMS (Martin and Synge, 1941; Völkl et al., 2013; Hopmann and Minceva, 2012; Goll et al., 2013). The results are shown in Fig. 6.

As expected, for all three columns a significant increase in productivity could be achieved by increasing the injection volume (Fig. 6a). At a flow rate of 40 ml min^{-1} , which was the highest possible flow rate for CPC at 1700 rpm in this study, the productivity could be increased by a factor of approximately 100. The highest theoretical productivity was always at the highest investigated flow rate for each column. This was 5 g per hour for CPC at a flow rate of 40 ml min^{-1} and a maximal

injection volume of 109 ml. With CPE (1700 rpm, 80 ml min^{-1} , maximal injection volume of 121 ml) and CPE spherical cells (2000 rpm, 80 ml min^{-1} , maximal injection volume of 129 ml) even 9.5 g per hour were theoretically achievable. At a flow rate of 40 ml min^{-1} , CPC demonstrated the highest productivity of the three columns. This is due to the higher resolution (see Fig. 3b), which is a result of the much higher column efficiency (see Fig. 2b).

Interestingly, the three columns show different behavior in terms of solvent consumption, as evident from Fig. 6b. While solvent consumption decreases slightly in CPE with increasing flow rate, the solvent consumption seems to stay approximately constant in CPE spherical cells and even slightly increases in CPC within the studied range of flow rate. However, the solvent consumption in all three columns is in the same range in case of maximized injection volumes (around 0.5 ml mg^{-1}). This is in contrast to the tendency received from the experiments with small injection volumes, where the solvent consumption clearly decreases with an increase in flow rate (see Fig. 5b).

3.4.3. Comparison of productivity and solvent consumption for different separation factors and maximal injection volume

Since the separation of the binary mixture of hydroquinone and pyrocatechol with a separation factor α of 3.67 is relatively easy, a short theoretical study was done to consider the influence of α on productivity (Fig. 7a–c) and solvent consumption (Fig. 7d–f) in descending mode. The column performances were compared at the three different flow rates 20 ml min^{-1} , 40 ml min^{-1} and 80 ml min^{-1} . It should be noted, that a flow rate of 80 ml min^{-1} could not be used in the CPC column due to pressure drop limitations. The partition coefficient of the first eluting compound, i.e. hydroquinone ($P_{DSC} = 0.6$) and the feed concentration (5 mg ml^{-1} of each compound) were kept constant. The partition coefficient of the second eluting compound was calculated from the set separation factor. The objective of the study was to find the maximal possible injection volume for which a base line separation is still possible. At each flow rate, the corresponding stationary phase retention and column efficiency, determined in the previous experiments and presented in Fig. 1b and 2b, were used. It was assumed that the number of theoretical plates of the second eluting component does not change with a change of the separation factor. This simplification should not have a significant influence on the conclusions of the simulation study. Namely, the number of theoretical plates in CPC at a flow rate of 20 and 40 ml min^{-1} is high (see Fig. 2b) and in a range in which the number of theoretical plates has a negligible influence on the shape of the elution profiles. In CPE and CPE spherical cells, the difference in the number of theoretical plates for the first and second eluting compound, i.e. hydroquinone and pyrocatechol, was not significant (see Fig. 2b) and therefore can be considered constant when varying α .

As expected, the injection volume and consequently productivity (Fig. 7a–c) increases with an increase of the separation factor, while the solvent consumption decreases (Fig. 7d–f). Due to the higher column efficiency of CPC, base line separation could be obtained for smaller separation factors compared to CPE and CPE spherical cells. For example, at a flow rate of 20 ml min^{-1} , a base line separation could be achieved for a separation factor of 1.8 in CPC, 2.3 in CPE spherical cells and 2.75 in CPE (see Fig. 7a–c). With the increase in flow

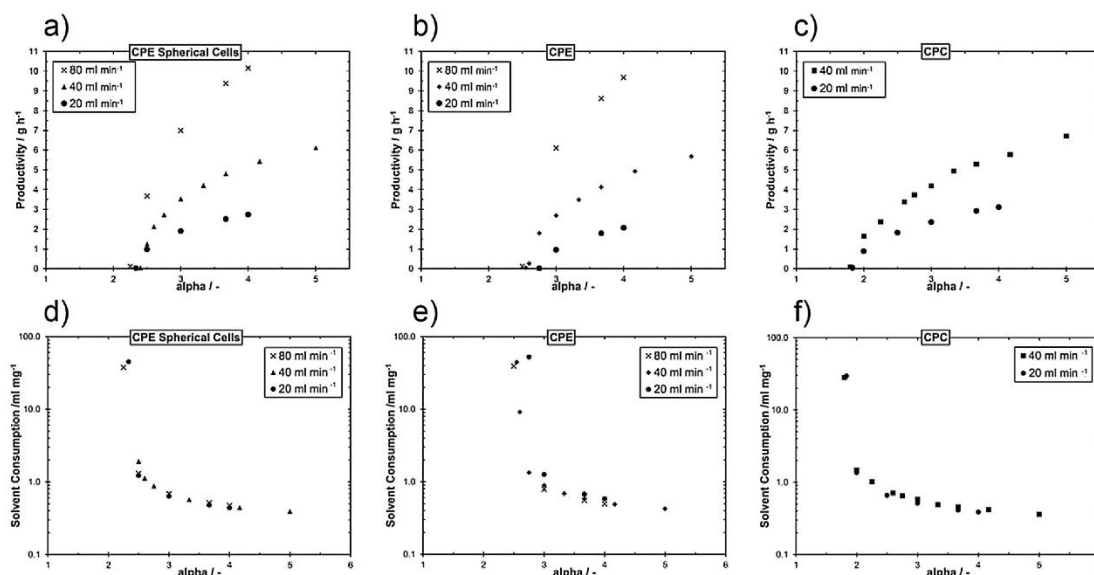


Fig. 7 – Theoretical study of the productivity as a function of the separation factor calculated based on the determined column efficiency and stationary phase retention at 80 ml min⁻¹, 40 ml min⁻¹ and 20 ml min⁻¹ from the pulse injections in descending mode of pyrocatechol and hydroquinone in (a) CPE spherical cells, (b) CPE and (c) CPC. In addition, the corresponding solvent consumption as a function of the separation factor in (d) CPE spherical cells, (e) CPE and (f) CPC.

rate, the separation factor at which base line separation is still possible decreases slightly in all columns. In each column, the productivity increases with the increase in flow rate for a given separation factor, while the solvent consumption is almost not affected. For separation factors above 2.5 the productivity increases significantly and solvent consumption decreases significantly with the increase of the flow rate in CPE and CPE spherical cells column. The maximal applicable flow rate is limited by pressure drop. Hence, for higher separation factors the CPE spherical cells column and the CPE column outperform the CPC column. However, the performances of CPE and CPE spherical cells become more similar with an increase in flow rate.

In conclusion from these two theoretical studies, a higher number of small cells as the CPC column can be recommended for more difficult separations with smaller separation factors, where high numbers of theoretical plates are needed that cannot be compensated by the higher stationary phase retention in columns with less but bigger cells even at higher flow rates. Columns with less but bigger cells could be suggested for relatively easy separations with higher separation factors in which higher injection volumes are possible despite lower numbers of theoretical plates. In addition, the purity and yield requirements also influence the productivity and solvent consumption of the desired separation. For lower purity and recovery requirements, the application of CPE spherical cells and CPE for a first purification or fractionation step from raw extracts in the whole separation process is conceivable.

4. Conclusions

A new hydrostatic column with spherical cells and insignificant duct volume, here called CPE spherical cells, was characterized in terms of stationary phase retention, column efficiency and peak resolution under the variation of flow rate and centrifugal acceleration. The column performance was evaluated by pulse injection experiments of hydroquinone

and pyrocatechol using the biphasic system heptane/ethyl acetate/methanol/water 1/2/1/2 (v/v/v/v). The results regarding the variation of flow rate were compared to two other hydrostatic columns of the same column volume with twin-cell design, one with similar cell volume and number of cells (CPE) and the other one with more but smaller cells (CPC). The separation performance of the new column with spherical cells is similar to the CPE column with twin-cells of similar size and number. Both columns could be operated at higher flow rates than the CPC, which is mainly due to the pressure drop limitation in the CPC. Compared to CPC, the stationary phase retention in CPE spherical cells was clearly the highest. Column efficiency was highest in CPC due to its significantly higher number of cells.

Best results in terms of productivity and solvent consumption at a given flow rate and a small injection volume for the model separation of hydroquinone and pyrocatechol (separation factor of 3.67) can be achieved using CPC. However, due to pressure limitations, this column could only be used with a flow rate of up to 40 ml min⁻¹. The other two columns outperform CPC when used at higher flow rates. As expected, for all three columns the solvent consumption decreases at small injection volumes with increasing flow rate. In a theoretical study, productivity and solvent consumption at maximized injection volumes show a similar performance of the CPE spherical cells and the CPE column, and both outperforming the CPC column at higher flow rates.

Further comparison of the columns by simulation varying different separation factors lead to the conclusion that columns with a higher number of small cells (CPC column) are more advantageous for more difficult separations with low separation factors (separation factor below 2.5). CPE and CPE spherical cells are proposed for easier separations and higher flow rates than achievable at CPC. There, CPE and CPE spherical cells result in a much faster separation and consequently higher productivity. In addition, CPE spherical cells performs slightly better than CPE. Considering the similar performance

of CPE spherical cells and the CPE column with twin-cells of similar size and number of cells, the CPE spherical cells column may also be suited for more unstable and more viscous solvent systems such as aqueous two-phase systems or deep eutectic solvent based systems.

Acknowledgements

The authors appreciate the financial support of the Deutsche Forschungsgemeinschaft 335 (German Research Foundation, DFG-Projekt MI1340/3-1). In addition, the authors thank Dr. Pfeiffer from AlphaCrom AG (Switzerland) for the loan of the pump and the UV-vis detector.

Appendix A. Supplementary data

Supplementary material related to this article can be found, in the online version, at doi:<https://doi.org/10.1016/j.cherd.2019.01.011>.

References

- Adelmann, S., Schembecker, G., 2011. Influence of physical properties and operating parameters on hydrodynamics in Centrifugal Partition Chromatography. *J. Chromatogr. A* 1218, 5401–5413.
- Adelmann, S., Baldhoff, T., Koepcke, B., Schembecker, G., 2013. Selection of operating parameters on the basis of hydrodynamics in centrifugal partition chromatography for the purification of nybomycin derivatives. *J. Chromatogr. A* 1274, 54–64.
- Berthod, A., 2002. *Countercurrent Chromatography*. Elsevier.
- Berthod, A., Faure, K., 2015. Separations with a liquid stationary phase: countercurrent chromatography or centrifugal partition chromatography. In: *Analytical Separation Science*.
- Chollet, S., Marchal, L., Meucci, J., Renault, J.-H., Legrand, J., Foucault, A., 2015. Methodology for optimally sized centrifugal partition chromatography columns. *J. Chromatogr. A* 1388, 174–183.
- Couillard, F., 2009. WO 2009/066014 A1.
- Couillard, F., 2010. US Patent 2010/0200488 A1.
- de La Poype, F., de La Poype, R., Durand, P., Foucault, A., Legrand, J., Patissier, G., Rosant, J.M., 2003. US Patent 2003/6537452 B1.
- Foucault, A.P., 1995. *Centrifugal Partition Chromatography*. M. Dekker.
- Foucault, A.P., Bousquet, O., Le Goffic, F., 1992. Importance of the parameter V_m/V_c in countercurrent chromatography: tentative comparison between instrument designs. *J. Liq. Chromatogr.* 15, 2691–2706.
- Foucault, A.P., Frias, E.C., Bordier, C.G., Goffic, F.L., 1994. centrifugal partition chromatography: stability of various biphasic systems and pertinence of the “Stoke’s Model” to describe the influence of the centrifugal field upon the efficiency. *J. Liq. Chromatogr.* 17, 1–17.
- Foucault, A., Legrand, J., Marchal, L., Durand, D., 2008. US Patent 2008/003546 A1.
- Foucault, A., Legrand, J., Marchal, L., Elie, C., Agaise, P., 2010. US Patent 2010/0252503 A1.
- Fumat, N., Berthod, A., Faure, K., 2016. Effect of operating parameters on a centrifugal partition chromatography separation. *J. Chromatogr. A* 1474, 47–58.
- Goll, J., Frey, A., Minceva, M., 2013. Study of the separation limits of continuous solid support free liquid–liquid chromatography: separation of capsaicin and dihydrocapsaicin by centrifugal partition chromatography. *J. Chromatogr. A* 1284, 59–68.
- Goll, J., Audo, G., Minceva, M., 2015. Comparison of twin-cell centrifugal partition chromatographic columns with different cell volume. *J. Chromatogr. A* 1406, 129–135.
- Hopmann, E., Minceva, M., 2012. Separation of a binary mixture by sequential centrifugal partition chromatography. *J. Chromatogr. A* 1229, 140–147.
- Hopmann, E., Goll, J., Minceva, M., 2012. Sequential centrifugal partition chromatography: a new continuous chromatographic technology. *Chem. Eng. Technol.* 35, 72–82.
- Ito, Y., Knight, M., Finn, T.M., 2013. Spiral countercurrent chromatography. *J. Chromatogr. Sci.* 51, 726–738.
- Kotland, A., Chollet, S., Autret, J.-M., Diard, C., Marchal, L., Renault, J.-H., 2015. Modeling pH-zone refining countercurrent chromatography: a dynamic approach. *J. Chromatogr. A* 1391, 80–87.
- Lorantfy, L., Németh, L., Kobács, Z., Rutterschmidt, D., Miskolc, Z., Rajsch, G., 2015. Development of industrial scale Centrifugal Partition Chromatography. In: *Planta Medica*. Georg Thieme Verlag, KG Rudigerstr. 14, D-70469 Stuttgart, Germany, pp. 1532.
- Lórántfy, L., Németh, L., 2016. WO Patent 2016/055821 A1.
- Mandova, T., Audo, G., Michel, S., Grougnet, R., 2017. Assessment of two centrifugal partition chromatography devices. Application to the purification of Centaurium erythraea methanolic extract. *Phytochem. Lett.* 20, 401–405.
- Marchal, L., Foucault, A., Patissier, G., Rosant, J.M., Legrand, J., 2000. Influence of flow patterns on chromatographic efficiency in centrifugal partition chromatography. *J. Chromatogr. A* 869, 339–352.
- Marchal, L., Legrand, J., Foucault, A., 2002. Mass transport and flow regimes in centrifugal partition chromatography. *AIChE J.* 48, 1692–1704.
- Marchal, L., Intes, O., Foucault, A., Legrand, J., Nuzillard, J.-M., Renault, J.-H., 2003. Rational improvement of centrifugal partition chromatographic settings for the production of 5-*n*-alkylresorcinols from wheat bran lipid extract: I. Flooding conditions—optimizing the injection step. *J. Chromatogr. A* 1005, 51–62.
- Martin, A.J.P., Synge, R.L.M., 1941. A new form of chromatogram employing two liquid phases, a theory of chromatography. 2. Application to the micro-determination of the higher monoamino-acids in proteins. *Biochem. J.* 35, 1358–1368.
- Murayama, W., Kobayashi, T., Kosuge, Y., Yano, H., Nunogaki, Y., Nunogaki, K., 1982. A new centrifugal counter-current chromatograph and its application. *J. Chromatogr. A* 239, 643–649.
- Schwiebheer, C., Merz, J., Schembecker, G., 2015. Investigation, comparison and design of chambers used in centrifugal partition chromatography on the basis of flow pattern and separation experiments. *J. Chromatogr. A* 1390, 39–49.
- Skalicka-Woźniak, K., Garrard, I., 2015. A comprehensive classification of solvent systems used for natural product purifications in countercurrent and centrifugal partition chromatography. *Nat. Prod. Rep.* 32, 1556–1561.
- Van Buel, M., Van Halsema, F., Van der Wielen, L., Luyben, K., 1998. Flow regimes in centrifugal partition chromatography. *AIChE J.* 44, 1356–1362.
- Völkl, J., Arlt, W., Minceva, M., 2013. Theoretical study of sequential centrifugal partition chromatography. *AIChE J.* 59, 241–249.

3.2. Paper II: Deep eutectic solvents in countercurrent and centrifugal partition chromatography

3.2.1. Summary

Citation

S. Roehrer, F. Bezold, E. M. García, M. Minceva, (2016). Deep eutectic solvents in countercurrent and centrifugal partition chromatography. *Journal of Chromatography A*, 1434, 102-110.

<https://doi.org/10.1016/j.chroma.2016.01.024>

Summary

In LLC, a huge variety of biphasic solvent systems has already been established, especially for the separation of medium-polar (natural) compounds. In recent years, an increasing demand for new non-aqueous biphasic solvent systems for the separation of very nonpolar substances has become apparent. Recently, a new class of solvents, the so-called deep eutectic solvents (DES), have emerged as especially promising for extraction applications. Therefore, the objective of this work was to investigate the applicability of this new solvent system class for LLC separations. DES are prepared by mixing hydrogen bond donors and hydrogen bond acceptors in a certain molar ratio to form a eutectic mixture with a substantially lower melting temperature compared to the melting temperature of the individual compounds. DES usually have a higher density and viscosity compared to conventional organic solvents and water. Hence, the DES-rich phase of a biphasic liquid system is also denser and more viscous. The use of rather viscous phases in comparison to organic-aqueous biphasic solvent systems in CPC is usually rather unsuitable, due to the limitation of a maximal pressure drop of 100 bar. Therefore, a column with large twin-cells, a centrifugal partition extractor (CPE), was selected to analyze the applicability of this new class of biphasic systems. A non-aqueous system composed of *n*-heptane/ethanol/DES with a DES made of choline chloride and levulinic acid in a molar ratio of 1:2 was demonstrated to be suitable for the separation of components within a wide range of hydrophobicity, which is accessible by the logarithmic octanol-water partition coefficient $\log P_{O/W}$ of the compounds. Hence, natural hydrophobic compounds such as β -ionone ($\log P_{O/W} = 3.8$) and α -tocopherol ($\log P_{O/W} = 12$) could be separated in the current study. This indicates that DES may be promising as a replacement for water in further biphasic systems. However, choline chloride and other ingredients of DES are known to be hygroscopic. Therefore, the water absorbance in the presence of ambient air was determined to be 5-10% in the first 2-3 days of exposure. The studied system was furthermore shown to be robust to the presence of such amounts of water, where no significant change in the partition coefficient of β -ionone was observed. This is especially advantageous for the preparative applications, since it eliminates water-protective precautions such as working under protective atmosphere. In addition, it was shown that the more viscous DES-rich phase could be used as both stationary and mobile phase in large twin-cells, which allows a greater flexibility for the design of the separation process.

Contributions

The author of this dissertation had a leading role in this work. Based on preliminary work from E.M. García, the author selected the (choline chloride: levulinic acid)-based biphasic system for the study of its applicability in the CPC column. The author performed most of the solute partitioning experiments in the selected system, performed all CPC experiments, discussed the results with F. Bezold and M. Minceva, and wrote the manuscript.



Contents lists available at ScienceDirect

Journal of Chromatography A

journal homepage: www.elsevier.com/locate/chroma

Deep eutectic solvents in countercurrent and centrifugal partition chromatography

Simon Roehrer^a, Franziska Bezold^a, Eva Marra García^b, Mirjana Minceva^{a,b,*}^a *Biothermodynamics, TUM School of Life and Food Sciences Weihenstephan, Technische Universität München, 85354 Freising, Germany*^b *Chair of Separation Science and Technology, Friedrich Alexander University Erlangen-Nuremberg, 91058 Erlangen, Germany*

ARTICLE INFO

Article history:

Received 20 October 2015

Received in revised form 5 January 2016

Accepted 9 January 2016

Available online 14 January 2016

Keywords:

Countercurrent chromatography
 Centrifugal partition chromatography
 Deep eutectic solvents
 Non-aqueous biphasic liquid systems
 Centrifugal partition extractor

ABSTRACT

Deep eutectic solvents (DESs) were evaluated as solvents in centrifugal partition chromatography, a liquid-liquid chromatography separation technology. To this end, the partition coefficients of ten natural compounds of different hydrophobicity were determined in non-aqueous biphasic systems containing DES. The influence of the composition of DESs and the presence of water in the biphasic system on the partition coefficient were also examined. In addition, several process relevant physical properties of the biphasic system, such as the density and viscosity of the phases, were measured. A mixture of three to four hydrophobic compounds was successfully separated in a centrifugal partition extractor using a heptane/ethanol/DES biphasic system.

© 2016 Elsevier B.V. All rights reserved.

1. Introduction

The term deep eutectic solvent (DES) refers to a mixture of compounds capable of associating with each other to form a eutectic mixture with a melting point substantially lower than that of each individual compound [1]. The hydrogen-bonding interactions between the compounds of the mixture, a hydrogen-bond donor (HBD) and a hydrogen-bond acceptor (HBA), are suggested as the main cause for the depression of the freezing point [1]. In general, DESs have melting points lower than 100 °C [2].

Since 2003, when Abbott and his co-workers presented the first DES [1] obtained by mixing quaternary ammonium salts (e.g., choline chloride) and urea, this new solvent family rapidly emerged as a new generation of designer solvents. Similar to ionic liquids, the physical properties of DES, such as the freezing point, density, viscosity, surface tension, and conductivity, can be tailored by combining different HBAs and HBDs, and to some extent by varying their molar ratio in the mixture [3–7].

A summary of hundreds of DESs can be found in the literature [2,8–14]. Choline chloride (ChCl), a mass-produced non-toxic quaternary ammonium salt used as an additive to chicken feed, is the

most widely used HBA, and urea, carboxylic acids, and polyols such as glycerol are the most popular HBAs [2]. Due to their biocompatibility, renewability, and biodegradability, natural deep eutectic solvents (NADES) have recently received special attention. They consist of abundant primary metabolites such as sugars, amino acids, organic acids, and a small amount of water [14].

In the literature, DESs are often presented as a more economical and eco-friendly alternative to ionic liquids. One of the most beneficial characteristics of DESs is their easy preparation, as DES is commonly prepared by heating the solid mixture of its constituents at a temperature below 100 °C. Many DESs are made from cheap, readily available, and toxicologically well characterized starting materials.

The number of DES applications is growing rapidly [2,11,15]. Besides their use as solvents in chemical and biological synthesis, electrochemistry, and the preparation of inorganic materials, significant attention is now being paid to their application in separation processes [3,14]. The main area of research is the use of DESs as extraction solvents in solid-liquid and liquid-liquid extraction [3,8,12,14,16–19]. DESs have been used to extract flavonoids [20,21], phenolic compounds [12,15], and aromatics [18,40] from plants. Shahbaz et al. [22] used DESs to extract glycerol from biodiesel. This first application of DES as a solvent in liquid-liquid extraction was followed by studies on the separation of mixtures of alcohols and esters [8], benzene from a benzene/hexane mixture [17], and BTEX aromatics (benzene, toluene, ethylbenzene and *m*-xylene) from *n*-octane [18,23]. Recently, Zeng et al. [16] inves-

* Corresponding author at: Biothermodynamics, TUM School of Life and Food Sciences Weihenstephan, Technische Universität München, 85354 Freising, Germany. Fax: +49 8161 71 3180.

E-mail address: mirjana.minceva@tum.de (M. Minceva).

tigated the partitioning of proteins in aqueous two-phase systems composed of DES (e.g. ChCl-urea) and K_2HPO_4 . Another approach for the extraction of compounds from mixtures is the in situ formation of DESs with the target compounds. This approach was used for the extraction of phenols from oils using quaternary ammonium salts [24,25].

To date, there is no publication on the use of DES in support-free liquid–liquid chromatography, also known as centrifugal partition chromatography (CPC) and countercurrent chromatography (CCC). A multi-solvent biphasic system is used in liquid-liquid chromatography, and the separation occurs as a result of the difference in the partitioning of the compounds of a mixture between the two liquid phases. One of the two phases is kept in place with the help of a centrifugal field, while the second phase is pumped through the column. The partition coefficient of the solutes to be separated is normally used as a screening parameter for the selection of a suitable biphasic system for the separation of a particular mixture. A system in which the partition coefficients range between 0.4 and 2.5 provides a good balance between the separation resolution and solvent consumption [26–28].

The most frequently used biphasic systems in CCC and CPC are composed of three to four solvents of different polarity [26,29–32]. Such systems are very practical, since the composition and the polarity of the phases can be tuned by varying the ratio of the solvents. For example, numerous biphasic systems with overall compositions between 1/0/1/0 and 0/1/0/1 (v/v/v/v) can be created using the solvent system heptane/ethyl acetate/methanol/water [30]. Even though these systems cover a wide range of polarities, they are often unsuitable for the separation of highly hydrophobic (lipophilic) and hydrophilic compounds. The partition coefficients are very high or very low for such compounds because they preferentially dissolve in one of the two phases [33].

With the increasing popularity of CCC and CPC as a powerful method for the purification of active compounds from plant extracts and biotechnological products, it is necessary to develop biphasic solvent systems for the separation of both hydrophobic and organic solvent sensitive biomolecules such as proteins and nucleic acids [34–36]. The DESs might be good solvent candidates for both types of systems, namely non-aqueous systems and organic-solvent-free aqueous two phase systems (ATPS).

In this study, we focus on non-aqueous solvent systems and explore the possibility of using DESs as a substitute for water in biphasic systems composed of water and organic solvents for liquid–liquid chromatographic applications. Recently published data about the solubility of several poorly water-soluble drugs and metabolites has clearly demonstrated the solvation power of DESs. In most cases the solubility of the biomolecules is considerably higher than in pure water [37,38].

To the best of the authors' knowledge, this is the first publication on the applicability of DESs in liquid-liquid chromatography. One of the objectives of this study was to identify DESs that would form biphasic liquid systems with commonly used solvents in CCC and CPC such as heptane and ethanol. To assess the applicability of DES-based biphasic systems in CCC and CPC, the partition coefficients of several natural compounds were evaluated. The selected compounds had octanol-water partition coefficients ($\log P_{O/W}$) ranging between -5.10 and 12.00 and thus covered a wide range of hydrophobicity.

In addition, the influence of water absorption on the partition coefficient, which resulted from the exposure of the DES to air, was determined. Physical properties, including the density and viscosity of both of the phases of the DES-based system, were measured and compared to standard CCC or CPC biphasic systems. Finally, a centrifugal partition extractor with a twin-cell design was used to separate mixtures of selected compounds.

2. Materials and methods

2.1. Chemicals

For the preparation of the DESs, choline chloride (purity $\geq 98\%$, Alfa Aesar, Germany) and betaine (purity $\geq 98.0\%$, Fluka/Sigma–Aldrich, Germany) were used as HBAs. The HBDs, including their purities and producer, are listed in Table 1. The abbreviation of the different DESs used in this study, the molar ratio of their corresponding HBD and HBA and the melting points of the DESs are also provided in this table. The melting points of the individual HBDs and HBAs are: 305°C (choline chloride), 293°C (betaine), 33°C (levulinic acid), 135°C (malonic acid), -13°C (ethylene glycol), 18°C (glycerol), 20°C (1,4-butanediol) [47].

The solvents heptane (EMSURE, purity 99%) and ethanol (LiChrosolv, purity 99.9%) were purchased from Merck KGaA (Darmstadt, Germany). A list of solutes, including their molecular formula, molecular weight, detection wavelength, octanol-water partition coefficient, purity, and producer, is provided in Table 2.

2.2. Equipment

2.2.1. UV-Vis spectrometer

The concentration of the solute in the two phases of the biphasic systems was determined by ultraviolet-visible (UV-Vis) spectroscopy using a Specord 50 Plus (Analytic Jena AG, Germany) at 20°C .

2.2.2. Density meter

The density of the phases of the solvent systems was measured with an oscillating U-tube density meter DMA 5000 from Anton Paar GmbH (Ostfildern-Scharnhausen, Germany) at 20°C .

2.2.3. Rheometer

A MCR-102 rheometer (Anton Paar GmbH, Ostfildern-Scharnhausen, Germany) was used for the determination of the dynamic viscosity. The samples were measured at 20°C .

2.2.4. Centrifugal partition extractor

The liquid-liquid chromatography experiments were carried out at room temperature in a centrifugal partition extractor (CPE) model SCPE-250-BIO from Armen Instrument (France), with a total column volume of 250 ml. The column was composed of 11 stainless steel disks coated with PTFE and was thus suitable for applications involving biomolecules. Each disk had 20 twin-cells with a cell volume of 0.961 ml. The maximum achievable rotational speed was 3000 rpm. The column could withstand a pressure drop of 100 bar.

The centrifugal partition extractor was connected to two isocratic HPLC pumps (Model 306 50 SC, Gilson, USA), which could deliver flow rates of up to 50 ml min^{-1} . The effluent was monitored with a diode-array detector (Model 171 from Gilson, USA). The sample was introduced through a six port manual injection valve.

2.3. Methods

2.3.1. Preparation of DES

The DESs were prepared by mixing the HBA (choline chloride or betaine) with the corresponding HBD according to the molar ratios provided in Table 1. After weighing in the particular amounts of HBA and HBD, the 20 ml vial was closed with a crimp cap. The mixture was stirred with a magnetic stirrer and heated at $80\text{--}85^\circ\text{C}$ until a single clear liquid phase was formed. In case of the preparation for the separation of the multicomponent mixture with the CPE,

Table 1

List of deep eutectic solvents: hydrogen bond acceptor (HBA), hydrogen bond donor (HBD), DES abbreviation, HBA/HBD mole ratio, DES melting point, and HBD purity and producer.

HBA	HBD	DES abbreviation	HBA/HBD mole ratio		DES melting point [°C]		HBD purity	HBD producer
Choline chloride	Levulinic acid	CLA	1:2		– ^a		98	Alfa Aesar
	Malonic acid	CMA	1:1		10 ^b		>99.5	Alfa Aesar
	Ethylene glycol	CEG	1:2		–66.01 ^b		≥99.5	Merck KGaA
	Glycerol	CGL	1:2	1:3	–36.15 ^b	–32.65 ^b	≥99	Merck KGaA
Betaine	Levulinic acid	BLA	1:3	1:4	–32 ^b	– ^a	99	Alfa Aesar
			1:2		– ^a		98	Alfa Aesar

^a Liquid at room temperature.

^b [9].

the DES was prepared in a laboratory bottle (1 L) without a crimp cap.

2.3.2. Water absorption

Directly after the preparation of the DES and subsequent cooling to room temperature, the water content in the DES was determined by Karl Fischer titration with a C20 compact coulometric titrator from Mettler Toledo (Switzerland). The kinetics of the water absorption was determined gravimetrically at room temperature. A precise quantity of DES was exposed to air, and its weight was measured over time with an analytical balance (precision of 0.1 mg) as described by Maugeri et al. [8].

2.3.3. Preparation of biphasic systems

The biphasic systems were prepared by mixing the respective amounts of the solvents at room temperature. The mixture was vigorously shaken and equilibrated at room temperature for at least two hours. For the liquid–liquid chromatography experiments the phases were split and placed in two separate containers. A freshly prepared biphasic system was used in each experiment.

2.3.4. Determination of the partition coefficients

The partition coefficients (defined in Section 3.2) of the selected solutes in the investigated biphasic systems were determined using the shake flask method. The solute was added to a previously prepared biphasic system at a concentration of 5 mmol per liter of the biphasic system. Afterwards, the two liquid phases were split and placed into two separated reservoirs for subsequent UV–Vis analysis. If necessary, the phases were diluted with ethanol. After recording the wavelength range from 190 to 400 nm, the partition coefficient of each solvent was determined at the wavelength listed in Table 2. A blank sample without solute was measured for each sample with the same dilution factor to take into account the influence of the solvent on the absorption spectrum. For each solute the experiments (except those presented in Fig. 3) were performed in triplicate.

Table 2

List of solutes, including name, abbreviation, molecular formula, molecular weight, octanol–water partition coefficient $P_{0/W}$, detection wavelength λ , purity, and producer.

Solute	Abbr.	Molecular formula	M [g/mol]	$\log P_{0/W}$ ^b	λ ^a [nm]	Purity	Producer
New coccine red	r	C ₂₀ H ₁₁ N ₂ Na ₃ O ₁₀ S ₃	604.5	–5.100	246	82.4 ± 0.5	Institute of Leather Industry, (Lodz Poland)
p-Arbutin	A	C ₁₂ H ₁₆ O ₇	272.3	–0.508	287	≥98	Alfa Aesar
Caffeine	C	C ₈ H ₁₀ N ₄ O ₂	194.2	–0.040	273	≥99	Sigma–Aldrich
Vanillin	V	C ₈ H ₈ O ₃	152.2	1.284	279	99	Alfa Aesar
Coumarin	M	C ₉ H ₆ O ₂	146.2	1.412	274	≥99	Sigma–Aldrich
Carvone	Ca	C ₁₀ H ₁₄ O	150.2	2.103	235	≥98.5	Fluka
Naringenin	N	C ₁₅ H ₁₂ O ₅	272.3	2.445	289	≥95	Sigma–Aldrich
β-Ionone	I	C ₁₃ H ₂₀ O	192.3	3.770	295	96	Sigma–Aldrich
Retinol	R	C ₂₀ H ₃₀ O	286.5	5.680 ^c	325	≥95	Sigma–Aldrich
α-Tocopherol	Y	C ₂₉ H ₅₀ O ₂	430.7	12.000 ^d	292	≥97	Alfa Aesar

^a In ethanol.

^b [28] except Retinol and α-Tocopherol.

^c Sigma–Aldrich, safety data sheet, product number 17772 (consulted 2015–08–27).

^d PubChem database, Alpha-tocopherol–Physical properties (consulted 2015–08–27) <http://pubchem.ncbi.nlm.nih.gov/rest/chemical/alpha-tocopherol>.

2.3.5. Liquid–liquid chromatography separation of a multicomponent mixture

Mixtures of solutes from Table 2 were separated with a DES-based biphasic system in ascending and descending mode in the CPE unit described in Section 2.2.4. The lower DES-rich phase was used as a stationary phase in the ascending mode and as a mobile phase in the descending mode.

At the beginning of the experiment, the column was filled with the stationary phase at a flow rate of 40 ml min^{–1}. Afterwards, the rotational speed was set to 2000 rpm and the mobile phase was pumped through the column until no more stationary phase eluted from the column. The mobile phase flow rate in ascending mode was 20 ml min^{–1} and in descending mode was 20 and 40 ml min^{–1}. The volume of the stationary phase inside the column was calculated as the difference between the total column volume and the volume of the stationary phase eluted from the column, considering the dead volume of the system.

The feed mixtures were injected via a 5 ml sample loop with a manual injection valve. In ascending mode 27.5 mg β-ionone, 25.3 mg retinol and 201.3 mg α-tocopherol dissolved in the upper phase were injected, whereas in descending mode 27.5 mg naringenin, 27.2 mg β-ionone, 27.4 mg retinol and 201.2 mg α-tocopherol dissolved in the lower phase were injected. The detector wavelength was set to 295 nm with a reference wavelength of 390 nm.

3. Results and discussion

3.1. Selection of a suitable DES-based biphasic system

Liquid–liquid equilibrium data of systems containing DESs are limited to phase diagrams of a few heptane/ethanol/DES-systems published by Oliveira et al. [39] and hexane/benzene/DES- and hexane/ethyl acetate/DES-systems published by Kareem et al. [17] and the group of Kroon [40].

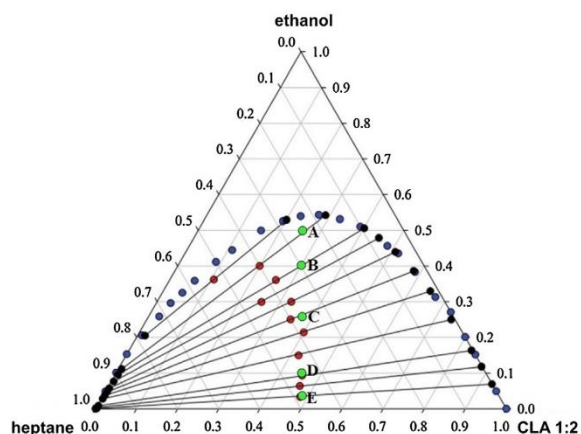


Fig. 1. Ternary diagram of heptane/ethanol/CLA 1:2 at 25 °C [adapted from 39]. A - 25/50/25 wt%, B - 30/40/30 wt%, C - 37.5/25/37.5 wt%, D - 45/10/45 wt%, and E - 48.5/3/48.5 wt%.

Due to the carcinogenic properties of benzene and the high UV cut-off of ethyl acetate (256 nm), a heptane/ethanol/DES-system was selected as a reference system in the present study. The ternary phase diagram is presented in Fig. 1.

The solvent system heptane/ethanol/CLA 1:2 (CLA: choline chloride and levulinic acid) had a considerably large miscibility gap. The upper phase was heptane-rich and the lower phase consisted mainly of ethanol and DES. In this study, five different systems, marked with the letters A to E in Fig. 1, were selected: A - 25/50/25 wt%, B - 30/40/30 wt%, C - 37.5/25/37.5 wt%, D - 45/10/45 wt%, and E - 48.5/3/48.5 wt%.

From system A to E, the composition of the upper phase (heptane-rich phase) did not change significantly, whereas the composition of the lower phase (DES-rich phase) did. Also, the amount of DES in the lower phase was observed to increase, while the amount of ethanol decreased.

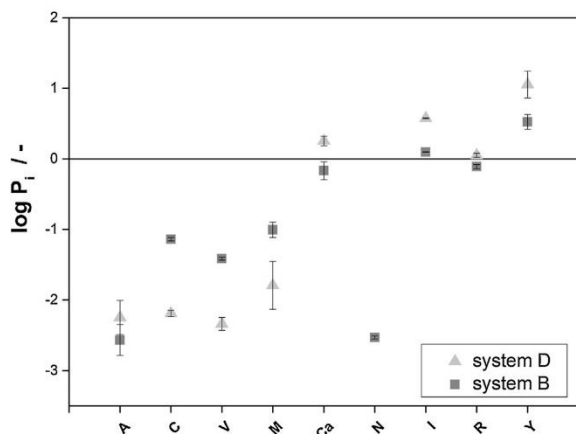


Fig. 2. Partition coefficients of different solutes in two heptane/ethanol/CLA 1:2 systems at 25 °C (system B: heptane/ethanol/CLA 1:2 (30/40/30 wt%) and system D: heptane/ethanol/CLA (1:2 45/10/45 wt%). Target compounds ordered by increasing hydrophobicity: A—p-arbutin, C—caffeine, V—vanillin, M—coumarin, Ca—carvone, N—naringenin, I— β -ionone, R—retinol, Y— α -tocopherol.

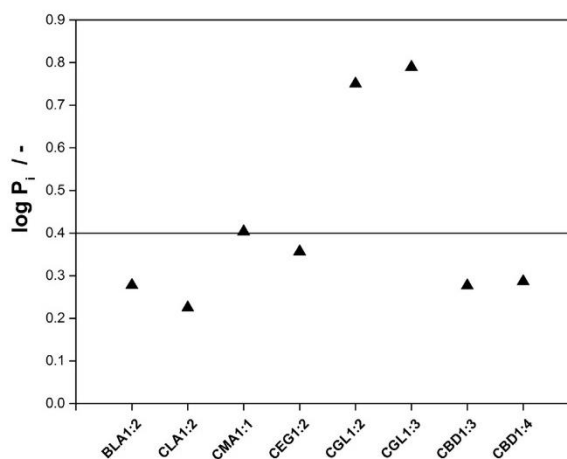


Fig. 3. Partitioning of β -ionone in different DES-based systems with a composition of heptane/ethanol/DES of 37.5/25/37.5 wt% (system C) at 25 °C. BLA (betaine-levulinic acid), CLA (choline chloride-levulinic acid), CMA (choline chloride- malonic acid), CEG (choline chloride-ethylene glycol), CGL (choline chloride-glycerol), CBD (choline chloride-1,4-butanediol).

3.2. Solute partitioning in heptane/ethanol/CLA 1:2 systems

In order to evaluate the applicability of DES-based biphasic systems in liquid-liquid chromatography, the partition coefficient of several solutes with different hydrophobicity were determined (Table 2). The preferred range of the partition coefficient was between 0.4 and 2.5. In this study, the partition coefficient P_i was defined as the ratio of the concentration of a solute i in the upper phase (c_i^{UP}) to its concentration in the lower phase (c_i^{LP}) at thermodynamic equilibrium (Eq. (1)).

$$P_i = \frac{c_i^{UP}}{c_i^{LP}} \quad (1)$$

The partition coefficient of β -ionone, a hydrophobic compound with an octanol-water partition coefficient of $\log P = 3.77$, was first measured in the heptane/ethanol/CLA 1:2 systems A (25/50/25 wt%) to E (48.5/3/48.5 wt%). The objective was to determine the influence of the biphasic system composition on the solute partitioning. The partition coefficients of β -ionone and their corresponding logarithmic value are presented in Table 3.

The partition coefficient of β -ionone increased from system A to E. The observed tendency was closely linked to the change in the composition of the phases of systems A to E. The composition of the upper heptane-rich phase did not change significantly, with observed concentrations of approximately 90 wt% heptane in system A to approximately 100 wt% heptane in system E (Fig. 1). On the other hand, the concentration of DES in the lower DES-rich phase increased significantly from system A to system E, with concentrations ranging from 30 wt% in system A to approximately 90 wt% in system E (see Fig. 1). When the concentration of the DES in the lower phase was higher, concentration of β -ionone in this phase was lower, which produced a higher partition coefficient. Most importantly, the result of this experiment was that the partition coefficient of β -ionone in systems A–C was in the preferred range of liquid-liquid chromatography, while systems D and E were quite close to the preferred range.

In a next step, the scope of the experiments was extended to ten natural compounds, presented in Table 2. The compounds had different octanol-water partition coefficients ($\log P_{O/W}$) ranging between -5.1 and 12.0 . Their partition coefficients were deter-

Table 3Composition of heptane/ethanol/CLA 1:2 systems A–E and partition coefficients of β -ionone in systems A–E.

System	System composition [wt%] heptane/ethanol/CLA1:2	System composition [v/v/v] ^a heptane/ethanol/CLA1:2	Partition coefficient P_1 [-]	Partition coefficient $\log P_1$ [-]
A	25/50/25	1.67/2.89/1	0.95	-0.02
B	30/40/30	1.67/1.93/1	1.25	0.10
C	37.5/25/37.5	1.67/0.96/1	1.64	0.21
D	45/10/45	1.67/0.32/1	3.71	0.57
E	48.5/3/48.5	1.67/0.09/1	4.31	0.63

^a Calculated with the densities of the pure compounds at 20 °C ρ (n-heptane) = 0.6838 g cm⁻³, ρ (ethanol) = 0.7893 g cm⁻³, ρ (CLA1:2) = 1.1402 g cm⁻³, based on PubChem database, <http://pubchem.ncbi.nlm.nih.gov> (consulted 2015-12-08).

mined in two heptane/ethanol/CLA 1:2 systems and are presented in Fig. 2. The systems had an overall composition of 45/10/45 wt% (system D) and 30/40/30 wt% (system B). The partition coefficients of new coccine red (r) in both systems and naringenin (N) in system D are not presented in Fig. 2, since their concentration in the upper phase was below the detection limit of the UV-vis detector and hence their partition coefficients could not be calculated. These compounds partition almost exclusively to the lower phase and therefore have extremely low partition coefficients.

The partition coefficient increased from arbutin (A) to α -tocopherol (Y) and except for naringenin (N) correlates to the trend of the octanol-water partition coefficients (Table 2). Naringenin (N) contains three hydroxy groups, and thus the possibility of forming intermolecular hydrogen bonds within the DES-rich lower phase was increased. This might possibly explain why naringenin (N) partitioned exclusively to the DES-rich phase. Also, the trend in the change of the partition coefficient values from systems B to D was different for different components. In general, the partition coefficient for hydrophobic compounds increased with increasing DES concentrations in the lower phase (e.g., the partition coefficient in system D was higher than in system B). An opposite trend was observed for the hydrophilic components, except for arbutin (A). It should be noticed that the high experimental error could be the reason for this observation.

The partition coefficients of carvone (Ca), β -ionone (I) and retinol (R) were in the preferred range of CCC and CPC, with $\log P_1$ values between -0.4 and 0.4. The partition coefficients of coumarin (M) and α -tocopherol (Y) were also quite close to this range. Concerning the partition coefficients of the different solutes, the biphasic solvent system containing heptane/ethanol/CLA 1:2 appeared to be a promising non-aqueous system for CCC and CPC applications, especially for hydrophobic substances.

3.3. Comparison of heptane/ethanol/DES systems containing different DESs

The influence of the type of DES on the solute partitioning was analyzed in the biphasic system consisting of heptane/ethanol/DES. Initially, several DESs that are liquid at room temperature were selected from the literature. The investigated DESs included betaine with levulinic acid (BLA 1:2) and choline chloride with several HBDs (Table 1). The HBDs combined with choline chloride were levulinic acid (CLA 1:2), malonic acid (CMA 1:1), ethylene glycol (CEG 1:2), glycerol (CGL 1:2 and CGL 1:3), and 1,4-butanediol (CBD 1:3 and CBD 1:4).

For the comparison of heptane/ethanol/DES systems made with different DESs, β -ionone was used as a representative solute. Since no LLE data were available for all of the studied DESs, the composition of the heptane/ethanol/DES (37.5/25/37.5 wt%) system, corresponding to system C in Fig. 1, was selected. This composition was chosen due to its position in the center of the miscibility gap of the solvent system. If no biphasic system formed with the investigated DES at this point, the miscibility gap of the system may

have been too small or non-existent and thus not of great interest for liquid-liquid chromatography applications.

The formation of two phases was observed for all of the investigated DESs. Fig. 3 shows the partition coefficients of β -ionone in heptane/ethanol/DES with a global composition of 37.5/25/37.5 wt%. In all tested DES-based biphasic systems, except the CGL systems ($\log P_1 = 0.75$ with CGL 1:2 and $\log P_1 = 0.79$ with CGL 1:3), the partition coefficient of β -ionone was in the preferred range ($\log P_1 < 0.4$).

The difference in polarity between GL and the other HBD (LA, MA, EG and BD), caused by the different amount of hydroxy groups per molecule, may have been the reason for the higher partition coefficients of β -ionone in the heptane/ethanol/CGL systems. In general, β -ionone had a higher affinity to less polar solvents due to its $\log P_{O/W}$ of 3.77. The higher the polarity of the lower phase (i.e., DES-rich phase), the lower the β -ionone concentration was expected to be in this phase. Consequently, the partition coefficient in this case increased.

3.4. Influence of water content in DES-based biphasic systems on the partitioning coefficient

The absorption of water as a result of the exposure of DES to air was evaluated gravimetrically for two organic acid-based DESs (betaine and levulinic acid: BLA 1:2, choline chloride and levulinic acid: CLA 1:2), and two alcohol-based DES (choline chloride and ethylene glycol: CEG 1:2, choline chloride and glycerol: CGL 1:2). The water absorption in the DESs over time is presented in Fig. 4. The water content in the DES is presented on the ordinate, expressed as the ratio of the weight of water to the weight of the pure DES in percent.

After eight days of air contact, the alcohol-based DESs (CEG 1:2, CGL 1:2) had absorbed more water than the acid-based DESs (BLA 1:2, CLA 1:2). The absorption was observed to proceed faster over the first 50 h before slowly approaching an equilibrium concentration. Similar results were reported by Maugeri et al. [8] for

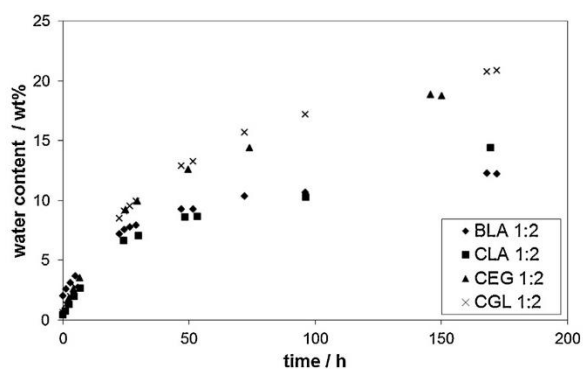


Fig. 4. Water absorption in BLA 1:2, CLA 1:2, CEG 1:2, CGL 1:2 over time.

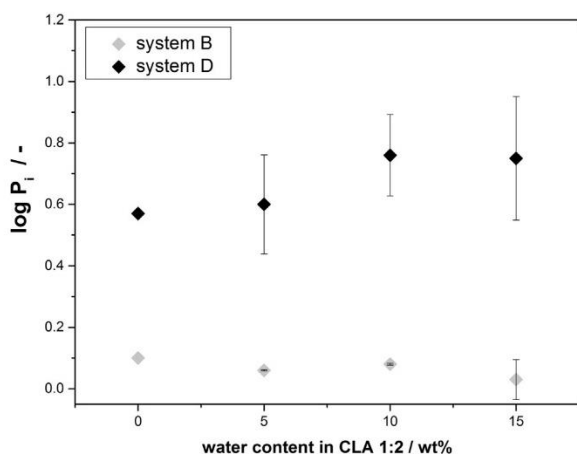


Fig. 5. Partition coefficients of β -ionone in heptane/ethanol/CLA 1:2 systems made of non-aqueous CLA 1:2 and CLA 1:2 with 5, 10, and 15 wt% of water (system B: 30/40/30 wt%; system D: 45/10/45 wt%).

CLA 1:2 (acid-based DES). Gutierrez et al. [41] studied a DES composed of choline chloride and urea or thiourea with concentrations of water > 50 wt%, and observed that the presence of a significant amount of water could weaken the hydrogen bonds between HBA and HBD, causing the DES to behave like an aqueous solution of its constituents (i.e., a water solution of HBA and HBD). Generally, the biphasic liquid systems in liquid-liquid chromatography are used shortly after their preparation. A typical separation run takes between a few minutes and a few hours, and thus the influence of water absorption over a longer period of time is not relevant.

Therefore, the influence of the water amount present in the DES on the partition coefficient of β -ionone in heptane/ethanol/CLA 1:2 was studied. A certain amount of water (0, 5, 10, and 15 wt%) was added to a freshly prepared DES composed of CLA 1:2. In the course of the preparation of the biphasic systems, this mixture of DES with water was then taken as the amount of pure DES. Two heptane/ethanol/DES systems were prepared: systems D and B. Afterwards, the partitioning of β -ionone in these systems was analyzed and is presented in Fig. 5. The standard deviation of the partition coefficient in system D was higher than in system B, which could be a result of the higher amount of DES in system D.

In both systems B (30/40/30 wt%) and D (45/10/45 wt%), no significant change in the partition coefficients of β -ionone with increasing water content in the DES was observed. This result consequently suggested that there was no strong need to work under a protective atmosphere while preparing the DES-based biphasic systems and during the separation run. Although this study should be extended to other DES systems and solutes to verify the findings, the preliminary results of this study should be of great interest for future industrial applications, since such working conditions are a major cost factor.

3.5. Physical properties of DES-based biphasic systems

Besides the partition coefficient P_i of the solutes, several physicochemical properties of biphasic solvent systems may affect the separation performance in liquid-liquid chromatography, including the difference in density of the two phases, the viscosity and interfacial tension (which influences the stationary phase retention), the mass transfer between the phases, and the pressure drop in the column [42].

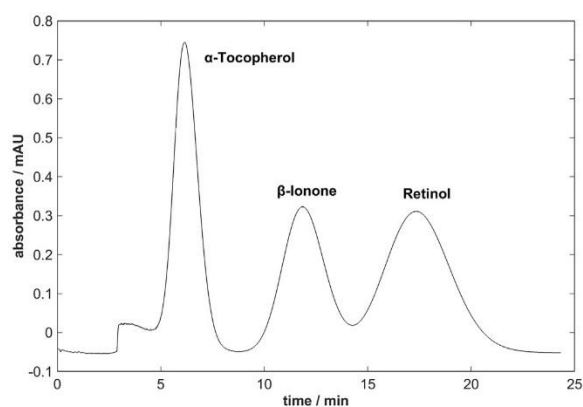


Fig. 6. Separation of a mixture of α -tocopherol, β -ionone, and retinol with a heptane/ethanol/CLA 1:2 system in ascending mode (mobile phase flowrate: 20 ml min⁻¹, revolution: 2000 rpm, detection wavelength: 295 nm). Stationary phase retention 76.2%; calculated partition coefficients: 0.33 (α -tocopherol), 0.93 (β -ionone), 1.51 (retinol).

The density, viscosity and settling time of the phases of four heptane/ethanol/DES biphasic systems with an overall composition of 37.5/25/37.5 wt% were measured at 20 °C. The systems are presented in Table 4 together with the data of some standard and newer liquid-liquid chromatography biphasic systems, including:

- one heptane/ethyl acetate/methanol/water system as a representative of a conventional organic solvent/water-based system;
- one polyethylene glycol (PEG)/phosphate salt system as a representative of a conventional aqueous two-phase system; and
- a novel ionic liquid/phosphate salt-based aqueous two-phase system (in this case, 1-Ethyl-3-methylimidazolium chloride ([EMIM] Cl) as an ionic liquid is shown).

All analyzed DES-based biphasic systems had a settling time in the range between 11 and 22 s, which is very similar to a traditionally used Arizona system, and showed similar densities. The differences in the density between the two phases were approximately 0.3 g cm⁻³, and thus the systems were suitable for liquid-liquid chromatography applications where systems with a density difference of at least 0.1 g cm⁻³ are favored. The density and dynamic viscosity of the upper phase of all DES-based biphasic systems were very similar and independent of the type of DES present in the biphasic system. This was an indication of the presence of an insignificant amount of DES in the upper phase of the studied heptane/ethanol/DES systems. The densities of the lower phase were very similar and were also close to the density of water, while the viscosities of the lower phase varied from system to system and strongly depended on the type of DES present. The main difference between the DES-based biphasic systems and the standard systems composed of water and an organic solvent, such as heptane/ethyl acetate/methanol/water, was the relatively high viscosity of the lower phase of the DES-based systems. However, in comparison to the aqueous two-phase systems, e.g., the PEG 1000/(K₂HPO₄/KH₂PO₄)/H₂O and [EMIM]Cl/(K₂HPO₄/KH₂PO₄)/H₂O systems, only one of the phases of the DES-based system is viscous (>1 mPas). An aqueous two-phase system containing PEG was recently tested with a CPE instrument (SCPE-250-BIO, Armen Instrument, France) with twin-cells and showed good stationary phase retention [46]. Hence, this unit was used for experiments with DES-based solvent systems.

Table 4
Density, dynamic viscosity and settling time of the phases of different biphasic liquid systems.

System	Composition	$\rho_{UP}[\text{g cm}^{-3}]$	$\rho_{LP}[\text{g cm}^{-3}]$	$\Delta\rho[\text{g cm}^{-3}]$	$\eta_{UP}[\text{mPa s}]$	$\eta_{LP}[\text{mPa s}]$	Settling time[s]
heptane/ethanol/BLA 1:2 ^a	37.5/25/37.5 (wt%)	0.690	0.981	0.291	0.596	9.276	18
heptane/ethanol/CLA 1:2 ^a	37.5/25/37.5 (wt%)	0.689	0.976	0.287	0.586	6.927	13
heptane/ethanol/CGL 1:2 ^a	37.5/25/37.5 (wt%)	0.695	1.010	0.315	0.604	17.033	22
heptane/ethanol/CEG 1:2 ^a	37.5/25/37.5 (wt%)	0.691	0.963	0.272	0.595	7.746	11
heptane/ethyl acetate/methanol/water ^{b,c}	7/3/6/5v/v/v/v	0.709	0.915	0.206	0.380	1.450	12
PEG 1000/(K ₂ HPO ₄ /KH ₂ PO ₄)/H ₂ O ^{b,d}	14.3/14.3/71.4 (wt%)	1.091	1.198	0.107	11.844	2.216	58
[EMIM]Cl/(K ₂ HPO ₄ /KH ₂ PO ₄)/H ₂ O ^{b,e}	22/20/58 (wt%)	1.127	1.399	0.272	3.162	5.263	28

^a 20 °C.

^b 25 °C.

^c [43].

^d [44].

^e [45].

3.6. Separation of multicomponent mixture with DES-based biphasic systems

The biphasic system heptane/ethanol/CLA 1:2 with an overall composition of 30/40/30 wt% was tested for the separation of a model mixture in both descending and ascending mode. Compounds with partition coefficients in the preferred range were selected for these experiments: α -tocopherol, retinol and β -ionone.

Fig. 6 presents the chromatogram resulting from the batch injection of a 5 ml mixture of β -ionone (27.5 mg), retinol (25.3 mg), and α -tocopherol (201.3 mg) performed in ascending mode with a mobile phase flow rate of 20 ml min⁻¹. The lower DES-rich phase was used as stationary phase. The stationary phase retention, i.e., the ratio of the volume of the stationary phase to the volume of the column, was 76.2%. No loss of stationary phase was observed during the separation run, and a complete separation of the three compounds was achieved. The partition coefficients calculated from the retention times of the components in this mode were 1.51 for retinol, 0.93 for β -ionone and 0.33 for α -tocopherol.

In descending mode, a mixture of naringenin (27.3 mg), β -ionone (27.2 mg), retinol (27.4 mg), and α -tocopherol (201.2 mg) was separated at mobile phase flow rates of 20 and 40 ml min⁻¹. Naringenin was selected as a void volume indicator in the descending mode because it partitions almost exclusively in the lower mobile phase and was therefore not retained. In both experiments, the mixture was dissolved in 5 ml of the mobile phase (DES-rich phase). The chromatograms are presented in Fig. 7a and b. The stationary phase retention was 74.8% at a mobile phase flow rate of 20 ml min⁻¹, and 61.6% at a mobile phase flow rate of 40 ml min⁻¹. There was no loss of stationary phase observed during the experimental runs. The calculated partition coefficients in descending mode at a flow rate of 20 ml min⁻¹ were 0.05 for naringenin, 0.79 for retinol, 1.25 for β -ionone and 3.24 for α -tocopherol, and at a flow rate of 40 ml min⁻¹ they were 0.16 for naringenin, 0.83 for retinol, 1.26 for β -ionone and 2.96 for α -tocopherol. They agreed considerably well with the values of the partition coefficient determined by shake flask experiments (Fig. 2). A higher separation resolution was achieved at a mobile phase flow rate of 20 ml min⁻¹ (Fig. 7a) compared to the rate at 40 ml min⁻¹ (Fig. 7b). This was attributed to the higher stationary phase retention at the lower mobile phase flow rate. However, by doubling the flow rate from 20 to 40 ml min⁻¹, the loss of resolution between retinol (R) and β -ionone (I) was not dramatic, only decreasing from 1 to 0.85. Considering that the resolution is proportional to the square root of the column length (i.e. the number of cells) and that the pressure drop in the column was far below the maximum allowed value, the loss of resolution at 40 ml min⁻¹ could be theoretically compensated by increasing the column length. Theoretically, at 40 ml min⁻¹ a resolution of 1 for retinol (R) and β -ionone (I) can be achieved by increasing the column length by about 40%

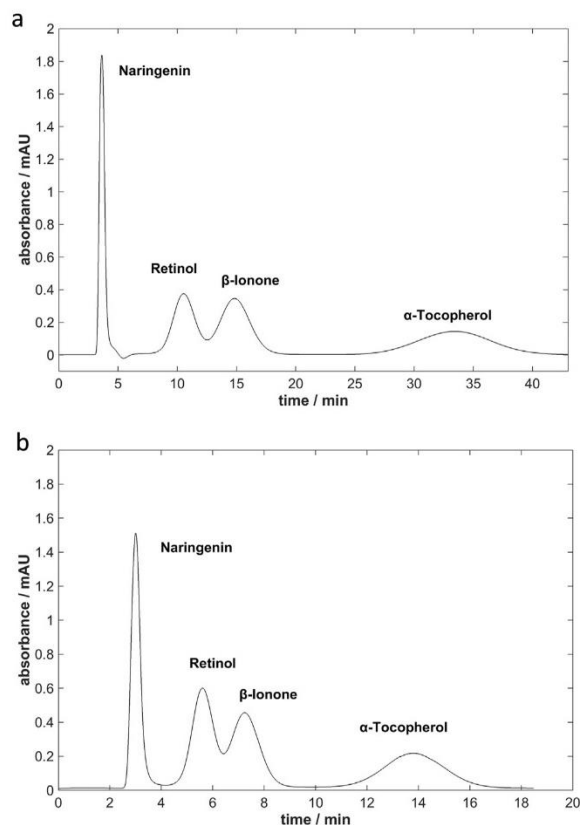


Fig. 7. Separation of a mixture of naringenin, retinol, β -ionone, and α -tocopherol with a heptane/ethanol/CLA 1:2 system in descending mode (revolution: 2000 rpm and detector wavelength: 295 nm).

(a) mobile phase flow rate 20 ml min⁻¹. Stationary phase retention 74.8%; calculated partition coefficients: 0.05 (naringenin), 0.79 (retinol), 1.25 (β -ionone), 3.24 (α -tocopherol).

(b) mobile phase flow rate 40 ml min⁻¹. Stationary phase retention 61.6%; calculated partition coefficients: 0.16 (naringenin), 0.83 (retinol), 1.26 (β -ionone), 2.96 (α -tocopherol).

$((1/0.85)^2 = 1.38 \approx 1.4)$. This would prolong the separation run by about 40%, from 17 min (see Fig. 7b) to approximately 24 min. Despite this increase in the experiment duration, the separation run will still be 40% shorter than the one at 20 ml min⁻¹ in the original column size $((40 \text{ min} - 24 \text{ min})/40 \text{ min} = 0.4)$. Consequently, the productivity would be approximately 65% higher than that achieved with the original column size at 20 ml min⁻¹.

These experiments demonstrated the potential of DES-based biphasic systems as alternative non-aqueous systems for the separation of hydrophobic molecules. Additionally, the DES-rich phase could be used either as the stationary or the mobile phase. Besides the relatively high viscosity of the DES-rich phase, the design of the twin-cells of the CPE column enabled the use of high flow rates while attaining relatively high stationary phase retention.

4. Conclusion

The applicability of deep eutectic solvent (DES)-based biphasic systems in liquid–liquid chromatography (LLC) was studied. The partition coefficients of ten natural compounds of different hydrophobicity were first determined in the non-aqueous biphasic system heptane/ethanol/DES (30/40/30 wt%), with a DES composed of choline chloride and levulinic acid in a molar ratio of 1:2. The partition coefficients of the hydrophobic compounds carvone ($\log P_{O/W} = 2.103$), β -ionone ($\log P_{O/W} = 3.770$), retinol ($\log P_{O/W} = 5.680$), and α -tocopherol ($\log P_{O/W} = 12.000$) were in, or very close to, the preferred range of liquid–liquid chromatography ($0.4 < P_1 < 2.5$). Compared to the conventional biphasic systems, the partition coefficient of these hydrophobic compounds could be successfully adjusted to the preferred range for LLC by using DES-based biphasic systems. In addition to the partition coefficient of the compounds, the physical properties of the systems could also be tuned not only by varying the composition of the biphasic systems, but also by varying different DESs (i.e., by different combinations of hydrogen bond donors and hydrogen bond acceptors). The physical properties (density, viscosity) of the DES-based biphasic systems were similar to the conventional biphasic systems, with the exception that the DES-rich phase had a higher viscosity.

The presence of up to 15 wt% water in the DES, which could have been a result of air exposure, was not observed to significantly affect the partition coefficients of the solutes in the studied systems. These preliminary results indicated that there was no strong need to work under a protective atmosphere while preparing and using the DES-based biphasic systems.

Finally, DES-based biphasic systems were demonstrated to be applicable for a separation performed in a centrifugal partition extractor (CPE). A mixture of hydrophobic compounds with a partition coefficient in the preferred range was successfully separated with the DES-rich phase as either the mobile phase or the stationary phase.

In conclusion, DESs have been shown to be a promising new class of solvents in LLC. They can be used to substitute water in biphasic systems that are composed of water and organic solvents. Although the recovery and re-use of DES is still an open topic for future studies, these new non-aqueous biphasic systems show great promise for the separation of hydrophobic substances.

Acknowledgements

The authors thank Prof. Wolfgang Arlt for supporting this study and Petra Kiefer and Lukas Weber for carrying out part of the experiments.

References

- [1] A.P. Abbott, G. Capper, D.L. Davies, R.K. Rasheed, V. Tambyrajah, Novel solvent properties of choline chloride/urea mixtures, *Chem. Commun.* 1 (2003) 70–71.
- [2] Q. Zhang, K. De Oliveira Vigier, S. Royer, F. Jerome, Deep eutectic solvents: syntheses, properties and applications, *Chem. Soc. Rev.* 41 (2012) 7108–7146.
- [3] A.P. Abbott, D. Boothby, G. Capper, D.L. Davies, R.K. Rasheed, Deep eutectic solvents formed between choline chloride and carboxylic acids: versatile alternatives to ionic liquids, *J. Am. Chem. Soc.* 126 (2004) 9142–9147.
- [4] R.C. Harris, *Physical Properties of Alcohol Based Deep Eutectic Solvents*, Ph.D. Thesis, University of Leicester, 2009.
- [5] M.A. Kareem, F.S. Mjalli, M.A. Hashim, I.M. AlNashef, Phosphonium-based ionic liquids analogues and their physical properties, *J. Chem. Eng. Data* 55 (2010) 4632–4637.
- [6] A. Yadav, S. Trivedi, R. Rai, S. Pandey, Densities and dynamic viscosities of (choline chloride + glycerol) deep eutectic solvent and its aqueous mixtures in the temperature range (283.15–363.15) K, *Fluid Phase Equilib.* 367 (2014) 135–142.
- [7] A. Pandey, R. Rai, M. Pal, S. Pandey, How polar are choline chloride-based deep eutectic solvents? *Phys. Chem. Chem. Phys.* 16 (2014) 1559–1568.
- [8] Z. Maugeri, P. Dominguez de María, Novel choline-chloride-based deep-eutectic-solvents with renewable hydrogen bond donors: levulinic acid and sugar-based polyols, *RSC Adv.* 2 (2012) 421.
- [9] B. Tang, K.H. Row, Recent developments in deep eutectic solvents in chemical sciences, *Monatsh. Chem.* 144 (2013) 1427–1454.
- [10] E.L. Smith, A.P. Abbott, K.S. Ryder, Deep eutectic solvents (DESs) and their applications, *Chem. Rev.* 114 (2014) 11060–11082.
- [11] B. Tang, H. Zhang, K.H. Row, Application of deep eutectic solvents in the extraction and separation of target compounds from various samples, *J. Sep. Sci.* 38 (2015) 1053–1064.
- [12] Y.T. Dai, J. van Spronsen, G.J. Witkamp, R. Verpoorte, Y.H. Choi, Ionic Liquids and Deep Eutectic Solvents in Natural Products Research: Mixtures of Solids as Extraction Solvents, *J. Nat. Prod.* 76 (2013) 2162–2173.
- [13] M. Francisco, A. van den Bruinhorst, M.C. Kroon, New natural and renewable low transition temperature mixtures (LTTMs): screening as solvents for lignocellulosic biomass processing, *Green Chem.* 14 (2012) 2153–2157.
- [14] M. Francisco, A. van den Bruinhorst, M.C. Kroon, Low-transition-temperature mixtures (LTTMs): a new generation of designer solvents, *Angew. Chem. Int. Edit. Engl.* 52 (2013) 3074–3085.
- [15] A. Paiva, R. Craveiro, I. Aroso, M. Martins, R.L. Reis, A.R.C. Duarte, Natural deep eutectic solvents—solvents for the 21st century, *ACS Sustainable Chem. Eng.* 2 (2014) 1063–1071.
- [16] Q. Zeng, Y. Wang, Y. Huang, X. Ding, J. Chen, K. Xu, Deep eutectic solvents as novel extraction media for protein partitioning, *Analyst* 139 (2014) 2565–2573.
- [17] M.A. Kareem, F.S. Mjalli, M.A. Hashim, I.M. AlNashef, Liquid–liquid equilibria for the ternary system (phosphonium based deep eutectic solvent–benzene–hexane) at different temperatures: a new solvent introduced, *Fluid Phase Equilib.* 314 (2012) 52–59.
- [18] M. Sarwono, M. Hadji-Kali, I. Alnashef, Application of deep eutectic solvents for the separation of aliphatics and aromatics, *Technology, Informatics, Management, Engineering, and Environment (TIME-E)*, International Conference on, IEEE (2013) (2013) 48–53.
- [19] M. Hayyan, M.A. Hashim, A. Hayyan, M.A. Al-Saadi, I.M. AlNashef, M.E.S. Mirghani, O.K. Saheed, Are deep eutectic solvents benign or toxic? *Chemosphere* 90 (2013) 2193–2195.
- [20] W. Bi, M. Tian, K.H. Row, Evaluation of alcohol-based deep eutectic solvent in extraction and determination of flavonoids with response surface methodology optimization, *J. Chromatogr. A* 1285 (2013) 22–30.
- [21] M.W. Nam, J. Zhao, M.S. Lee, J.H. Jeong, J. Lee, Enhanced extraction of bioactive natural products using tailor-made deep eutectic solvents: application to flavonoid extraction from *Flos sophorae*, *Green Chem.* 17 (2015) 1718–1727.
- [22] K. Shahbaz, F. Mjalli, M. Hashim, I. AlNashef, Using deep eutectic solvents based on methyl triphenyl phosphonium bromide for the removal of glycerol from palm-oil-based biodiesel, *Energy Fuels* 25 (2011) 2671–2678.
- [23] S. Mulyono, H.F. Hizaddin, I.M. Alnashef, M.A. Hashim, A.H. Fokeeha, M.K. Hadji-Kali, Separation of BTEX aromatics from n-octane using a (tetrabutylammonium bromide+ sulfolane) deep eutectic solvent—experiments and COSMO-RS prediction, *RSC Adv.* 4 (2014) 17597–17606.
- [24] K. Pang, Y. Hou, W. Wu, W. Guo, W. Peng, K.N. Marsh, Efficient separation of phenols from oils via forming deep eutectic solvents, *Green Chem.* 14 (2012) 2398–2401.
- [25] W. Guo, Y. Hou, W. Wu, S. Ren, S. Tian, K.N. Marsh, Separation of phenol from model oils with quaternary ammonium salts via forming deep eutectic solvents, *Green Chem.* 15 (2013) 226–229.
- [26] J. Brent Friesen, G.F. Pauli, G.U.E.S.S.—a generally useful estimate of solvent systems for CCC, *J. Liq. Chromatogr. Relat. Technol.* 28 (2005) 2777–2806.
- [27] S. Adelmann, T. Balhoff, B. Koepcke, G. Schembecker, Selection of operating parameters on the basis of hydrodynamics in centrifugal partition chromatography for the purification of nymbycin derivatives, *J. Chromatogr. A* 1274 (2013) 54–64.
- [28] J.B. Friesen, G.F. Pauli, Rational development of solvent system families in counter-current chromatography, *J. Chromatogr. A* 1151 (2007) 51–59.
- [29] A. Berthod, *Countercurrent chromatography: The Support-Free Liquid Stationary Phase*, Elsevier Science & Technology, Amsterdam, 2002.
- [30] A.P. Foucault, *Centrifugal partition chromatography Chromatographic Series*, vol. 68, M. Dekker, New York, 1995.
- [31] F. Oka, H. Oka, Y. Ito, Systematic search for suitable two-phase solvent systems for high-speed counter-current chromatography, *J. Chromatogr. A* 538 (1991) 99–108.
- [32] I.J. Garrard, L. Janaway, D. Fisher, Minimising solvent usage in high speed high loading, and high resolution isocratic dynamic extraction, *J. Liq. Chromatogr. Relat. Technol.* 30 (2007) 151–163.
- [33] I.A. Sutherland, D. Fisher, Role of counter-current chromatography in the modernisation of Chinese herbal medicines, *J. Chromatogr. A* 1216 (2009) 740–753.

- [34] G.F. Pauli, S.M. Pro, J.B. Friesen, Countercurrent separation of natural products#, *J. Nat. Prod.* 71 (2008) 1489–1508.
- [35] K. Skalicka-Woźniak, I. Garrard, A comprehensive classification of solvent systems used for natural product purifications in countercurrent and centrifugal partition chromatography, *Nat. Prod. Rep.* 32 (2015) 1556–1561.
- [36] J.B. Friesen, J.B. McAlpine, S.-N. Chen, G.F. Pauli, Countercurrent separation of natural products: an update, *J. Nat. Prod.* 78 (2015) 1765–1796.
- [37] Y. Dai, J. van Spronsen, G.J. Witkamp, R. Verpoorte, Y.H. Choi, Natural deep eutectic solvents as new potential media for green technology, *Anal. Chim. Acta* 766 (2013) 61–68.
- [38] H.G. Morrison, C.C. Sun, S. Neervannan, Characterization of thermal behavior of deep eutectic solvents and their potential as drug solubilization vehicles, *Int. J. Pharm.* 378 (2009) 136–139.
- [39] F.S. Oliveira, A.B. Pereiro, L.P. Rebelo, I.M. Marrucho, Deep eutectic solvents as extraction media for azeotropic mixtures, *Green Chem.* 15 (2013) 1326–1330.
- [40] A.S.B. Gonzalez, M. Francisco, G. Jimeno, S.L.G. de Dios, M.C. Kroon, Liquid–liquid equilibrium data for the systems {LTTM + benzene + hexane} and {LTTM + ethyl acetate + hexane} at different temperatures and atmospheric pressure, *Fluid Phase Equilib.* 360 (2013) 54–62.
- [41] M.a.C. Gutieirrez, M.L. Ferrer, C.R. Mateo, F. del Monte, Freeze-drying of aqueous solutions of deep eutectic solvents: a suitable approach to deep eutectic suspensions of self-assembled structures, *Langmuir* 25 (2009) 5509–5515.
- [42] M.J. van Buel, L.A. van der Wielen, K.C.A.M. Luyben, Pressure drop in centrifugal partition chromatography, *J. Chromatogr. A* 773 (1997) 1–12.
- [43] S. Adelmann, G. Schembecker, Influence of physical properties and operating parameters on hydrodynamics in Centrifugal Partition Chromatography, *J. Chromatogr. A* 1218 (2011) 5401–5413.
- [44] J. Goll, M. Minceva, Unpublished research data.
- [45] F. Bezold, J. Goll, M. Minceva, Study of the applicability of non-conventional aqueous two-phase systems in counter-current and centrifugal partition chromatography, *J. Chromatogr. A* 1388 (2015) 126–132.
- [46] J. Goll, G. Audo, M. Minceva, Comparison of twin-cell centrifugal partition chromatographic columns with different cell volume, *J. of Chromatogr. A* 1406 (2015) 129–135.
- [47] PubChem database (consulted 2015–12–07) <http://pubchem.ncbi.nlm.nih.gov>.

3.3. Paper III: Influence of temperature on the separation performance in solid support-free liquid-liquid chromatography

3.3.1. Summary

Citation

S. Roehrer, M. Minceva, (2019). Influence of temperature on the separation performance in solid support-free liquid-liquid chromatography. *Journal of Chromatography A*, 1594, 129-139.

<https://doi.org/10.1016/j.chroma.2019.02.011>

Summary

In LLC, stationary and mobile phase correspond to two phases of a biphasic liquid solvent system that is in thermodynamic equilibrium. The liquid-liquid equilibrium of the system is a function of temperature. Therefore, the composition of the two liquid phases and their physical properties (density, viscosity, interfacial tension) are potentially susceptible to a temperature change. The objective of this work was to analyze the influence of a temperature increase on the separation performance. In this context, the temperature may change due to dissipation, as a result of friction within the piston pumps or due to the rotation of the column including mechanical seals, as well as by external environmental influences, i.e. changes in the room temperature. In this context, two frequently used systems in LLC, the aqueous-organic biphasic solvent system *n*-heptane/ethyl acetate/methanol/water (Arizona N) and the non-aqueous system *n*-hexane/ethyl acetate/acetonitrile, were analyzed. Although only small changes in the phase composition of mobile and stationary phase at liquid-liquid equilibrium and the partitioning of the solutes could be observed for Arizona N, the non-aqueous system was significantly affected between 25 °C and 40 °C. It was shown that changes occur especially in the physical properties of the phases, causing a significant decrease in stationary phase retention and resolution, which cannot be compensated by the observed increase in column efficiency as a result of enhanced mass transfer between the phases. Interestingly, it was found that an additional destabilizing effect of the system occurred when a temperature difference between mobile phase inlet temperature and column temperature exceeds only 10 °C. Hence, this study demonstrates the necessity of an efficient temperature control system for satisfactory separations with temperature sensitive systems. In terms of the aqueous-organic system, even a slightly beneficial effect was observed with an increase of the temperature, where a slight increase in stationary phase retention occurred. Hence, for such systems temperature may also be used purposefully to modify and enhance the separation. The measurement of system stability together with settling time was identified as an easy but reliable indicator for temperature susceptibility and can be used as a standard procedure during separation method development.

Contributions

The author of this dissertation was the lead scientist in all parts of the work. He planned and coordinated the work, conducted or supervised all data acquisition and performed most of the laboratory work. L. Braumann measured part of the LLE data and D. André performed part of the CCC pulse injections and density measurements. T. Goudoulas assisted the author with the determination of the dynamic viscosity of the phases. The manuscript was written by the author and discussed with M. Minceva.



Contents lists available at ScienceDirect

Journal of Chromatography A

journal homepage: www.elsevier.com/locate/chroma

Influence of temperature on the separation performance in solid support-free liquid-liquid chromatography



Simon Roehrer, Mirjana Minceva*

Biothermodynamics, TUM School of Life and Food Sciences Weihenstephan, Technical University of Munich, Maximus-von-Imhof-Forum 2, 85354 Freising, Germany

ARTICLE INFO

Article history:

Received 3 December 2018

Received in revised form 25 January 2019

Accepted 4 February 2019

Available online 15 February 2019

Keywords:

Countercurrent chromatography
Centrifugal partition chromatography
Column temperature
Resolution
Stationary phase retention
Non-aqueous biphasic systems

ABSTRACT

In a biphasic liquid system, temperature affects the phase composition, so that a change in temperature can even turn the system into a single-phase system. Furthermore, temperature influences the physical properties of the phases, such as density, viscosity and interfacial tension. In this work, temperature was evaluated as an influencing factor for the separation performance in solid support-free liquid-liquid chromatography, i.e. countercurrent chromatography and centrifugal partition chromatography. To this end, two biphasic systems were selected: the non-aqueous solvent system *n*-hexane/ethyl acetate/acetonitrile (11.2/2.0/5.3 v/v/v at 25 °C) and the aqueous-organic system *n*-heptane/ethyl acetate/methanol/water (1/1/1/1 v/v/v/v at 25 °C). The effect of elevated temperature on the separation was systematically analyzed between 25 °C and 40 °C. The results were related to the changes in the liquid-liquid equilibria of the solvent systems and physical properties of the phases. The temperature influence on the stationary phase retention, column efficiency and separation resolution was analyzed. An appropriate temperature control of the column was shown to be essential in order to avoid destabilizing the biphasic system and enable a satisfactory separation for temperature sensitive systems. In this context, the influence of different column and mobile phase inlet temperature on the separation performance was investigated by pulse injections. In addition, the stability and settling time of the biphasic systems were evaluated as indicators whether temperature susceptibility needs to be considered during method development in order to prevent a decrease in separation resolution.

© 2019 Elsevier B.V. All rights reserved.

1. Introduction

In recent years, solid support-free liquid-liquid chromatography (LLC), i.e. countercurrent chromatography (CCC) and centrifugal partition chromatography (CPC), has become a powerful separation technique with increasing popularity in the field of active natural compounds [1,2]. The number of applications has risen tremendously in the last decade [2,3]. Consequently, the variety of biphasic solvent systems used in different applications has increased as well [3]. Most often, a biphasic liquid system composed of 2–4 solvents is used as mobile and stationary phase for the separation in LLC [3–6]. Up to now, almost exclusively organic solvent-based biphasic systems are applied at preparative scale. These include both non-aqueous systems and aqueous-organic systems, such as the well-known solvent system families HEMWat

composed of *n*-hexane/ethyl acetate/methanol/water or Arizona with *n*-heptane/ethyl acetate/methanol/water [4,6].

For all solvent systems, the phases are usually prepared by mixing predefined volume portions of the solvents. Subsequently, the phases are normally equilibrated at room temperature or at a certain temperature with the help of a water bath, and split into two different containers before using them in a CCC or CPC separation run. However, the temperature of the mobile and stationary phase often is not controlled during the separation inside the column. An increase in column temperature may occur during the separation process in units with no or insufficient temperature control of the column and/or the inlet temperature of the mobile phase, e.g. due to a missing temperature controlled solvent reservoir. While current lab-scale CCC units are equipped with external temperature control systems where a liquid cooling fluid circulates to cool the column housing, fans are usually installed in CPC units for convective cooling of the column with ambient air. Hence, the user cannot actively modify the column temperature. It is well known from conventional liquid chromatography with solid stationary phases, that temperature is a crucial parameter that influences the separa-

* Corresponding author.

E-mail address: mirjana.minceva@tum.de (M. Minceva).

<https://doi.org/10.1016/j.chroma.2019.02.011>

0021-9673/© 2019 Elsevier B.V. All rights reserved.

tion, i.e. adsorption isotherms, hydrodynamics, and mass transfer [7–10]. Especially for the application at preparative scale this might be an important issue to be evaluated during method development in order to ensure process stability and reproducibility.

In LLC, the temperature influences the liquid-liquid equilibrium (LLE) of the biphasic solvent systems i.e. the compositions of the mobile and stationary phases. On the one hand, the change in phase composition alters the partitioning of solutes between the phases. On the other hand, the physical properties of the phases are influenced, such as density, viscosity and interfacial tension. In this context, hydrodynamics play an essential role and influence the separation [11–14]. As a result, stationary phase retention, phase distribution in the column (contact area between the phases) and the diffusion coefficients of the solutes, which are determining the mass transfer rate are influenced. In summary, the temperature can impact all three parameters that determine the resolution: partition coefficient, stationary phase retention and column efficiency. How strongly the temperature affects the separation depends on the particular solvent system. Hence, the influence may be more critical for some systems than others. In some cases, a temperature change might lead to one phase or may cause the formation of a third phase.

Liquid-liquid equilibrium data of aqueous-organic and non-aqueous biphasic systems at different temperatures with corresponding physical properties of the phases are limited. In addition, data is often difficult to compare between the sources due to different solvent grades used. For LLE measurements, mostly analytical grade solvents are used, while in LLC solvents varying from technical grade to analytical grade. Up to now, the temperature influence on the separation in LLC is addressed in only few publications and have not been studied systematically [4,15–18]. Berthod et al. [19] performed the first study on the influence of temperature on the parameters governing a LLC separation. The study was performed with an octanol-water system at temperatures between 15 °C and 35 °C, and a CPC column that was placed in an adjustable temperature box. In addition to the change of the partition coefficient, they have observed an increase of the column efficiency that was attributed to the significant decrease of the viscosity of the octanol-rich phase with the increase of temperature. In general, non-aqueous biphasic solvent systems, i.e. systems containing ethyl acetate, are described to be potentially susceptible to temperature in LLC [5]. In some cases, a decrease of the biphasic area with rising temperatures is observed, e.g. for the system *n*-hexane/dichloromethane/acetonitrile, resulting in a single-phase system [17]. Further, a change in the partition coefficient was observed [20], which can affect the resolution of a certain separation in different ways [18,21]. An improved separation performance with a higher resolution at higher temperatures was observed by Ito et al. [21] for butanol-water-based systems and by Friesen et al. [18] for the aqueous-organic system HEMWat especially due to an improved stationary phase retention at higher temperatures. Nevertheless, the influence of temperature on LLE differs for different solvent systems and hence has to be evaluated separately. A general decrease in viscosity and an increase in efficiency with increasing temperature was observed for most studied systems [21]. Therefore, working at higher temperatures might be advantageous for systems with a highly viscous mobile phase in order to improve CCC separations [22].

In conventional liquid chromatography with a solid stationary phase, the influence of temperature is already well explored, while a systematic investigation of the influence on the separation in solid support-free liquid-liquid chromatography (LLC) is still missing. In the current study, two different frequently used solvent systems, an aqueous-organic solvent-based Arizona system (*n*-heptane/ethyl acetate/methanol/water, 1/1/1/1 v/v/v/v at 25 °C) and a non-aqueous solvent system *n*-hexane/ethyl

acetate/acetonitrile (11.2/2.0/5.3 v/v/v at 25 °C) were selected as reference systems. For the two systems, a systematic evaluation of the influence of temperature on the phase composition and physical properties of the phases was performed. Its effects on the stationary phase retention, partition coefficient, efficiency and separation resolution were analyzed. Subsequently the influence of column and mobile phase inlet temperature on the separation performance was investigated at different temperatures and evaluated by pulse injections.

2. Materials and methods

2.1. Chemicals

For the preparation of the biphasic systems, the solvents *n*-hexane (purity: ≥95%, Honeywell, Germany), *n*-heptane (purity: ≥99%, Merck KGaA, Germany), acetonitrile (purity: ≥99%, J.T. Baker, Netherlands), ethyl acetate and methanol (purity: ≥99%, Merck KGaA, Germany) were used. Milli-Q water was obtained from a Milli-Q Direct Water Purification System from Merck Millipore (Germany).

In this study, the solutes methyl paraben (MP, purity: 99%), ethyl paraben (EP, 99%), propyl paraben (PP, 99%), butyl paraben (BP, 99%), D/L-tryptophan (99%), and α -tocopherol (99%) were obtained from Alfa Aesar GmbH & Co KG (Germany), while β -ionone (96%) and S-carvone (≥98.5%) were purchased from Sigma Aldrich (Germany).

2.2. Equipment and methods

2.2.1. Preparation of the biphasic liquid systems and feed mixtures

The biphasic liquid systems *n*-heptane/ethyl acetate/methanol/water (1/1/1/1 v/v/v/v at 25 °C, 7.01/10.50/25.38/57.11 mol%, 20.2/26.7/23.4/29.7 wt%) and *n*-hexane/ethyl acetate/acetonitrile (11.2/2.0/5.3 v/v/v at 25 °C, 41.43/9.92/48.65 mol%, 55.4/13.6/31.0 wt%) were prepared by mixing the corresponding portions of the solvents at ambient temperature and pressure. The mixture was then vigorously shaken and equilibrated at the selected temperatures between 25 °C and 40 °C for at least two hours in a water bath. After that, the phases were split and placed in two separate containers at the selected temperature. The containers were temperature controlled with a water bath.

Feed solutions were prepared by adding appropriate amounts of the solutes to the mobile phase used for the pulse injections, upper phase in ascending mode or lower phase in descending mode. For the pulse injections with the *n*-heptane/ethyl acetate/methanol/water system in descending mode, D/L-tryptophan, methyl-, ethyl-, propyl- and butyl paraben were used at a sample concentration of 2 mg ml⁻¹ respectively. In the case of the non-aqueous system *n*-hexane/ethyl acetate/acetonitrile, β -ionone (2 mg ml⁻¹), S-carvone (5 mg ml⁻¹) and butyl paraben (2 mg ml⁻¹) were used. In ascending mode, α -tocopherol (10 mg ml⁻¹) was used instead of butyl paraben.

2.2.2. Determination of the physical properties

The physical properties of the phases of the equilibrated solvent systems were determined at distinct temperatures between 25 and 40 °C. The biphasic systems were prepared according to section 2.2.1 in 20 ml flasks and the respective temperature was set in the equipment settings.

The density of the phases of the biphasic solvent systems was measured with an oscillating U-tube density meter DM 40 from Mettler Toledo (Columbus, USA). The measuring principle is a vibrational tube. The swinging is correlated with the density of the probe

at a certain temperature. The dynamic viscosity was determined with a MCR-502 rheometer from Anton Paar GmbH (Ostfildern-Scharnhausen, Germany). A titanium parallel plate geometry with a diameter of 60 mm and a distance of 30 μm was used with a constant shear rate of 10 s^{-1} . The plate distance during sample application was 1 mm. The interfacial tension between the phases of the biphasic systems was measured with a drop volume tensiometer (DVT 50) from KRÜSS GmbH (Germany). For the measurements, a capillary with a diameter of 0.254 mm was used. The experimentally determined phase densities (shown in section 3.1.) were used as input parameters for the tensiometer to determine the interfacial tension. It must be noted that two different methods were used to determine the interfacial tension: *falling drop* with the drops of lower phase dispersing in the upper phase and vice versa the *rising drop*.

2.2.3. Determination of settling time

For the two studied biphasic solvent systems, the respective amounts of the solvents were added to a sealable 20 ml flask, vigorously shaken and adjusted with a water bath to the particular temperature for at least 2 h in order to achieve thermodynamic equilibrium. Afterwards the phase boundary between upper and lower phase was marked, the vial was vigorously shaken for 10 s and the settling time was measured with a stopwatch. Phase separation was assumed as soon as a clear phase boundary was formed.

2.2.4. Analysis of phase composition

For the GC-analysis, calibration curves were established for the analyzed solvents diluted in THF. For both systems, samples of upper and lower phase diluted in THF were analyzed as described subsequently.

The phase composition of the *n*-heptane/ethyl acetate/methanol/water (1/1/1/1 v/v/v/v at 25 °C, 20.2/26.7/23.4/29.7 wt%) system was analyzed using a Nexis GC 2030 coupled with a thermal conductivity detector (TCD) from Shimadzu (Germany). A Restek Rxi-624Sil MS capillary column (30 m length, 0.25 mm inner diameter, 1.4 μm film thickness) was used in split mode and helium as carrier gas with a linear velocity controlled flow of 23 cm s^{-1} . The inlet temperature was set to 250 °C with a split-ratio of 50 during injection. An injection volume of 1 μl was applied. The initial column temperature was set to 35 °C and maintained for 2.5 min before a temperature gradient of 15 °C min^{-1} to 50 °C was applied. The temperature was kept for additional 5 min. Then, another temperature gradient of 30 °C min^{-1} to 160 °C was applied. The TCD temperature was set to 260 °C.

The phase composition of the *n*-hexane/ethyl acetate/acetonitrile (11.2/2.0/5.3 v/v/v at 25 °C, 55.4/13.6/31.0 wt%) system was analyzed using a Nexis GC 2030 coupled with a flame ionization detector (FID) from Shimadzu (Germany). A Restek Rxi-17Sil MS capillary column (30 m length, 0.25 mm inner diameter, 0.25 μm film thickness) was used in split mode and helium as carrier gas with a linear velocity controlled flow of 23 cm s^{-1} . The inlet temperature was set to 300 °C with a split-ratio of 50 during injection. An injection volume of 1 μl was applied. The initial column temperature was set to 50 °C and maintained for 5 min before a temperature gradient of 30 °C min^{-1} to 140 °C was applied. The final temperature was kept for additional 7 min. The FID temperature was set to 300 °C.

2.2.5. Countercurrent chromatography experiments

CCC pulse injections were performed on a countercurrent chromatography column, model HPCCC-Mini Centrifuge (0.8 mm i.d.) from Dynamic Extractions (Wales), with a total column volume of 18.2 ml. Two isocratic Gilson 306 pumps (Gilson, USA), equipped with an 806 Manometric Module (Gilson, USA), were used for

delivering the mobile and stationary phases. The elution profiles were monitored with a DAD 171 diode array detector (Gilson, USA) at wavelengths of 255 nm and 280 nm. Pulse injections were carried out with the non-aqueous solvent system *n*-hexane/ethyl acetate/acetonitrile (11.2/2.0/5.3 v/v/v at 25 °C) and the aqueous-organic system *n*-heptane/ethyl acetate/methanol/water (1/1/1/1 v/v/v/v at 25 °C).

At the beginning of each experiment, the column was filled with the phase intended to be used as stationary phase. Afterwards, the rotational speed was set to 1900 rpm and the mobile phase was pumped through the column at 1 ml min^{-1} for at least one column volume. The reported stationary phase retention was determined from the collected amount of stationary phase after pumping one column volume of mobile phase. The samples were introduced through a manual 6-port valve and an injection loop of 72 μl (<1% of the total column volume). The mobile phase was continuously pumped at 1 ml min^{-1} and stationary phase loss, if there was any, was recorded during the run. For all experiments, a tempered water bath was used in order to keep the containers filled with stationary and mobile phase at constant temperature. In addition, an external temperature control system (FL 300, Julabo, Germany) was connected to the CCC column and manually controlled to set a particular column temperature at the temperature controller of the bobbin. The measuring cylinder for the column outlet was placed in a tempered water bath and sealed up with Parafilm® to avoid evaporation of the eluate.

Two different types of CCC experiments were carried out: pulse injections at constant temperature, i.e. same mobile phase inlet temperature and column temperature, and pulse injections at constant but different mobile phase inlet temperature and column temperature. For the experiments with different mobile phase inlet temperature and column temperature, the mobile phase inlet temperature was set to 25 °C while the column temperature was set to 35 °C or 40 °C. This was intended to imitate a column without or with efficient temperature control in order to show the effect of temperature change during the separation.

2.2.6. Centrifugal partition chromatography (CPC) experiments

Experiments were carried out on a centrifugal partition chromatography (CPC) column, model SCPC 250, from Armen Instrument (now called CPC 250, Gilson Purification SAS, France), as described by Hopmann et al. [23]. Two single columns are connected in series resulting in a total column volume of 182.1 ml. The column was equipped with two HPLC gradient pumps (Armen Instrument, France) and the effluent monitored with a UV detector (ECOM DAD600 2 W L 200–600 nm, Czech Republic) at 255 nm and 280 nm. The experimental procedure of the pulse injection experiment is similar to the procedure described in section 2.2.5 for a CCC column. In CPC, the rotational speed was set to 1700 rpm and the flow rate to 12 ml min^{-1} . The injection loop had a volume of 1 ml (<1% of the total column volume). A water bath was used in order to keep the mobile phase inlet temperature constant at 25 °C. For the CPC pulse injections two different types of column cooling were used: For the experiments “without additional cooling”, the integrated fan was used for cooling the column with ambient air. For the experiments “with additional cooling”, additional vessels with ice were placed on top of the cabin in order to keep the column temperature preferably constant at ambient temperature and to minimize uncontrolled warming of the column. Unfortunately, the actual column temperature could not be determined and hence, no defined column temperature could be controlled as in the CCC experiments. Still, the experiments simulate experimental conditions under approximately ambient temperature conditions or increasing column temperature.

3. Results and discussion

In the current study, the impact of temperature on two solvent systems, the non-aqueous system *n*-hexane/ethyl acetate/acetonitrile and the aqueous-organic *n*-heptane/ethyl acetate/methanol/water was investigated. The system *n*-hexane/ethyl acetate/acetonitrile is widely used in LLC, for example, for the separation of carotenoids and terpenoids [24]. The *n*-heptane/ethyl acetate/methanol/water system is applied to the separation of a vast number of diverse medium polar compounds [3]. First, the temperature influence on the phase composition and specific phase properties (Section 3.1) was determined between 25 °C and 40 °C. The temperature range was selected in order to study a possible and representative operating range between room temperature and extreme conditions, e.g. a hot summer, which could occur in the lab when no air conditioning is available. In addition, the maximum recommended operating temperature by the CCC manufacturer is 40 °C. Furthermore, the influence of column temperature and mobile phase inlet temperature on the separation performance in LLC was analyzed with pulse injections of model solutes at both same and different mobile phase inlet temperatures and column temperatures (Section 3.2).

3.1. Influence of temperature on the phase composition and specific phase properties

In LLC publications, the system compositions are commonly given in volume portions without referring to any temperature, since room temperature is assumed. However, the same volume portions at different temperatures would lead to different molar and mass ratios. For the evaluation of the temperature influence on the phase composition and system specific properties, i.e. physical properties of the phases, the following system compositions were selected:

- (i) *n*-hexane/ethyl acetate/acetonitrile 11.2/2.0/5.3 v/v/v at 25 °C (41.43/9.92/48.65 mol%, 55.4/13.6/31.0 wt%), which is located in the middle of the miscibility gap to ensure that it does not turn into a monophasic system with a small temperature change (see reference system in the phase diagram Fig. A in supplementary data). In the following sections, the system is just called Hex/EtOAc/ACN.
- (ii) *n*-heptane/ethyl acetate/methanol/water 1/1/1/1 v/v/v/v at 25 °C (7.01/10.5/25.38/57.11 mol%, 20.2/26.7/23.4/29.7 wt%), known as Arizona N system.

The phase compositions of the two systems between 25 °C and 40 °C are presented in Fig. 1. For the *n*-hexane/ethyl acetate/acetonitrile (Fig. 1a-b, see also supplementary data Table B), the amount of acetonitrile (3) is increased and that of hexane (1) is decreased in the upper phase at 40 °C compared to 25 °C. It is reverse but less pronounced for the lower phase. The amount of ethyl acetate (2) in both phases seems to be almost unaffected within the studied temperature range. The measured phase composition slightly differs from the data reported by Qiao et al. [25]. The most probable reason for the observed differences is the purity of the solvents used. In the work of Qiao et al. [25] analytical grade solvents were used, while in this work technical HPLC grade solvents were applied as commonly used in LLC. However, in both works similar influence of the temperature on the miscibility gap was observed. The miscibility gap slightly decreases with the increase in temperature (see supplementary data Fig. A). In comparison, the phase composition of the *n*-heptane/ethyl acetate/methanol/water system Arizona N was clearly less affected by the temperature increase within the studied range (Fig. 1c-d, see also supplementary data Table C). Nevertheless, in both systems the phase composi-

tion does not change significantly with an increase in temperature. Hence, no significant change of the partition coefficients of the solutes to be separated with temperature is expected for either system.

The densities and viscosities of the phases, interfacial tension, and the settling time of the systems were measured at different temperatures between 25 °C and 40 °C. Subsequently, the system stability was calculated and compared.

After preparation, the systems were equilibrated, separated, and analyzed at the studied temperatures. In Fig. 2, the results of the measurements are presented as a function of temperature.

For both systems, the density of the phases, upper (Hex/EtOAc/ACN: 1%, Arizona N: 2%) and lower (Hex/EtOAc/ACN: 3%, Arizona N: 2%) phase, slightly decreases with an increase in temperature. In addition, the density difference between the phases slightly decreases ($\Delta\rho < 0.02 \text{ g cm}^{-3}$) for the Hex/EtOAc/ACN system (Fig. 2a), while it stays almost constant ($\Delta\rho < 0.002 \text{ g cm}^{-3}$) for Arizona N (Fig. 2b). It should be noticed that the density difference of the Hex/EtOAc/ACN is below 0.1 g cm^{-3} , which in literature is referred to as a minimum in order to achieve good stationary phase retention in LLC and to avoid a loss of stationary phase during the separation (bleeding) [13].

In general, the dynamic viscosity of the phases of both systems is relatively low. For the Hex/EtOAc/ACN system (Fig. 2c), the viscosities of both, upper and lower phase are lower than the respective phase viscosities of the Arizona N (Fig. 2d) system and do not appear to be significantly influenced by temperature. Similarly, no changes were observed for the upper phase of Arizona N. However, for the lower phase of Arizona N, a decrease in viscosity could be determined for increasing temperature between 25 °C and 35 °C. This is due to the higher water content in the lower phase, which contributes most to the change of the viscosity in that phase. With the used setup, no measurement of the viscosity at 40 °C was possible, since no constant values could be obtained due to evaporation.

Besides the density difference and viscosity, the interfacial tension is an essential factor to evaluate the stability of a biphasic system as this parameter often correlates with the stationary phase retention in the LLC column. In this study, two different measurements were performed: falling drop and rising drop. The two measurements differ in the phase used as dispersed phase. Consequently, the falling drop corresponds to the descending mode while the rising drop to the ascending mode in LLC separations. The interfacial tension clearly declines for the Hex/EtOAc/ACN system (Fig. 2e) with an increase in temperature. For the Arizona N system (Fig. 2f), only a slight decrease could be observed in the same temperature range. Similar to the density difference between the phases, the interfacial tension is higher in the Arizona N system.

Finally, the settling time of the two systems was determined at different temperatures between 25 °C and 40 °C. An increase of the settling time could be observed for the Hex/EtOAc/ACN system (Fig. 2g). In contrast, the settling time decreased for the Arizona N system (Fig. 2h). It should be noted that the Hex/EtOAc/ACN system has a very short settling time below 10 s in the studied temperature range. Both systems have a settling time clearly below 60 s, which is described in literature [4,5,16] to be a suitable biphasic system for the application in CCC and CPC.

According to literature, both interfacial tension and density difference influence the behavior and flow pattern of the biphasic system. A decrease in interfacial tension and density difference enhances the dispersion of the phases and consequently the mass transfer inside the column, but has an adverse effect on the stationary phase retention in the column. For CPC columns, starting from the Stoke's model, Foucault [13] derived the so-called system stability parameter (Eq.1), which can be used for a fast evaluation of expected stationary phase retention and flow pattern in the column (i.e. mass transfer areas). For a given solvent system, the tenden-

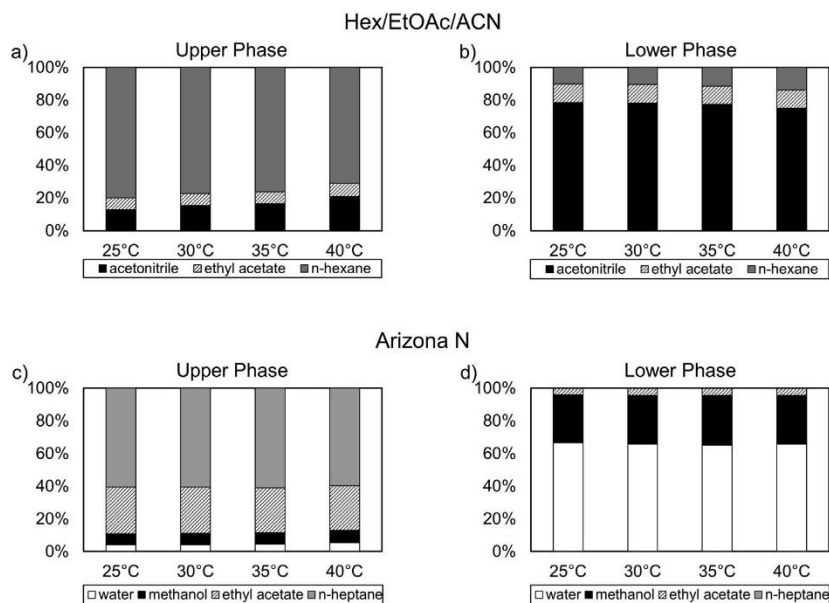


Fig. 1. Liquid-liquid equilibrium phase composition in mole fractions for the upper (a) and lower phase (b) of the *n*-hexane/ethyl acetate/acetonitrile system 41.43/9.92/48.65 mol% (11.2/2.0/5.3 v/v/v at 25 °C, 55.4/13.6/31.0 wt%) and the upper (c) and lower phase (d) of the *n*-heptane/ethyl acetate/methanol/water system Arizona N 7.01/10.50/25.38/57.11 mol% (1/1/1/1 v/v/v/v at 25 °C, 20.2/26.7/23.4/29.7 wt%) at different temperatures.

cies of the stationary phase retention, e.g. as a function of flow rate or temperature, are generally similar in CCC and CPC columns. Hence, when the stationary phase retention decreases in CPC, it also decreases in CCC. The hypothesis of the study is that systems with a stability factor being almost independent from temperature changes, also do not show significant changes in stationary phase retention as a function of temperature. Therefore, this parameter can be applied to forecast the behavior of a system in both column types. However, it must be noted that some non-stable systems might not be retained in CCC while they are in CPC. The system stability is defined as the ratio of these two parameters:

$$\text{System stability} = \frac{\gamma}{\Delta\rho} \quad (1)$$

Here, γ represents the interfacial tension and $\Delta\rho$ the density difference between the two liquid phases.

To this end, Foucault categorized biphasic systems in three groups. Systems with a value of $\frac{\gamma}{\Delta\rho}$ below 10 were classified as “less stable” with non-stable or small droplets and low stationary phase retention. Systems with a quotient higher than 50 are described as “more stable” with large droplets and higher stationary phase retention, but slow mass transfer due to the low mass transfer area. Values between 10 and 50 correspond to “stable systems”, exhibiting an optimum regarding stationary phase retention and mass transfer area. As apparent from Fig. 2i, the Hex/EtOAc/ACN system shows a rather low stability, varying between $15 \text{ cm}^3 \text{ s}^{-2}$ at 25 °C and $5 \text{ cm}^3 \text{ s}^{-2}$ at 40 °C. Hence, a stationary phase loss in the LLC column is expected above room temperature.

In terms of Arizona N (Fig. 2j), almost constant system stability could be determined in the studied temperature range, staying in the proposed optimal range. Arizona N has a higher system stability compared to the Hex/EtOAc/ACN system and can be categorized into the suggested optimal range of “stable systems”.

3.2. Influence of temperature on the separation performance

Subsequently, the influence of mobile phase inlet temperature and column temperature on the separation performance was compared at temperatures between 25 °C and 40 °C. It was further shown how temperature, as a crucial factor, could affect an established LLC method or could even be purposefully used to modify separation performance or time.

3.2.1. Separation performance at constant column and mobile phase inlet temperatures

Stationary phase retention, column efficiency and resolution were analyzed by keeping mobile phase inlet temperature and column temperature constant. The stationary phase retention (S_F) is defined as the fraction of the column volume occupied by the stationary phase:

$$S_F = \frac{V_{SP}}{V_C} \quad (2)$$

where V_{SP} is the volume of the stationary phase and V_C is the volume of the column.

In Fig. 3a and b the stationary phase retention at different but constant column and mobile phase inlet temperatures obtained with the CCC unit is presented for the two systems. For the Hex/EtOAc/ACN system (Fig. 3a), the stationary phase retention decreases with increasing temperature within the studied range from 25 °C to 40 °C. This is in accordance to the previously determined system specific properties, where density difference, interfacial tension and settling time, as well as the system stability decreased at higher temperatures. While there was no stationary phase loss observed at 25 °C, a stationary phase loss was observed during the run with an increase in temperature. This was expected from the decrease in system stability. At 40 °C, a stationary phase loss of up to 1 ml in descending mode (1.5 ml in ascending mode) occurred in total continuously during the run between injection and the elution of the last compound.

In contrast, the stationary phase retention increased for the Arizona N system (Fig. 3b) under the same conditions. No stationary phase loss occurred in the whole temperature range. This is in line with the constant stability of Arizona N as a function of temperature and at the same time a decrease in viscosity of the lower (mobile) phase in descending mode. Furthermore, this is consistent with the results of Friesen et al. [18] who observed an increase in stationary phase retention in elution extrusion experiments at increased column temperatures between 5 °C and 35 °C.

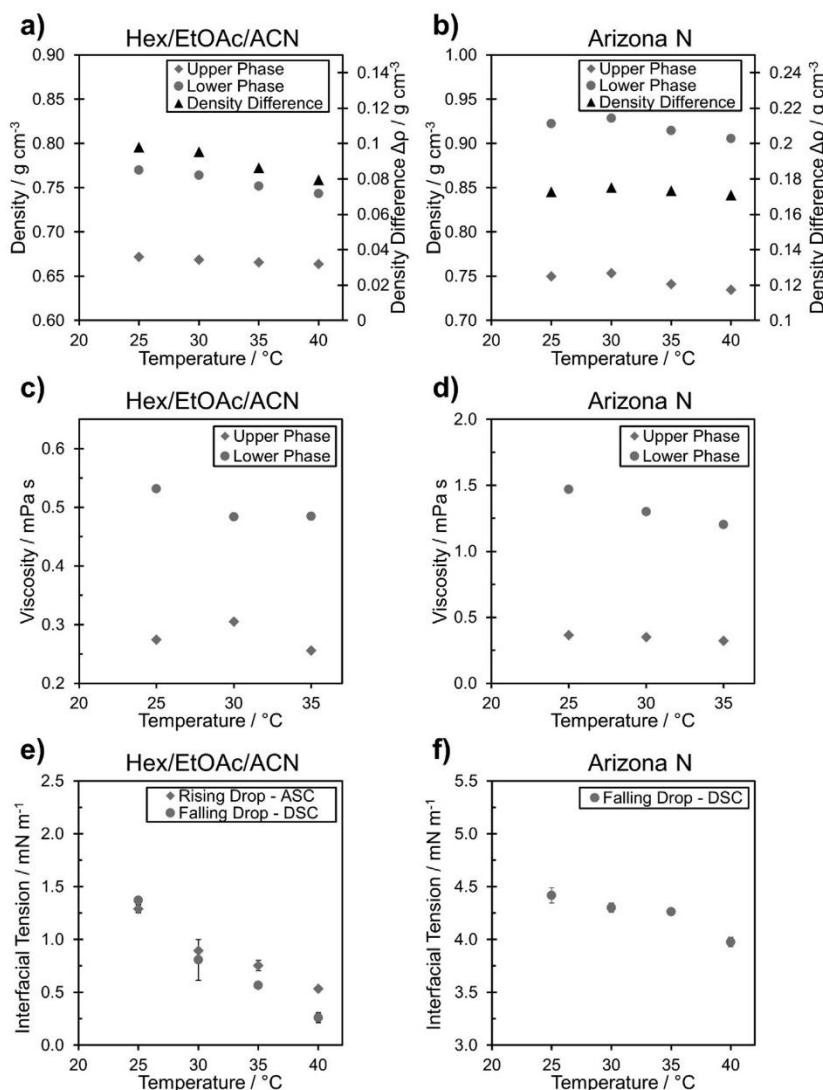
CCC pulse injection experiments of different model solutes were performed at varying temperatures between 25 °C and 40 °C, where the same column temperature and mobile phase inlet temperature was selected. Model solutes were selected with partition coefficients in or close to the sweet-spot range ($0.4 < P_i < 2.5$). For the Arizona N system, methyl paraben, ethyl paraben, propyl paraben, and butyl paraben were used as model solutes. For the Hex/EtOAc/ACN system, butyl paraben, S-carvone, and β -ionone were used in descending mode (see representative chromatograms in supplementary data Fig. C and D).

The partition coefficient (P_i) of each compound was determined from the obtained chromatograms according to Eq. 3.:

$$P_i = \frac{V_{R,i} - (1 - S_F) \cdot V_C}{S_F \cdot V_C} \quad (3)$$

where V_R is the retention volume of compound i , V_C is the column volume, and S_F the stationary phase retention.

As shown in Fig. 3c and d, the temperature change has only a minor effect on the partitioning of the model solutes in the studied systems. A slight increase of the partition coefficients could be observed for the Hex/EtOAc/ACN system for solutes with partition coefficients below 1. In comparison, the determined partition coefficients decreased in ascending mode between 25 °C and 40 °C for compounds with $P_i > 1$, while they increased for those with $P_i < 1$ (see supplementary Fig. B(c)). For Arizona N, a slight decrease for ethyl paraben and propyl paraben has been observed. However, for butyl paraben with a partition coefficient above the sweet spot range ($P_i > 2.5$), the effect is more pronounced and subsequently, a clear decrease in the partition coefficient was determined. Interestingly,



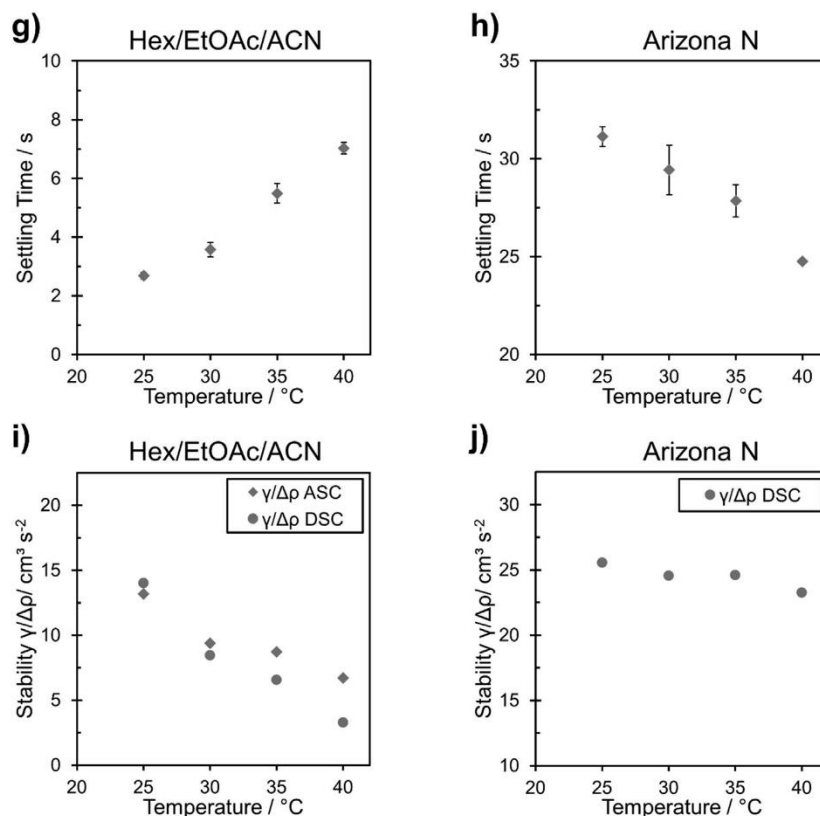


Fig. 2. System specific properties of the biphasic system as a function of temperature for the Hex/EtOAc/ACN (left column) and Arizona N system (right column): (a/b) density and density difference, (c/d) viscosity, (e/f) interfacial tension, (g/h) settling time, and (i/j) system stability.

although there is only a relatively small change in the system composition with an increase in temperature, this can clearly affect the partitioning especially of compounds with a partition coefficient above 1. Finally, the change in phase composition has a distinct influence on both the physical properties of the phases as well as the partitioning of the solutes between the phases. Although the partition coefficients seem to slightly change towards equal distribution between the phases ($P_i = 1$) with an increase in temperature for both studied systems, this is system specific and cannot be generalized. However, this observation is in line with the general trend of biphasic solvent systems to turn into a single phase with rising temperature.

The column efficiency, also called number of theoretical plates (N_i), was calculated from the recorded UV-Vis signals with Eq. 4.

$$N_i = \left(\frac{t_{R,i}}{\sigma_i} \right)^2 \quad (4)$$

where $t_{R,i}$ is the retention time of component i and σ_i the corresponding standard deviation of the peak.

In Fig. 3e and f, the number of theoretical plates (N_i) for the studied model solutes are shown as a function of temperature between 25 °C and 40 °C. For the Hex/EtOAc/ACN system, a tremendous increase in efficiency with increasing temperature could be observed (see supplementary Fig. B(b) for ascending mode). This is most likely due to a higher dispersion of the mobile phase in the stationary phase as a result of reduced system stability, leading to an increase of the contact area between the two phases. In addition, the increase in temperature leads to an increase of diffusivity in the

liquid phases. Both, a higher phase contact area and diffusivity coefficient, result in a higher mass transfer rate at higher temperatures. For the parabens in the aqueous-organic system Arizona N, only a slight increase in efficiency could be observed. This observation is in agreement with less pronounced changes of the physical properties of this system, i.e. a slight decrease in the viscosity of the lower phase but constant system stability with an increase in temperature. Hence, also the contact area of the phases and diffusivity are clearly less affected.

The resolution between the solutes as a function of temperature is presented in Fig. 3g (Hex/EtOAc/ACN system) and Fig. 3h (Arizona N) in descending mode, respectively. The resolution between two compounds is defined according to Eq. 5. The resolution in this study was calculated according to Eq. 6, assuming a Gaussian peak shape ($w = 4\sigma$).

$$R_S = \frac{2(t_{R,j} - t_{R,i})}{w_j + w_i} \quad (5)$$

$$R_S = \frac{t_{R,j} - t_{R,i}}{2(\sigma_j + \sigma_i)} \quad (6)$$

Here, $t_{R,i}$ and $t_{R,j}$ are the retention times of a first and a second eluting component, respectively; w_i and w_j are their peak widths at base line; σ_j and σ_i are the peak standard deviations at base line.

As mentioned before, the resolution R_S of the peaks is influenced by the parameters S_F , N_i , and P_i . Consequently, a different behavior of the two systems regarding the resolution could be observed. A clear decrease in resolution was observed for the Hex/EtOAc/ACN

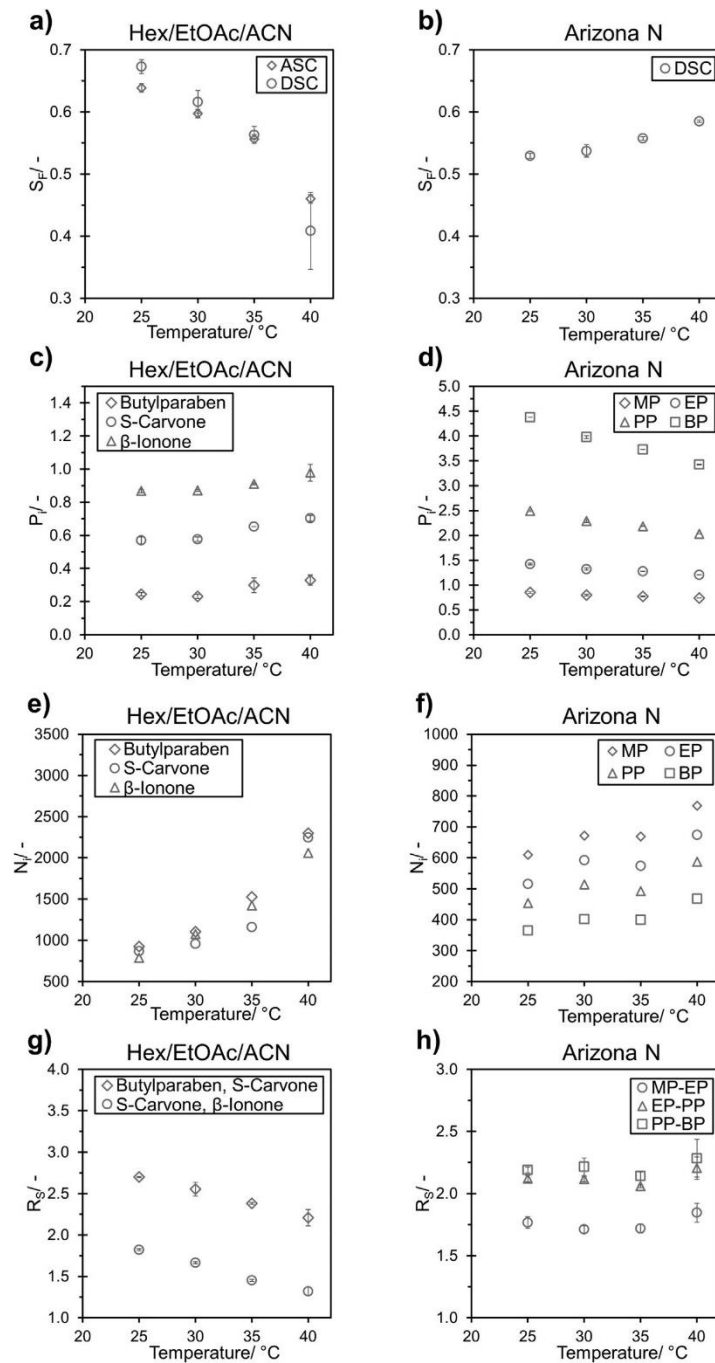


Fig. 3. Influence of temperature on the separation for the Hex/EtOAc/ACN (left column) and Arizona N (right column) system in the CCC column on: stationary phase retention (a–b), partition coefficients of selected model compounds (c–d), column efficiency (e–f), and peak resolution in descending mode (g–h). Experimental conditions: mobile phase flow rate 1 ml min^{-1} , 1900 rpm, $V_{inj} = 72 \mu\text{l}$.

system resulting in a slight peak overlapping ($R_S < 1.5$) between S-carvone and β -ionone at 40°C mainly due to a clear decrease in S_F , since P_1 does not significantly change and even the increase in N could not compensate for this trend. A similar trend of a decrease

in resolution with an increase in temperature could be observed also in ascending mode (see supplementary Fig. B(d)). In the Arizona N system, S_F was less affected and even slightly increased. At the same time the separation factors ($\alpha = P_j/P_1$) slightly decrease,

while N slightly increased. Hence, also the resolution was just slightly affected here as a function of temperature. This is in line to the observations of Friesen et al. [18], who observed an improved peak resolution with HEMWat systems at higher temperatures.

In conclusion, an increase in temperature influences stationary phase retention, solute partitioning, efficiency, and consequently, the resolution. The influences result from the modification of phase compositions and physical properties of the phases, which is manifested differently in the two studied systems as a function of temperature. Especially, the non-aqueous system Hex/EtOAc/ACN is more susceptible to temperature and as a result, the resolution decreases with temperature. Interestingly, the solute partitioning is only slightly affected. In contrast, the system stability of the aqueous-organic system Arizona N stays almost constant with an increase in temperature. Hence, the resolution stays almost constant. For both systems, the change in system stability sufficiently correlates with the change in resolution. In this context, the change in S_F with an increase in temperature is apparently the main influencing factor. In addition, this tendency also seems to be concomitant with the change in settling time.

An increase in settling time consequently suggests a decrease in stationary phase retention with an increase in temperature. Even though the system sensitivity on temperature change can be anticipated more accurately by system stability, the change of settling time provides a simpler alternative to determine temperature susceptibility. Another useful check of temperature sensitivity would be to simply determine at which temperature the system turns to monophasic. The change of settling time furthermore indicates a change in hydrodynamic behavior and the mass transfer between the phases. With this preliminary test, the user can quickly determine whether a temperature influence should be a consideration during separation method development and scale-up.

However, this test does not take into account any change in solute partitioning, which could occur for different solvent systems. Therefore, we recommend also the determination of P for at least one compound at different temperatures, e.g. at the lowest and highest temperature level in the expected range. This enables the user to determine whether or not the partition coefficients may change with temperature.

3.2.2. Separation performance at different column and mobile phase inlet temperatures

As shown in the previous section, a temperature increase clearly affects the separation with the non-aqueous biphasic system Hex/EtOAc/ACN and reduces the resolution between the peaks. In LLC, very often a convective cooling system, i.e. a fan, is used without a temperature control unit. Consequently, the column temperature is influenced by the solvent system, operating conditions such as mobile phase flow rate and rpm, environmental influences such as ambient air temperature as well as the total operating time of the unit. As a result, the column temperature is often neither recorded nor adequately controlled. Therefore, a constant temperature level of mobile phase inlet temperature and column temperature as described in section 3.2.1 often cannot be realized and an increase of the column temperature during the separation process or daytime/time of the year can be observed. In this context, a tempered water bath is usually used in order to keep the mobile phase inlet temperature constant. Subsequently, as a result of increasing column temperature, a difference between mobile phase inlet temperature and column temperature occurs. Hence, a temperature gradient exists and a re-equilibration between the two phases inside the column takes place during the separation process. In the current study, this scenario was attempted. A lab-scale CCC was used to set a specific column temperature of 35 °C while keeping the mobile phase inlet temperature at 25 °C. Subsequently the separation performance was analyzed by pulse injections and

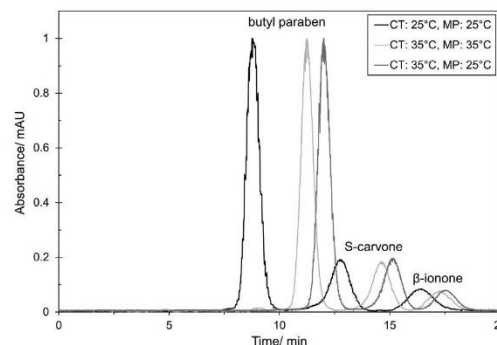


Fig. 4. CCC pulse injections of butyl paraben, S-carvone and β -ionone at different column temperatures (CT) and mobile phase inlet temperatures (MP) (Hex/EtOAc/ACN system, descending mode, 1 ml min⁻¹ mobile phase flow rate, 1900 rpm, $V_{inj} = 72 \mu\text{l}$, detector wavelength 255 nm, S_F at injection: 0.67 (25 °C CT&MP), 0.58 (35 °C CT&MP), 0.55 (35 °C CT, 25 °C MP)).

compared with pulse injections performed at the same column and mobile phase temperature of 25 °C and 35 °C.

As apparent from Fig. 4, the pulse injection at 35 °C (mobile phase inlet temperature and column temperature) results in higher retention times and a decrease in resolution compared to 25 °C. For example, the R_S value between butyl paraben and S-carvone decreased from 2.7 to 2.4. As described in section 3.2.1., this is mainly due to lower stationary phase retention but similar partition coefficients (Note: $P_1 < 1$ for all three compounds). Interestingly, when using a column temperature of 35 °C while keeping the mobile phase inlet temperature at 25 °C, the retention times further increase and the resolution is slightly lower compared to the separation at a constant mobile phase and column temperature of 35 °C ($R_S = 2.3$). The re-equilibration of the phases inside the column due to the temperature difference causes stationary phase loss (bleeding) and decreases the stationary phase retention compared to the separations at constant column and mobile phase inlet temperature of 25 °C or 35 °C. At constant 35 °C a slight stationary phase loss of 0.5 ml was observed in descending mode during the run, while a much higher stationary phase loss of more than 2 ml was observed with 25 °C mobile phase temperature and 35 °C column temperature. The temperature difference seems to additionally destabilize the system. Hence, the much stronger stationary phase loss leads to a higher retention time of the solutes and consequently a further decrease in resolution. With a higher column temperature of 40 °C and the same mobile phase temperature of 25 °C, this effect is even more pronounced which causes a further decrease in resolution (see supplementary Fig. F).

In ascending mode (see Fig. E in supplementary data), a similar effect with stationary phase loss could be observed. Analogous to descending mode, the stationary phase loss causes a reduced resolution with an increase in temperature. Hence, the retention time was longer for solutes with $P_1 < 1$, while it was decreased for $P_1 > 1$. Analogous to descending mode, additional destabilizing with continuous stationary phase loss of about 2 ml during the run was observed, when applying a different column temperature (35 °C) and mobile phase inlet temperature (25 °C). Similarly, a higher column temperature of 40 °C with a mobile phase inlet temperature of 25 °C caused even higher stationary phase loss and subsequently further reduced resolution (see supplementary Fig. G).

For the same solvent system, Hex/EtOAc/ACN, a pulse injection was performed in descending mode on a semi-preparative CPC column with a mobile phase inlet temperature of 25 °C. The CPC column in this study is equipped with a fan for convective cooling, but has no temperature control system. Consequently, the current

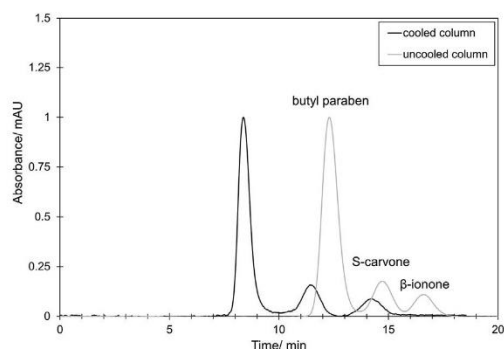


Fig. 5. CPC pulse injections of butyl paraben, S-carvone and β -ionone with a mobile phase inlet temperature of 25 °C and a column with (cooled column) and without (uncooled column) additional cooling (Hex/EtOAc/ACN system, descending mode, 12 ml min⁻¹ mobile phase flow rate, 1700 rpm, V_{inj} = 1 ml, detector wavelength 255 nm, S_T at injection: 0.67 (cooled column), 0.46 (uncooled column)).

column temperature during the run can neither be kept constant nor accurately be measured. Additional cooling was improvised by placing tubs filled with ice on top of the column housing in order to cover the whole top of the housing. Pulse injections were performed in descending mode with (cooled column) and without (uncooled column) additional cooling. Similar to the previous CCC experiments, a significant influence on the elution profile was observed in Fig. 5. In both cases, stationary phase loss occurred during the run, which was more pronounced when performing the separation without additional cooling. This lead to a clear decrease in resolution compared to the separation with additional cooling. Thus, no base line separation was achievable anymore. Similarly, a stationary phase loss with and an even higher loss without additional cooling occurred. Subsequently, a clear decrease in peak resolution could be observed also in ascending mode (see Fig. H in supplementary data) between the two pulse injections with and without additional cooling.

4. Conclusion

The influence of the temperature between 25 °C and 40 °C on LLC separations was studied using a non-aqueous organic solvent-based system *n*-hexane/ethyl acetate/acetonitrile (11.2/2.0/5.3 v/v/v at 25 °C) and an aqueous-organic system *n*-heptane/ethyl acetate/methanol/water (1/1/1/1 v/v/v/v at 25 °C, Arizona N).

Temperature change influences the systems differently. The effect was stronger in case of the non-aqueous system, whose physical properties were significantly affected even by a small change in the liquid-liquid equilibrium caused by temperature change. However, in both systems, increasing temperature resulted in only a small change of the partition coefficients.

Similarly, pulse injection experiments show that increasing temperature has a greater influence on the non-aqueous system where a decrease in resolution was observed. This was mainly caused by a decrease in stationary phase retention and could not be compensated by the observed increase in efficiency. In contrast, a slight increase in both stationary phase retention and efficiency was observed for Arizona N, leading to a slight improvement of the resolution. Furthermore, a difference of 10 °C between the inlet mobile phase and the column temperature resulted in a destabilization of the non-aqueous system. This caused additional loss of stationary phase (bleeding) and decreased the separation resolution. A similar behavior was observed on a semi-preparative CPC column where column temperature increased during the separation as no additional cooling equipment was present.

Finally, temperature should be considered as an influencing factor in the development of LLC separation methods and instruments. For some systems, a constant and controlled column and mobile phase inlet temperature could be used purposefully to modify and fine-tune a separation. However, an efficient way of temperature control for CCC and CPC columns of different scale needs to be investigated. An integrated online monitoring of the temperature at the column inlet and outlet, and an automated temperature control could be of interest especially when performing 24/7 industrial applications. Thus, in order to establish a robust separation method for subsequent scale-up, we suggest the evaluation of temperature susceptibility of the chosen system. A reliable indicator of this is a change in system stability, whereas the measurement of settling time represents a simpler alternative.

Acknowledgement

We acknowledge Dominic André and Lukas Braumann for carrying out part of the experiments. The authors thank Dr. Goudoulas (Chair of Fluid Dynamics of Complex Biosystems, Technical University of Munich) for his assistance during the viscosity measurements. We thank Prof. Thommes (Chair of Separation Science & Technology, University of Erlangen-Nürnberg) for giving us the possibility to measure the interfacial tension in their lab. The authors thank Prof. Briesen (Chair of Process Systems Engineering, Technical University of Munich) for giving us the opportunity to do the density measurements in their lab.

Appendix A. Supplementary data

Supplementary material related to this article can be found, in the online version, at doi:<https://doi.org/10.1016/j.chroma.2019.02.011>.

References

- [1] G.F. Pauli, S.M. Pro, J.B. Friesen, Countercurrent separation of natural products, *J. Nat. Prod.* 71 (2008) 1489–1508.
- [2] J.B. Friesen, J.B. McAlpine, S.-N. Chen, G.F. Pauli, Countercurrent separation of natural products: an update, *J. Nat. Prod.* 78 (2015) 1765–1796.
- [3] K. Skalicka-Woźniak, I. Garrard, A comprehensive classification of solvent systems used for natural product purifications in countercurrent and centrifugal partition chromatography, *Nat. Prod. Rep.* 32 (2015) 1556–1561.
- [4] A.P. Foucault, *Centrifugal Partition Chromatography*, M. Dekker, 1995.
- [5] A. Berthod, *Countercurrent Chromatography*, Elsevier, 2002.
- [6] F. Oka, H. Oka, Y. Ito, Systematic search for suitable two-phase solvent systems for high-speed counter-current chromatography, *J. Chromatogr. A* 538 (1991) 99–108.
- [7] F.D. Antia, C. Horváth, High-performance liquid chromatography at elevated temperatures: examination of conditions for the rapid separation of large molecules, *J. Chromatogr. A* 435 (1988) 1–15.
- [8] F. Gritti, G. Guiochon, Adsorption mechanisms and effect of temperature in reversed-phase liquid chromatography. Meaning of the classical Van't Hoff plot in chromatography, *Anal. Chem.* 78 (2006) 4642–4653.
- [9] T. Teutenberg, Potential of high temperature liquid chromatography for the improvement of separation efficiency—a review, *Anal. Chim. Acta* 643 (2009) 1–12.
- [10] S. Heinisch, J.-L. Rocca, Sense and nonsense of high-temperature liquid chromatography, *J. Chromatogr. A* 1216 (2009) 642–658.
- [11] S. Adelmann, G. Schembecker, Influence of physical properties and operating parameters on hydrodynamics in centrifugal partition chromatography, *J. Chromatogr. A* 1218 (2011) 5401–5413.
- [12] L. Marchal, A. Foucault, G. Patissier, J.M. Rosant, J. Legrand, Influence of flow patterns on chromatographic efficiency in centrifugal partition chromatography, *J. Chromatogr. A* 869 (2000) 339–352.
- [13] A. Foucault, E.C. Frias, C. Bordier, F.L. Goffic, Centrifugal partition chromatography: stability of various biphasic systems and pertinence of the “Stoke’s model” to describe the influence of the centrifugal field upon the efficiency, *J. Liq. Chromatogr. Relat. Technol.* 17 (1994) 1–17.
- [14] M. Van Buel, F. Van Halsema, L. Van der Wielen, K. Luyben, Flow regimes in centrifugal partition chromatography, *AIChE J.* 44 (1998) 1356–1362.
- [15] Y. Ito, J.-M. Menet, Coil planet centrifuges for high-speed countercurrent chromatography, *Chromatogr. Sci.* 82 (1999) 87–119.
- [16] W.D. Conway, *Countercurrent Chromatography: Apparatus, Theory, and Applications*, Wiley-VCH, 1990.

- [17] S. Baldermann, K. Ropeter, N. Köhler, P. Fleischmann, Isolation of all-trans lycopene by high-speed counter-current chromatography using a temperature-controlled solvent system, *J. Chromatogr. A* 1192 (2008) 191–193.
- [18] J.B. Friesen, G.F. Pauli, GUESSmix-guided optimization of elution–extrusion counter-current separations, *J. Chromatogr. A* 1216 (2009) 4225–4231.
- [19] A. Berthod, D.W. Armstrong, Centrifugal partition chromatography. VI. Temperature effects, *J. Liq. Chromatogr.* 11 (1988) 1457–1474.
- [20] Y. Wei, F. Wang, S. Wang, Y. Zhang, Modelling counter-current chromatography using a temperature dependence plate model, *J. Chromatogr. B* 933 (2013) 30–36.
- [21] Y. Ito, W.D. Conway, Experimental observations of the hydrodynamic behavior of solvent systems in high-speed counter-current chromatography: III. Effects of physical properties of the solvent systems and operating temperature on the distribution of two-phase solvent systems, *J. Chromatogr. A* 301 (1984) 405–414.
- [22] S. Ignatova, N. Sumner, N. Colclough, I. Sutherland, Gradient elution in counter-current chromatography: a new layout for an old path, *J. Chromatogr. A* 1218 (2011) 6053–6060.
- [23] E. Hopmann, J. Goll, M. Minceva, Sequential centrifugal partition chromatography: a new continuous chromatographic technology, *Chem. Eng. Technol.* 35 (2012) 72–82.
- [24] P. De Souza, L. Rangel, S. Oigman, M. Elias, A. Ferreira-Pereira, N. De Lucas, G. Leitão, Isolation of two bioactive diterpenic acids from *Copaifera glycyarpa* oleoresin by high-speed counter-current chromatography, *Phytochem. Anal.* 21 (2010) 539–543.
- [25] M. Qiao, S. Yang, L. Qu, Liquid–liquid equilibrium data for (*n*-hexane+ ethyl acetate+ acetonitrile) ternary system at (298.15, 308.15, and 318.15) K, *Fluid Phase Equilib.* 419 (2016) 84–87.

3.4. Paper IV: Evaluation of inter-apparatus separation method transferability in countercurrent chromatography and centrifugal partition chromatography

3.4.1. Summary

Citation

S. Roehrer, M. Minceva, (2019). Evaluation of inter-apparatus separation method transferability in countercurrent chromatography and centrifugal partition chromatography, *Separations*, 6(3), 36

<https://doi.org/10.3390/separations6030036>

Summary

The objective of this work was to establish a fast short-cut approach for an easy and straightforward estimation of separation method transferability between columns in LLC. Scale-up and method transfer in CCC and CPC are often based on trial-and-error approaches. In the current study, it was demonstrated that a direct separation method transfer with linear scale-up factors is not generally valid between columns of different size and design, especially when columns with different geometries are used. It was shown that the most commonly used approach in LLC where similar stationary phase retention is targeted in the two columns, can reach its limits. Based on a comprehensive evaluation of the separation performance of different columns it could be demonstrated that similar stationary phase retention does not guarantee similar separation performance. It is shown that within the typical operating range of each column, linear correlations of the stationary phase retention and efficiency can be assumed. This correlation can be used to calculate the resolution at different flow rates, which helps to quickly estimate the transferability of a particular separation method. For the determination of the linear correlations only two pulse injection experiments at different flow rates are needed, one preferably at the lower end and one at the higher end of the typical flow rate range of the column. The approach was demonstrated with five columns that differ in type (CCC and CPC) and size (lab-scale and semi preparative-scale). The proposed approach saves experimental time and effort, thus enabling a more targeted and universally valid strategy for unexperienced users. Furthermore, the study emphasizes that both separation method transferability and the subsequent selection of best operating conditions in terms of maximal productivity and minimal solvent consumption for a required purity and recovery can be estimated even faster as well as in a more purposeful way when combined with simulations.

Contributions

The author of this dissertation was the lead scientist in all parts of the work. He planned the work, performed the experiments, and conducted the data acquisition as well as the evaluation of the results. Part of the data from the CPE pulse injections was obtained from R. Morley. The manuscript was written by the author and discussed with M. Minceva.

3.4.2. Manuscript



Article

Evaluation of Inter-Apparatus Separation Method Transferability in Countercurrent Chromatography and Centrifugal Partition Chromatography

Simon Roehrer and Mirjana Minceva *

Biothermodynamics, TUM School of Life and Food Sciences Weihenstephan, Technical University of Munich, Maximus-von-Imhof-Forum 2, 85354 Freising, Germany

* Correspondence: Mirjana.minceva@tum.de; Tel.: +49-8161-71-6170

Received: 8 April 2019; Accepted: 12 July 2019; Published: 24 July 2019



Abstract: In the countercurrent chromatography and centrifugal partition chromatography, separation method transfer and scale-up is often described as an easy and straightforward procedure. Separation methods are usually developed on lab scale columns and subsequently transferred using linear scale-up factors to semi-preparative or preparative columns of the same column design. However, the separation methods described in the literature have been developed on various columns of different design and size. This is accompanied by differences in the separation behavior of the columns and therefore makes separation method transfer difficult. In the current study, the separation performances of different columns were evaluated and compared. Linear correlations of stationary phase retention and column efficiency as a function of flow rate were found to be applicable for the calculation of separation resolution in the typical operating range of each column. In this context, a two-point short-cut approach for a fast column characterization is recommended. This allows a quick prediction of the separation method transferability between columns, which saves experimental time and effort. In the current study, the transferability between five different columns from lab scale countercurrent chromatography (CCC) (18 mL) to semi-preparative centrifugal partition chromatography (CPCs) (250 mL) with different cell numbers and design is investigated.

Keywords: column characterization; resolution; separation performance; inter-apparatus method transfer

1. Introduction

Solid support-free liquid-liquid chromatography (LLC) is a powerful technique with increasing popularity for the separation of active compounds from plant extracts and biotechnological products. In general, two fundamental column designs exist: hydrodynamic columns better known as countercurrent chromatography (CCC), and hydrostatic columns known as centrifugal partition chromatography (CPC). CCC columns consist of a coil that is wound on a bobbin that rotates around its own axis and revolves around a second axis of a centrifuge [1,2]. CPC columns have only one axis of rotation with a constant centrifugal field. Conventional CPC columns consist of several identical annular disks that are connected in series, with polytetrafluoroethylene (PTFE) plates in between acting as seals. Each disk contains a certain number of cells that are circumferentially engraved and interconnected by narrow short channels, referred to as ducts [3–5]. Due to continuous developments, many subgroups with various column designs emerged for each of the two categories [3–5]. CCC columns, for example, differ in its rotary motion, ratios of the rotation radii (β -values), and different coil or tubing diameters and geometries, while CPC columns often have different cell and duct design as well as size. In literature, a huge number of applications have been established on many different columns. However, the columns

often differ significantly in column design as well as size. Consequently, suitable operating parameters (e.g., flow rate, rotational speed) and separation performances (e.g., stationary phase retention, column efficiency) between the columns are also different. Therefore, efficient and systematic strategies are needed to quickly transfer separation methods between different apparatuses.

In conventional liquid chromatography (LC), e.g., High-performance liquid chromatography (HPLC), clear rules exist on how to transfer batch separation methods between columns. Here, columns are of cylindrical shape and packed with a solid stationary phase. The design parameters are column diameter, length and stationary phase particle size. In general, sample load, i.e., the feed sample concentration and relative volumetric column loading, is kept constant and the same or a better number of theoretical stages is aimed for. To achieve these criteria when transferring a separation method, usually the particle size and the column length are kept the same, while the cross sectional area and the mobile phase flow rate are adjusted in order to guarantee the same mobile phase velocity in both columns [6]. In literature, this approach was studied also for applicability in CCC and CPC. The same mobile phase linear velocity was used in both columns when transferring the separation method between columns [7]. However, this is difficult, especially in CPC, since the cross-sectional area of the CPC cells is not constant and changes along the cells of different geometries. It was shown, that an average theoretical cross sectional area calculated as the ratio of cell volume and height does not give satisfactory results when cells clearly differ in design and/or size [7].

So far, LLC applications are mostly developed at lab scale columns with a volume between 10 and 300 mL. As commonly known, a good separation performance is related to a high stationary phase retention [4]. This is probably the reason, why the separation method transfer in CCC and CPC is commonly done by adjusting operating parameters, i.e., rotational speed and flow rate, in order to keep the stationary phase retention in both columns the same. Then, usually linear scale-up factors are used for calculating the injection volume or mass load, e.g., the ratio of column volumes in CPC and CCC, or coil lengths in CCC columns [7–11]. Although this has been often used as a fast and relatively satisfactory strategy, it is not a generally valid separation method transfer approach.

Another approach is the model-based methodology for optimizing a CPC column size for a particular separation introduced by Chollet et al. [12]. Varying hydrodynamics and mass transfer efficiency in different columns are taken into account enabling the calculation of an optimal column length. This approach allows the design of an optimized tailor-made column for a particular application, but requires preliminary tests for the determination of the model parameters as well as experience in modelling. Commercial columns are usually standardized and have a fix size. Therefore, this approach is not directly applicable for the separation method transfer in standardized and non-adjustable columns.

Bouju et al. proposed the free-space between the peaks method for the intra-apparatus method transfer between differently sized CPC columns with same cell geometry [13]. With this strategy, a separation method developed at lab scale can be easily transferred to large scale columns using the relation of the space between the peaks determined by pulse injections with low injection volumes ($V_{inj} = 1\% V_C$) on the two columns. Then, the injection volume is maximized on the first column and the maximum injection volume on the second column is directly calculated using the previously determined ratio of the space between the peaks. However, this method assumes in advance that the transfer of the separation method between the two columns is possible and no adjustment or selection of suitable operating parameters is provided. Hence, this approach can only be directly applied, if a higher separation resolution occurs on the column where the method is intended to be transferred.

According to literature, columns of same size but different design or cell geometries behave differently as a function of operating conditions such as flow rate and rotational speed (g -field) [14–18]. Differences in stationary phase retention and column efficiency have a clear influence on the separation resolution and process performances, including product purity, recovery, achievable productivity, and solvent consumption [16,19–24]. Hence, a reliable and easy strategy for the separation method transfer between columns independent of their size and type is needed that considers the separation performances of different column designs.

In this sense, two general questions arise before the actual transfer of a separation method: 1. is the method transferable at all; 2. which operating conditions have to be selected in order to achieve the highest possible productivity and at the same time a preferably low solvent consumption for pre-set purity and/or recovery requirements. At this point, the current work addresses the prediction and evaluation of separation method transferability in LLC. Hence, the separation method transferability between different columns is discussed. A systematic approach for the column characterization and method transfer is proposed in order to achieve comparable resolution of the separation on different CCC/CPC devices. For the column characterization a mixture of four parabens and the common aqueous-organic solvent based biphasic solvent system Arizona N was used, which is composed of *n*-heptane/ethyl acetate/methanol/water 1/1/1/1 *v/v/v/v*. In the study, different LLC columns available in our lab were used, namely a small 18.2 mL lab scale CCC and four different semi-preparative CPC columns with the same nominal total column volume of 250 mL, but different cell design and peripheral setups. It should be noted that the intention of this study was not to compare the separation performance of the different columns, but to establish a fast strategy for the estimation of separation method transferability between two columns.

2. Materials and Methods

2.1. Chemicals

The solvents *n*-heptane, ethyl acetate and methanol of the biphasic solvent system were all of analytical grade (EMSURE, purity 99%) from Merck KGaA (Darmstadt, Germany). Milli-Q water was obtained from a Milli-Q Direct Water Purification System from Merck Millipore (Darmstadt, Germany). The solutes *D/L*-tryptophan (racemic mixture), methyl paraben (MP), ethyl paraben (EP), propyl paraben (PP), and butyl paraben (BP) with a purity of $\geq 99\%$ were purchased from Alfa Aesar GmbH & Co KG (Karlsruhe, Germany).

2.2. Equipment

The experiments were carried out with different liquid–liquid chromatographic columns listed in Table 1. The hydrodynamic CCC-Mini column is a hydrodynamic J-type centrifuge with a 0.8 mm ID PTFE tube, a beta value range between 0.5 and 0.78, and a total column volume of 18.2 mL. The CCC-Mini was connected to a cooling unit (FL 300, Julabo, Seelbach, Germany) and an isocratic HPLC pump (Gilson 306, Gilson, Middleton, WI, USA), which could deliver flow rates of up to 50 mL min⁻¹. The effluent was monitored with a UV-detector (Gilson 171 UV-DAD-detector, Gilson, Middleton, WI, USA) at a wavelength of 255 nm. The sample was introduced through a manual 6-port valve and an injection loop of 72 μ L (<1% V_C).

Table 1. List of investigated columns, including name, acronym, column type, cell type, total column volume, and total number of cells.

Column Name	Acronym	Column Type	Cell Type	V_C /mL	No. of Cells
DE Mini Centrifuge	CCC	hydrodynamic	-	18.2	-
SCPC 250	CPC 1800	hydrostatic	twin-cells	250 (182) *	1800
CPC 250	CPC 864	hydrostatic	twin-cells	250 (242) *	864
CPC 250 PRO SPECIAL BIO Version	CPE 240	hydrostatic	twin-cells	250 (244) *	240
CPC 250 PRO SC prototype	CPE 196 spherical cells	hydrostatic	spherical cells	250 (240) *	196

* Experimentally determined total column volume (V_C) with Arizona N.

The SCPC-250 column consists of two single columns connected in series with an experimentally determined total volume of 182 mL. Each of the single columns has 10 disks with 90 engraved twin cells, resulting in total 1800 twin cells. The maximum achievable rotational speed is 3000 rpm (715 g) and the whole column can be operated at a maximum pressure drop of 100 bar. The CPC unit was connected to two isocratic preparative HPLC pumps with maximum flow rates of 50 mL min⁻¹, one for filling the column with the stationary phase and the other one for pumping the mobile phase during the

separation. The effluent was monitored with a UV detector (ECOM DAD600 2WL 200–600 nm, Prague, Czech Republic) at 255 nm. The feed sample was introduced through a six-port manual injection valve, and an injection loop of 1 mL ($<1\% V_C$) was used.

The CPC 250 column has an experimentally determined total column volume of 242 mL and consists of eight disks, each disk contains 108 engraved twin cells, in total 864 cells. The disks are made of stainless steel and sealed by PTFE plates. The maximum achievable rotational speed is 3000 rpm (729 g) and the maximum pressure drop is 100 bar. The CPC unit was connected to a PLC 2250 purification system including a preparative HPLC pump with maximum flow rate of 250 mL min^{-1} . The effluent was monitored with an integrated Gilson UV-DAD detector at 255 nm. The feed sample was introduced through an automated injection valve, and an injection loop of 1 mL ($<1\% V_C$) was used.

The column CPC 250 PRO SPECIAL BIO VERSION with an experimentally determined total volume of 244 mL has 12 disks, where each disk contains 20 engraved twin-cells; in total 240 cells. The disks are made of stainless steel and are additionally coated with PTFE for applications with biomolecules. The disks are sealed by PTFE plates. The column can be operated at a pressure drop of up to 100 bar and a maximal rotational speed of 3000 rpm (715 g). The column was connected to an isocratic HPLC pump (AZURA P2.1L, KNAUER, Berlin, Germany), which could deliver flow rates of up to 220 mL min^{-1} . The effluent was monitored with a UV-detector (AZURA MWD 2.1L, KNAUER, Berlin, Germany) at a wavelength of 255 nm. The sample was introduced through a manual 6-port valve and an injection loop of 1 mL ($<1\% V_C$).

The CPC 250 PRO SC prototype with an experimentally determined total volume of 240 mL has a monobloc design made of stainless steel and contains 196 spherical cells in total. The cells are connected to each other with small ducts with a total volume of only 5 mL. Due to the different column design, no sealing PTFE plates between the column disks are necessary, allowing an operation of the column with a maximal pressure drop of 200 bar and a rotational speed of 4000 rpm (2450 g). A detailed description of the design and production process can be found in the corresponding patent [25]. The column was connected to an isocratic preparative HPLC pump (PrepStar 218 Solvent Delivery Module, Varian, Palo Alto, CA, USA), which could deliver flow rates of up to 200 mL min^{-1} . The effluent was monitored with a UV-Vis detector (ProStar 325 UV-Vis Detector, Varian, Palo Alto, CA, USA) and a SUPER PREP 4 \times 0.15 mm detector cell at a wavelength of 255 nm. The sample was introduced through a six-port manual injection valve. An injection loop of 1 mL ($<1\% V_C$) was used.

For the sake of clarity, in the following text the columns are referred to by their acronyms introduced in Table 1.

2.3. Methods

2.3.1. Preparation of the Biphasic Liquid Systems and Feed Samples

The biphasic liquid system *n*-heptane/ethyl acetate/methanol/water 1/1/1/1 (*v/v/v/v*), Arizona N, was prepared by mixing the corresponding volume portions of the solvents at room temperature. The mixture was vigorously shaken and equilibrated at room temperature for at least two hours. For the experiments the phases were split and placed in two separate containers at room temperature. Feed solutions were prepared by adding appropriate amounts of the solutes to the mobile phase used for the pulse injections, lower phase in descending mode. The pulse injections for the characterization of all columns were performed in descending mode with *D/L*-tryptophan, methyl paraben, ethyl paraben, propyl paraben and butyl paraben. A sample concentration of 2 mg mL^{-1} was used for all five solutes, respectively.

2.3.2. Pulse Injection Experiments

Pulse injections of the mixtures in each column were performed in descending mode. For all measurements, the columns were first filled with the intended stationary phase, i.e., the upper phase.

After that, the rotational speed was set to the desired value and mobile phase was pumped through the column with the respective flow rates until no more stationary phase was eluting from the column, but at least one column volume. A feed mixture of D/L-tryptophan and four parabens was injected via a sample loop and the effluent was monitored with a UV-Vis detector at the specific wavelength (Note: In the CPE spherical cells experiments, no butyl paraben was injected). The stationary phase retention was calculated from the retention volume of the tracer D/L-tryptophan (partition coefficient equal to 0 in the Arizona N system).

3. Results

3.1. Approach of Column Characterization-Based Separation Method Transferability

In this work, the evaluation of separation method transferability between different columns is studied. The columns differ in type, size and design, but also in the typical operating range in terms of relative centrifugal acceleration (g -field) and mobile phase flow rate. Hence, the column performance is different in every single column as a result of differences in flow pattern, mass transfer area and solute residence time distribution [16,19–22,26,27]. The different column characteristics can be described by a different stationary phase retention, column efficiency and peak resolution.

The objective is to evaluate whether a transfer of the separation from one unit to another is possible by keeping the resolution between the target compounds constant. First, the different columns are characterized with pulse injections of small injection volume ($V_{inj} \leq 1\% V_C$). This is a similar procedure to LC, where an insignificant injection volume and low feed concentrations are used for the characterization of the column so that column load influences on the elution profile can be neglected [6,28,29]. Subsequently, the stationary phase retention, column efficiency and resolution between the peaks is determined in dependence of flow rate at a set rotational speed. Based on the determined resolution, separation method transferability between the columns can be easily foreseen for the selected type of solvent systems. In this manner, three general possibilities can occur: a resolution between the target compounds higher, equal, or lower compared to the original separation method.

However, the previously described situation, where both columns are extensively characterized with the same solvent system and solute, is usually not given. Often, an application found in literature is intended to be established on the column in the author's own lab. Still, the separation method transferability could be estimated purposefully as illustrated schematically in Figure 1 without extensive experimental trial and error attempts. First, the separation found in literature is evaluated in terms of separation performance, i.e., resolution. Then, the column where the separation method should be transferred to is characterized: a few pulse injections are performed, in the typical operating range of flow rate and a suitable but constant g -field of the column, the resolution is determined, and transferability evaluated. If the obtained resolution is higher than in the original column, further optimization in terms of injection volume, productivity, and solvent consumption could be directly followed. For this purpose, the information about experimentally determined stationary phase retention and column efficiency from the pulse injection experiments and the cell model can be used for simulations [30–32]. This approach saves experimental effort and time, and enables a targeted separation method transfer, which is further discussed in Section 3.3.

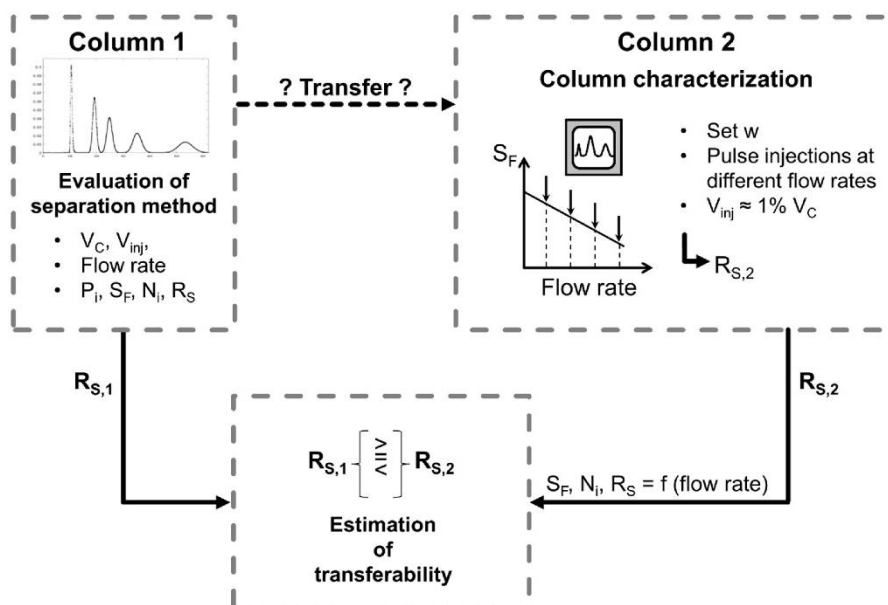


Figure 1. Schematic procedure of the evaluation of the separation method transferability between two different columns.

In the current study, the solvent system *n*-heptane/ethyl acetate/methanol/water 1/1/1/1 *v/v/v/v*, Arizona N, is used and methyl paraben, ethyl paraben, propyl paraben, and butyl paraben are selected as model compounds. In addition, *D/L*-tryptophan is used as a tracer compound in descending mode, i.e., lower phase as mobile phase.

3.2. Column Characterization

Five columns of different size and design (see Table 1) were characterized in terms of stationary phase retention, column efficiency and resolution as a function of mobile phase flow rate. The rotational speed (*w*) for each column was kept constant and individually selected. The selected rotational speeds are in a range where a further increase of the rotational speed has no significant positive influence on the stationary phase retention and column efficiency, and complies with the pressure drop limitations of each column. This is usually known from previous studies with similar solvent systems [17,33] or suggested by the producer of the column. The rotational speed was set as following: CCC (1900 rpm, 216 g), CPC 1800 (1700 rpm, 230 g), CPC 864 (1737 rpm, 230 g), CPE 240 (1700 rpm, 230 g), CPE 196 spherical cells (2000 rpm, 613 g). The experimental data for the characterization of the CPE 240 are taken from Morley et al. [34].

3.2.1. Stationary Phase Retention

The stationary phase retention (S_F) is the fraction of the column volume occupied by the stationary phase:

$$S_F = \frac{V_S}{V_C} \tag{1}$$

where V_S is the volume of the stationary phase and V_C is the volume of the column.

In Figure 2 the stationary phase retention as a function of the mobile phase flow rate is shown for all studied columns in descending mode (lower phase as mobile phase). The maximum studied flow rate was selected according to the maximum flow rate recommended by the manufacturer (CCC), the maximum allowed pressure drop of the column (CPC 1800, CPE 240), the maximum applicable flow

rate for the applied detector (CPE 196 spherical cells), or simply due to a low stationary phase that is suboptimal for a sufficient separation in LLC (CPC 864). For all columns, a linear decrease with an increase in flow rate was observed within the studied range. This is in line with similar studies from literature for both, CCC [5,18,33,35–40] and CPC [14,16,20,22,24,38,41] of different column sizes and geometries within a certain flow rate range. However, it should be noted that this only applies up to a certain flow rate. Above that, especially in CPC columns, an abrupt drop in stationary phase retention can occur and a linear correlation between S_F and flow rate is no longer possible [14,16,38,41]. In the studied columns, no abrupt decrease in stationary phase retention was observed at a certain flow rate. With the studied solvent system, a good stationary phase retention above 0.6 is achievable in all columns. For the studied operating parameters, the CPE 196 spherical cells column had the highest stationary phase retention while the biggest range of S_F was observed with the CPC 864.

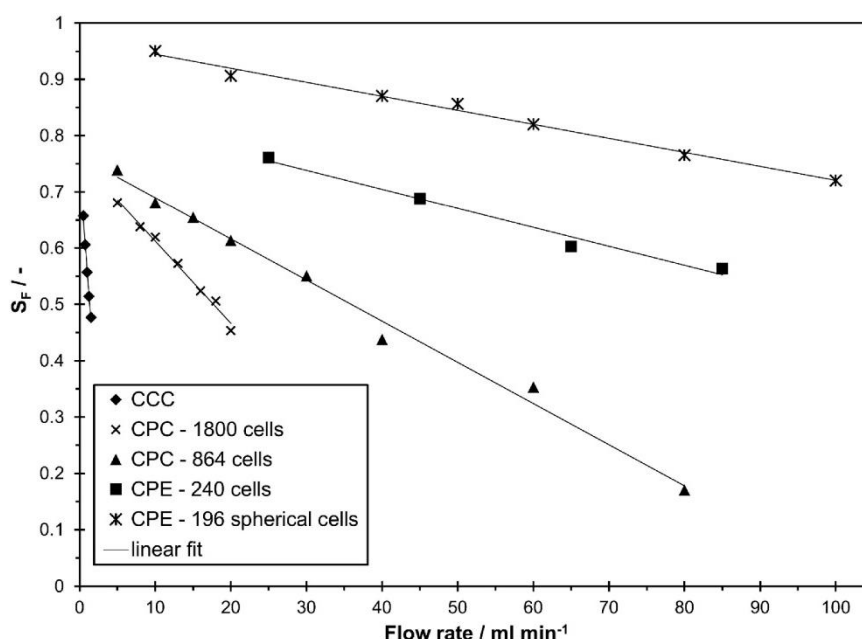


Figure 2. Stationary phase retention in descending mode in different countercurrent chromatography (CCC) and centrifugal partition chromatography (CPC) columns as a function of mobile phase flow rates for the solvent system *n*-heptane/ethyl acetate/methanol/water 1/1/1/1 *v/v/v/v*.

3.2.2. Column Efficiency and Resolution of the Columns

In addition to a high stationary phase retention, a high column efficiency is beneficial for a good separation i.e., high resolution. In all studied columns, the efficiency is determined with pulse injection experiments of the model compounds methyl paraben, ethyl paraben, propyl paraben and butyl paraben at different mobile phase flow rates in descending mode. The column efficiency, also called number of theoretical plates (N_i), was calculated from the recorded UV-Vis signal with Equation (2).

$$N_i = \left(\frac{t_{R,i}}{\sigma_i} \right)^2 \tag{2}$$

where $t_{R,i}$ is the retention time of component *i* and σ_i^2 the corresponding peak variance.

In Figure 3, the efficiency of methyl paraben is shown as a function of flow rate in descending mode. A linear increase with an increase in flow rate was observed for all columns in the studied range. However, all studied columns with different designs clearly differ in column efficiency. As expected, a

higher number of theoretical plates is determined in CPC columns with a higher number of physical cells. It is worth mentioning that the CPE 240 and CPE 196 spherical cells have a much higher single cell efficiency compared to the other two CPCs. Still, the total number of theoretical plates of CPC 1800 and CPC 864 is clearly higher than in the two CPEs which is due to the higher number of physical cells. Similarly, the lab scale CCC outperforms the two CPEs in terms of column efficiency and a similar N_i is achievable compared to the two CPC columns. In all columns and at all flow rates, the number of theoretical plates is highest for the first eluting compound methyl paraben and lowest for the last eluting compound butyl paraben.

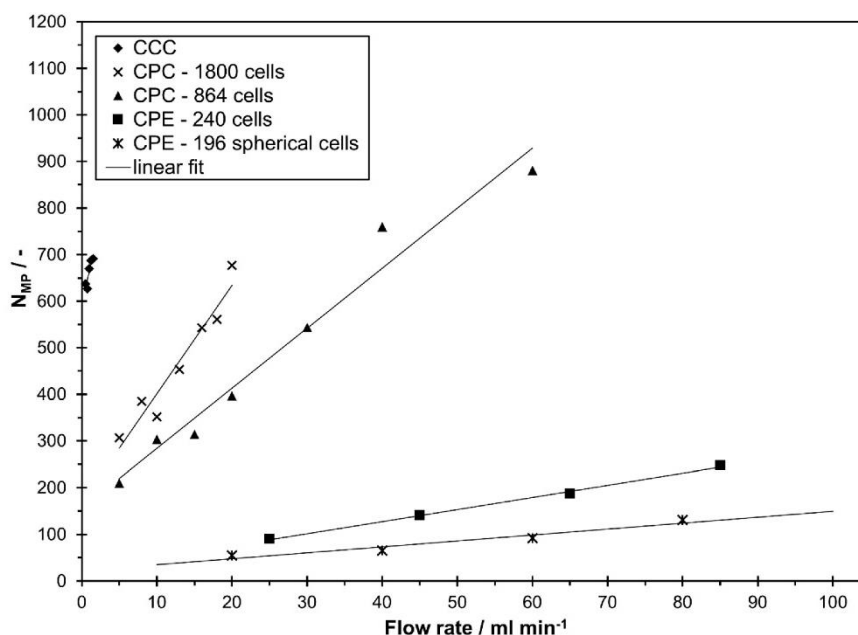


Figure 3. Number of theoretical plates (efficiency) of methyl paraben in descending mode of different CCC and CPC columns as a function of mobile phase flow rates for the solvent system *n*-heptane/ethyl acetate/methanol/water 1/1/1/1 v/v/v/v.

The resolution between two peaks is defined according to Equation (3). The resolution in this study was calculated according to Equation (4), assuming a Gaussian peak shape ($w = 4 \sigma$).

$$R_S = \frac{2(t_{R,j} - t_{R,i})}{w_j + w_i} \tag{3}$$

$$R_S = \frac{t_{R,j} - t_{R,i}}{2(\sigma_j + \sigma_i)} \tag{4}$$

where $t_{R,i}$ and $t_{R,j}$ are the retention times of the first and second eluting compound; w_i and w_j are the corresponding peak widths at base line; σ_j and σ_i are the peak standard deviations.

The resolution can also be described by the partition coefficient P_i , column efficiency N_i , and stationary phase retention S_F (Equation (5)):

$$R_S = S_F \frac{1}{4} \sqrt{N} \frac{(P_j - P_i)}{1 - S_F \left[1 - \frac{P_j + P_i}{2} \right]} \tag{5}$$

where N is the mean value of the number of theoretical plates of both components ($N = (N_i + N_j)/2$) [42].

The partition coefficient of a solute is solvent system dependent and described by the thermodynamic equilibrium. Hence, for the same solvent system, P_i and P_j are the same for all columns. The partition coefficient of a compound i can be calculated from the chromatogram of a pulse injection at a certain flow rate (F) according to Equation (6):

$$P_i = \frac{F t_{R,i} - (1 - S_F) V_C}{S_F V_C} \quad (6)$$

As described by Berthod et al. [43] for the homologous series of alkyl benzenes, a linear correlation of the partition coefficients can be applied to the parabens used in this study. Based on the chromatogram of a CCC pulse injection at 1 mL min^{-1} (see chromatogram in Figure A1 in Appendix A), $\log P = 0.231n_C - 0.305$ with n_C representing the number of methylene groups ($P_{MP} = 0.84, P_{EP} = 1.44, P_{PP} = 2.44, P_{BP} = 4.22$). In contrast, S_F and N_i are solvent system, column and operating parameter dependent, and determine the difference in resolution between different columns. Once S_F and N_i are known, Equation (5) can be used to calculate the resolution.

Using the linear correlations of S_F and N , the peak resolution can be calculated according to Equation (5) in the whole flow rate range. As apparent from Figure 4, showing experimental values of R_S as well as calculated values with Equation (5) and the linear correlations of S_F and N from Figures 2 and 3, the calculated and experimental R_S values are in good agreement with minor deviations of up to 0.15. Only in terms of the CPE 240 a deviation of up to 0.2 was observed at a flow rate of 85 mL min^{-1} . In this sense, the accuracy of the calculated values is good enough for a first approximation of the resolution when estimating the transferability of a certain separation method.

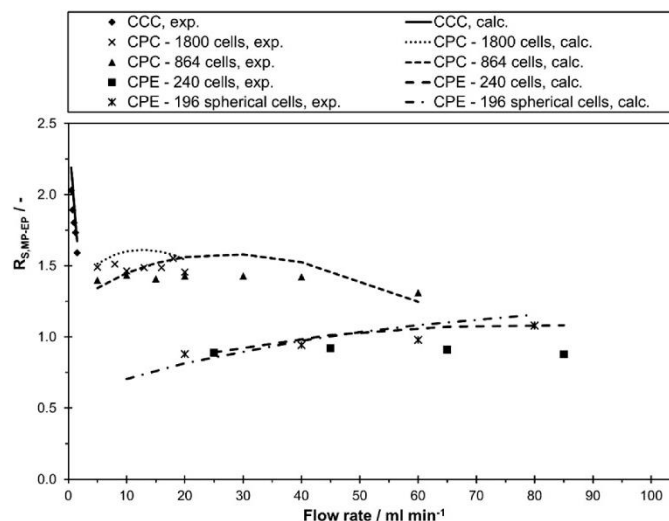


Figure 4. Separation resolution, experimental and calculated values using Equation (5) and the linear correlations of S_F and N , between methyl paraben and ethyl paraben in descending mode of different CCC and CPC columns as a function of mobile phase flow rates for the solvent system *n*-heptane/ethyl acetate/methanol/water 1/1/1/1 *v/v/v/v*.

In the current study, the highest resolution could be determined in the lab scale CCC. However, a clear decrease in resolution between methyl paraben and ethyl paraben was determined with an increase in flow rate from 0.5 mL min^{-1} ($R_S = 2.05$) to 1.5 mL min^{-1} ($R_S = 1.6$). Consequently, these two compounds could be separated completely with the lab scale CCC in the whole flow rate range.

In contrast, the resolution at CPC 1800 and CPC 864 stayed almost constant with an increase in flow rate. While a complete base line separation ($R_S \geq 1.5$) between methyl paraben and ethyl paraben was still possible in CPC 1800, a small peak overlapping occurred in CPC 864. The CPE 240 and CPE 196 spherical cells show a similar behavior within the studied flow rate range, but with a clearly lower resolution compared to CPC and CCC. Interestingly, the CPE 196 spherical cell even slightly outperforms the CPE 240 at higher flow rates. Additionally, it can be directly anticipated from Figure 4 whether a higher, similar or lower peak resolution can be expected for a certain pulse injection in the investigated columns. In this work, a separation method transfer is possible in the following order of the resolution: CCC > CPC 1800 > CPC 864 > CPE 196 spherical cells > CPE 240. This trend becomes even clearer in Figure 5, where corresponding chromatograms with pulse injections are shown. In terms of CCC, a median flow rate of 1 mL min^{-1} is shown. For CPC 864 and CPE 196 spherical cells, representative flow rates were arbitrarily selected since R_S does not change (CPC 864) or just slightly increases (CPE 196 spherical cells) within the studied flow rate range (see Figure 4).

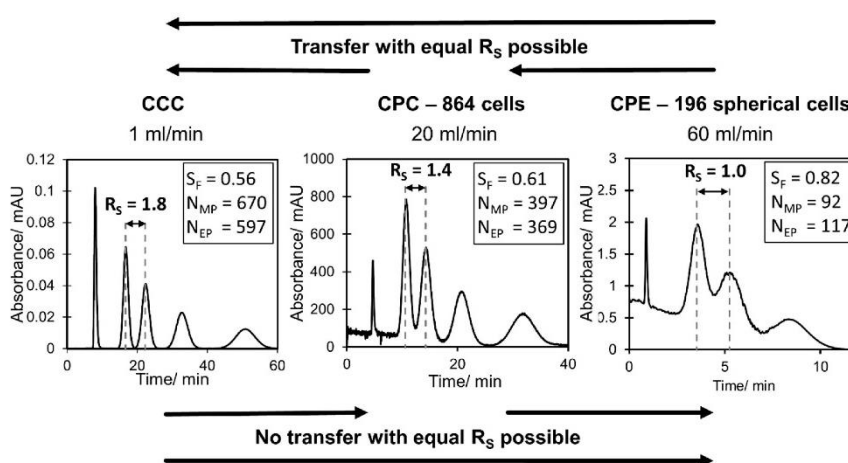


Figure 5. Representative chromatograms of paraben pulse injections in CCC, CPC 864 and CPE 196 spherical cells at different flow rates.

In summary, the partition coefficient of compound i is the same in all columns and independent of operating conditions, since P_i is a thermodynamic parameter. In contrast, linear correlations for S_F and N_i as a function of flow rate can be obtained. S_F decreases and N_i increases with an increase in flow rate in all studied columns. In terms of resolution the columns behaved differently. The shown trends are consistent with previous CCC and CPC studies [14,15,17,18,44]. Although the resolution appears to be mostly linear dependent on the flow rate in Figure 4, this is not necessarily the case for all possible flow rates, since, according to Equation (5), R_S is not a linear function of S_F and N_i . The big difference in the achievable resolution between CPC and CPE can be easily explained by the much higher number of physical cells in the CPC columns.

In order to evaluate the applicability of the commonly used separation method transfer between two columns based on the same stationary phase retention, the resolution is presented as a function of stationary phase retention in Figure 6. As is apparent from the figure, R_S between two peaks can clearly differ in the various columns for a certain value of S_F . For example, at a stationary phase retention of 0.6 the resolution varies between 0.9 (CPE 240) and 1.9 (CCC). Consequently, the frequently used method transfer strategy with same S_F and linear scale-up factors between the columns is not generally applicable.

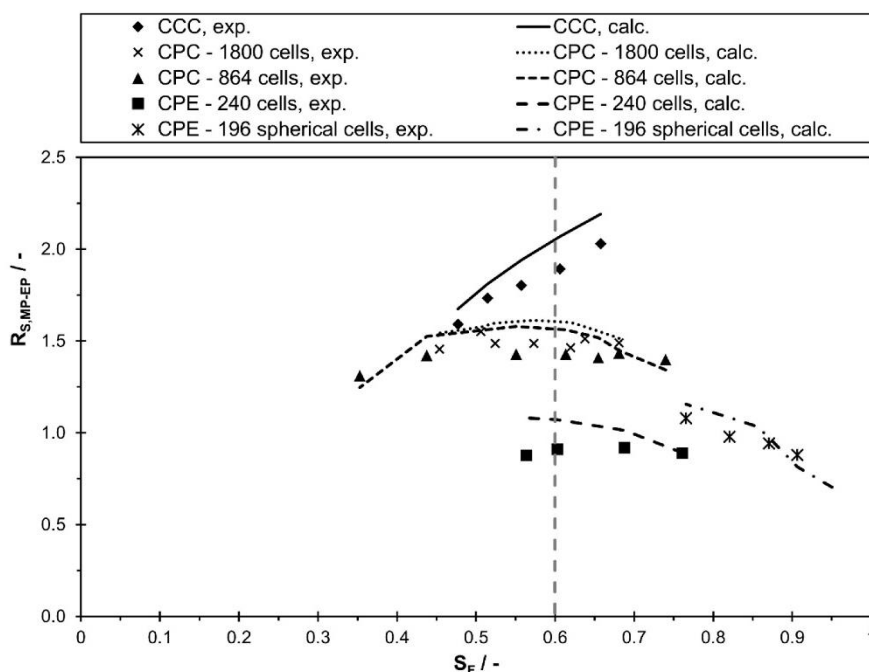


Figure 6. Separation resolution, experimental and calculated values using Equation (5) and the linear correlations of S_F and N , between methyl paraben and ethyl paraben in descending mode of different CCC and CPC columns as a function of stationary phase retention for the solvent system *n*-heptane/ethyl acetate/methanol/water 1/1/1/1 v/v/v/v.

3.3. Short-Cut Approach for Evaluation of Separation Method Transferability

In this section, a two-point short-cut approach for a preliminary evaluation of separation method transferability is proposed (Figure 7). According to the results of the column characterization study (Section 3.2) shown in Figures 2–4, S_F linearly correlates with the flow rate at a constant rotational speed. In addition, N_i can be assumed as linearly dependent on the flow rate in the studied range. Therefore, two pulse injections are sufficient to determine the mentioned linear correlations with a satisfactory accuracy. In this context, a typical operating range of the column in terms of flow rate is selected based on previous experience or manufacturer’s information. The suitable rotational speed is chosen to achieve a good compromise between good stationary phase retention and pressure drop. Initially, a pulse injection of the separation method to be transferred with a preferably small injection volume ($V_{inj} \approx 1\% V_C$) is performed at a relatively low flow rate within the common operating range. The flow rate is then increased stepwise and the stationary phase retention is determined at each stage by measuring the eluted stationary phase at hydrodynamic equilibrium. The flow rate is increased in a way that S_F decreases linearly until a stationary phase retention between 0.4 and 0.5 is achieved, which represents a reasonable minimum value of S_F for a good separation resolution in liquid–liquid chromatography [4]. If an abrupt decrease in S_F occurs before or a maximum pressure drop is reached, the column needs to be refilled with stationary phase and equilibrated at a flow rate lower than the one where the abrupt decrease of S_F occurred or below the maximum pressure drop. Subsequently, a second pulse injection is performed at the highest flow rate suitable according to the previous criteria. Finally, the chromatograms of both pulse injections, one at low and the other at a higher flow rate, are analyzed in terms of S_F , N_i , and P_i . In all columns the same values of P_i are obtained, since P_i is a thermodynamic parameter. Then, linear correlations of S_F and N_i as a function of flow rate can be assumed. The resolution can then be calculated according to Equation (5) in the whole flow rate

range and one could quickly assess whether a separation method transfer with aimed resolution (e.g., $R_{S,2} = R_{S,1}$) is possible between two columns.

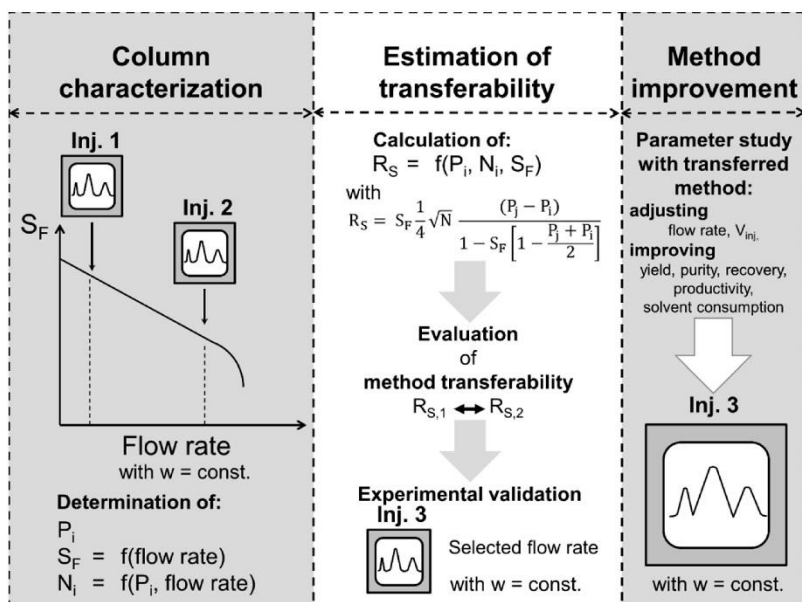


Figure 7. Scheme of the short-cut method for the evaluation of separation method transferability.

After the transferability of the separation method has been determined, an experimental validation at the particular flow rate at which the previous criteria are fulfilled can be performed and by this time, the separation method is transferred. A further improvement of the transferred method could follow by applying the space between the peaks method [13] or additional simulations as part of theoretical parameter studies. This can be done by a parameter study, where different flow rates and injection volumes can be evaluated by applying the linear correlations of S_F and N_i from the short-cut method as input, e.g., as part of a simulation study based on the equilibrium cell model [30,45]. In this context, individual requirements such as purity, yield, productivity, and solvent consumption can be assessed. For a more comprehensive and reliable model-based optimization of the separation performance, a more extensive characterization of the column like in Section 3.2 with additional pulse injections could be recommended especially for the optimization and fine tuning of operating conditions at preparative or industrial scale [46,47]. Finally, it could be shown that transferability between columns can be determined by performing a two-point short-cut characterization. We believe that the proposed approach saves experimental effort and time.

4. Discussion and Conclusions

The objective of this work was to establish a systematic approach for the estimation of separation method transferability between different columns in countercurrent chromatography and centrifugal partition chromatography. In this sense, the separation method transferability was studied with the solvent system *n*-heptane/ethyl acetate/methanol/water 1/1/1/1 *v/v/v/v* and a mixture of four parabens.

The separation performance of five columns was compared in terms of stationary phase retention, column efficiency and resolution in dependence of flow rate. It was shown, that all studied columns behave differently as a function of flow rate. Nevertheless, a linear correlation of stationary phase retention and column efficiency as a function of flow rate was obtained within a certain flow rate range. This can be used to estimate whether a separation method is transferable and in which flow rate

range a similar resolution is achievable. Moreover, the results of this study show that the commonly used separation method transfer strategy between two columns, where a flow rate is selected in order to keep the stationary phase retention in both columns the same and linear scale-up factors are chosen, can reach its limits. Evidently, similar stationary phase retention does not guarantee similar separation resolution.

A comprehensive evaluation of the columns in terms of stationary phase retention and column efficiency allows solute and solvent system specific parameters to be obtained and used for the (model-based) optimization of the operating parameters (e.g., injection volume and flow rate). A fast characterization of the columns can be done by a two-point short-cut method based on two pulse injection experiments at different flow rates. This saves not only experimental effort, but also material and time, which is costly, especially on a preparative scale. This approach can be applied during scale-up between two columns available on site as well as for the estimation of transferability of a separation method from literature. Furthermore, it would be useful for the CCC/CPC community to characterize existing commercially available and most frequently used CCC/CPC columns with the most commonly used solvent systems and model components (for example those from GUESSmix). This information would be a helpful contribution for a preliminary evaluation of separation method transferability between columns, i.e., labs, and established methods from literature.

Author Contributions: Both authors contributed substantially to the work reported: Conceptualization, S.R.; Data curation, S.R.; Formal analysis, S.R.; Investigation, S.R.; Methodology, S.R.; Resources, M.M.; Supervision, M.M.; Validation, S.R.; Visualization, S.R.; Writing—original draft, S.R.; Writing—review and editing, S.R. and M.M.

Funding: This work was supported by the German Research Foundation (DFG) and the Technical University of Munich (TUM) in the framework of the Open Access Publishing Program.

Acknowledgments: The authors thank Pfeiffer from AlphaCrom AG (Switzerland) for the loan of the pump and detector for the CPC spherical cells experiments. The authors thank Gilson International B.V. (Germany) for the loan of the CPC-250 and the PLC 2250 purification system setup. We thank Raena Morley for carrying out part of the CPE experiments.

Conflicts of Interest: The authors declare no conflict of interest.

Appendix A

The following are additional data to this article:

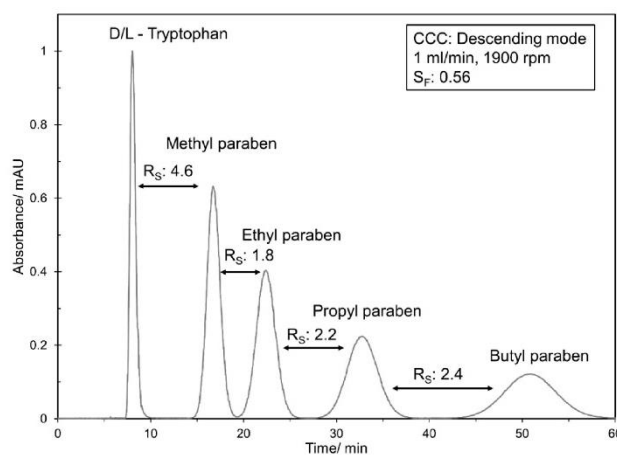


Figure A1. CCC pulse injection of D/L-tryptophan, methyl paraben, ethyl paraben, propyl paraben and butyl paraben with the solvent system *n*-heptane/ethyl acetate/methanol/water 1/1/1/1 v/v/v/v in descending mode (1 mL min⁻¹, 1900 rpm, V_{inj} = 72 μL, detector wavelength 255 nm).

References

1. Ito, Y. High-speed countercurrent chromatography. *Nature* **1987**, *326*, 419–420. [[CrossRef](#)]
2. Ito, Y. Origin and evolution of the coil planet centrifuge: A personal reflection of my 40 years of ccc research and development. *Sep. Purif. Rev.* **2005**, *34*, 131–154. [[CrossRef](#)]
3. Berthod, A.; Faure, K. Separations with a Liquid Stationary Phase: Countercurrent Chromatography or Centrifugal Partition Chromatography. In *Analytical Separation Science*; Wiley-VCH Verlag GmbH & Co. KGaA: Weinheim, Germany, 2015.
4. Berthod, A. *Countercurrent Chromatography*; Elsevier: Amsterdam, The Netherlands, 2002; Volume 38.
5. Foucault, A.P. *Centrifugal Partition Chromatography*; Chromatographic Science Series; M: Dekker: New York, NY, USA, 1995; Volume 68.
6. Schmidt-Traub, H.; Schulte, M.; Seidel-Morgenstern, A. *Preparative Chromatography*, 2nd ed.; Wiley-VCH Verlag GmbH & Co. KGaA: Weinheim, Germany, 2012.
7. Das Neves Costa, F.; Hubert, J.; Borie, N.; Kotland, A.; Hewitson, P.; Ignatova, S.; Renault, J.H. Schinus terebinthifolius countercurrent chromatography (part iii): Method transfer from small countercurrent chromatography column to preparative centrifugal partition chromatography ones as a part of method development. *J. Chromatogr. A* **2017**, *1487*, 77–82. [[CrossRef](#)]
8. Sutherland, I.A.; Audo, G.; Bourton, E.; Couillard, F.; Fisher, D.; Garrard, I.; Hewitson, P.; Intes, O. Rapid linear scale-up of a protein separation by centrifugal partition chromatography. *J. Chromatogr. A* **2008**, *1190*, 57–62. [[CrossRef](#)]
9. Wood, P.; Ignatova, S.; Janaway, L.; Keay, D.; Hawes, D.; Garrard, I.; Sutherland, I.A. Counter-current chromatography separation scaled up from an analytical column to a production column. *J. Chromatogr. A* **2007**, *1151*, 25–30. [[CrossRef](#)]
10. Das Neves Costa, F.; Vieira, M.N.; Garrard, I.; Hewitson, P.; Jerz, G.; Leitão, G.G.; Ignatova, S. Schinus terebinthifolius countercurrent chromatography (part ii): Intra-apparatus scale-up and inter-apparatus method transfer. *J. Chromatogr. A* **2016**, *1466*, 76–83. [[CrossRef](#)]
11. Sutherland, I.; Hewitson, P.; Ignatova, S. Scale-up of counter-current chromatography: Demonstration of predictable isocratic and quasi-continuous operating modes from the test tube to pilot/process scale. *J. Chromatogr. A* **2009**, *1216*, 8787–8792. [[CrossRef](#)]
12. Chollet, S.; Marchal, L.; Jeremy, M.; Renault, J.H.; Legrand, J.; Foucault, A. Methodology for optimally sized centrifugal partition chromatography columns. *J. Chromatogr. A* **2015**, *1388*, 174–183. [[CrossRef](#)]
13. Bouju, E.; Berthod, A.; Faure, K. Scale-up in centrifugal partition chromatography: The “free-space between peaks” method. *J. Chromatogr. A* **2015**, *1409*, 70–78. [[CrossRef](#)]
14. Fumat, N.; Berthod, A.; Faure, K. Effect of operating parameters on a centrifugal partition chromatography separation. *J. Chromatogr. A* **2016**, *1474*, 47–58. [[CrossRef](#)]
15. Goll, J.; Audo, G.; Minceva, M. Comparison of twin-cell centrifugal partition chromatographic columns with different cell volume. *J. Chromatogr. A* **2015**, *1406*, 129–135. [[CrossRef](#)]
16. Schwienheer, C.; Merz, J.; Schembecker, G. Investigation, comparison and design of chambers used in centrifugal partition chromatography on the basis of flow pattern and separation experiments. *J. Chromatogr. A* **2015**, *1390*, 39–49. [[CrossRef](#)]
17. Roehrer, S.; Minceva, M. Characterization of a centrifugal partition chromatographic column with spherical cell design. *Chem. Eng. Res. Des.* **2019**, *143*, 180–189. [[CrossRef](#)]
18. Peng, A.; Hewitson, P.; Sutherland, I.; Chen, L.; Ignatova, S. The effect of increasing centrifugal acceleration/force and flow rate for varying column aspect ratios on separation efficiency in counter-current chromatography. *J. Chromatogr. A* **2018**, *1581–1582*, 80–90. [[CrossRef](#)]
19. Van Buel, M.; Van Halsema, F.; Van der Wielen, L.; Luyben, K. Flow regimes in centrifugal partition chromatography. *AIChE J.* **1998**, *44*, 1356–1362. [[CrossRef](#)]
20. Marchal, L.; Foucault, A.; Patissier, G.; Rosant, J.M.; Legrand, J. Influence of flow patterns on chromatographic efficiency in centrifugal partition chromatography. *J. Chromatogr. A* **2000**, *869*, 339–352. [[CrossRef](#)]
21. Marchal, L.; Legrand, J.; Foucault, A. Mass transport and flow regimes in centrifugal partition chromatography. *AIChE J.* **2002**, *48*, 1692–1704. [[CrossRef](#)]

22. Adelmann, S.; Baldhoff, T.; Koepcke, B.; Schembecker, G. Selection of operating parameters on the basis of hydrodynamics in centrifugal partition chromatography for the purification of nybomycin derivatives. *J. Chromatogr. A* **2013**, *1274*, 54–64. [[CrossRef](#)]
23. Foucault, A.P.; Frias, E.C.; Bordier, C.G.; Goffic, F.L. Centrifugal partition chromatography: Stability of various biphasic systems and pertinence of the “stoke’s model” to describe the influence of the centrifugal field upon the efficiency. *J. Liq. Chromatogr.* **1994**, *17*, 1–17. [[CrossRef](#)]
24. Adelmann, S.; Schembecker, G. Influence of physical properties and operating parameters on hydrodynamics in centrifugal partition chromatography. *J. Chromatogr. A* **2011**, *1218*, 5401–5413. [[CrossRef](#)]
25. Couillard, F. Connecting channels and cells for centrifugal partition chromatographs. Wo 2009/066014 a1, 28 May 2009.
26. Marchal, L.; Intes, O.; Foucault, A.; Legrand, J.; Nuzillard, J.-M.; Renault, J.-H. Rational improvement of centrifugal partition chromatographic settings for the production of 5-n-alkylresorcinols from wheat bran lipid extract. *J. Chromatogr. A* **2003**, *1005*, 51–62. [[CrossRef](#)]
27. Peng, A.; Hewitson, P.; Sutherland, I.; Chen, L.; Ignatova, S. How changes in column geometry and packing ratio can increase sample load and throughput by a factor of fifty in counter-current chromatography. *J. Chromatogr. A* **2018**, *1580*, 120–125. [[CrossRef](#)]
28. Guiochon, G.; Felinger, A.; Shirazi, D.G.; Katti, A.M. *Fundamentals of Preparative and Nonlinear Chromatography*; Elsevier: Amsterdam, The Netherlands, 2006.
29. Nicoud, R.-M. *Chromatographic Processes*; Cambridge University Press: Cambridge, UK, 2015.
30. Martin, A.J.P.; Syngé, R.L.M. A new form of chromatogram employing two liquid phases. A theory of chromatography. 2. Application to the micro-determination of the higher monoamino-acids in proteins. *Biochem. J.* **1941**, *35*, 1358–1368. [[CrossRef](#)]
31. Kostanian, A.E. Modelling counter-current chromatography: A chemical engineering perspective. *J. Chromatogr. A* **2002**, *973*, 39–46. [[CrossRef](#)]
32. Kostanyan, A.E. General regularities of liquid chromatography and countercurrent extraction. *Found. Chem. Eng.* **2006**, *40*, 587–593. [[CrossRef](#)]
33. Ignatova, S.; Sutherland, I. A fast, effective method of characterizing new phase systems in ccc. *J. Liq. Chromatogr. Relat. Technol.* **2003**, *26*, 1551–1564. [[CrossRef](#)]
34. Morley, R.; Minceva, M. Unpublished work. 2018.
35. He, C.H.; Zhao, C.X. Retention of the stationary phase for high-speed countercurrent chromatography. *AIChE J.* **2007**, *53*, 1460–1471. [[CrossRef](#)]
36. Du, Q.Z.; Wu, C.J.; Qian, G.J.; Wu, P.D.; Ito, Y. Relationship between the flow-rate of the mobile phase and retention of the stationary phase in counter-current chromatography. *J. Chromatogr. A* **1999**, *835*, 231–235. [[CrossRef](#)]
37. Sutherland, I.; Du, Q.; Wood, P. The relationship between retention, linear flow, and density difference in countercurrent chromatography. *J. Liq. Chromatogr. Relat. Technol.* **2001**, *24*, 1669–1683. [[CrossRef](#)]
38. Foucault, A.; Bousquet, O.; Le Goffic, F. Importance of the parameter v_m/v_c in countercurrent chromatography: Tentative comparison between instrument designs. *J. Liq. Chromatogr.* **1992**, *15*, 2691–2706. [[CrossRef](#)]
39. Sutherland, I.A.; Booth, A.J.; Brown, L.; Kemp, B.; Kidwell, H.; Games, D.; Graham, A.S.; Guillon, G.G.; Hawes, D.; Hayes, M.; et al. Industrial scale-up of countercurrent chromatography. *J. Liq. Chromatogr. Relat. Technol.* **2001**, *24*, 1533–1553. [[CrossRef](#)]
40. Wood, P.L.; Hawes, D.; Janaway, L.; Sutherland, I.A. Stationary phase retention in ccc: Modelling the j-type centrifuge as a constant pressure drop pump. *J. Liq. Chromatogr. Relat. Technol.* **2003**, *26*, 1373–1396. [[CrossRef](#)]
41. Kotland, A.; Chollet, S.; Autret, J.M.; Diard, C.; Marchal, L.; Renault, J.H. Modeling ph-zone refining countercurrent chromatography: A dynamic approach. *J. Chromatogr. A* **2015**, *1391*, 80–87. [[CrossRef](#)]
42. Berthod, A.; Faure, K. Revisiting resolution in hydrodynamic countercurrent chromatography: Tubing bore effect. *J. Chromatogr. A* **2015**, *1390*, 71–77. [[CrossRef](#)]
43. Berthod, A.; Bully, M. High-speed countercurrent chromatography used for alkylbenzene liquid-liquid partition coefficient determination. *Anal. Chem.* **1991**, *63*, 2508–2512. [[CrossRef](#)]
44. Bousquet, O.; Foucault, A.P.; Goffic, F.L. Efficiency and resolution in countercurrent chromatography. *J. Liq. Chromatogr.* **1991**, *14*, 3343–3363. [[CrossRef](#)]

45. Völkl, J.; Arlt, W.; Minceva, M. Theoretical study of sequential centrifugal partition chromatography. *AIChE J.* **2013**, *59*, 241–249. [[CrossRef](#)]
46. Goll, J.; Minceva, M. Continuous fractionation of multicomponent mixtures with sequential centrifugal partition chromatography. *AIChE J.* **2017**, *63*, 1659–1673. [[CrossRef](#)]
47. Morley, R.; Minceva, M. Operating mode selection for the separation of intermediately-eluting components with countercurrent and centrifugal partition chromatography. *J. Chromatogr. A* **2019**. [[CrossRef](#)]



© 2019 by the authors. Licensee MDPI, Basel, Switzerland. This article is an open access article distributed under the terms and conditions of the Creative Commons Attribution (CC BY) license (<http://creativecommons.org/licenses/by/4.0/>).

3.5. Strategies for the isolation and purification of bioactive minor components from plant extracts using LLC

3.5.1. Process concept for solute capture and enrichment with LLC

LLC is conventionally used in classical batch elution mode by performing a pulse injection of the mixture to be separated, ideally in the form of a rectangular concentration profile of the injected solutes at the column entrance. Due to dispersive effects, the components elute from the column in the form of a (dispersed) peak. Hence, the concentration of the collected purified components is lower than their concentration in the feed mixture. Marchal et al. [172] suggested an unconventional application of LLC columns, namely for the extraction of target compounds from a complex mixture. In this process concept, which is inspired from the adsorption-desorption process concept, the feed mixture is continuously pumped into the column and the target component is retained by the stationary phase in the column. The enriched target component is then recovered from the column in an “extrusion” step, where the liquid stationary phase including the target component is pumped out from the column. The process concept was demonstrated in a CPC column for the extraction of β -carotene from a microalgae fermentation broth [172].

Continuing the idea of Marchal et al. [172], in this work LLC was evaluated to selectively enrich and purify minor compounds from natural extracts. A solvent system is selected in which the partition coefficient of the target component is high and at the same time higher than most of the major impurities present in the mixtures. The process is realized in two steps. In the first step, the capture and pre-purification step, the feed mixture dissolved in the mobile phase is loaded on the column. The target compound is retained in the column, while the impurities with lower partition coefficients travel faster through the column than the target compound and start eluting from the column. Consequently, the stationary phase inside the column is enriched with the target compound. The second step, the extrusion step, ideally begins at the latest directly before the target compound starts eluting from the column. This point in time is also called switching time t_{switch} . In the extrusion step, the target compound is recovered by pumping the stationary phase out from the column. The extrusion can be realized in elution-extrusion mode or back-extrusion mode. As explained in Section 2.6, in elution-extrusion mode the stationary phase is pumped into the column instead of mobile phase while the pumping direction is kept the same. In back-extrusion mode, mobile phase is continued to be pumped into the column while the pumping direction is switched. As a result of the two-step process, an enriched and at the same time pre-purified extract is obtained. Such a selective capture, enrichment and pre-purification directly from the raw extract can make further purification steps more convenient.

In this work, the process was used for the capture and enrichment of the bioactive minor compound xanthohumol C from a natural hop extract. Xanthohumol C was captured and enriched in the column, while the main impurity xanthohumol was removed (**Paper V**). A systematic model-based approach for the process design is proposed. The steps of the method are presented in Figure 18.

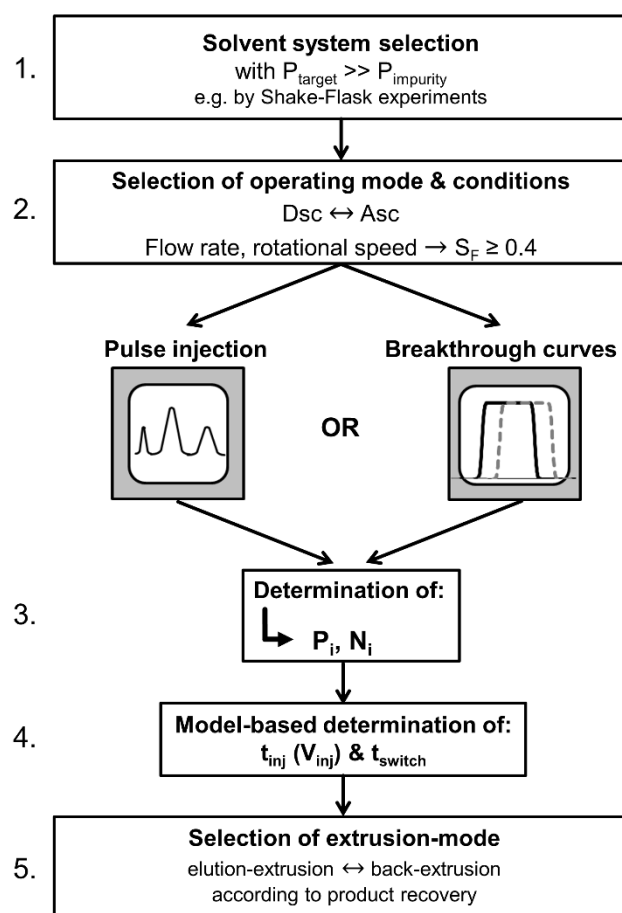


Figure 18: Schematic illustration of the process design workflow of a process for the capture and enrichment of minor compounds from complex mixtures using a LLC column.

In the first step, a biphasic liquid solvent system is selected in a way that the partition coefficient of the target compound has a high affinity to one of the phases, i.e. $P_{\text{target}} \gg 1$, since the objective is to retain the target component in the column. This is in contrast to classical elution mode where a partition coefficient with almost equal distribution between the phases is desired, i.e. P_{target} in the sweet spot range ($0.4 < P_{\text{target}} < 2.5$). The solvent system can be selected by shake-flask experiments or by using predictive thermodynamic models.

In the next step, the operating mode needs to be selected, i.e. which phase should be used as stationary or mobile phase. In this sense, ascending or descending mode are selected so that the target compound has a higher partition coefficient compared to the main impurities. After that, like for conventional batch mode, operating conditions (flow rate, rotational speed) are selected where a good stationary phase retention with $S_F \geq 0.4$ can be achieved.

In the current approach, a model-based process design by applying the cell model is intended to be used to determine the applicable injection volume and t_{switch} . As input parameters for the model, the column efficiency N_i is needed, which is system specific, i.e. it is a function of the solvent system, solutes, operating conditions and the column design. This can be determined either by pulse injections with low injection volume ($V_{\text{inj},1\%} \leq 1\% V_C$) of the feed mixture or by performing breakthrough curves with the single compounds. In the case of a

complex natural mixture such as the hop extract in **Paper V**, pulse injections are more convenient since single compounds are not available. In the following preliminary study with model compounds, this is exemplarily done by breakthrough curves.

In the following, the appropriate column load, i.e. injection volume, and switching time t_{switch} can be determined based on the experimentally determined model parameters S_F , N_i , and P_i . The injection duration t_{inj} or injection volume V_{inj} could be determined by simulating batch injections with different injection volumes. V_{inj} is adjusted so that at the end of the classical elution mode, the switching point t_{switch} , the major impurities have completely eluted from the column while the breakthrough of the target compound has not been started yet.

Finally, the mode used for the recovery of the enriched product needs to be selected. This can be achieved either by pumping new stationary phase into the column (elution-extrusion mode) or by changing the flow direction and continuing with the pumping of the mobile phase (back-extrusion mode).

Before applying the approach to a complex natural mixture, the steps three to five were validated experimentally using a model mixture and solvent system. The experimental data were simulated using the cell model (Section 2.7.2.) in order to evaluate the accuracy of the model. The objective was to evaluate the system stability, when introducing large injection volumes to the column. The first two steps of the process workflow are identical to the process development steps in conventional LLC pulse injection experiments in elution mode. Hence, this was not part of this preliminary study with the model system. The single steps were demonstrated with a model feed mixture composed of two parabens, methyl paraben (MP) and butyl paraben (BP), and the biphasic liquid solvent system Arizona N (*n*-heptane/ethyl acetate/methanol/water 1/1/1/1 v/v/v/v). The partition coefficients of MP and BP determined by shake flask experiments in the current study were $P_{\text{MP}} = 0.7 \pm 0.2$ and $P_{\text{BP}} = 3.8 \pm 0.5$. The linear range of the partition equilibrium was previously determined and reported to be in the range between 0 and 30 mg ml⁻¹ total paraben concentration [125]. For the current study, a feed concentration far below this upper limit of the linear concentration range, i.e. a paraben concentration c_{paraben} of 0.2 mg ml⁻¹ per paraben, was selected to perform the breakthrough curves.

In Fig. 19, breakthrough curves with the single parabens were performed in descending mode to determine the column efficiency and partition coefficients of the single parabens. The elution profile was analyzed by frontal analysis (Section 2.1) in order to calculate the system specific separation parameters ($P_{\text{MP,Dsc}} = 0.982$, $N_{\text{MP,Dsc}} = 797$, $P_{\text{BP,Dsc}} = 3.366$, $N_{\text{BP,Dsc}} = 347$) on a semi-preparative CPC column ($V_C = 246.65$ ml, $F = 18$ ml min⁻¹, $S_F = 0.5$).

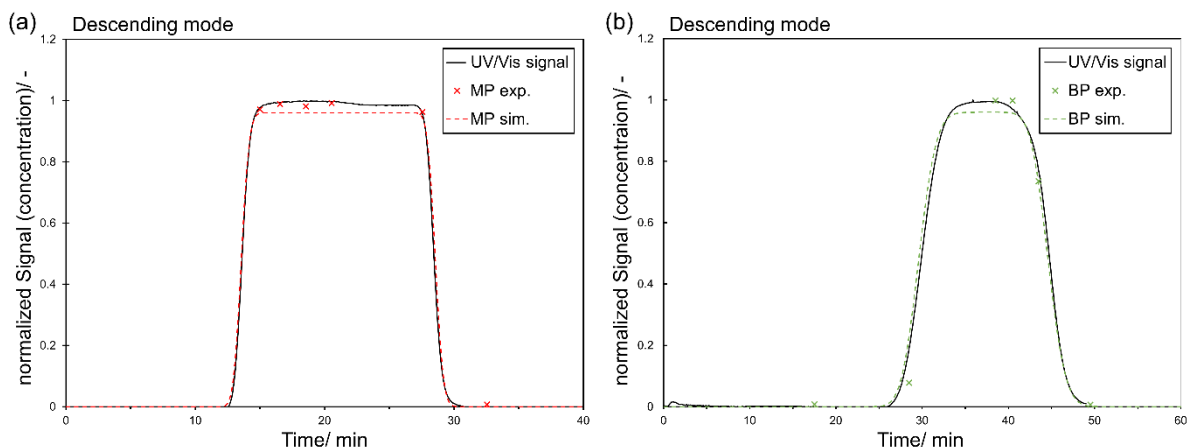


Figure 19: Breakthrough curves of methyl paraben (MP) and butyl paraben (BP) performed on a CPC column in descending mode including UV/Vis signals at 255 nm (UV/Vis signal), experimental elution profiles from HPLC offline analysis (exp.) with corresponding simulation (sim.) using the cell model: descending mode (a) MP ($P_{MP} = 0.982$, $N_{MP} = 797$) and (b) BP ($P_{BP} = 3.366$, $N_{BP} = 347$) with operating parameters: Arizona N, 1700 rpm, $V_C = 246.65$ ml, $S_F = 0.5$, $F = 18$ ml min^{-1} , $t_{inj} = 15$ min ($V_{inj} = 270$ ml);

It must be noted that in the current study, the partition coefficients of the parabens determined by breakthrough curves slightly differ from the linear range of the partition equilibria. This is due to hydrodynamic effects in the column. As described in literature [31, 113, 169], back mixing can occur in the CPC cells. This impacts the residence time distribution of the compounds in each cell by re-circulating part of the stationary and mobile phase inside the cell. In addition, dead zones can occur due to non-ideal phase mixing in the cells [31, 113, 169]. When analyzing the elution profiles of breakthrough curves (or pulse injections), such effects are included in the calculated values and can be the reason for the difference in the determined partition coefficients between different columns. Hence, it is often easier or more convenient to use the partition coefficients determined by breakthrough curves (or pulse injections) rather than shake-flask experiments for the calculations and to perform the simulations.

The applicability of the cell model (Section 2.7.2.) was also validated for high injection volumes. In the following, this is demonstrated by performing breakthrough curves in descending mode with a binary mixture of MP and BP (Fig. 20). Significant peak overlapping was intended to analyze whether the components influence the elution of the other components or the occurring co-elution might lead to any loss of stationary phase. As apparent from Fig. 20, the reconstructed elution profiles of MP and BP confirm the simulations based on the parameters previously determined with the single compounds. Fortunately, no stationary phase loss occurred, which confirmed the process to be stable in the linear range of the liquid-liquid equilibrium. Consequently, the breakthrough time (t_B) of the compounds was also not affected. The parameter t_B is defined as the point in time where a compound starts eluting from the column (Eq. 13).

Although this is expected from linear chromatography in conventional LC, such high injection volumes including breakthrough curves have not been used in LLC until now. The objective

was to confirm that S_F stays constant and no column bleeding or other hydrodynamic effects occur during the long injection duration.

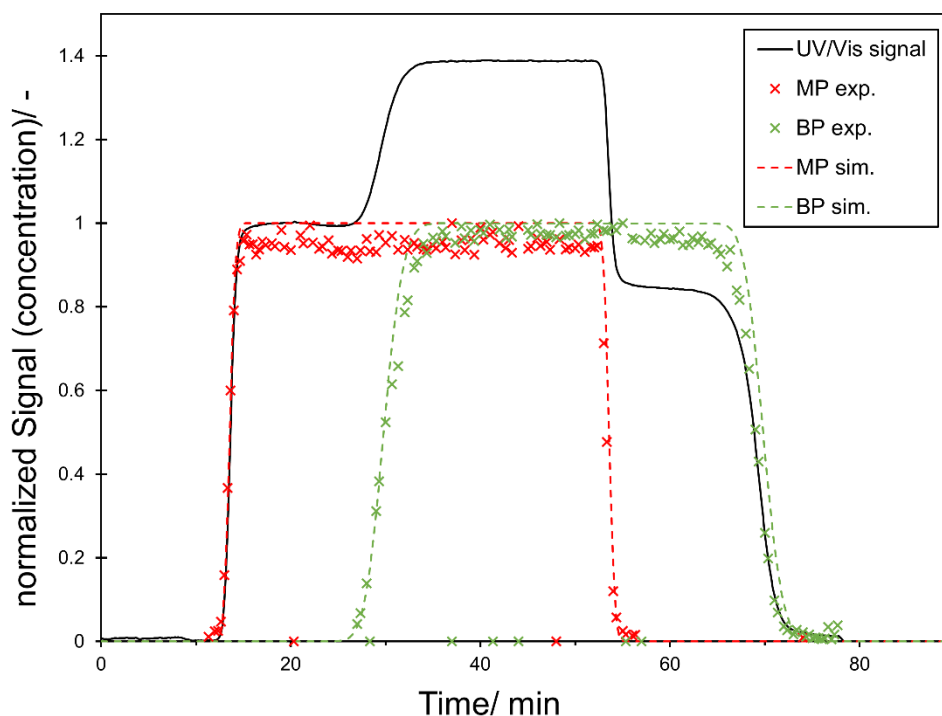


Figure 20: Breakthrough curve of methyl paraben (MP) and butyl paraben (BP) performed on a CPC column in descending mode including UV/Vis signal at 255 nm (UV/Vis signal), experimental elution profile from HPLC offline analysis (exp.) with corresponding simulation (sim.) using the cell model, respectively. Operating parameters: descending mode with MP ($P_{MP} = 0.982$, $N_{MP} = 797$, $c_{MP} = 0.2 \text{ mg ml}^{-1}$) and BP ($P_{BP} = 3.366$, $N_{BP} = 347$, $c_{BP} = 0.2 \text{ mg ml}^{-1}$), Arizona N, 1700 rpm, $V_C = 246.65 \text{ ml}$, $S_F = 0.5$, $F = 18 \text{ ml min}^{-1}$, $t_{inj} = 40 \text{ min}$ ($V_{inj} = 720 \text{ ml}$);

In the current case, BP represents the target compound and MP the most relevant impurity in the current model system. Hence, BP is retained in the column, while MP elutes from the column. Based on simulations in classical elution mode with various injection volumes, an injection duration t_{inj} of 12 min ($V_{inj} = 216 \text{ ml}$) could be determined in a way that at the end of the classical elution mode, the switching point t_{switch} , MP has completely eluted from the column while the breakthrough of BP has not been started yet. These criteria are fulfilled at $t_{switch} = 26.8 \text{ min}$.

Finally the two options for the extrusion of the stationary phase, back extrusion (Fig. 21) and elution-extrusion (Fig. 22), were evaluated. In both cases, partly a co-elution of mobile and stationary phase could be observed after switching the mode, which results in a further solute mass transfer between the phases as part of a non-ideal piston effect during the extrusion. This differs from the theoretical assumptions and observations in CCC literature, where the two phases are pushed out of the column separately and no co-elution of the two phases occurs. Although the duration of the extrusion theoretically is the same, in practice it took about 5 min longer in the back-extrusion mode compared to the elution-extrusion mode to extrude the BP completely from the column at a given flow rate. Hence, this also contributes to a slightly

higher solvent consumption in the back-extrusion mode. Especially at industrial scale, this might be a selection criterion between the two extrusion modes. An advantageous side effect is that the column in elution-extrusion mode is already filled with stationary phase at the end of the experiment and the next separation can directly be started without changing the phases inside the column. In conclusion, both extrusion modes are applicable, since the elution step as well as the selection of the switching time is independent of the extrusion. However, the elution-extrusion mode was found to be more advantageous in comparison to the back-extrusion mode.

As a result from this preliminary study, the model-based design can be applied to subsequently determine the appropriate injection volume and switching time for the selective compound enrichment with breakthrough curves in LLC. Subsequently, this approach was transferred to the purification of xanthohumol C from a raw hop extract (**Paper V**).

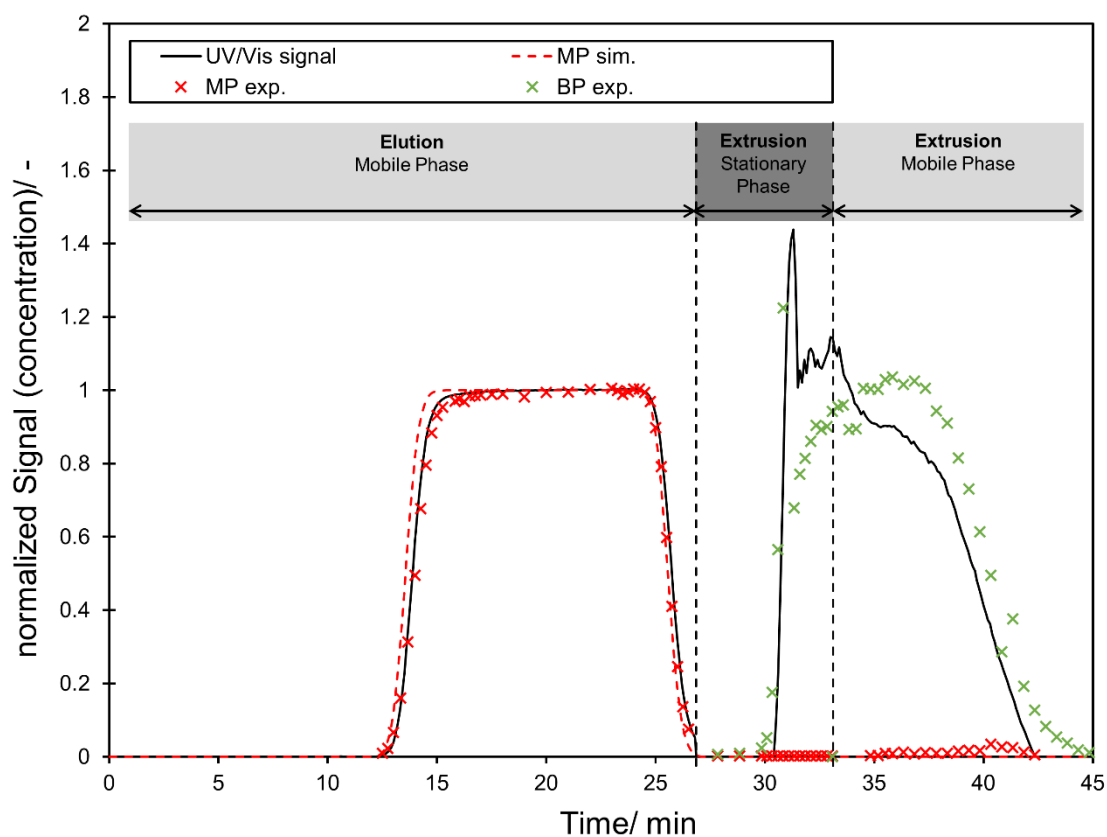


Figure 21: Separation of methyl paraben (MP) and butyl paraben (BP) in back-extrusion mode with a CPC column feed load of $V_{inj} = 216$ ml ($t_{inj} = 12$ min) and a switching point (t_{switch}) after 26.8 min, including UV/Vis signal at 255 nm (UV/Vis signal), experimental elution profiles from HPLC offline analysis (exp.), and the corresponding simulated elution profile (sim.) of MP ($P_{MP} = 0.982$, $N_{MP} = 797$) using the cell model. Operating parameters: elution mode in descending mode, Arizona N, 1700 rpm, $V_C = 246.65$ ml, $S_F = 0.5$, $F = 18$ ml min^{-1} , $c_{Feed} = c_{MP} = c_{BP} = 0.2$ mg ml^{-1} .

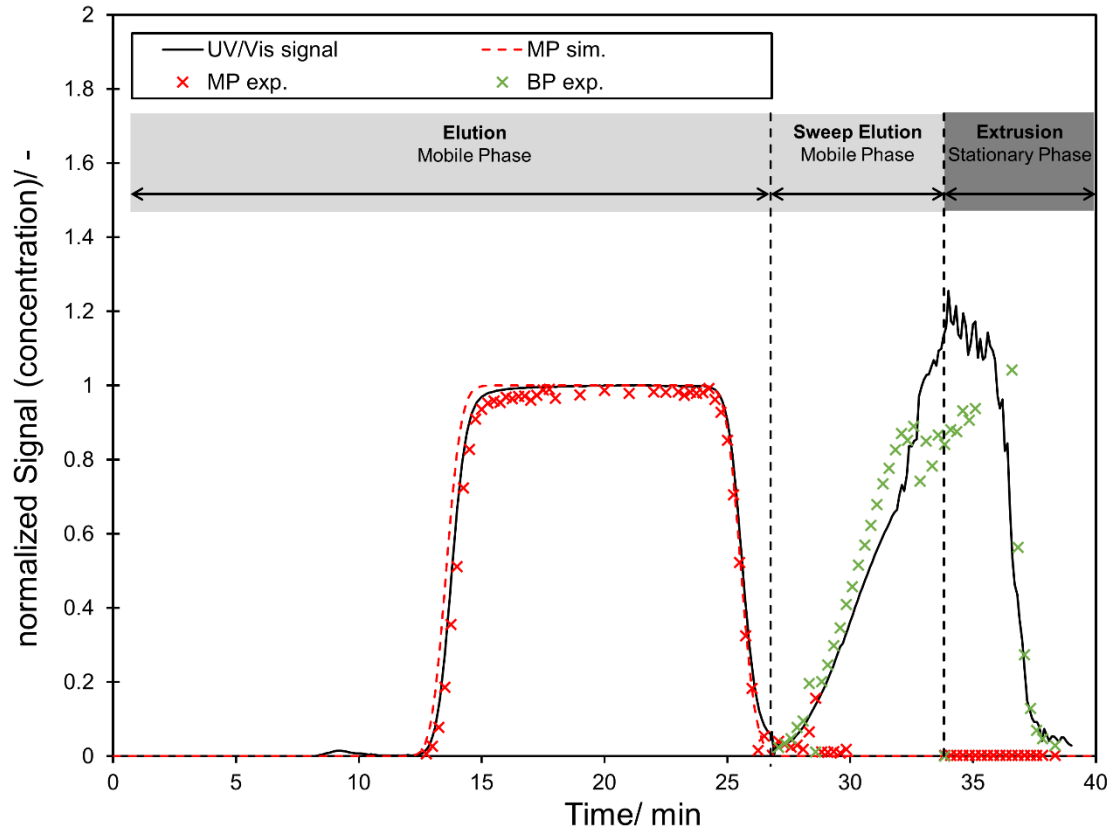


Figure 22: Separation of methyl paraben (MP) and butyl paraben (BP) in elution-extrusion mode with a CPC column feed load of $V_{inj} = 216$ ml ($t_{inj} = 12$ min) and a switching point (t_{switch}) after 26.8 min, including UV/Vis signal at 255 nm (UV/Vis signal), experimental elution profiles from HPLC offline analysis (exp.), and the corresponding simulated elution profile (sim.) of MP ($P_{MP} = 0.982$, $N_{MP} = 797$) using the cell model. Operating parameters: elution mode in descending mode, Arizona N, 1700 rpm, $V_C = 246.65$ ml, $S_F = 0.5$, $F = 18$ ml min^{-1} , $c_{Feed} = c_{MP} = c_{BP} = 0.2$ mg ml^{-1} .

3.5.2. Paper V: Xanthohumol C, a minor bioactive hop compound: Production, purification strategies and antimicrobial test

3.5.2.1. Summary

Citation

S. Roehrer, J. Behr, V. Stork, M. Ramires, G. Médard, O. Frank, K. Kleigrewer, T. Hofmann, M. Minceva, (2018). Xanthohumol C, a minor bioactive hop compound: production, purification strategies and antimicrobial test. *Journal of Chromatography B*, 1095, 39-49

<https://doi.org/10.1016/j.jchromb.2018.07.018>

Summary

In the field of natural products, minor plant components were shown to be potentially more bioactive than related major compounds. A promising natural resource for such highly potent bioactive natural products is hops, which has been used as a medicinal herb for centuries. However, minor hop compounds are often not available in sufficient quantities or can be obtained only with very time- and cost-intensive procedures, e.g. by many pulse injections by using preparative HPLC columns. This severely restricts comprehensive studies on their bioactivity and efficacy. In this work, production and purification strategies were investigated at the example of the minor hop compound xanthohumol C (XNC), a derivative of the well-known and already widely studied xanthohumol (XN). Different production and separation strategies for the purification of XNC from a XN-enriched raw hop extract, where only 0.24-2.2% XNC are present, were evaluated. As part of a two-step liquid-liquid chromatographic process, 95% pure XNC could be captured and enriched selectively from the extract. However, the productivity was low due to the low content of XNC in the starting mixture. In order to further increase the purity and productivity, an alternative production route was established. This approach is based on the fact that the desired target component XNC is a derivative of the major component XN. First, XN is isolated with LLC and converted into the target component XNC with the help of a rapid and simple semi-synthesis. In this context, two options for the ring-closure of the prenylated chalcone from XN to XNC were evaluated. Subsequently, XNC was purified by LLC batch injections in classical elution mode from the reaction product. It was demonstrated that LLC in combination with semi-synthesis could be a powerful tool for the production of natural minor compounds with a high purity of >99%. In addition, it was shown that LLC is an efficient technology for the isolation of natural minor components in high purity and amounts needed for subsequent bioactivity tests. The anticarcinogenic potential of the isolated XNC was studied in **Paper VI**.

Contributions

The author of this dissertation had a leading role in this work. The author did the conceptual design of the work, conducted or supervised all data acquisition and experiments, and interpreted the data. The author designed the separations, semi-syntheses, analysis and microbial tests. J. Behr supported the author with the design of the microbial tests and the interpretation of the corresponding results. V. Stork and M. Ramires performed part of the separations and microbial tests. Synthesis 2 was conducted in collaboration with G. Médard. O. Frank conducted the NMR measurement and helped with the interpretation of the NMR spectra. K. Kleigrewé and T. Hofmann supported the author with the performance and interpretation of the tandem mass spectrometry experiments. The author wrote the manuscript and discussed the results with J. Behr and M. Minceva.

3.5.2.2. Manuscript

Journal of Chromatography B 1095 (2018) 39–49



Contents lists available at ScienceDirect

Journal of Chromatography B

journal homepage: www.elsevier.com/locate/jchromb



Xanthohumol C, a minor bioactive hop compound: Production, purification strategies and antimicrobial test



Simon Roehrer^a, Juergen Behr^b, Verena Stork^a, Mara Ramirez^a, Guillaume Médard^c, Oliver Frank^d, Karin Kleigrew^b, Thomas Hofmann^d, Mirjana Minceva^{a,*}

^a Biothermodynamics, TUM School of Life and Food Sciences Weihenstephan, Technical University of Munich, Maximus-von-Inhof-Forum 2, 85354 Freising, Germany

^b Bavarian Center for Biomolecular Mass Spectrometry, TUM School of Life and Food Sciences Weihenstephan, Technical University of Munich, Gregor Mendel Strasse 4, 85354 Freising, Germany

^c Chair of Proteomics and Bioanalytics, TUM School of Life and Food Sciences Weihenstephan, Technical University of Munich, Emil-Erlenmeyer-Forum 5, 85354 Freising, Germany

^d Chair of Food Chemistry and Molecular Sensory Science, TUM School of Life and Food Sciences Weihenstephan, Technical University of Munich, Lise-Meitner-Strasse 34, 85354 Freising, Germany

ARTICLE INFO

Keywords:

Countercurrent chromatography
Centrifugal partition chromatography
Xanthohumol
Xanthohumol C
Antimicrobial bioactivity
Humulus lupulus

ABSTRACT

Hop has been attracting scientific attention due to its favorable bioactivity properties. It is thus desirable to relate these properties to the specific hop compounds and extract these compounds in highly purified form in order to enhance the effect. The aim of the present study is the isolation of a sufficient amount of the highly purified prenylated minor hop compound xanthohumol C (XNC) for characterizing its bioactivity. Two strategies for the production of XNC were evaluated. The first strategy involved a capture of natural XNC from a xanthohumol (XN)-enriched hop extract (XF) by countercurrent chromatography. In the second approach, a one-step semi-synthesis of XNC was performed starting from XN, which had previously been separated from a natural XN-enriched hop extract. Both methods delivered XNC in sufficient amount and purity (> 95%, HPLC), whereas the second strategy was preferable in terms of purity (> 99%, HPLC) as well as productivity and solvent consumption. The methods were validated by identifying and quantifying XNC using LC-MS, LC-MS/MS and ¹H NMR analysis. The XNC obtained in this way was supplied to several bacterial, yeast and fungal cultures in order to evaluate its antimicrobial effects. For comparison, microorganisms were also treated with the natural XN-enriched hop extract, as well as the prenylated hop compound XN. While still reducing cell proliferation, XNC was found to be less effective than both XF and XN for all studied bacteria and yeasts. Furthermore, for *Bacillus subtilis*, a strongly pH-dependent minimal inhibition concentration was observed for all three bioactive compounds, lowest at a p_H of 5 and highest at a p_H of 7.

1. Introduction

In the past few years, natural phenolic plant compounds have shown promise not only because of their antimicrobial and antiviral effects but also for cancer treatment and chemoprevention [1, 2]. In this context, there is an increasing interest in hops. Hop (*Humulus lupulus* L.) is widely used in the brewing industry to give beer its characteristic flavor and bitterness. Additionally, hop is well known as a medicinal plant with many bioactive effects. It contains a wide variety of biologically active phenolic compounds [3–6]. The most studied polyphenolic substances (xanthohumol, isoxanthohumol, 6-prenylnaringenin, 8-prenylnaringenin, desmethylxanthohumol) belong to the group of prenylflavonoids. Xanthohumol (XN) is the most abundant prenylated

chalcone in hops [7]. Great importance has been placed on this compound due to its multiple biological activities, including antimicrobial and anticancer effects. Xanthohumol shows co-action with several antibiotics [8, 9]. However, its bioactivity against gram positive bacteria decreases when used in combination with other hop compounds [9]. These investigations strongly emphasize the potential of XN and its analogues as promising compounds for the prevention and treatment of many diseases [2, 3, 6, 7, 10–15]. Due to all these properties of already known and well investigated hop compounds, there is an increasing interest, thus making other naturally occurring minor hop chalcones available for further bioactivity studies.

Some minor chalcones, such as xanthohumol H or 3'-geranyl-6'-O-methylchalconaringenin [16], are even more bioactive in comparison

* Corresponding author.

E-mail address: mirjana.minceva@tum.de (M. Minceva).

<https://doi.org/10.1016/j.jchromb.2018.07.018>

Received 15 February 2018; Received in revised form 19 June 2018; Accepted 15 July 2018

Available online 18 July 2018

1570-0232/ © 2018 Published by Elsevier B.V.

to XN [4, 7, 17]. One of these promising naturally occurring minor chalcones is xanthohumol C (XNC) [18, 19]. It has lately received much attention due to its antiproliferative, cytotoxic [20], neuro-protective [21] and antioxidative [16] activities. XNC, also called dehydroxycycloanthohumol, was first identified in the 1990s by Stevens et al. [20, 22]. The chemical structure of XNC differs from that of XN by a ring closing of the prenyl side chain with the hydroxyl group at position 4' (see Fig. 4). Miranda et al. [20] already observed a significant anti-proliferative and cytotoxic effect of various prenylated flavonoids. They assumed that pure XNC inhibited the growth of MCF-7 breast cancer cells at lower concentrations compared to XN and isoxanthohumol. In a recent study, XNC was identified as the most active compound within a group of hop-derived prenylflavonoids for the differentiation of neuronal precursor cells [21].

While XN and other major phenolic hop compounds are already well characterized in literature, pharmacological data concerning minor compounds such as XNC is scarce. In order to perform pharmacological testing, sufficient highly purified quantities of these compounds must be made available. Due to their low concentration, a powerful method for isolating these compounds from natural hops is necessary and such methods are still being investigated [23]. In the case of XNC, one approach is the total chemical synthesis of the complex molecule from simpler precursors, as described by Lee et al. [23] and Vogel et al. [16]. An alternative method is the one-step semi-synthesis of XNC starting from XN as proposed by Aigner et al. [24]. In this reaction, XN is converted to XNC with 2,3-dichloro-5,6-dicyano-p-benzoquinone (DDQ) [24]. The XNC obtained in this way must be purified further. Existing methods for the isolation and purification of XNC are complex and involve several extraction and chromatographic steps, such as flash chromatography and preparative HPLC [7, 25].

In the current study, solid support-free liquid-liquid chromatography (LLC), better known as countercurrent chromatography (CCC) and centrifugal partition chromatography (CPC), is evaluated as an alternative separation technique for the purification of XN and XNC. This method promises high product recovery with low irreversible adsorption. Compared to conventional liquid chromatography, both the mobile and the stationary phase are liquid in LLC. They are obtained by mixing specific amounts of two or more solvents, which form two liquid phases. The stationary phase is held in place in a specially designed column with the help of a centrifugal field, while the mobile phase is pumped through the column. The separation occurs as a result of the difference in the partitioning of the compounds of a mixture between the two liquid phases [26–28]. Components with lower partition coefficients travel faster through the column than components with higher partition coefficients. Due to the liquid nature of the stationary phase and wide variety of solvents that can be used, this technique allows for the creation of tailor-made biphasic liquid systems, i.e. tailor-made mobile and stationary phases, which makes this separation technology extremely versatile. A wide variety of biphasic solvent systems has already been established in the history of LLC, such as the solvent system families HEMWat (*n*-hexane/ethyl acetate/methanol/water) and Arizona (*n*-heptane/ethyl acetate/methanol/water) [26–33]. In addition, the whole volume of liquid stationary phase, which typically occupies 50 to 70% of the column volume, is available for the solutes, thus making high sample loading feasible.

In 1997, Hermans-Lokkerbol et al. introduced CPC for the preparative separation of bitter acids from hop extracts [34]. Chen et al. [25] and Chadwick et al. [35] later reported on the potential of CCC for the isolation of prenylated phenolics from hops. Among other compounds, they isolated > 95% pure XN (determined by HPLC at 370 nm) using the HEMWat solvent system family. Alvarenga et al. [36] and Dietz et al. [5] also used CCC and the HEMWat solvent system family for generating *tailor-made* extracts from natural hops for a targeted analysis of their biological activity.

In the current study, two different approaches for obtaining XNC, starting from a XN-enriched hop extract named Xantho-Flav™ (XF) were

established (see Fig. 1). In the first approach, a two-step CCC purification process including a capture and enrichment stage of XNC followed by a CCC batch separation was used. In the second approach, two possible reaction routes for a one-step semi-synthesis from XN to XNC were compared and followed by XNC purification with CCC batch separation. Finally, the antimicrobial properties of XF, XN and XNC were screened for typical representative bacteria (gram positive and gram negative) and fungi (yeasts and molds) in order to evaluate their antimicrobial potential.

2. Materials and methods

2.1. Materials

2.1.1. Chemicals

The pre-concentrated commercial xanthohumol (65–90%) crude extract, Xantho-Flav™ (XF), was supplied by the Hopsteiner GmbH (Germany). For the CCC and CPC experiments, the *n*-hexane (purity: ≥ 95%) solvent was purchased from Honeywell (Germany). Ethyl acetate for liquid chromatography (purity: ≥ 98%), and methanol for analysis (purity: ≥ 99.9%) were purchased from Merck KGaA (Germany). The deionized water was obtained from an in-house network system. For analysis, Milli-Q water from a Milli-Q Direct Water Purification System from Merck Millipore (Germany) and acetonitrile from J.T. Baker (Netherlands) were used.

For the semi-syntheses, (diacetoxyiodo)benzene (Ph(OAc)₂, purity: ≥ 98%), 2,2,6,6-tetramethylpiperidinyloxy (TEMPO, purity: ≥ 98%), 2,3-dichloro-5,6-dicyano-p-benzoquinone (DDQ, purity: 98%) and anhydrous benzene (purity ≥ 99.8%) were purchased from Sigma-Aldrich (USA). Anhydrous tetrahydrofuran (THF, purity: ≥ 99%) and 1,4-dioxane (purity: ≥ 98%) were purchased from Alfa Aesar (Germany).

2.1.2. Microorganisms and cultivation

All microorganisms were kindly provided by the Chair of Technical Microbiology (TMW, Technical University of Munich, Germany) and were part of the TMW strain collection. *Escherichia coli* (TMW 2.436) (37 °C, with agitation) and *Bacillus subtilis* (TMW 2.246) (30 °C, without agitation) were grown in lysogeny broth (LB) medium. Yeast extract, peptone ex casein, NaCl and agar for solid medium, were purchased from Carl Roth® (Germany). *Lactobacillus brevis* (TMW 1.313) (30 °C, without agitation) and *Pedococcus damnosus* (TMW 2.1535) (30 °C, without agitation) were grown in MRS agar (De Man, Rogosa and Sharpe) and O₂ reduced environments (AGS CampyGen™; Oxoid Limited, UK). For the growth media, yeast extract, cysteine-HCl, agar and MnSO₄·H₂O were purchased from Carl Roth® (Germany). Meat extract, KH₂PO₄, NH₄Cl, Tween 80, glucose, maltose, MgSO₄·7 H₂O were obtained from Merck KGaA (Germany) and fructose from Omni Life Science (Germany). K₂HPO₄ was purchased from AppliChem (Germany).

The yeasts *Saccharomyces cerevisiae* (TMW 3.009) and *Saccharomyces pastorianus* (TMW 3.288) were cultivated in yeast extract-peptone-glycerol (YPG) medium at room temperature without agitation. Malt extract was obtained from AppliChem (Germany) and peptone ex soya and agar from Carl Roth® (Germany).

The molds *Aspergillus niger* (TMW 4.1068), *Penicillium roqueforti* (TMW 4.1599), *Penicillium expansum* (TMW 4.1363), and *Rhizopus stolonifer* (TMW 4.1544) were cultivated with malt extract agar (MEA) at room temperature. Yeast extract, peptone ex casein and agar were purchased from Carl Roth® (Germany), while glucose was purchased from Merck KGaA (Germany).

The media for all microorganisms were adjusted to pH values of 5, 6 and 7 with concentrated hydrochloric acid (Carl Roth®, Germany). Cycloheximide (Carl Roth®, Germany) as positive control for antibiotic effects was used for fungi and chloramphenicol (Carl Roth®, Germany) for bacteria. All hop compounds were dissolved in dimethyl sulfoxide (DMSO, purity: > 99.5%) from Sigma-Aldrich (USA) for the bioactivity

tests, and DMSO was used as negative control. The zone of inhibition assay was conducted with discs (BBL™ Sensi-Disc™ Susceptibility Test Discs) from Becton Dickinson (USA). To avoid evaporation, cells in 96-well plates were coated with paraffin oil from Sigma-Aldrich (USA).

2.2. Methods

2.2.1. Preparation of biphasic liquid systems

The biphasic liquid systems for the CCC and CPC separations were prepared by mixing the respective amounts of the solvents at room temperature. The mixture was vigorously shaken and equilibrated at room temperature for at least two hours. For the CCC and CPC experiments, the phases were split and placed in two separate containers. A freshly prepared biphasic system was used in each experiment.

2.2.2. Determination of the partition coefficients

The partition coefficients (defined in Section 3.1) of the selected hop compounds in the investigated biphasic systems were determined using the shake flask method. The hop extract Xantho-Flav™ was added to two equal volumetric portions of upper and lower phase, 5 mL respectively, of a previously equilibrated biphasic system. Due to the detection limit of the minor hop compounds, a concentration of the extract of 10 mg mL⁻¹ per volume of the total biphasic system was used. After equilibration at room temperature, the two liquid phases were split and placed into two separate vials for LC-MS and UV-Vis analysis at 290 nm and 370 nm.

2.2.3. Countercurrent chromatography (CCC) experiments

CCC experiments were carried out on a countercurrent chromatography column, model HPCCC-Mini Centrifuge (0.8 mm i.d.) from Dynamic Extractions (Wales), with a column volume of 18.2 mL. Two isocratic Gilson 306 pumps (Gilson, USA), equipped with an 806 Manometric Module (Gilson, USA), were used for delivering the mobile and stationary phases. The elution profiles were monitored with a DAD 171 diode array detector (Gilson, USA) at a wavelength of 370 nm. The CCC experiments were performed at room temperature.

Two different types of CCC experiments were carried out: pulse injections and elution-extrusion experiments. At the beginning of each experiment, the column was filled with the stationary phase. Afterwards, the rotational speed was set to 1900 rpm and the mobile phase was pumped through the column at 1 mL min⁻¹ until no more stationary phase eluted from the column.

For the CCC pulse injection experiments, the samples were then injected via a 0.5 mL sample loop with a manual injection valve and the mobile phase was continuously pumped at 1 mL min⁻¹.

The elution-extrusion countercurrent chromatography (EECCC) consists of two steps: an elution step (equivalent to pulse injection) followed by an extrusion step in which mobile and stationary phase, including the retained components, is pushed out from the column by pumping a fresh stationary phase into the column. Contrary to the CCC pulse injections, a considerably larger amount of the hop extract Xantho-Flav™ (2.2 mg mL⁻¹ dissolved in mobile phase, V_{inj} = 48 mL) was introduced continuously using the mobile phase pump. After 152.1 min, the elution mode was switched to extrusion mode, where initially the mobile phase portion and subsequently the stationary phase portion in the column, including the retained compounds, were pushed out. This was reached by pumping fresh stationary phase into the column at a flow rate of 1 mL min⁻¹ for at least one column volume. All CCC runs were manually fractionated after injection in fraction intervals of 30 s or 1 min. The collected fractions were analyzed by LC-MS. From each experiment, the selected CCC fractions containing XNC were combined, solvents were evaporated, and the sample finally lyophilized in a Free Zone Plus 2.5 freeze dry system from Labconco (USA).

2.2.4. Centrifugal partition chromatography (CPC) experiments

Experiments were performed at room temperature in a centrifugal partition column (CPC), model SCPC 250, from Armen Instrument (now called CPC 250, Gilson Purification SAS, France), described by Hopmann et al. [37]. The column consists of two single columns connected in series with a total column volume of 250 mL. The column was equipped with two HPLC gradient pumps (Armen Instrument, France) and the effluent monitored with a UV detector (ECOM DAD600 2WL 200–600 nm, Czech Republic) at 290 nm and 370 nm. A fraction collector (LS 5600, Armen Instrument, France) was used for collecting fractions during the separation run. The experimental procedure of the pulse injection experiment is equivalent to the procedure described in Section 2.2.6 for a CCC column. In CPC, the rotational speed was set to 1700 rpm and the flow rate to 14 mL min⁻¹. The injection loop had a volume of 5 mL. The run was fractionated with the help of a fraction collector in intervals of 30 s or 1 min. The fractions were analyzed by LC-MS afterwards. The CPC fractions containing XN were combined, solvents were evaporated, and the sample finally lyophilized in a Free Zone Plus 2.5 freeze dry system from Labconco (USA).

2.2.5. Semi-syntheses of xanthohumol C from xanthohumol

Semi-synthesis 1. The synthesis protocol was adapted from George et al. [38], suggested for the synthesis of hyperguinone B. TEMPO (90 mg, 0.578 mmol) and PhI(OAc)₂ (102.4 mg, 0.137 mmol), each previously dissolved in 5 mL of THF and stored at -80 °C, were slowly added sequentially to a solution of purified XN (102.4 mg, 0.289 mmol) in 10 mL of THF at -80 °C under a nitrogen atmosphere. After 5 min, the reaction was quenched with water (10 mL) and extracted with diethylether (3 × 10 mL). The combined organic layer was dried on MgSO₄, filtered through a 0.2 μm nylon filter and evaporated under vacuum. Further lyophilization gave a yellow powder which was subsequently purified as described in Section 3.4.

Semi-synthesis 2. The protocol used for the chemical synthesis of XNC from XN was proposed by Aigner et al. [24] and adapted from Jain et al. [39]. 2,3-Dichloro-5,6-dicyanobenzoquinone (DDQ, 128 mg, 0.56 mmol) was added to a solution of XN (200 mg, 0.56 mmol) in 1 mL dry benzene and 2 drops of 1,4-dioxane under an argon atmosphere. The reaction mixture was irradiated with microwaves at 120 °C (Monowave 300 microwave reactor from Anton Paar, Austria) for 3 min. Ethyl acetate (approximately 20 mL) was added and the solids filtered off by vacuum filtration (ceramic filter, pore size 10–16 μm), which allowed to remove most of the non-reacted DDQ. The crude product was purified by CCC pulse injections as described in Section 3.4.

2.2.6. Analytical methods

Liquid chromatography and mass spectrometry (LC-MS) analysis. Liquid chromatography analyses coupled with mass spectrometry (LC-MS) were carried out using a LCMS-2020 single quadrupole mass spectrometer equipped with a Prominence HPLC system including an auto-sampler SIL-20 A, a solvent delivery module LC-20 AB Prominence and a photodiode array UV/VIS detector SPD-M20 A, each from Shimadzu (Japan), respectively. For the mass spectrometry, a Dual Ion Source (DUIS) was used and analysis was carried out in the negative ionization mode. The separation was performed with a reversed-phase silica Acclaim 120, C18, analytical column (4.6 × 250 mm, 5 μm) from Dionex (Germany). Milli-Q water (A) and acetonitrile (B) including 0.05% formic acid (FA), respectively, were used as mobile phase at a flow rate of 1 mL min⁻¹ (gradient: 0 min 20% B, 1 min 20% B, 21.75 min 90% B, 28.75 min 90% B, 29.75 min 20% B, 34 min 20% B). The injection volume of the sample was 5 μL. A flow rate splitter was used to set the flow rate that enters the mass spectrometer to 0.2 mL.

Mass spectrometric profile data were acquired from 50 m/z to 800 m/z in negative ionization with a scan speed of 5000 u/s and an interface voltage of -4.5 kV using nitrogen as collision gas.

Liquid chromatography and high resolution tandem mass spectrometry (LC-MS/MS) analysis. LC-MS/MS analyses were carried out on a Nexera X2 UPLC system from Shimadzu (Japan), including the SIL-30AC autosampler and the LC-30AC solvent delivery module, coupled with a Triple-TOF[®] 6600 mass spectrometer (AB Sciex, Germany). For the mass spectrometry, an electrospray ionization (ESI) with negative ionization was used. The analysis was performed with Kinetex XB reversed-phase silica, C18 analytical column (100×2.1 mm, $1.7 \mu\text{m}$, 100 \AA) from Phenomenex (Germany). Milli-Q water (A) and acetonitrile (B) were used as mobile phase at a flow rate of 0.4 mL min^{-1} (gradient: 0 min 30% B, 0.3 min 30% B, 4.0 min 100% B, 5.0 min 100% B, 7.0 min 30% B). The injection volume of the sample was $5 \mu\text{L}$. Mass spectrometric data were acquired in high sensitivity mode (8 MS/MS measurements per measuring cycle) from 50 m/z to 1500 m/z in negative ionization and an ion spray voltage of -4.5 kV using nitrogen as collision gas.

Nuclear magnetic resonance spectroscopy (NMR) analysis. The structure of the purified target compound XNC was verified by ¹H NMR (nuclear magnetic resonance) spectroscopy. The ¹H NMR analysis was performed on a 500 MHz Avance III spectrometer (Bruker, Germany) and the ¹H quantitative NMR (qNMR) for purity assessment was performed on a 400 MHz Avance III spectrometer (Bruker, Germany), using the parameters from literature [40]. For the qNMR, a 5 mM solution of purified XNC in deuterated methanol ($600 \mu\text{L}$) (MeOD) from Sigma-Aldrich (USA) was used.

2.2.7. Antimicrobial bioactivity tests

The zone of inhibition assay was applied to determine the effect of the hop extract XF, XN and XNC in microorganisms. Small discs for the inhibition assay were prepared by immersion in $100 \mu\text{M}$ and 1 mM of bioactive compounds in DMSO. From a cell suspension, 10^7 bacteria or

yeasts, or 10^5 spores of molds were spread on a solid agar plate and the prepared discs subsequently placed on the agar plate. After incubation, a clear zone was observed around the discs containing the antimicrobial components and its diameter was measured.

The minimal inhibition concentrations (MIC) were determined by turbidity change in liquid medium. The optical density at a wavelength of 600 nm ($\text{OD}_{600\text{nm}}$) of a cell suspension of *B. subtilis*, *S. cerevisiae* and *S. pastorianus* was adjusted to 0.05. From this cell suspension, $198 \mu\text{L}$ were added to each well of a 96-well plate (Sarstedt AG & Co., Germany) and $2 \mu\text{L}$ of the different concentrations of bioactive substances were added to each well. The cells were additionally coated with paraffin oil. Microorganisms were incubated under the respective conditions and the presence of growth was determined by visible observation. All experiments were performed in triplicate.

3. Results and discussion

The concentration of the target compound xanthohumol C (XNC) in the starting material (xanthohumol (XN)-enriched hop extract Xantho-Flav[™]) is very low, only 0.24 to 2.2%. In terms of productivity and solvent consumption, a direct separation of XNC by conventional pulse injections is therefore not feasible. In this work, two different approaches for obtaining XNC from XN-enriched hop extract, both involving solid support-free liquid-liquid chromatography (CCC/CPC), were evaluated. The process flow is presented in Fig. 1. In the first approach, a two-step CCC purification including a XNC capture and enrichment step, followed by a XNC separation step, is used (Section 3.2). In the second approach, one-step semi-synthesis of XNC from purified XN (Section 3.3) is followed by XNC CCC separation. Two possible reaction routes for the semi-synthesis of XNC from XN were evaluated and compared (Section 3.4).

After completing the separation of XNC, the antimicrobial properties of XF, XN and XNC were screened (Section 3.5) on typical representatives of bacteria (gram positive and gram negative) and fungi (yeasts and molds) in order to compare the antimicrobial activity of XNC with that of the other two compounds.

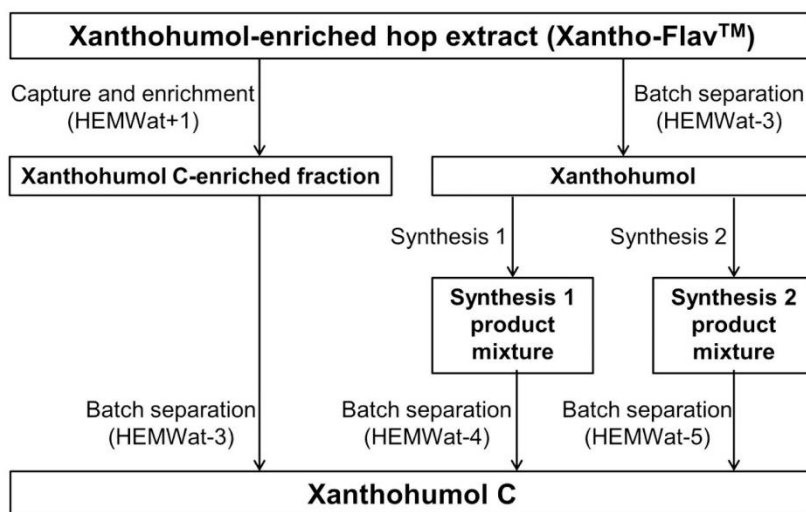


Fig. 1. Different process approaches for the production and purification of xanthohumol C starting from the xanthohumol (XN)-enriched hop extract Xantho-Flav[™].

3.1. Separation and purification of xanthohumol from hop extract

For the one-step semi-synthesis (Section 3.3) as well as for the bioactivity study (Section 3.5), highly pure xanthohumol (XN) is required. Hence, XN was separated from XN-enriched hop extract Xantho-Flav™ (XF) using solid support-free liquid-liquid chromatography. First, the composition of the starting material, the XN-enriched hop extract, was determined by LC-MS. The main constituents relevant for this study and the minor hop chalcone xanthohumol C (XNC) are listed in Table 1 with their characteristic mass to charge ratio (m/z) at negative ionization and their content in the extract calculated using the UV signal recorded at 370 nm.

The first step in designing a CCC or CPC separation is the selection of a suitable biphasic solvent system. The partition coefficient P_i of the target components is used as a screening and selection parameter. The partition coefficient P_i in CCC/CPC is defined as the ratio of the concentration of a solute i in the stationary phase (c_i^{SP}) to its concentration in the mobile phase (c_i^{MP}) at thermodynamic equilibrium (Eq. 1). For the classical elution mode, P_i should preferably be in the *sweet spot* range ($0.4 < P_i < 2.5$). Values outside this range lead to low resolution or high solvent consumption and diluted products.

$$P_i = \frac{c_i^{SP}}{c_i^{MP}} \quad (1)$$

The *n*-hexane/ethyl acetate/methanol/water (HEMWat) solvent system family [31], consisting of 16 systems with different

Table 1

Main compounds and the minor hop compound xanthohumol C with their characteristic mass to charge ratio (m/z) at negative ionization and content in the xanthohumol (XN)-enriched hop extract Xantho-Flav™.

Compound	Abbreviation	m/z ($[M-H]^-$)	Content ^a /%
1 Isoxanthohumol	IX	353	0.05–0.14
2 8-Prenylnaringenin	8-PN	339	0.06–0.12
3 Desmethylxanthohumol	DMX	339	0.38–1.02
4 6-Prenylnaringenin	6-PN	339	0.06–0.20
5 Xanthohumol	XN	353	65–90
6 Xanthohumol C	XNC	351	0.24–2.2

^a Calculated using the UV signal recorded at 370 nm.

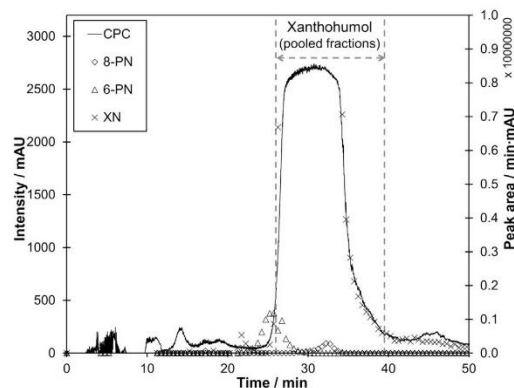


Fig. 2. Chromatogram of CPC separation of xanthohumol (XN) from Xantho-Flav™ with the solvent system HEMWat-3 (*n*-hexane/ethyl acetate/methanol/water, 6/4/6/4 v/v/v/v) at the wavelength of 370 nm, including the LC-MS offline analysis of the collected fractions containing xanthohumol and the main impurities 8-prenylnaringenin (8-PN) and 6-prenylnaringenin (6-PN) at 370 nm (ASC mode: 14 mL min^{-1} , $c_{inj} = 55.6 \text{ mg mL}^{-1}$, $V_{inj} = 5 \text{ mL}$, 1700 rpm , $S_F = 0.47$).

compositions and polarities, was screened. This solvent system family has already been successfully used by Chadwick et al. [35] and Chen et al. [25] for the isolation of different prenylated phenolic hop compounds, e.g. xanthohumol and 8-prenylnaringenin. The partition coefficients of the main constituents of the XN-enriched hop extract were experimentally determined by shake flask experiments. A list of partition coefficients obtained in the different HEMWat-systems is presented in Table A of the Supplementary material.

Based on the results of the shake flask experiments, the solvent system HEMWat-3 (6/4/6/4 v/v/v/v) was selected for the purification of XN. This solvent system ensures that the partition coefficient of XN is in the *sweet spot* range and maximizes the separation factor between XN and remaining compounds. The separation was performed first with an analytical CCC column (18.2 mL column volume) in ascending mode (ASC, upper phase as mobile phase) at 1 mL min^{-1} and 1900 rpm. The feed mixture was injected in the column ($V_{inj} = 0.5 \text{ mL}$) with a concentration of 40 mg mL^{-1} , which was prepared by dissolving XF in the mobile phase (see Supplementary Fig. A adapted from [41]). The separation could successfully be transferred to a semi-preparative CPC column (250 mL column volume), by keeping constant the ratio of feed mass load to total column volume ($m_{load} : V_C = 1.1 \text{ mg mL}^{-1}$) and the stationary phase retention. The stationary phase retention is the volume of stationary phase in the column divided by the total column volume. In order to keep the same stationary phase retention ($S_F = 0.47$) as in the analytical CCC column, a mobile phase flow rate of 14 mL min^{-1} was used. A feed with a concentration of 55.6 mg mL^{-1} of XF ($V_{inj} = 5 \text{ mL}$) was used and the rotational speed was set to 1700 rpm.

The chromatogram of the CPC separation is shown in Fig. 2 (adapted from [41]). Even though there is a small peak overlapping of 6-PN and 8-PN with XN, 98.6% pure XN (HPLC, 370 nm) could be obtained with a recovery of 90%. The XN fraction obtained from the CPC separation was then evaporated, freeze dried and used as purified XN for the semi-syntheses of XNC (Section 3.3) and in the bioactivity studies (Section 3.6).

3.2. Capture and purification of natural xanthohumol C from hop extract with CCC

In this section, the two-step CCC purification process for obtaining pure XNC from XN-enriched hop extract Xantho-Flav™ (XF) is evaluated (see left-hand side in Fig. 1). In the first step, XNC was captured and enriched using CCC in so-called elution-extrusion mode (EECC). In the second step, the XNC recovered in the first step was separated from the remaining impurities using the conventional elution CCC mode.

EECC consists of two steps: an elution and an extrusion step [42]. During the elution step, the column is loaded with the sample and some of the components contained in the sample mixture are eluted. Typically, the elution step is stopped when the target compound has eluted out of the column. This is followed by the extrusion step, in which a fresh stationary phase is pumped in the column instead of the mobile phase. In this step, the entire column content, i.e. mobile and stationary phases and the components dissolved therein, are pushed out of the column. Therefore, it is no longer necessary to wait for the elution of highly retained impurities that would elute after the target compound. Thus, EECC accelerates the separation process and reduces the amount of consumed solvent.

In contrast to the classical application procedure described above, EECC is used in this work to capture and enrich XNC. Instead of switching to extrusion following the elution of the target compound, the target compound is retained in the column, while the major impurities present in XF, i.e. XN, are separated through elution. Hence, a solvent system has to be selected, in which the partition coefficient of XNC is considerably higher than the partition coefficient of the main impurity XN. Therefore, the amount of XNC in the retained fraction is enriched. However, it must be noticed that the partition coefficient of the target compound should not be too high in order to ensure their elution in a reasonable time.

Based on partition coefficients from shake flask experiments (see Supplementary Table A), different HEMWat systems were evaluated in terms of XNC productivity and solvent consumption. This was done by

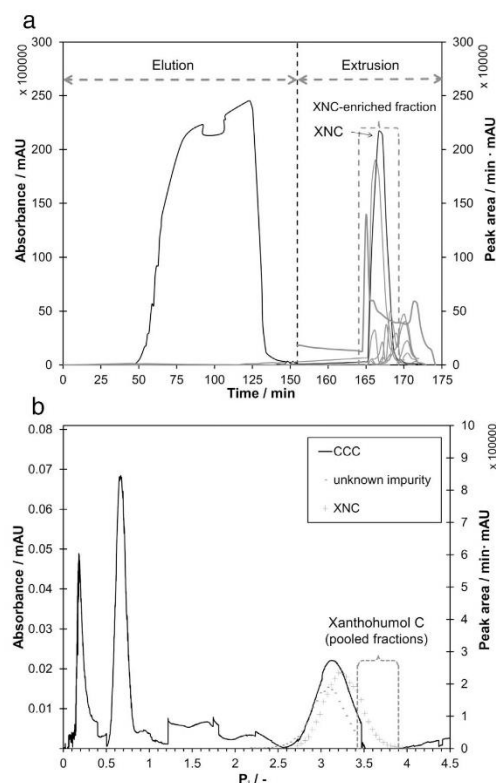


Fig. 3. (a) Chromatogram of EIECCC experiment for XNC capture from Xantho-Flav™ with the solvent system HEMWat+1 (hexane/ethyl acetate/methanol/water, 4/6/5/5 v/v/v/v) at the wavelength of 370 nm, including the LC-MS offline analysis of the collected fractions during the extrusion step at 370 nm (DSC mode: 1 mL min^{-1} , $c_{inj} = 2.44 \text{ mg mL}^{-1}$, $V_{inj} = 48 \text{ mL}$, 1900 rpm , $S_F = 0.54$). For the sake of clarity, the data of the offline analysis are shown with continuous lines. (b) Chromatogram of CCC separation of xanthohumol C from XNC-enriched fraction (see Fig. 3a) with the solvent system HEMWat-3 (hexane/ethyl acetate/methanol/water, 6/4/6/4 v/v/v/v) at the wavelength of 370 nm, including the LC-MS offline analysis of the collected fractions containing XNC and an unknown impurity at 370 nm (DSC mode: 1 mL min^{-1} , $c_{inj} = 2.2 \text{ mg mL}^{-1}$, $V_{inj} = 0.5 \text{ mL}$, 1900 rpm , $S_F = 0.63$).

simulation using the cell model [43], also known as the plate model, implemented in gPROMS Model Builder v4.2 software from Process Systems Enterprise (London, UK) [44–46]. The maximum possible injection volume, and with it the optimal time of switching between elution and extrusion step, were determined for the systems HEMWat-3/–1/0/+1, using the experimentally determined partition coefficients of XN and XNC, and the stationary phase retention S_F at 1 mL min^{-1} and 1900 rpm in DSC mode (lower phase as mobile phase) for each studied system. For the simulations, a column efficiency of $N_i = 100$ was assumed for all compounds.

Subsequently, the solvent system HEMWat+1 (hexane/ethyl acetate/methanol/water, 4/6/5/5 v/v/v/v) was selected, where XNC ($P_{XNC} = 19.2$) is much stronger retained than the major compound XN ($P_{XN} = 3.1$). A maximal injection volume of 48 mL was determined and the extrusion could be started directly before the breakthrough of XNC from the column, namely after 152.1 min . In addition, the feed concentration of 2.44 mg mL^{-1} (XF dissolved in mobile phase) was experimentally selected

in order to avoid stationary phase loss during the run.

As it could be seen from the chromatogram in Fig. 3a, XN, the main compound in the XN-enriched extract Xantho-Flav™, elutes during the elution step. In the extrusion step, XNC was fully recovered and other minor compounds with similar partition coefficients to XNC co-eluted and therefore are also collected in the product fraction (see Fig. 3a). The relative amount of XNC (HPLC, 370 nm) in the XNC-enriched product fraction collected during the extrusion step was 21% and hence clearly increased compared to the initial amount of 0.24 to 2.2% XNC in XF. The XNC-enriched product fraction was then evaporated and freeze dried.

Subsequently, another batch separation step had to be conducted (see Fig. 3b) for obtaining pure XNC. The solvent system HEMWat-3 (6/4/6/4 v/v/v/v) was selected for this, as it ensured a sufficient separation factor of XNC and remaining minor impurities. However, a co-elution of XNC and an unknown impurity occurred, which made peak-cutting necessary for obtaining highly purified (> 95%) XNC with a recovery of 15%, see Fig. 3b. The separation was performed in descending mode (DSC) with an analytical CCC column at 1 mL min^{-1} , 1900 rpm . A feed of 0.5 mL with a concentration of 2.2 mg mL^{-1} , prepared by dissolving the XNC-enriched product in mobile phase, was injected. Highly purified (95%) XNC (HPLC, 370 nm) could be recovered in this separation step.

Considering that XNC is present in XF in a very low amount (0.24 to 2.2%) and the productivity is limited by the available amount, about 0.24 mg of the minor hop chalcone XNC could be recovered per gram of Xantho-Flav™ after the EIECCC capturing step, followed by the CCC batch separation. Hence, a high amount of extract has to be processed to provide sufficient amounts of XNC. However, it should be pointed out that compared to many single pulse injections in series, this method saves separation time and reduces solvent consumption as well as avoids excessive dilution of the target compound.

3.3. Chemical semi-synthesis of xanthohumol C

As an alternative to the approach described in Section 3.2, a sufficient amount of pure XNC for bioactivity studies can be obtained by chemical synthesis from XN. However, the total chemical synthesis of XNC includes several synthesis and separation steps, and thus it is complicated and very time consuming [16, 23]. Therefore, the strategy of combining a one-step semi-synthesis with a liquid-liquid chromatographic separation (see right-hand side in Fig. 1) was evaluated in this work. For the one-step semi-synthesis, two different reaction routes for an oxidative cyclization from XN to XNC (see Fig. 4), were examined by using the CPC purified XN (see Section 3.1) to process route 1 (synthesis 1) and route 2 (synthesis 2).

In the first semi-synthesis (synthesis 1), proposed by George et al. [38] for the synthesis of hyperquinone B, XN is treated with PhI(OAc)_2 in the presence of TEMPO (see Section 2.2.5). George et al. [38] report a high selectivity for the reaction of hyperquinone B, for which they suggest a mechanism involving a selective hydride abstraction by TEMPO cation followed by a 6π -electrocyclization. In the case of XN, this reaction yields three XNC isomers with the same mass to charge ratio (m/z 351), most likely due to the presence of two phenolic oxygen atoms, which could be involved in the cyclization. However, after lyophilization of the product mixture, no other XNC isomers could be identified by LC-MS analysis anymore (UV-Vis analysis at 370 nm and m/z 351). We assume that these isomers were UV sensitive and degenerated during the lyophilization step under ambient light.

The second alternative semi-synthesis (synthesis 2), proposed by Aigner et al. [24], enables the selective cyclization of XN to XNC with the help of dichloro-dicyanobenzoquinone (DDQ, see Section 2.2.5). The reaction yield of synthesis 2 was higher than of synthesis 1. The reaction yield is the ratio of the amount of XNC that was converted from XN to the amount of XN before the conversion. It was determined by the UV signal from LC-MS analysis of the synthesis product at 370 nm. In synthesis 1, only about 1.4% of XN could be converted to XNC, while in synthesis 2 as much as 12% of XN were converted into XNC. Starting from 200 mg of purified XN, about 2.8 mg of XNC were obtained in

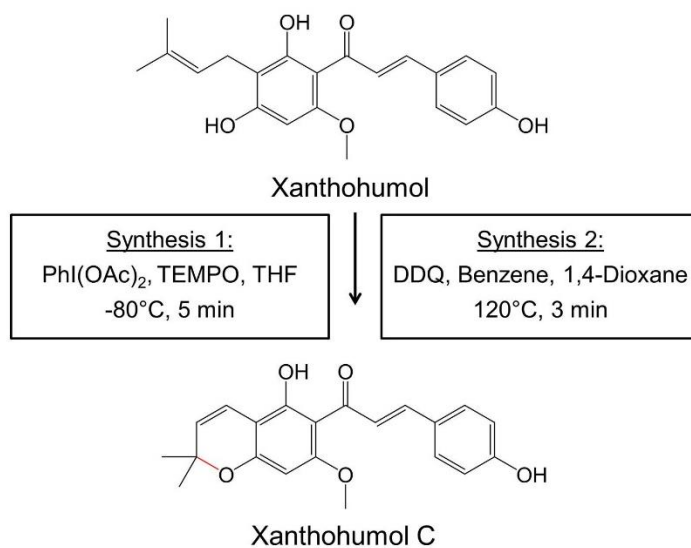


Fig. 4. Two reaction routes, synthesis 1 and 2, for a one-step semi-synthesis of xanthohumol C (XNC) from xanthohumol (XN) by oxidative cyclization of CPC purified XN.

synthesis 1 and about 15 mg of XNC in synthesis 2. Consequently, synthesis crude products with a XNC content of about 9% (synthesis 1) and 20.6% (synthesis 2) could be obtained.

To conclude, XNC can be synthesized in one-step semi-syntheses. It must be noted, however, that the product mixtures of both semi-synthetic routes still contain significant amounts of impurities of side reactions and unreacted reactants such as TEMPO or DDQ that need to be removed. Both reactions could also be performed with the crude XN-enriched extract Xantho-Flav™. However, this would lead to additional impurities in the product mixture and hence further complicate the subsequent purification of XNC. Therefore, this possibility was not pursued any further in this study.

3.4. Purification of xanthohumol C obtained by chemical semi-syntheses

A CCC batch separation was used as a final purification step of XNC for both synthesis products. Preliminary selection of the solvent systems for the separation of the product mixtures was made based on the partition coefficient of XNC and XN, since no information was available about the partitioning of the other reactants and reaction side products present. Hence, the considered biphasic solvent systems were first narrowed down based on the partition coefficient of XNC, i.e. P within or close to the *sweet spot*. The systems fulfilling this criterion were then evaluated based on their separation factor between XNC and XN, with larger separation factors α being favored.

3.4.1. XNC purification from synthesis 1

For the first synthesis, the solvent system HEMWat-4 (hexane/ethyl acetate/methanol/water, 7/3/6/4 v/v/v/v) was selected. The separation was performed in descending mode (lower phase as mobile phase, 1 mL min⁻¹, V_{inj} = 0.5 mL, 1900 rpm). The synthesis product was injected dissolved in the mobile phase with a concentration of 13 mg mL⁻¹. This was the maximal concentration at which no stationary phase loss occurred during the separation. The stationary phase retention was 0.62. As shown in Fig. 5a, a complete separation of fully recovered XNC (purity: > 99%, HPLC at 370 nm) from XN and other reactants could be achieved.

3.4.2. XNC purification from synthesis 2

XNC produced with the second synthesis could be purified with the solvent system HEMWat-5 (hexane/ethyl acetate/methanol/water, 7/3/7/3 v/v/v/v) and the same process conditions (DSC mode, c_{inj} = 13 mg mL⁻¹, V_{inj} = 0.5 mL, 1900 rpm, S_F = 0.69). The injected concentration was selected equivalent to synthesis 1, to avoid stationary phase loss during the separation. As shown in Fig. 5b, a baseline separation was achieved and 99.8% pure XNC (HPLC at 370 nm) was obtained with a recovery of over 95%.

In this system, the partition coefficient of XNC is lower than in the system HEMWat-4 that was used for the purification from synthesis 1, which results in a shorter separation time. A complete separation was still achieved with this solvent system due to the lower partition coefficient of the different impurities present in the synthesis 2 product mixture compared to the synthesis 1 product mixture.

In comparison, the purification of XNC from synthesis 2 product is more efficient, due to both a shorter separation time (lower solvent consumption) and a higher XNC content in the injected mixture: about 0.68 mg mL⁻¹ XNC in synthesis 2 compared to 0.068 mg mL⁻¹ XNC in synthesis 1. In each case, the most suitable solvent system was selected: HEMWat-4 for synthesis 1 and HEMWat-5 for synthesis 2. The selected solvent systems ensure that XNC starts eluting directly after even minor impurities, whose UV signal intensities are too low to be seen as a peak in Fig. 5, as they have left the column. The purity of the XNC obtained from both synthesis products exceeds 99%. Hence, considering the respective yield, the purification of synthesis 2 clearly outperforms the separation of XNC from the synthesis 1 product mixture. In both cases, an increase in feed load leads to stationary phase loss during the separation.

To conclude, two strategies for the production of pure XNC were evaluated: a two-step CCC purification of XNC directly from the XN-enriched extract Xantho-Flav™ (XF) and an alternative strategy combining chemical one-step semi-synthesis of XNC from purified XN followed by a CCC separation step. With the first strategy, a XNC isolation with 95% purity from XF using only CCC was achieved. However, yield and productivity were very low (0.24 mg XNC per gram XF, productivity of 0.0003 mg XNC per hour per mL column volume), limited by the small amount of XNC available in the extract XF. In terms of

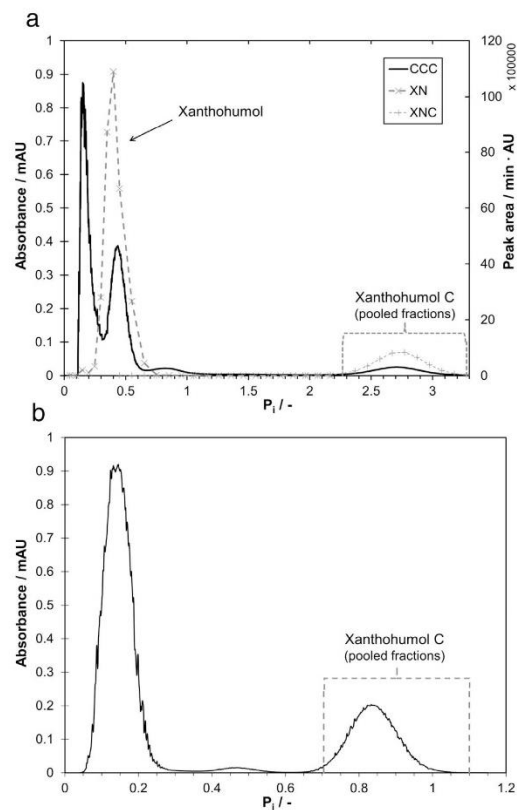


Fig. 5. (a) Chromatogram of CCC separation of XNC from the synthesis 1 product with the solvent system HEMWat-4 (hexane/ethyl acetate/methanol/water, 7/3/6/4 v/v/v/v) at the wavelength of 370 nm, including the LC-MS offline analysis of the collected fractions containing XN and XNC at 370 nm (DSC mode: $1 \text{ mL} \cdot \text{min}^{-1}$, $c_{inj} = 13 \text{ mg mL}^{-1}$, $V_{inj} = 0.5 \text{ mL}$, 1900 rpm, $S_F = 0.62$). (b) Chromatogram of CCC separation of XNC from the synthesis 2 product with the solvent system HEMWat-5 (hexane/ethyl acetate/methanol/water, 7/3/7/3 v/v/v/v) at the wavelength of 370 nm (DSC mode: $1 \text{ mL} \cdot \text{min}^{-1}$, $c_{inj} = 13 \text{ mg mL}^{-1}$, $V_{inj} = 0.5 \text{ mL}$, 1900 rpm, $S_F = 0.69$).

productivity, solvent consumption and especially purity, the alternative strategy was much more efficient. With this strategy, 99% pure XNC was obtained. It must be noted, however, that the second semi-synthesis (synthesis 2) outperformed the first option (synthesis 1). About 70 mg of XNC could be produced per gram of Xantho-Flav™ (0.04 mg XNC per hour per mL column volume) compared to 12 mg (0.003 mg XNC per hour per mL column volume) of XNC obtained through synthesis 1. Consequently, > 4 g of XNC could be produced with a typical industrial-scale column (5 L) and synthesis 2 per day.

Finally, it can be summarized that promising minor hop chalcones such as the XN analogue XNC can be made available efficiently in combination with semi-synthesis and CCC even in higher amounts and purities for further bioactivity studies.

3.5. Characterization of xanthohumol C

The purified target compound XNC from synthesis 2 (see pooled fractions in Fig. 5b) was further characterized by evaporating the solvents from the pooled fractions and subsequently freeze drying the sample. Purity and molecular structure were analyzed by LC-MS, LC-MS/MS and ^1H NMR. From the LC-MS analysis in Fig. 6, > 99% pure XNC was achieved based on the UV-Vis absorption profile (Fig. 6a at 370 nm). XNC was further identified by mass spectrometry at negative ionization (Fig. 6b, m/z 351).

In addition, XNC was also characterized by LC-MS/MS, as shown in Fig. 7. The molecular composition of $\text{C}_{21}\text{H}_{20}\text{O}_5$ and the specific fragmentation pattern of the ESI MS/MS spectra of XNC confirmed the molecular structure (Fig. 7b, the specific fragmentation pattern of XN (m/z 353) is provided in supplementary data, Fig. B). XN and XNC have similar fragmentation patterns (XNC major fragments $[\text{M}-\text{H}]^-$: m/z 351.1256/231.0664/119.0503; XN major fragments $[\text{M}-\text{H}]^-$: m/z 353.1423/323.0939/295.0634/233.0846/218.0592/175.0047/119.0517). The fragment m/z 231 of XNC compared to the respective fragment m/z 233 of XN indicates the ring closure of the prenyl unit. Even though the molecular structure of a compound cannot be confirmed by MS/MS data, fast and sufficient characterization can be achieved by comparing the fragmentation pattern.

The structure of XNC was confirmed by comparison to the ^1H NMR results of Dresel [47].

^1H NMR (500 MHz, MeOD; COSY): δ [ppm]: 1.43 [s, 6H, H-C (4'/5')]; 3.94 [s, 3H, H-C (1'')]; 5.52 [d, 1H, $J = 9.8 \text{ Hz}$, H-C (2'')]; 6.03 [s, 1H, H-C (6)]; 6.62 [d, 1H, $J = 9.8 \text{ Hz}$, H-C (1'')]; 6.83 [m, 2H, $J = 8.6 \text{ Hz}$, H-C (3'/5')]; 7.51 [m, 2H, $J = 8.6 \text{ Hz}$, H-C (2'/6')]; 7.71 [d, 1H, $J = 15.5 \text{ Hz}$, H-C (3)]; 7.78 [d, 1H, $J = 15.5 \text{ Hz}$, H-C (2)].

Additionally, the purity of XNC was determined by ^1H qNMR (400 MHz, MeOD; 25 °C). For the measurement, a 5 mM MeOD solution of the purified XNC was used and a recovery of 72.8% was determined (for the spectrum, see Supplementary Fig. C). Only residual water and some minor solvent residues (< 5%) were found as impurities. This is in accordance to literature [40], where considerable amounts of residual water were measured in natural isolates even though they were previously freeze-dried.

3.6. Antimicrobial bioactivity tests

For the antimicrobial bioactivity tests, a spectrum of different fungi and bacteria were incubated at concentrations of 100 μM and 1000 μM of XF, XN and XNC. Microbial growth was determined by disc diffusion assay, as explained in Section 2.2.7 Simpson et al. [48, 49] observed that hop acids have a higher antibacterial effect at lower pH values and that the transmembrane pH gradient is influenced by these substances. Therefore, all experiments were done with pH values of the incubation medium of 5, 6 and 7 to identify the effects of XF, XN and XNC on microbial growth at different pH.

For all evaluated molds, *Aspergillus niger*, *Penicillium roqueforti*, *Penicillium expansum*, and *Rhizopus stolonifera* no inhibition by any of the investigated compounds could be observed for the selected concentrations and pH values.

Regarding yeasts, *Saccharomyces pastorianus* was inhibited by 1000 μM XN and XF regardless of the pH. *Saccharomyces cerevisiae* showed no cell growth at 1000 μM of XF and XN, while for XNC, a small pH independent inhibition zone could be observed at 1000 μM . A small inhibition zone could also be observed at 100 μM of XN, XNC and XF with a pH of 5.

Moreover, the growth of *E. coli*, *Lactobacillus brevis* and *Pediococcus damnosus* was not inhibited. As shown in previous studies [50, 51], the growth of gram negative bacteria, such as *E. coli*, is not inhibited by hop compounds. The gram positive bacteria *L. brevis* and *P. damnosus* were originally isolated from spoiled beer. It is possible that the bacteria are familiar with polyphenols from hops and thus gained tolerance or

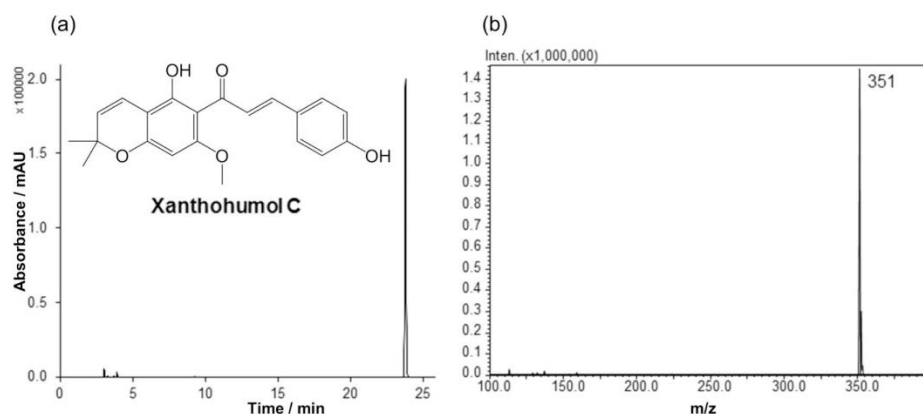


Fig. 6. LC-MS analysis of purified XNC (m/z 351) from synthesis 2 with (a) the chromatogram at a wavelength of 370 nm and (b) the corresponding mass spectrum in negative ionization mode.

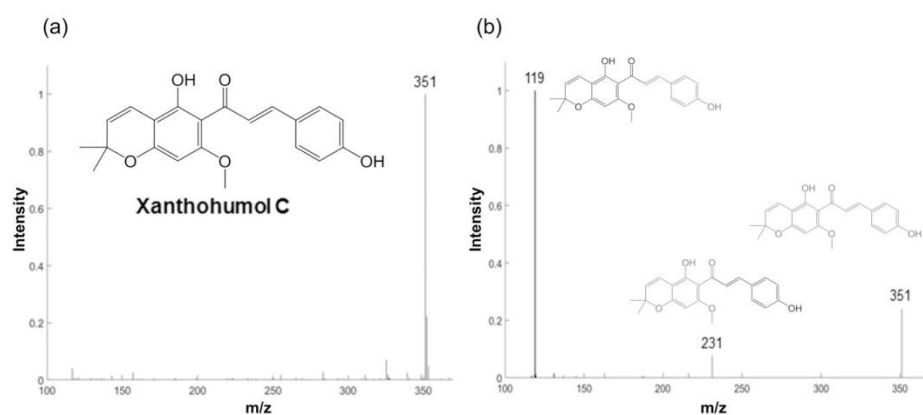


Fig. 7. LC-MS/MS analysis of purified XNC from synthesis 2 with (a) the MS spectrum of XNC (m/z 351) in negative ionization mode and (b) the corresponding MS/MS fragmentation pattern.

Table 2

Microbial inhibition zone diameters for considered microorganisms *S. cerevisiae*, *S. pastorianus* and *B. subtilis* after incubation with XF, XN and XNC at different pH values and concentrations.

	pH	<i>S. cerevisiae</i>		<i>S. pastorianus</i>		<i>B. subtilis</i>	
		100 μ M	1000 μ M	100 μ M	1000 μ M	100 μ M	1000 μ M
XF/ cm	5	0.67 \pm 0.03	0.83 \pm 0.06	X	0.83 \pm 0.03	1.03 \pm 0.20	1.86 \pm 0.06
	6	X	0.78 \pm 0.03	X	0.82 \pm 0.03	1.15 \pm 0.07	1.35 \pm 0.09
	7	X	0.78 \pm 0.03	X	0.80 \pm 0.05	X	1.15 \pm 0.15
XN/ cm	5	0.65 \pm 0	0.83 \pm 0.03	X	0.81 \pm 0.01	1.08 \pm 0.16	1.82 \pm 0.08
	6	X	0.77 \pm 0.03	X	0.78 \pm 0.03	1.05 \pm 0.07	1.27 \pm 0.06
	7	X	0.78 \pm 0.03	X	0.80 \pm 0	X	1.10 \pm 0.15
XNC/ cm	5	0.65 \pm 0	0.68 \pm 0.03	X	X	0.87 \pm 0.10	1.38 \pm 0.19
	6	X	0.65 \pm 0	X	X	0.95 \pm 0.21	1.00 \pm 0.1
	7	X	0.64 \pm 0.01	X	X	X	0.83 \pm 0.06

resistance, which might explain their growth in the presence of XN, XNC or XF. Cell growth of gram positive *B. subtilis* was inhibited at a pH of 5 and 6 at both studied concentrations, 100 μ M and 1000 μ M, for XF, XN and XNC. At a pH of 7, an inhibition was only observed at 1000 μ M

for all three hop probes. The inhibition zone diameters that were obtained are summarized in Table 2.

To conclude, XNC inhibited the cell growth of all studied microbial organisms less than XN and XF. The disc diffusion assay enabled a

screening of the inhibitory potential of these hop compounds. A cross comparison between either the different compounds or the different microorganisms was possible by determining the minimum inhibitory concentrations (MIC), which was suggested by Bhattacharya et al. [52] as a more accurate quantitative comparison of various hop constituents. Consequently, the MIC for *S. cerevisiae*, *S. pastorianus* and *B. subtilis* were determined by visual observation of turbidity at pH values of 5, 6 and 7. The minimal inhibition concentration is defined as the lowest concentration of the compound that shows no visible growth [53]. As shown in Table 3, XNC exhibited lowest inhibitory potential with MICs above 5000 μM for the studied yeast. As expected from the disc diffusion assay measurements, the inhibition of gram positive *B. subtilis* is pH-dependent but still only at high concentrations (500 μM at a pH of 5 to 5000 μM at pH 7). Compared to XNC, the MIC of XF and XN is significantly lower for all three pH values and species. In addition, the MIC of XF and XN at all three pH values and species is similar. For *S. cerevisiae* and *S. pastorianus*, no significant pH dependency could be observed. For *B. subtilis*, the MIC is lowest at a pH of 5 (97 μM) and highest at a pH of 7 (2000 μM). In all three organisms, there was no relevant difference between the MIC of XN and XF at a given pH value. Consequently, XN is likely the main reason for the antimicrobial inhibition, since it is the major constituent of XF.

To determine whether the compounds are bactericidal or fungicidal or just inhibit growth, a sample of incubated organisms with the MIC of the compounds was incubated again without XN, XNC and XF. Apparently, the inhibition was reversible and normal growth of all organisms could be observed.

Table 3

Minimal inhibition concentrations for considered microorganisms *S. cerevisiae*, *S. pastorianus* and *B. subtilis* after incubation with XF, XN and XNC at different pH values.

	pH	<i>S. cerevisiae</i>	<i>S. pastorianus</i>	<i>B. subtilis</i>
XF/ μM	5	667 \pm 58	600 \pm 0	97 \pm 6
	6	600 \pm 0	567 \pm 58	500 \pm 0
	7	500 \pm 0	633 \pm 58	2000 \pm 0
XN/ μM	5	667 \pm 58	567 \pm 58	87 \pm 6
	6	600 \pm 0	600 \pm 0	633 \pm 115
	7	500 \pm 0	600 \pm 0	2000 \pm 0
XNC/ μM	5	> 5000	> 5000	500 \pm 0
	6	> 5000	> 5000	4667 \pm 577
	7	> 5000	> 5000	5000 \pm 0

4. Conclusion

This work evaluated different separation strategies for the purification of the minor hop chalcone xanthohumol C (XNC) from a commercial xanthohumol (XN)-enriched hop extract (Xantho-Flav™, XF). A two-step liquid-liquid chromatographic process, consisting of a XNC capturing and enrichment step performed in elution-extrusion mode, followed by a XNC separation in elution mode was developed, leading to 95% purity (HPLC, 370 nm).

In addition, an alternative and even more efficient production strategy that consisted of a one-step semi-synthesis of XNC from XN followed by a liquid-liquid chromatographic separation in elution mode was established. With this alternative strategy, > 99% purity (HPLC, 370 nm) and a yield of up to 70 mg of XNC per gram of XF could be obtained. XNC was identified by LC-MS/MS and a fragmentation pattern was determined. Further, the structure of pure XNC could be verified by ^1H qNMR, with only water as the main residue.

In the last part of the study, the bioactivities of XNC, XN and the commercial hop extract XF were evaluated and compared. It was shown that the antimicrobial potential of XNC is not significant compared to XN and XF. For the treatment of molds and gram negative bacteria, no inhibition was observed. However, pH-independent inhibition for

yeasts (*Saccharomyces pastorianus*, *Saccharomyces cerevisiae*) and significantly pH-dependent inhibition for the gram positive bacteria *Bacillus subtilis* suggest different inhibition mechanisms of the considered hop compounds.

To sum up, solid support-free liquid-liquid chromatography (CCC/CPC) was shown to be a highly promising technology for isolating and purifying minor hop compounds in sufficient amounts for their further analysis and evaluation as a bioactive compound. The proposed methods thus provide a further step towards the exploitation of bioactive and antimicrobial effects of minor hop compounds.

Acknowledgements

We acknowledge M. Biendl from Hopsteiner (S. H. Steiner, Hopfen GmbH, 84048 Mainburg, Germany) for providing the hop extract Xantho-Flav™. The authors thank Prof. R. Vogel (Chair of Technical Microbiology, Technical University of Munich) for allowing us to carry out the microbial bioactivity experiments in his lab.

Appendix A. Supplementary data

Supplementary data to this article can be found online at <https://doi.org/10.1016/j.jchromb.2018.07.018>.

References

- [1] S. Malik, *Biotechnology and Production of Anti-Cancer Compounds*, Springer International Publishing, 2017.
- [2] M. Karabín, T. Hudcová, I. Jelínek, P. Dostálek, Biologically active compounds from hops and prospects for their use, *Compr. Rev. Food Sci. Food Saf.* 15 (2016) 542–567.
- [3] M. Biendl, *Hops and Health*. MBAA TQ, (2009), pp. 1–7 (doi: 10.1094, TQ-46-2-0416-01).
- [4] J. Olšovská, P. Cermak, V. Bostiková, P. Bostik, M. Dusek, A. Mikyska, V. Jandovská, K. Bogdanova, M. Kolar, *Humulus lupulus* L. (Hops) – a valuable source of compounds with bioactive effects for future therapies, *Mil. Med. Sci. Lett. (Voj. Zdrav. Listy)*, 85 (2016), p. 19.
- [5] B.M. Dietz, S.-N. Chen, R.F.R. Alvarenga, H. Dong, D. Nikolić, M. Biendl, R.B. van Breemen, J.L. Bolton, G.F. Pauli, Designer extracts as tools to balance estrogenic and chemopreventive activities of botanicals for women's health, *J. Nat. Prod.* 80 (8) (2017) 2284–2294, <https://doi.org/10.1021/acs.jnatprod.7b00284>.
- [6] J.F. Stevens, J.E. Page, Xanthohumol and related prenylflavonoids from hops and beer: to your good health!, *Phytochemistry* 65 (2004) 1317–1330.
- [7] M. Liu, P. Hansen, G. Wang, L. Qiu, J. Dong, H. Yin, Z. Qian, M. Yang, J. Miao, Pharmacological profile of xanthohumol, a prenylated flavonoid from hops (*Humulus lupulus*), *Molecules* 20 (2015) 754.
- [8] P. Natarajan, S. Katta, I. Andrei, V.B.R. Ambati, M. Leonida, G. Haas, Positive antibacterial co-action between hop (*Humulus lupulus*) constituents and selected antibiotics, *Phytomedicine* 15 (2008) 194–201.
- [9] M. Rozalski, B. Micota, B. Sadowska, A. Stochmal, D. Jedrejek, M. Wieckowska-Szakiel, B. Rozalska, Antiadherent and antibiofilm activity of *Humulus lupulus* L. derived products: new pharmacological properties, *Biomed. Res. Int.* 2013 (2013).
- [10] S. Venturilli, M. Burkard, M. Biendl, U.M. Lauer, J. Frank, C. Busch, Prenylated chalcones and flavonoids for the prevention and treatment of cancer, *Nutrition* 32 (2016) 1171–1178.
- [11] C. Gerhäuser, A. Alt, E. Heiss, A. Gamal-Eldeen, K. Klimo, J. Knauff, I. Neumann, H.-R. Scherf, N. Frank, H. Bartsch, H. Becker, Cancer chemopreventive activity of xanthohumol, a natural product derived from hop 1 support for this work has been provided by Verein zur Förderung der Krebsforschung in Deutschland e.V. and by Wissenschaftsförderung der Deutschen Brauwirtschaft eV These data were presented, in part, at the 92nd annual meeting of the American Association of Cancer Research, March 24–28, 2001 in New Orleans, LA (64), *Molecular Cancer Therapeutics*, 1 (2002), pp. 959–969.
- [12] C. Gerhäuser, Broad spectrum anti-infective potential of xanthohumol from hop (*Humulus lupulus* L.) in comparison with activities of other hop constituents and xanthohumol metabolites, *Mol. Nutr. Food Res.* 49 (2005) 827–831.
- [13] Y. Kang, M.-A. Park, S.-W. Heo, S.-Y. Park, K.W. Kang, P.-H. Park, J.-A. Kim, The radio-sensitizing effect of xanthohumol is mediated by STAT3 and EGFR suppression in doxorubicin-resistant MCF-7 human breast cancer cells, *Biochim. Biophys. Acta Gen. Subj.* 1830 (2013) 2638–2648.
- [14] P. Zanoli, M. Zavatti, Pharmacognostic and pharmacological profile of *Humulus lupulus* L., *J. Ethnopharmacol.* 116 (2008) 383–396.
- [15] L. Legette, C. Karnpracha, R.L. Reed, J. Choi, G. Bobe, J.M. Christensen, R. Rodríguez-Proteau, J.Q. Purnell, J.F. Stevens, Human pharmacokinetics of xanthohumol, an antihyperglycemic flavonoid from hops, *Mol. Nutr. Food Res.* 58 (2014) 248–255.
- [16] S. Vogel, J.R. Heilmann, Synthesis, cytotoxicity, and antioxidative activity of minor prenylated chalcones from *Humulus lupulus*, *J. Nat. Prod.* 71 (2008) 1237–1241.

- [17] E. Nuti, B. Bassani, C. Camodeca, L. Rosalia, A. Cantelmo, C. Gallo, D. Baci, A. Bruno, E. Orlandini, S. Nencetti, D.M. Noonan, A. Albini, A. Rossello, Synthesis and antiangiogenic activity study of new hop chalcone xanthohumol analogues, *Eur. J. Med. Chem.* 138 (2017) 890–899.
- [18] M. Forino, S. Pace, G. Chianese, I. Santagostini, M. Werner, C. Weinigel, S. Rummeler, G. Fico, O. Werz, O. Tagliatalella-Scafati, Humulifucol and bioactive prenylated polyphenols from hops (*Humulus lupulus* cv. "Cascade"), *J. Nat. Prod.* 79 (2016) 590–597.
- [19] D. Nikolic, R.B. Van Breenen, Analytical methods for quantitation of prenylated flavonoids from hops, *Curr. Anal. Chem.* 9 (2013) 71–85.
- [20] C. Miranda, J. Stevens, A. Helmrich, M. Henderson, R. Rodriguez, Y.-H. Yang, M. Deinzer, D. Barnes, D. Buhler, Antiproliferative and cytotoxic effects of prenylated flavonoids from hops (*Humulus lupulus*) in human cancer cell lines, *Food Chem. Toxicol.* 37 (1999) 271–285.
- [21] E. Oberbauer, C. Urmann, C. Steffenhagen, L. Bieler, D. Brunner, T. Fartner, C. Humpel, B. Bäumer, C. Bandtlow, S. Couillard-Despres, Chroman-like cyclic prenylflavonoids promote neuronal differentiation and neurite outgrowth and are neuroprotective, *J. Nutr. Biochem.* 24 (2013) 1953–1962.
- [22] S. Vogel, Synthese prenylierter Chalkone aus Hopfen und Bestimmung ihrer cytotoxischen und antioxidativen Aktivität, (2008).
- [23] Y.R. Lee, L. Xia, Concise total synthesis of biologically interesting pyranochalcone natural products: citranobin, boesenbergin A, boesenbergin B, xanthohumol C, and glabrachromene, *Synthesis* 2007 (2007) 3240–3246.
- [24] I. Aigner, E. Oberbauer-Hofmann, S. Couillard-Despres, F.J. Rivera, H. Riepl, C. Urmann, M. Biendl, Chromane-like Cyclic Prenylflavonoids for the Medical Intervention in Neurological Disorders, US20170128411 A1, (2016).
- [25] Q.-h. Chen, M.-l. Fu, M.-m. Chen, J. Liu, X.-j. Liu, G.-q. He, S.-c. Pu, Preparative isolation and purification of xanthohumol from hops (*Humulus lupulus* L.) by high-speed counter-current chromatography, *Food Chem.* 132 (2012) 619–623.
- [26] A. Berthod, K. Faure, Separations with a liquid stationary phase: countercurrent chromatography or centrifugal partition chromatography, *Analytical Separation Science*, 2015, pp. 1177–1206, <https://doi.org/10.1002/9783527678129.assep046>.
- [27] A.P. Foucault, Centrifugal Partition Chromatography, M. Dekker, 1995.
- [28] A. Berthod, Countercurrent Chromatography, Elsevier, 2002.
- [29] K. Skalikova-Woźniak, I. Garrard, A comprehensive classification of solvent systems used for natural product purifications in countercurrent and centrifugal partition chromatography, *Nat. Prod. Rep.* 32 (2015) 1556–1561.
- [30] J.B. Friesen, J.B. McAlpine, S.-N. Chen, G.F. Pauli, Countercurrent separation of natural products: an update, *J. Nat. Prod.* 78 (2015) 1765–1796.
- [31] J. Brent Friesen, G.F. Pauli, GUESS—A generally useful estimate of solvent systems for CCC, *J. Liq. Chromatogr. Relat. Technol.* 28 (2005) 2777–2806.
- [32] I. Sutherland, L. Brown, S. Forbes, G. Games, D. Hawes, K. Hostettmann, E. McKerrill, A. Marston, D. Wheatley, P. Wood, Countercurrent chromatography (CCC) and its versatile application as an industrial purification & production process, *J. Liq. Chromatogr. Relat. Technol.* 21 (1998) 279–298.
- [33] Y. Ito, Golden rules and pitfalls in selecting optimum conditions for high-speed counter-current chromatography, *J. Chromatogr. A* 1065 (2005) 145–168.
- [34] A. Hermans-Lokkerbol, A. Hoek, R. Verpoorte, Preparative separation of bitter acids from hop extracts by centrifugal partition chromatography, *J. Chromatogr. A* 771 (1997) 71–79.
- [35] L.R. Chadwick, H.H. Fong, N.R. Farnsworth, G.F. Pauli, CCC sample cutting for isolation of prenylated phenolics from hops, *J. Liq. Chromatogr. Relat. Technol.* 28 (2005) 1959–1969.
- [36] R.F. Ramos Alvarenga, J.B. Friesen, D. Nikolić, C. Simmler, J.G. Napolitano, R. van Breenen, D.C. Lankin, J.B. McAlpine, G.F. Pauli, S.-N. Chen, K-targeted metabolomic analysis extends chemical subtraction to DESIGNER extracts: selective depletion of extracts of hops (*Humulus lupulus*), *J. Nat. Prod.* 77 (2014) 2595–2604.
- [37] E. Hopmann, J. Goll, M. Minceva, Sequential centrifugal partition chromatography: a new continuous chromatographic technology, *Chem. Eng. Technol.* 35 (2012) 72–82.
- [38] J.H. George, M.D. Hesse, J.E. Baldwin, R.M. Adlington, Biomimetic synthesis of polycyclic polyprenylated acylphloroglucinol natural products isolated from *Hypericum papuanum*, *Org. Lett.* 12 (2010) 3532–3535.
- [39] A. Jain, R. Gupta, P. Sarpal, Synthesis of (+) lupiniforum, di-O-methyl xanthohumol and isoxanthohumol and related compounds, *Tetrahedron* 34 (1978) 3563–3567.
- [40] O. Frank, J.K. Kreissl, A. Daschner, T. Hofmann, Accurate determination of reference materials and natural isolates by means of quantitative 1H NMR spectroscopy, *J. Agric. Food Chem.* 62 (2014) 2506–2515.
- [41] M. Ramires, Synthesis and Purification of Xanthohumol C from Xanthohumol Hop Extract, Instituto Superior Técnico, Universidade de Lisboa, 2016.
- [42] A. Berthod, J.B. Friesen, T. Inui, G.F. Pauli, Elution–extrusion countercurrent chromatography: theory and concepts in metabolic analysis, *Anal. Chem.* 79 (2007) 3371–3382.
- [43] A.J.P. Martín, R.L.M. Synge, A new form of chromatogram employing two liquid phases, A theory of chromatography, 2. Application to the Micro-determination of the Higher Monoamino-acids in Proteins, 35 1941, pp. 1358–1368.
- [44] J. Völk, W. Arlt, M. Minceva, Theoretical study of sequential centrifugal partition chromatography, *AIChE J.* 59 (2013) 241–249.
- [45] E. Hopmann, M. Minceva, Separation of a binary mixture by sequential centrifugal partition chromatography, *J. Chromatogr. A* 1229 (2012) 140–147.
- [46] J. Goll, A. Frey, M. Minceva, Study of the separation limits of continuous solid support free liquid–liquid chromatography: separation of capsaicin and dihydrocapsaicin by centrifugal partition chromatography, *J. Chromatogr. A* 1284 (2013) 59–68.
- [47] M. Dresel, Struktur und sensorischer Beitrag von Hopfenhartharzen zum Bittergeschmack von Bier sowie zellbasierte Studien zu deren Resorption und Metabolismus, Verlag Dr. Hut, 2013.
- [48] W. Simpson, A. Smith, Factors affecting antibacterial activity of hop compounds and their derivatives, *J. Appl. Microbiol.* 72 (1992) 327–334.
- [49] W. Simpson, Ionophoric action of trans-isohumulone on *Lactobacillus brevis*, *Microbiology* 139 (1993) 1041–1045.
- [50] M. Stompor, B. Żarowska, Antimicrobial activity of Xanthohumol and its selected structural analogues, *Molecules* 21 (2016) 608.
- [51] B. Kramer, J. Thielmann, A. Hickisch, P. Muranyi, J. Wunderlich, C. Hauser, Antimicrobial activity of hop extracts against foodborne pathogens for meat applications, *J. Appl. Microbiol.* 118 (2015) 648–657.
- [52] S. Bhattacharya, S. Virani, M. Zavro, G.J. Haas, Inhibition of *Streptococcus mutans* and other oral streptococci by hop (*Humulus lupulus* L.) constituents, *Econ. Bot.* 57 (2003) 118–125.
- [53] C. Carson, K. Hammer, T. Riley, Broth micro-dilution method for determining the susceptibility of *Escherichia coli* and *Staphylococcus aureus* to the essential oil of *Melaleuca alternifolia* (tea tree oil), *Microbios* 82 (1995) 181–185.

3.5.3. Paper VI: Analyzing Bioactive Effects of the Minor Hop Compound Xanthohumol C on Human Breast Cancer Cells using Quantitative Proteomics

3.5.3.1. Summary

Citation

S. Roehrer, V. Stork, C. Ludwig, M. Minceva, J. Behr, (2019). Analyzing Bioactive Effects of the Minor Hop Compound Xanthohumol C on Human Breast Cancer Cells using Quantitative Proteomics. *PLoS ONE*, 14(3), e0213469.

<https://doi.org/10.1371/journal.pone.0213469>

Summary

Hops has been known as a medicinal plant for centuries. However, it is difficult to relate certain observed activities or effects to specific hop compounds since they are rarely available in high purity. Hence, there is still a lack of knowledge whether certain activities can be allocated to single hop compounds at all or whether the activity is the result of complex interactions between major and minor compounds. The objective of this work was to compare the anticarcinogenic potential of the promising minor hop compound xanthohumol C (XNC) with the already well-known and widely studied hop compound xanthohumol (XN). In a comprehensive cell-culture study with the MCF-7 breast cancer cell line, a higher antiproliferative and cytotoxic effect of XNC could be observed in comparison to both XN and a XN-enriched extract where XNC is present in low amounts (0.24-2.2%). Remarkably, XNC has shown an even higher effect in vitro (IC_{50} : 4.18 μ M) when compared to other natural products currently considered to be of high potential, such as resveratrol (IC_{50} : 100 μ M) or curcumin (IC_{50} : 35 μ M) [173]. This study emphasizes the high potential of liquid-liquid chromatography as a powerful technique to provide highly pure minor hop compounds for further evaluation of anticarcinogenic or chemopreventive effects. In combination with state-of-the-art quantitative proteomics and comprehensive statistical analysis, an efficient procedure for the fast investigation of the bioactivity of natural compounds including possible modes of action was established. This method contributes to a more targeted exploitation of hops and natural resources in general as active ingredients or additives in future anticarcinogenic drugs or preventive foods in order to enhance their desired effects.

Contributions

The author of this dissertation had a leading role in this work. He planned and coordinated the entire workflow, conducted or supervised all data acquisition, and performed the data analysis as well as interpretation. V. Stork performed the cell culture experiments supervised by the author and assisted in the analysis of the results. In collaboration with the author, C. Ludwig and J. Behr performed the mass spectrometry experiments including raw data processing with MaxQuant, and consulted with the interpretation of the proteomics results. The manuscript was written by the author and discussed with all co-authors of the manuscript.

3.5.3.2. Manuscript

RESEARCH ARTICLE

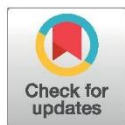
Analyzing bioactive effects of the minor hop compound xanthohumol C on human breast cancer cells using quantitative proteomics

Simon Roehrer¹, Verena Stork¹, Christina Ludwig², Mirjana Minceva¹, Jürgen Behr^{2a*}

1 Biothermodynamics, TUM School of Life and Food Sciences Weihenstephan, Technical University of Munich, Freising, Germany, **2** Bavarian Center for Biomolecular Mass Spectrometry, TUM School of Life and Food Sciences Weihenstephan, Technical University of Munich, Freising, Germany

✉ Current address: Leibniz-Institute for Food Systems Biology at the Technical University of Munich, Freising, Germany

* juergen.behr@tum.de



OPEN ACCESS

Citation: Roehrer S, Stork V, Ludwig C, Minceva M, Behr J (2019) Analyzing bioactive effects of the minor hop compound xanthohumol C on human breast cancer cells using quantitative proteomics. *PLoS ONE* 14(3): e0213469. <https://doi.org/10.1371/journal.pone.0213469>

Editor: Suman S. Thakur, Centre for Cellular and Molecular Biology, INDIA

Received: October 27, 2018

Accepted: February 21, 2019

Published: March 15, 2019

Copyright: © 2019 Roehrer et al. This is an open access article distributed under the terms of the [Creative Commons Attribution License](https://creativecommons.org/licenses/by/4.0/), which permits unrestricted use, distribution, and reproduction in any medium, provided the original author and source are credited.

Data Availability Statement: The data underlying this study have been deposited to the PRIDE repository and is indexed on ProteomeXchange under accession number PXD010785. Alternatively, the data may be directly accessed via either the project webpage (<http://www.ebi.ac.uk/pride/archive/projects/PXD010785>) or FTP download link (<ftp://ftp.pride.ebi.ac.uk/pride/data/archive/2019/03/PXD010785>).

Funding: This work was supported by the German Research Foundation (DFG) and the Technical

Abstract

Minor prenylated hop compounds have been attracting increasing attention due to their promising anticarcinogenic properties. Even after intensive purification from natural raw extracts, allocating certain activities to single compounds or complex interactions of the main compound with remaining impurities in very low concentration is difficult. In this study, dose-dependent antiproliferative and cytotoxic effects of the promising xanthohumol (XN) analogue xanthohumol C (XNC) were evaluated and compared to XN and a XN-enriched hop extract (XF). It was demonstrated that the cell growth inhibition of human breast cancer cell line (MCF-7) significantly increases after being treated with XNC compared to XN and XF. Based on label-free data-dependent acquisition proteomics, physiological influences on the proteome of MCF-7 cells were analyzed. Different modes of action between XNC and XN treated MCF-7 cells could be postulated. XNC causes ER stress and seems to be involved in cell-cell adhesion, whereas XN influences cell cycles and DNA replication as well as type I interferon signaling pathway. The results demonstrate the utility of using quantitative proteomics for bioactivity screenings of minor hop compounds and underscore the importance of isolating highly pure compounds into their distinct forms to analyze their different and possibly synergistic activities and modes of action.

Introduction

Hop (*Humulus lupulus* L.) is well known as a medical plant with many bioactive effects. Due to the trend of evaluating natural compounds for its diverse bioactive effects, hop has been attracting increasing interest as a natural resource for promising biologically active phenolic compounds. In this context, natural compounds have shown promise due to their antimicrobial, antiviral and also anticarcinogenic or (chemo)preventive effects [1, 2]. Hop contains a huge variety of prenylated phenolic compounds [3–6]. The most abundant prenylated chalcone in hops is xanthohumol (XN) [7]. Great importance has been placed on this compound

University of Munich (TUM) in the framework of the Open Access Publishing Program.

Competing interests: The authors have declared that no competing interests exist.

due to its multiple biological activities, including anti-inflammatory [8], neuro-protective [9, 10], anti-microbial [11, 12], anticarcinogenic [13–15] and even radio-sensitizing [16] effects. Furthermore, promising results from in vivo and in vitro studies with several cancer cell lines, including MCF-7 breast cancer cells, have shown its antiproliferative activity [13–15, 17]. Xanthohumol shows co-action with several antibiotics [11, 12], but is less active in combination with other hop compounds [12] against gram-positive bacteria. Moreover, XN showed anti-obesity effects by inhibiting the differentiation of preadipocytes and inducing apoptosis in mature adipocytes by using the mouse cell line 3T3-L1 [18, 19]. All these explorations strongly suggest XN and its analogues as potential compounds for the prevention and treatment of many diseases [2, 3, 6, 7, 14, 16, 20–23]. Especially naturally occurring minor chalcones from hops gained interest due to their different investigated properties. Dietz et al. showed an efficacy improvement of bioactive hop compounds linked to the concentration of minor compounds in the natural extract [5]. Interestingly, many of these seem to be even more bioactive in comparison to XN [4, 7, 24, 25]. 8-prenylnaringenin is known as one of the most potent phytoestrogen [6], desmethylxanthohumol shows e.g. anti-oxidant activity [26], isoxanthohumol inhibits angiogenesis [27], and 6-prenylnaringenin has anti-fungal activities against *Trichophyton* spp. [28]. Another recently upcoming minor chalcone is xanthohumol C (XNC), which has lately received much attention due to its antiproliferative, cytotoxic [15, 17], neuro-protective [9], and anti-oxidative activities [24, 29, 30]. Xanthohumol C, also called dehydrocyclo-xanthohumol, was first identified by Stevens et al. [31] and its molecular structure differs to xanthohumol due to a ring closure of the prenyl-side chain with the hydroxyl group at position 4' (see Fig 1A). Miranda et al. [15] already showed a significant antiproliferative and cytotoxic effect of various prenylated flavonoids and assumed an inhibition capacity only of XNC at lower concentrations compared to XN and iso-xanthohumol for the growth of MCF-7 breast cancer cells. In contrast, Popłoński et al. [17] recently showed a lower in vitro antiproliferative activity of XNC compared to XN in prostate, colon, and breast cancer cell lines. In another study, XNC was identified as the most active compound within a group of hop-derived prenyl-flavonoids for the differentiation of neuronal precursor cells [9]. While XN and other major phenolic hop compounds are already well characterized in literature, pharmacological data concerning minor compounds such as XNC are scarce due to its limited availability via isolation from natural sources and therefore is still in the process of investigation [32]. In addition, in natural products studies it is often difficult to link a certain bioactivity to a single compound due to the presence of many minor impurities and their unknown influence on the analyzed target compound.

The potential of liquid-liquid chromatography, i.e. countercurrent chromatography (CCC) and centrifugal partition chromatography (CPC), has recently been shown to provide even minor hop compounds in sufficient amount and high purity for antimicrobial or pharmacological testing [33]. In the current study, a XN-enriched hop extract (Xantho-Flav[®], XF) was used as a natural resource containing 65–85% XN and a huge variety of other different minor compounds such as XNC (0.24–2.2%). Subsequently, the bioactive effects of purified XNC (>99.8%) were evaluated and compared to pure XN (>98.6%). Both compounds were previously gained from XF with liquid-liquid chromatography [33].

The objective of this study was to compare the effects of single compounds to the natural crude resource, the XN-enriched hop extract XF, as a complex multicomponent mixture. XF contains a huge variety of minor compounds that theoretically could interact with each other and hence enhance or reduce the bioactive effect, or evoke the biological effect only in combination with each other.

Mass spectrometry based proteomics has been exploited as a powerful technology for capturing complex information about proteome structure and function. This can be used to gain

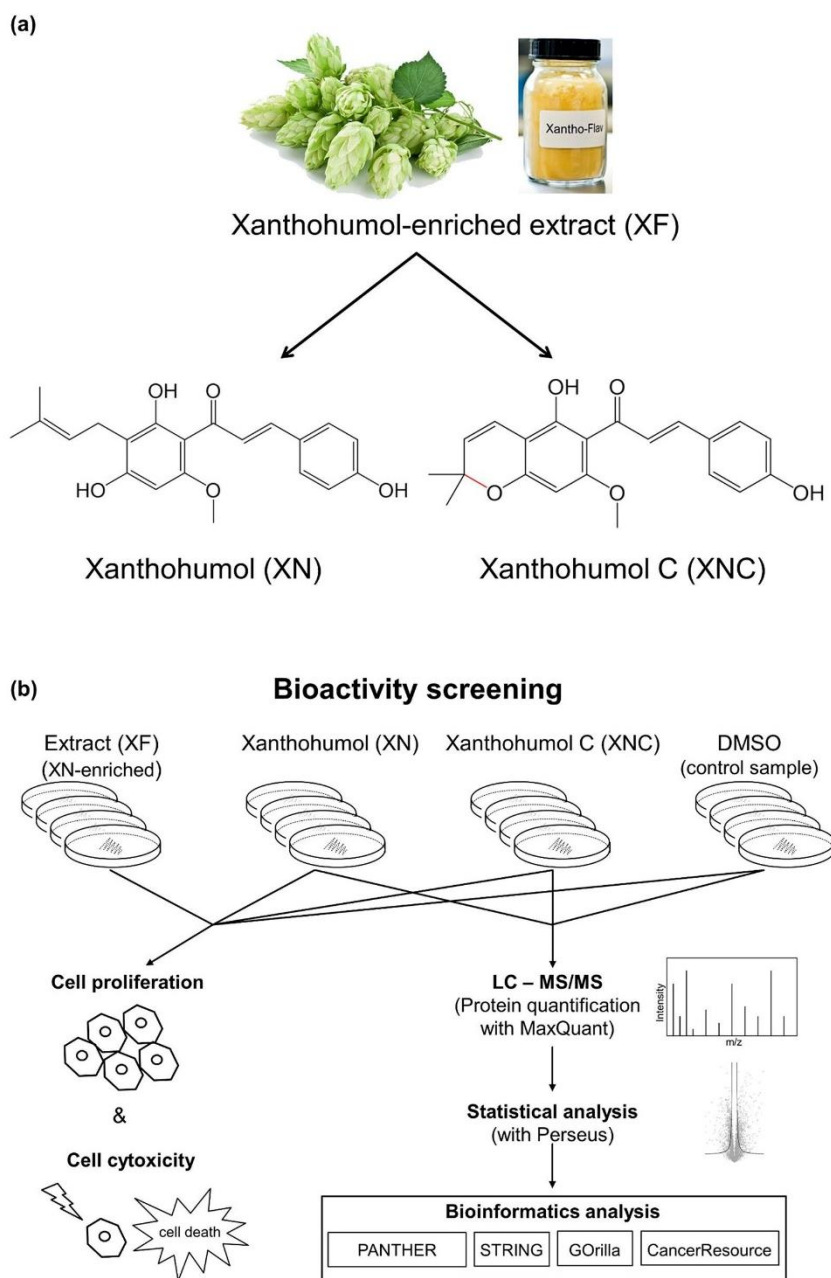


Fig 1. (a) Molecular structures of the hop compounds xanthohumul (XN) and xanthohumul C (XNC) obtained from the xanthohumul-enriched hop extract Xantho-Flav (XF). (b) Overview of the total workflow of the study.

<https://doi.org/10.1371/journal.pone.0213469.g001>

an understanding of the biological processes ongoing in cellular samples of interest [34–39]. In the context of compound-protein interactions quantitative proteomics can provide molecular insights into biological pathways and processes influenced by a given compound [40, 41].

In this study, we established an experimental approach for the bioactivity analysis of promising minor hop compounds (see flow chart in Fig 1B). First, the dose dependent antiproliferative and cytotoxic effect of XN and XNC were evaluated in MCF-7 cell culture experiments and compared to a complex crude hop extract, the commercially available XN-enriched hop extract (XF). Subsequently, protein expression in the MCF-7 cell line after XN and XNC treatment was analyzed by label-free data-dependent acquisition proteomics and the results evaluated by various bioinformatics tools, such as Perseus, PANTHER, STRING, and GOrilla. Such analysis could give a fast overview of possible functions that can guide for further specific analysis. This enables a targeted approach and consequently also reduces experimental time as well as sample amounts of such rare highly purified minor natural products.

Materials and methods

Chemicals

The pre-concentrated commercial xanthohumol (65–85%, HPLC) crude extract, Xantho-Flav (XF), was supplied by the company Hopsteiner (Germany). Xanthohumol (>98.6%, HPLC) and xanthohumol C (>99.8%, HPLC) were purified by liquid-liquid chromatography (CCC/CPC) as described in a previous work [33]. Chemical structures were drawn with Marvin 17.2.27.0, 2017, ChemAxon <http://www.chemaxon.com>.

Cell culture

The MCF-7 breast cancer cell line was kindly provided by the Chair of Proteomics and Bioanalytics (Technical University of Munich, Germany), originally purchased from the National Cancer Institute (NCI, USA). The complete growth media of MCF-7 cells consisted of Gibco (Dulbecco's Modified Eagle Medium, DMEM, high glucose) from Thermo Fisher Scientific Inc. (USA) and 10% fetal bovine serum (FBS) from Sigma-Aldrich (USA). The media for bioactivity assays composed of DMEM, high glucose, HEPES, no phenol red from gibco (Thermo Fisher Scientific Inc., USA) and 5% FBS. For sub-culturing cells phosphate-buffered saline (PBS) from Merck KGaA (Germany) and a trypsin-EDTA solution from Sigma-Aldrich (USA) were used.

Proliferation was determined by the CellTiter 96 Aqueous Non-Radioactive Cell Proliferation Assay from Promega (USA), which contains 3-(4,5-dimethylthiazol-2-yl)-5-(3-carboxymethoxyphenyl)-2-(4-sulfophenyl)-2H-tetrazolium, inner salt (MTS) and the electron coupling reagent phenazine methosulfate (PMS).

Equipment and implementation of cell culture bioactivity tests

The cells were cultivated in T-75 (75 cm²) or T-25 (25 cm²) flasks (Falcon Tissue Culture Flasks, Corning Inc., USA) at 37°C in a humidified atmosphere of 95% air / 5% CO₂, until 80% confluency. In each new T-75 flask between $8.5 \cdot 10^5$ and $1.1 \cdot 10^6$ MCF-7 cells were plated. For bioactivity screenings, cells were centrifuged (120 rcf, 20°C, 10 min) and the complete growth medium was exchanged with media for bioactivity assays. Per well 5 000 MCF-7 cells were plated into a 96-well microtiter plate (Corning Inc., USA). After 1 day of incubation, the cells were treated with the test substances XN, XNC and XF in varying concentrations (100, 75, 50, 25, 10, 7.5, 5, 2.5, 1, 0.1, 0.01 μM) dissolved in DMSO (maximal 0.2% v/v). As control DMSO without a component was used (0.2% v/v).

At the day of treatment (day 0), a proliferation assay was conducted on cells without stimulation (without bioactive compounds) for calculating cytotoxicity. After incubation for 2, 4 and 6 days, the proliferation assay was performed on all treated cells and the control samples. Therefore, old medium was removed, cells were washed with 150 μL PBS, and 100 μL of fresh medium was added for the bioactivity tests. The MTS/PMS-solution (ratio 20 to 1) was added (16 μL) and incubated for 90 minutes at 37°C, 5% CO₂. As described in the technical bulletin (Promega Corp., USA), MTS is converted to an aqueous, soluble formazan by dehydrogenase enzymes found in metabolically active cells [42]. The absorbance of the formazan was recorded at 490 nm by the “infinite M200 multimode microplate reader” (Tecan Group Ltd., Switzerland). The experiments were performed in triplicate.

Antiproliferative effects were calculated as a ratio of OD_{490nm} in XN, XNC, and XF treated wells and the wells treated with DMSO. Cytotoxicity was determined as the ratio between OD_{490nm} in a treated well and OD_{490nm} at day 0 (day of treatment) (technical bulletin, Promega Corp., USA). Statistical analyses were determined by Student's *t*-test. In all cases, *P* values <0.05 were considered statistically significant.

Cell culture preparation for proteomics analysis

For the proteomic experiments, MCF-7 cells were cultured as described in the cell culture section before and transferred to T-25 cm² flasks. After one day of incubation, cells were treated with XN, XNC, and DMSO as control. For the treatment, the IC₅₀ concentration determined by antiproliferative assays was used, respectively (XN: 12.25 μM , XNC: 4.18 μM). After two more days of incubation, medium was removed completely and cells were washed two times with PBS. Finally, 1 mL PBS was added, cells were scraped from the surface of the flask and transferred to an Eppendorf Protein LoBind Tube (Eppendorf, Germany). Cells were centrifuged at 16000 rcf, for 10 min, and 4°C. Supernatant was completely discarded and the pellet was shock frozen in dry ice, containing 80% EtOH and stored at -80°C until protein extraction was performed. The pelletized MCF-7 cells were sampled in quadruplicates.

Sample preparation for proteomics analysis

The stored cell pellets were thawed slowly on ice and resuspended in lysis buffer (8 M urea, 5 mM EDTA di-sodium salt, 100 mM (NH₄)HCO₃, 1 mM Dithiothreitol (DDT), 10% (v/v) protease inhibitor cocktail (SigmaFast 10x stock), pH 8.0) by thoroughly up- and down-pipetting and subsequent ultrasonication for 40 seconds. Total protein concentration of the lysate was determined using the BCA method (Pierce BCA protein assay kit, ThermoFisher, Germany). 100 μg protein extract was used per sample for in-solution digestion. Proteins were reduced with 10 mM DTT (at 30°C for 30 min), and subsequently carbamidomethylated with 55 mM chloroacetamide in the dark at room temperature for 60 min. Proteins were digested with 1 μg trypsin (1:100 trypsin:protein) for 3 hours at 37°C and another 1 μg of trypsin overnight at 37°C. Digested peptide samples were desalted according to the manufacturer's instructions by C18 solid phase extraction using Sep-Pak columns (Waters, WAT054960) [43]. Purified peptide samples were dried in a SpeedVac and resuspended in 2% acetonitrile, 98% H₂O, 0.1% formic acid to a final concentration of 0.25 μg μL^{-1} as determined by Nanodrop measurement.

Liquid chromatography and tandem mass spectrometry

Generated peptides were analyzed on a Dionex Ultimate 3000 nano LC system coupled to a Q-Exactive HF mass spectrometer (Thermo Scientific, Germany). Peptides were delivered to a trap column (75 μm \times 2 cm, self-packed with Reprosil-Pur C18 ODS-3 5 μm resin, Dr. Maisch, Ammerbuch) at a flow rate of 5 μL min⁻¹ in solvent A0 (0.1% formic acid in water). Peptides

were separated on an analytical column (75 $\mu\text{m} \times 40$ cm, self-packed with Reprosil-Gold C18, 3 μm resin, Dr. Maisch, Ammerbuch) using a 120 min linear gradient from 4–32% solvent B (0.1% formic acid, 5% DMSO in acetonitrile) and solvent A1 (0.1% formic acid, 5% DMSO in water) at a flow rate of 300 nL min^{-1} . The mass spectrometer was operated in data-dependent acquisition (DDA) mode, automatically switching between MS and twenty MS2 spectra.

MS1 spectra were acquired over a mass-to-charge (m/z) range of m/z 360–1 300 at a resolution of 60 000 (at m/z 200) using a maximum injection time of 10 ms and an AGC target value of 3×10^6 . Up to 20 peptide precursors were isolated (isolation window m/z 1.7, maximum injection time 50 ms, AGC value 2×10^5), fragmented by HCD using 25% NCE and analyzed at a resolution of 30 000 with a scan range from m/z 200 to 2 000. Precursor ions that were singly-charged, unassigned or with charge states $>6+$ were excluded. The dynamic exclusion duration of fragmented precursor ions was 35 s.

Peptide and protein identification, intensity-based absolute quantification (iBAQ) and label-free quantification (LFQ) of proteins

The proteomic experiments were performed with MCF-7 cells treated with XN or XNC as well as with a control sample containing only DMSO as a solvent. Peptide and protein identification and label free quantification were performed with MaxQuant (version 1.5.8.3, <http://www.coxdocs.org/doku.php?id=:maxquant:start>) [44] (see MaxQuant configuration in [S3 File](#)) by searching the MS2 data against all protein sequences obtained from UniProt—Reference proteome Homo sapiens (UP000005640, canonical, 20 236 reviewed entries, last modified on July 18, 2017) using the embedded search engine Andromeda [45]. Carbamidomethylated cysteine was a fixed modification; oxidation of methionine, and N-terminal protein acetylation were variable modifications. Trypsin/P was specified as the proteolytic enzyme and up to two missed cleavage sites were allowed. Precursor and fragment ion tolerances were 10 ppm and 20 ppm, respectively. Label-free quantification (LFQ) [46] and data matching between consecutive analyses were enabled within MaxQuant. Search results were filtered for a minimum peptide length of seven amino acids, 1% peptide and 1% protein FDR plus common contaminants and reverse identifications. Each condition was monitored in four biological replicates (see all identified peptides in [S1 File](#)).

Intensity-based absolute quantification (iBAQ) values, which are proportional to the molar protein quantities in the samples, were used to relatively compare the concentration of different proteins within one sample. iBAQ protein intensity values were retrieved from the MaxQuant software as the sum of all peptide intensities per proteins divided by the number of theoretical peptides per protein. For protein quantification between samples, label free quantification (LFQ) [46] intensities were obtained (see all identified protein groups in [S2 File](#)).

After raw data processing with MaxQuant, quality control (QC) was performed by using the R-based QC pipeline *Proteomics Quality Control* (PTXQC package). Measured bias, consistency, and errors were analyzed by creating a QC report (see [S4 File](#)) containing a set of QC metrics [47].

Statistical analysis with Perseus

MaxQuant results were further statistically analyzed using the MaxQuant associated software suite Perseus (version 1.6.0.7, <http://www.coxdocs.org/doku.php?id=perseus:start>). First, raw data from XN and XNC treated replicates were filtered by excluding potential contaminants, reverse and only identified by site proteins leading to a table of all identified proteins ([S2 File](#)). This data set was further filtered based on the criterion that at least 3 non-zero values must be present in at least one treatment or control group. Missing values were imputed on the basis of

a Gaussian distribution using the Perseus algorithm to allow for statistical analysis, resulting in all quantified proteins (S5 File). Statistical significance was assessed by the Student's t-test between control and treated groups. Quantitative differences between the analyzed groups were considered to be statistically significant for adjusted $p < 0.05$. The Log₂ (Fold Ratios) of the proteins were calculated in all condition comparisons and means and as well as standard deviations (SD) of the differences were calculated. Proteins displaying large magnitude changes within a defined cutoff (1 SD) were classified as differentially expressed (DE) proteins and visualized in volcano plots. The data were expressed as the mean (\pm 1 SD) and further categorized as: upregulated or downregulated proteins (S6–S9 Files). The significance of the differences was determined by the Student's t-test.

Bioinformatics analysis

The identified proteins were classified and compared by different bioinformatics tools, such as PANTHER, STRING, GOrilla, to obtain further information about protein annotation, molecular function, biological process, subcellular localization, protein interactions and their potential pathways.

The PANTHER classification system (version 13.0, <http://www.pantherdb.org>) was used for protein identification and classification in terms of molecular function, biological process and cellular component [48]. For that, protein IDs (UniProtKB) of identified, quantified, and DE proteins including up- and downregulated DE proteins after XN and XNC treatment were submitted to PANTHER and *Homo sapiens* was selected as the organism. In addition to the obtained protein amounts, the mapped protein IDs were subsequently statistically analyzed with the chi-squared test (X^2) for comparison between the samples. Again, $p < 0.005$ indicates significance and $p < 0.001$ was selected for indicating a highly significant difference.

The signaling pathways and protein interactions of proteins with changed expression levels were identified with the help of the STRING-tool (Version 10.5, <https://string-db.org>). In analogy to the PANTHER analysis, protein IDs were submitted and active interaction sources were selected: experiments, co-expression, neighborhood, gene fusion, and co-occurrence. For the protein network visualization, only the main interactions were considered. A default medium confidence score (>0.4) was used for XN. In terms of XNC, a high confidence score (>0.7) was used in order to reduce the high number of proteins. However, no protein interactions at high confidence score were found for XN. In addition, disconnected nodes in the network were hidden [49, 50].

Further, visualization of shared DE proteins between XN and XNC treated cells was achieved with the online plotting tool Venny 2.1.0 (Version 2.1.0, <http://bioinfogp.cnb.csic.es/tools/venny>). The intersections and complements are plotted based on protein IDs.

A functional enrichment analysis was performed for the identification of significantly over-represented or underrepresented proteins in molecular function, biological process and cellular component. For that, the protein IDs were submitted for the organism *Homo sapiens* to the tool GOrilla (<http://cbl-gorilla.cs.technion.ac.il>) [51]. For each of the different Gene Ontology (GO) categories, an enrichment factor, FDR p-values and corresponding p-values were calculated (details see S1 and S2 Tables). Accessions with p-values of more than 10^{-3} and FDR adjusted p-values of more than 10^{-2} were automatically removed from the corresponding enrichment table.

Single proteins were also analyzed by open access database CancerResource (<http://data-analysis.charite.de/care/>). Drug targets were searched by gene identifiers, and possible cancer relevant pathways and mutation profiles were examined in more detail.

Results and discussion

Evaluation of antiproliferative effects of xanthohumol (XN), xanthohumol C (XNC), and a XN-enriched extract (XF) on MCF-7 breast cancer cell line

In previous studies, XN and several analogues demonstrated antiproliferative and cytotoxic effects in human cancer cell lines, such as human breast cancer cells (MCF-7), colon cancer cells (HT-29) or ovarian cancer cells (A-2780). [15] The activities of xanthohumol derivatives are highlighted as promising new bioactive compounds. [25, 52] In addition to their various bioactive effects, natural products usually show a low toxicity and can therefore be used as favorable preventive substances or as additives that enhance the effect of e.g. cytostatic drugs against breast cancer. In this study, XNC was evaluated for its antiproliferative and cytotoxic effects on breast cancer cells (MCF-7) and its activity is compared to the reference XN and the XN-enriched hop extract Xantho-Flav (XF) containing a high amount of XN (65–85%) as well as a huge variety of different minor hop compounds in very low concentrations (including 0.24–2.2% of XNC).

The antiproliferative effects of XN, XNC and XF on MCF-7 cell line were determined with the MTS-assay (for details see [Materials and methods](#) section) [42]. In [Fig 2](#) the relative growth-inhibitory activity of the three compounds in MCF-7 cells after a treatment of 2 (a), 4 (b) and 6(c) days is shown.

Cells incubated with XN always grew best. Interestingly, the raw extract XF, which consists of about 80% XN, inhibited cell growth more than pure XN. This seems to indicate strong effects of minor components included in XF. One of these minor compounds is the minor hop chalcone XNC. Cells incubated only with XNC, showed the strongest growth inhibition.

In addition, the inhibition concentration of the compounds at 50% cell growth inhibition (IC_{50}) was determined for all three compounds. In all cases, the IC_{50} was lowest after 6 days of incubation. There was no decreased sensitivity of the cancer cells after 6 days of exposure, whereby the generation of resistances can be excluded for this period of time. After all three periods of treatment, the IC_{50} of XNC was lowest and the one of XN the highest. After two days of incubation, the IC_{50} of XNC (4.18 μ M) was by a factor of 2 lower compared to XF (8.84 μ M), and only a third compared to XN (12.25 μ M). After four days (XNC: 1.9 μ M, XF: 4.3 μ M, XN: 8.8 μ M) and six days (XNC: 1.70 μ M, XF: 2.2 μ M, XN: 7.1 μ M), the difference between XNC and XN was even more distinct. Interestingly, XN and XF show similar growth after 2 days of incubation ([Fig 2A](#)), but clearly differ after 4 ([Fig 2B](#)) and especially 6 days ([Fig 2C](#)). This indicates some kind of a delayed effect of XF, resulting in a stronger effect of XF compared to the pure compound XN. Statistical significance was determined by Student's *t*-test (*p*-value < 0.05). Interestingly, only XNC showed a significant relative cell growth inhibition at 2.5 μ M after 4 and 6 days of incubation. In accordance with literature [15, 24, 53], XNC shows significant antiproliferative effects compared to XN. It is noteworthy that a higher antiproliferative activity of XN and in particular XNC after two days of incubation was observed compared to the data of Popłoński et al. [17], who showed a higher IC_{50} concentration for both compounds (XN: 8.1±0.8 μ M, XNC: 15.0±1.8 μ M) as well as a different tendency with XN as the more active compound. A possible reason for the different tendency might be the use of different purification methods. An isolation of XN and XNC based on flash chromatography or liquid-liquid chromatography could result in different purities and hence a different interaction of the target compound with minor impurities that could potentially influence activity. Another reason could be a difference in the cell line itself due to the unstable genome of cancer cells that can result in different gene expression and properties between different labs. Other effects like isomerization of XN and XNC induced by thermal treatment [6] or alkaline conditions [54] are rather unlikely due to the selected experimental conditions and the relatively

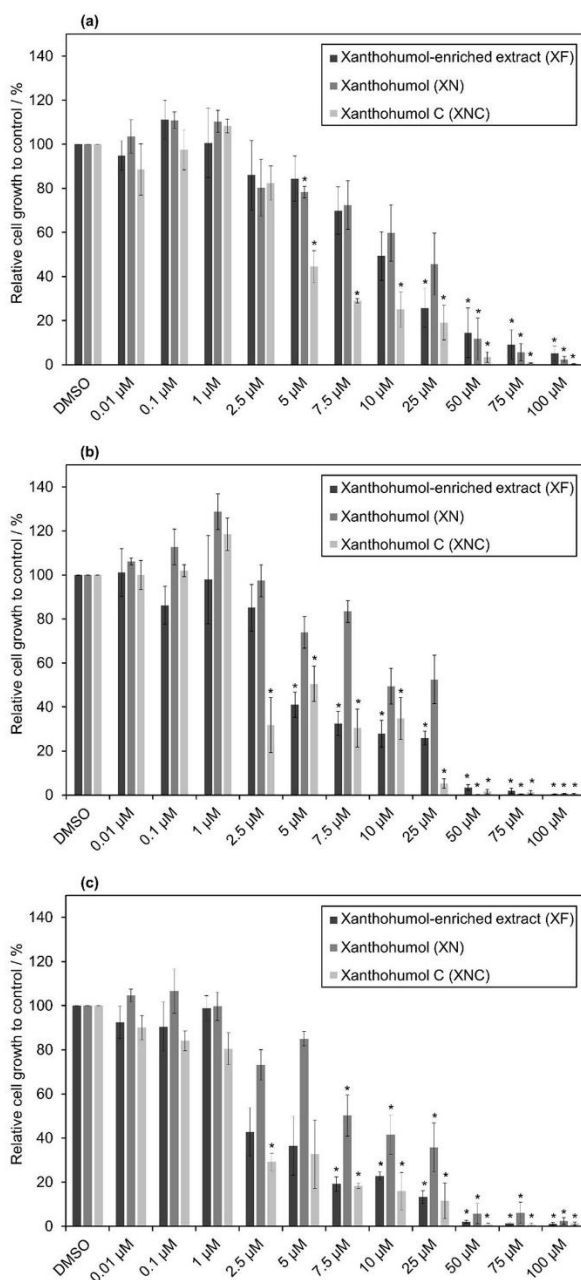


Fig 2. Relative cell growth of MCF-7 cells determined by MTS-assay after 2 (a), 4 (b) and 6 (c) days of incubation at different concentrations of XF, XN and XNC (* statistical significance to control, p-value < 0.05).

<https://doi.org/10.1371/journal.pone.0213469.g002>

short experimental time of few days. Nevertheless, all results show an *in vitro* antiproliferative activity in a similar concentration range and emphasize the anticarcinogenic potential of the investigated minor hop compounds. In comparison to other promising natural phenolic agents, such as resveratrol (IC_{50} : 100 μ M) or curcumin (IC_{50} : 35 μ M), XNC shows a much higher antiproliferative effect against MCF-7 cells after two days [55].

Cytotoxic effects of XN, XNC and XF on MCF-7 cells

Cytotoxicity was calculated in analogy to Miranda et al. [15] by comparing OD units of treated cells with OD units of untreated cells at day 0, which is the start of the compound incubation. Cell death was indicated by lower cell viabilities after treating the cells compared to cell viability before treatment. The cytotoxic effect on the MCF-7 cell line is shown in Fig 3 after 2 (a), 4 (b) and 6 (c) days of incubation with different concentrations of XN, XNC, and XF. After two days of incubation, XNC was the most cytotoxic compound and showed cell death even at a concentration of 5 μ M.

After 4 and 6 days of incubation this effect was already observed at a concentration of 2.5 μ M (XNC). Above 50 μ M all of the substances were cytotoxic to MCF-7 cells. At a concentration below 1 μ M the cell death was not affected by the components. Statistical significance was determined by Student's *t*-test (*p*-value < 0.05) indicating cell death induced by the three compounds. Interestingly, after 2 days, only XNC showed cytotoxic effects at low concentrations, while after 4 and 6 days the difference in cytotoxicity between the compounds is decreasing.

From the cell culture studies, i.e. antiproliferative and cytotoxic analysis, it can be assumed that XF as a complex mixture might affect various cell processes just like the single compounds. For a deeper understanding of the effects on molecular level, pure compounds are necessary in order to avoid misinterpretation of the experimental results and to find the effects of the actual single target compounds.

Quantitative proteomics analysis of MCF-7 cells

In order to get insights into pharmacological influence or anticarcinogenic behavior of the hop compounds xanthohumol C (XNC) and xanthohumol (XN), a quantitative proteomics approach was used to analyze the global proteome of MCF-7 breast cancer cells in order to find possible molecular mechanisms of XN and XNC treatment [56, 57]. Although proteomics studies have been applied to hop and its bioactivity before [58–60], data about how minor hop compounds, such as XN and XNC, affect the proteome of cancer cells are still lacking. In this study, the global proteome of MCF-7 human breast cancer cells was quantified after treatment with XN and XNC. Further, the involved biological processes are characterized using bioinformatics analysis tools. This global proteome characterization enabled an evaluation of possible effects of XN and XNC in order to generate new hypotheses about how these compounds might influence the function of the cells on a molecular level. This strategy can easily be extended and applied to screenings of a wider range of other bioactive minor hop compounds as well as to other cancer cell lines.

The cells were treated with the IC_{50} concentration (XN: 12.25 μ M, XNC: 4.18 μ M) for two days in quadruplicate and measured by label-free data-dependent acquisition proteomics. Additionally, DMSO was used as a control condition. As shown in Fig 4A, in total 6 009 proteins could be identified using the software MaxQuant, which covers about 30% of the 20 236 entries from UniProt database reference proteome. From these, 4 363 proteins were quantified with good reproducibility (at least three valid measurements out of four replicate measurements), of which 74 were differentially expressed (DE) (41 down- and 33 upregulated) in case of XN (S1 Fig including molecular functions) and 742 (366 down- and 376 upregulated) in

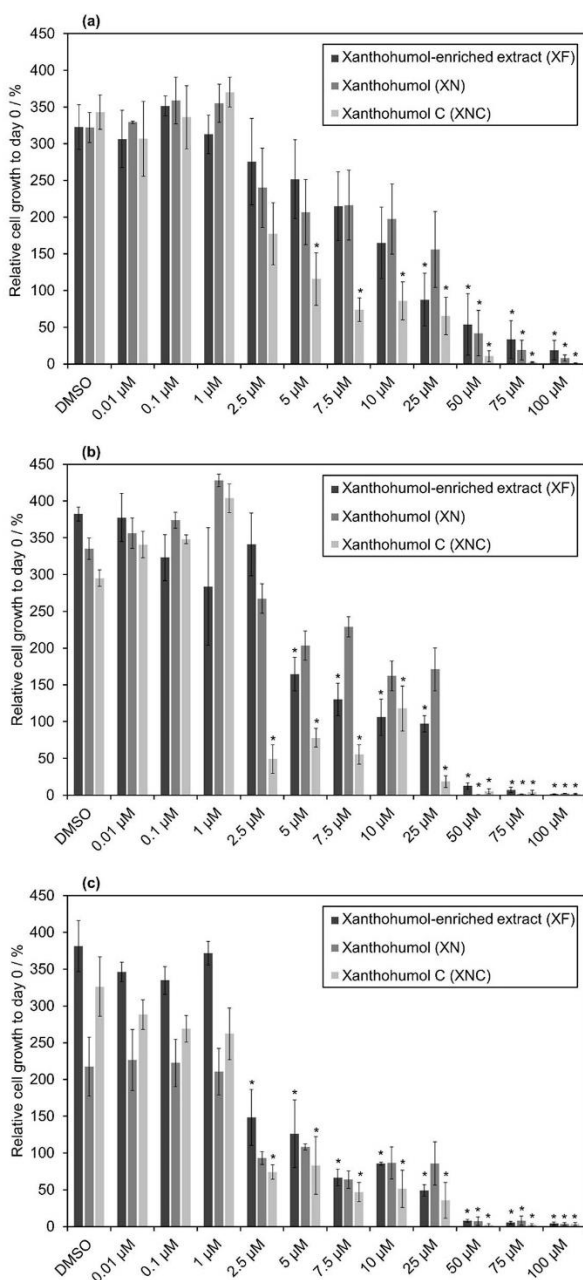


Fig 3. Cytotoxic effect on MCF-7 cells after 2 (a), 4 (b) and 6 (c) days of incubation with different concentrations of XF, XN and XNC (* statistical significance to control, p-value < 0.05). Note: Experiments with XN treatment in Fig 3B were only performed in duplicate.

<https://doi.org/10.1371/journal.pone.0213469.g003>

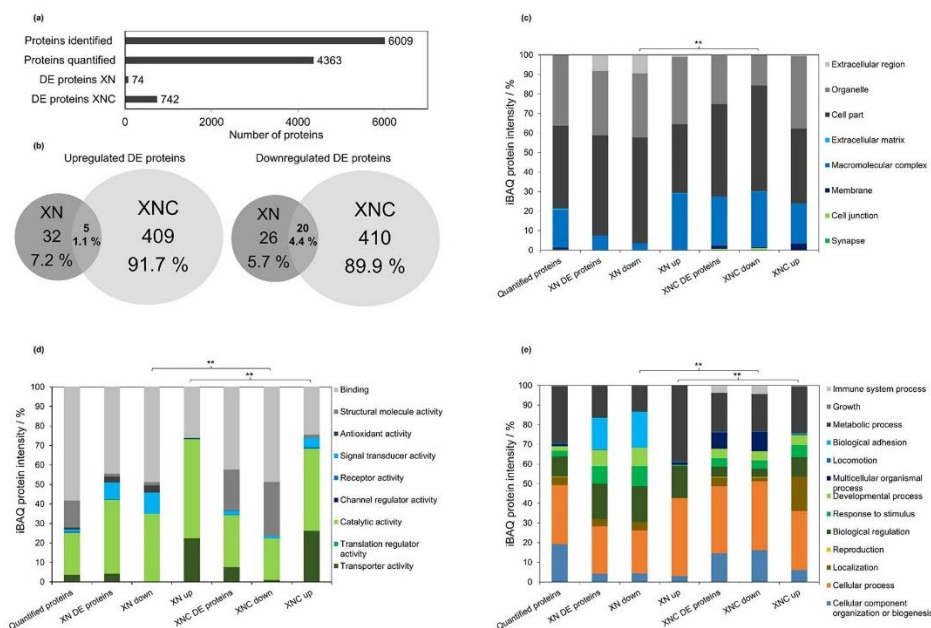


Fig 4. Global proteome characterization from MCF-7 cells after treatment with XN and XNC at IC₅₀ concentration. (a) Comparison of the number of identified, quantified, and differentially expressed (DE) proteins. (b) Comparison of shared up- and downregulated DE proteins (c) Predicted cellular localization of quantified and DE proteins in percentage based on iBAQ intensities (d) Predicted molecular function of quantified and DE proteins in percentage based on iBAQ intensities (e) Predicted biological process of quantified and DE proteins in percentage based on iBAQ intensities. (* significant difference, $p < 0.005$; ** highly significant difference, $p < 0.001$).

<https://doi.org/10.1371/journal.pone.0213469.g004>

case of XNC (S2 Fig including molecular functions). The number of DE proteins seems to be concomitant to the higher activity and growth inhibition of XNC in the cell culture experiments. A higher effect of XNC could cause stronger defense mechanisms of the MCF-7 cell, which consequently results in more DE proteins. The comparison between the XN and XNC regulated proteome shows not only a large difference in the total number of DE proteins but also in the low number of shared DE proteins. An overlap of only 5 upregulated (1.1%) and 20 downregulated (4.4%) proteins as shown in Fig 4B was found. In addition, the shared proteins were spread over different possible pathways and functions, so that no specific common function could be found. This indicates different target structures and modes of action between XN and XNC.

Next, a protein classification was performed by applying a gene ontology (GO) analysis with the PANTHER classification system on various functional and cellular levels. Quantified and DE proteins were analyzed in terms of cellular localization, molecular function and biological processes (Fig 4C–4E). For all three categories, a difference (p -value < 0.001) between DE proteins after treatment with XN and XNC was determined. In addition, DE proteins were further analyzed by differentiating DE proteins in up- and downregulated proteins after treatment of XN or XNC and statistical significance was calculated by the chi-squared test. For XN and XNC comparisons, significance was conducted between up- and downregulated proteins respectively. A complete coverage of all subcellular compartments was observed, revealing a successful sample preparation including harvest, cell disruption, and digestion.

Applying the analysis of cellular localization (Fig 4C), it was possible to associate DE proteins with mainly organelle, cell part, macromolecular complex, membrane and extracellular regions. The predicted cellular localization after XN and XNC treatment clearly differs in downregulated proteins. In terms of XN treated MCF-7 cells a higher percentage of DE proteins from extracellular region were downregulated, while for XNC a higher amount of proteins from macromolecular complexes was downregulated. In upregulated proteins, XNC and XN mainly differ in the higher amount of upregulated membrane proteins for XNC.

Concerning molecular function (Fig 4D), mostly proteins assigned to binding and catalytic activity could be found. Both downregulated and upregulated proteins are different between XN and XNC. Noteworthy is that the signal transducer activity is downregulated in XN compared to an upregulation in XNC. In addition, the structural molecule activity is more severely downregulated with XNC.

In allocating the DE proteins to certain biological processes (Fig 4E), downregulated proteins differentiate in biological adhesion in XN, and immune system processes and multicellular organismal processes in XNC. In terms of upregulated proteins, a higher amount of proteins involved in localization, developmental processes and response to stimulus after treatment with XNC was observed.

In general, a multifactorial response from treatment with hop compound XN and XNC becomes apparent from this analysis. Due to many different influenced proteins and functions, the biological activity of XN and XNC cannot be assigned to one specific cluster of function or target structure.

Next we specifically investigated statistically significant differences between XN or XNC treated MCF-7 cells and the DMSO control cells as shown in the volcano plot analysis in Fig 5. In MCF-7 cells after treatment with XN, reductases (aldo-keto reductase) and proteins involved in the interferon pathway were significantly downregulated. In contrast, upregulated proteins (kinesin family members, KIF, and minichromosome maintenance complexes, MCM) were allocated to the laminin pathway. Proteins from the laminin pathway also contribute to cell growth and cell adhesion and are therefore involved in catalytic activity, binding and receptor activity. This is also in accordance to functional network analysis (see S3 and S4 Figs), where a strong interaction of these upregulated proteins could be observed. Besides kinesin family members (KIF) and minichromosome maintenance complexes (MCM), also aurora kinases (AURK) were present in the network. These proteins are implicated in mitotic spindle elongation, cell cycle, and deoxyribonucleic acid (DNA) replication. This is expected, since these proteins (i.e. kinesin family members) were shown to be overexpressed associated with breast cancer cell growth [61]. Based on western blot analysis, Shimo et al. [61] suggested this protein family as a promising molecular target for anticancer treatment. A downregulation could possibly suppress the growth of such breast cancer cells. In addition, MCM proteins were described as promising markers for targeting cancer cells, since they are involved in DNA replication and therefore mostly upregulated in cancer cells [62, 63]. Aurora kinases B and C are also upregulated in correspondence with cancer cell growth and implicated to several biological cell processes. Consequently, the described upregulation mainly confirms the cell stress response after treatment with XN.

On the side of downregulation after treatment with XN, especially proteins involved in type I interferon signaling pathway were affected, including SQSTM1, ISG15, OAS1, OAS3, IRF9, STAT1, PARP9, and DTX3L. In general, interferon is involved in the JAK/STAT (Janus kinase/ signal transducer and activator of transcription) signaling pathway and hence induces cell apoptosis (see also cancer data base: <http://data-analysis.charite.de/care/>). Musgrove et al. described an in vitro downregulation of the interferon pathway in tamoxifen resistant breast cancer cells [64]. Furthermore, they concluded from the downregulation of the interferon

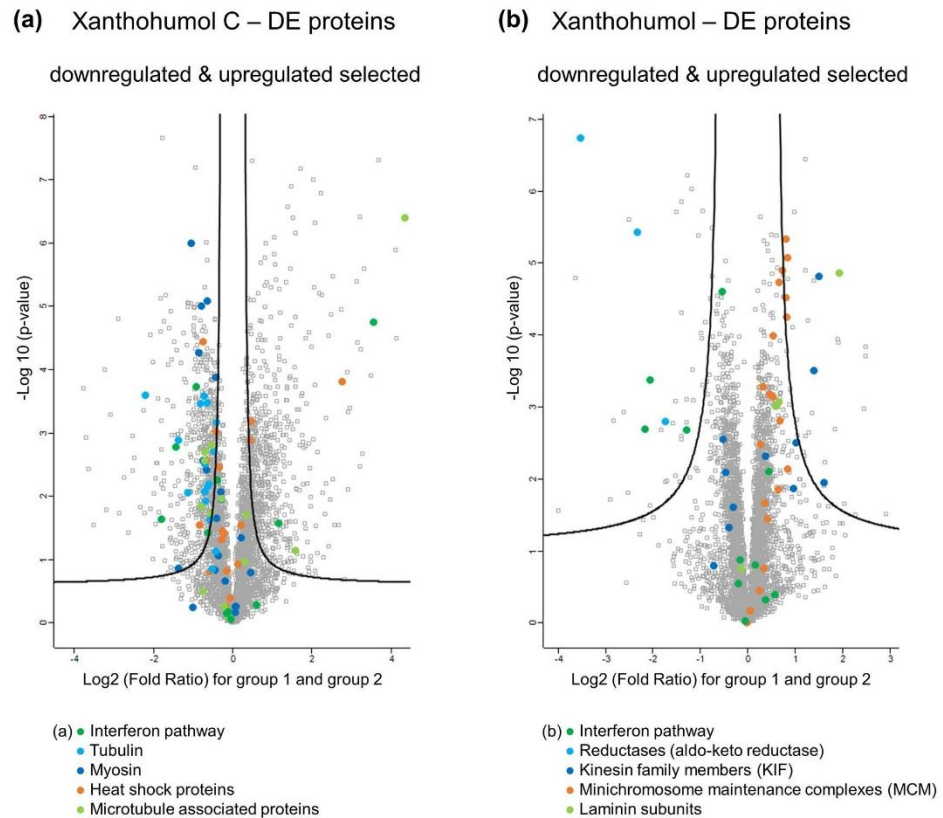


Fig 5. Volcano plots represent significant differences between MXF-7 treated cells (group 1) and DMSO control cells (group 2) for XNC (a) and XN (b). Significant up- and downregulated proteins that could be assigned to one function or family are marked. The protein names are listed in supporting information S6–S9 Files.

<https://doi.org/10.1371/journal.pone.0213469.g005>

pathway among others, a reason for therapeutic resistances against tamoxifen and other antiestrogens. Consequently, a downregulation of proteins involved in the type I interferon signaling pathway might be an adjustment of MCF-7 cells to treatment with XN. To sum up the xanthohumol analysis, a general stress response of MCF-7 cells was found after treatment.

Compared to treatment with XN, a much higher number of proteins were differentially expressed after treatment with XNC. As mentioned before, this could be associated with the higher activity of XNC. Mostly proteins part of tubulin and myosin were downregulated (see functional network in S4(b) Fig), whose molecular function is involved in binding and catalytic activity. In contrast, so called heat shock proteins (HSP) signaling cell stress and influencing structural molecule activity were upregulated (see HSPA5, HSPA13, HSP90B1, HSP40 in functional network, S4(a) Fig). An enrichment analysis of the different functional categories of all upregulated proteins leads to an overrepresentation of microtubule-associated protein 1 light chain 3 alpha and beta, and beta 2 (MAP1LC3A / MAP1LC3B / MAP1LC3B2), which are involved in the cellular response to nitrogen levels, autophagy of mitochondrion, and mitochondrion disassembly. However, these enriched upregulated DE proteins occurred as single

nodes only and hence, could not be assigned to a certain network within the functional network analysis. Nevertheless, the upregulation of these proteins might explain the cytotoxic effect of XNC in MCF-7 cells. A list of all enriched molecular functions is provided in supplementary S1 and S2 Tables including GO terms and description. The upregulated heat shock proteins are generally expressed as a reaction to endoplasmic reticulum (ER) stress and are involved in protein folding. In addition, they protect proteins' secondary structure under extreme conditions and are involved in mitogen-activated protein kinases (MAPK) signal pathways. This might be a reason for cell apoptosis as a consequence after cell treatment with XNC (see also cancer data base: <http://data-analysis.charite.de/care/>). As reported by Nollen et al. [65], both upregulation and downregulation of these proteins, i.e. HSP70 or HSP90, can result in aberrant growth control, developmental malformations and cell death. This might depend on the relative amount of these proteins. In addition, Chen et al. [66] described a downregulation of a different HSP (i.e. HSP27) after MCF-7 treatment with the antitumor drug doxorubicin and showed a target related action on the HSP27 expression. It is assumed that the influence on the HSP level might be useful for the control of breast tumor growth [67–70]. In our study, upregulated HSP levels were found. However, no HSP27 was detected after treatment with XN or XNC, which requires further specific analysis in this issue of different altered HSP levels.

In terms of the downregulated proteins after treatment with XNC, i.e. tubulin (e.g. TUBA1A, TUBA1B, TUBA1C, TUBA3D, TUBB6), myosin (e.g. MYL12A, MAL12B, MYL6, MYL9, MYH7B, MYH9) and various kinases (e.g. CDKs, MAPKs, PAK, PKC) were detected. Tubulin and myosin participate in cell-cell adhesion or cell-matrix adhesion such as tight junction and focal adhesion. A downregulation of these proteins might affect cell-cell contacts, resulting in a reduction of cell growth or cell death. This is in accordance with the enrichment analysis (see summary in S1 and S2 Tables), which indicates a significant overrepresentation of proteins involved in the regulation of cell proliferation and the homotypic cell-cell adhesion. A downregulation of tubulin and myosin by XNC might result in an inhibition of microtubule dynamics. As described by Rathinasamy et al. [71] for the compound griseofulvin and Banerjee et al. [72] for the compound curcumin, a suppression of microtubule dynamics inhibits the proliferation of MCF-7 cells and induces cell apoptosis. This indicates also a possible reason for the proliferative and cytotoxic effect of XNC in our study. Since kinases are involved in cell proliferation, DNA damage checkpoint regulation and pathway repair, they are often deregulated in cancer. Therefore, our analysis suggests XNC also as a potential anticancer agent for targeting various kinases [73–75]. Downregulation of tubulin, myosin and various kinases could possibly be related to the cytotoxic effect of XNC in MCF-7 cell line. However, further experiments that proof this hypothesis are needed. Noteworthy and similar to the treatment with XN, also proteins involved in the type I interferon signaling pathway (ISG15, OAS1, OAS3, IRF9, STAT1, and IFI35) were downregulated in XNC treated cells. This might be an indication for a MCF-7 defense mechanism to the compound treatment with XN and XNC.

To conclude the proteomics analysis, the comparison between the XN and XNC regulated proteomes suggests different modes of action. The strong effect of pure XNC on the growth of MCF-7 compared to XN seems to be related to the downregulation of cell-cell adhesion proteins, i.e. cytoskeletal proteins such as tubulin, myosin and various kinases, and the suppression of microtubule dynamics. In terms of XN, the downregulation of the interferon pathway and JAK/STAT signaling pathway seems to cause cell apoptosis. These findings underscore also the cytotoxic effects of the compounds observed in the cell culture experiments before.

Confirming the proteomics approach with a much higher number of affected proteins, pure XNC shows a stronger effect on the growth of MCF-7 compared to pure XN. The

higher effect of the XN -enriched extract XF in the cell culture experiments, including also small amounts of XNC and other minor hop compounds, demonstrates the supporting activity of minor hop compounds. Further, our results demonstrate the potential of pure minor hop compounds to be more active than extracts still containing a bunch of minor compounds as impurities. Concluding, minor hop compounds could also be deployed in a targeted way and added to anticarcinogenic drugs or preventive food additives to enhance their bioactivity.

Conclusions

In this study, we explored the effect of xanthohumol C (XNC) compared to xanthohumol (XN) and the commercial XN -enriched hop extract Xantho-Flav (XF) on human breast cancer cell line MCF-7 in vitro. All three showed dose-dependent antiproliferative and cytotoxic effects after 2, 4, and 6 days of incubation. Remarkably, XN was less cytotoxic than the XN -enriched extract XF, while the activity of XNC was highest. All three compounds clearly differed in their half maximal inhibitory concentration (IC_{50} after two days XNC: 4.18 μ M, XF: 8.84 μ M, XN: 12.25 μ M). This promises the bioactive potential of minor prenylated hop chalcones for further applications in cancer research and indicates hop as a versatile natural resource of active minor compounds with potential anticarcinogenic effects. The results demonstrate a higher anticarcinogenic or chemopreventive potential of the studied hop compounds compared to other phenolic compounds such as resveratrol (IC_{50} : 100 μ M) or curcumin (IC_{50} : 35 μ M) [55]. The study indicates the need of highly pure minor compounds to clearly associate certain effects with single compounds.

Further, the quantitative proteomics approach provided a comprehensive view on the proteome composition of XN and XNC treated MCF-7 cells. Based on the differences in protein expression, this approach gave insights in molecular mechanisms and possible target structures, which indicate different modes of action between XN and XNC treated cells. XN upregulated proteins involved in cell cycles and DNA replication and downregulated proteins of the type I interferon signaling pathway. In contrast, upregulated proteins after XNC treatment were responses to ER stress and downregulated proteins were involved in cell-cell adhesion. In addition, XNC possibly modulated kinase expression. The applied proteomics approach has the potential to be a state-of-the-art technique for bioactivity screenings of promising bioactive minor hop compounds. The study emphasizes the potential of liquid-liquid chromatography to isolate highly pure natural compounds from complex mixtures in sufficient amounts, which is needed to analyze the bioactivity of each compound specifically. By this, previously unavailable natural minor compounds could be provided in high purity. In addition, XNC might also be a promising preventive or anticarcinogenic target for the use together with current anticarcinogenic drugs to enhance antiproliferative and cytotoxic effects.

Supporting information

S1 Fig. DE proteins after xanthohumol treatment. Differentially expressed proteins in xanthohumol treated MCF-7 with their respective molecular function. Proteins are sorted by their differences in expression compared to control cells, showing only proteins with 2.5 fold up- or downregulation based on \log_2 transformed LFQ intensities. (TIF)

S2 Fig. DE proteins after xanthohumol C treatment. Differentially expressed proteins in xanthohumol C treated MCF-7 with their respective molecular function. Proteins are sorted by their differences in expression compared to control cells, showing only proteins with 2.5

fold up- or downregulation based on log₂ transformed LFQ intensities.

(TIF)

S3 Fig. Functional signal networks after xanthohumol treatment. Functional signal networks of up- (a) and downregulated (b) proteins in xanthohumol treated MCF-7. In (b), proteins were marked that are involved in the type I interferon signaling pathway.

(TIF)

S4 Fig. Functional signal networks after xanthohumol C treatment. Functional signal networks of up- (a) and downregulated (b) DE proteins in xanthohumol C treated MCF-7. (a): Heat shock proteins were marked in grey. (b): In blue kinases were marked, in grey proteins involved in tubulin, and in black proteins implemented in the type I interferon signaling pathway.

(TIF)

S1 Table. Enrichment analysis of upregulated proteins after xanthohumol C treatment.

Enrichment analysis of upregulated proteins in xanthohumol C treated MCF-7 implemented in the web tool GOrilla. Gene ontology terms, description of the molecular function in which enriched proteins were involved, p-values, false discovery rates (FDR), and enrichment factors are shown.

(PDF)

S2 Table. Enrichment analysis of downregulated proteins after xanthohumol C treatment.

Enrichment analysis of downregulated proteins in xanthohumol C treated MCF-7 implemented in the web tool GOrilla. Gene ontology terms, description of the molecular function in which enriched proteins were involved, p-values, false discovery rates (FDR), and enrichment factors are shown.

(PDF)

S1 File. All identified peptides as output from MaxQuant.

(XLSX)

S2 File. All identified protein groups as output from MaxQuant.

(XLSX)

S3 File. MaxQuant configuration.

(XML)

S4 File. Quality control report performed with raw data from MaxQuant.

(PDF)

S5 File. All quantified proteins.

(XLSX)

S6 File. Downregulated DE proteins after treatment with Xanthohumol C.

(XLSX)

S7 File. Upregulated DE proteins after treatment with Xanthohumol C.

(XLSX)

S8 File. Downregulated DE proteins after treatment with Xanthohumol.

(XLSX)

S9 File. Upregulated DE proteins after treatment with Xanthohumol.

(XLSX)

Acknowledgments

We acknowledge M. Biendl from Hopsteiner (S. H. Steiner, Hopfen GmbH, 84048 Mainburg, Germany) for the provision of the hop extract Xantho-Flav. We are thankful to Prof. Küster and K. Kramer (Chair of Proteomics and Bioanalytics, Technical University of Munich) for providing the MCF-7 cells and fruitful discussions about the experimental setup. The authors want to greatly thank Prof. Hauner and M. Hubersberger (Chair of Nutritional Medicine, Technical University of Munich) for giving us the possibility to perform the cell culture experiments in their lab and for supporting us during the cell culture experiments. The authors thank H. Kienberger (Bavarian Center for Biomolecular Mass Spectrometry) for technical assistance.

Author Contributions

Conceptualization: Simon Roehrer, Jürgen Behr.

Data curation: Simon Roehrer, Jürgen Behr.

Formal analysis: Simon Roehrer, Verena Stork, Jürgen Behr.

Investigation: Simon Roehrer, Verena Stork, Jürgen Behr.

Methodology: Simon Roehrer, Verena Stork, Jürgen Behr.

Project administration: Simon Roehrer, Jürgen Behr.

Resources: Mirjana Minceva, Jürgen Behr.

Supervision: Mirjana Minceva, Jürgen Behr.

Visualization: Simon Roehrer, Verena Stork.

Writing – original draft: Simon Roehrer, Verena Stork.

Writing – review & editing: Christina Ludwig, Mirjana Minceva, Jürgen Behr.

References

1. Malik S. *Biotechnology and Production of Anti-Cancer Compounds*: Springer International Publishing; 2017.
2. Karabín M, Hudcová T, Jelínek L, Dostálek P. Biologically active compounds from hops and prospects for their use. *Compr Rev Food Sci F*. 2016; 15(3):542–67. <https://doi.org/10.1111/1541-4337.12201>
3. Biendl M. Hops and Health. *MBAA TQ*: 1–7. 2009.
4. Olsovska J, Cermak P, Bostikova V, Bostik P, Dusek M, Mikyska A, et al. Humulus Lupulus L. (Hops)—A valuable source of compounds with bioactive effects for future therapies. *Mil Med Sci Lett (Voj Zdrav Listy)*. 2016; 85(1):19. <https://doi.org/10.31482/mmsl.2016.004>
5. Dietz BM, Chen S-N, Alvarenga RFR, Dong H, Nikolić D, Biendl M, et al. DESIGNER Extracts as Tools to Balance Estrogenic and Chemopreventive Activities of Botanicals for Women's Health. *J Nat Prod*. 2017; 80(8):2284–94. <https://doi.org/10.1021/acs.jnatprod.7b00284> PMID: 28812892
6. Stevens JF, Page JE. Xanthohumol and related prenylflavonoids from hops and beer: to your good health! *Phytochemistry*. 2004; 65(10):1317–30. <https://doi.org/10.1016/j.phytochem.2004.04.025> PMID: 15231405
7. Liu M, Hansen P, Wang G, Qiu L, Dong J, Yin H, et al. Pharmacological Profile of Xanthohumol, a Prenylated Flavonoid from Hops (*Humulus lupulus*). *Molecules*. 2015; 20(1):754. <https://doi.org/10.3390/molecules20010754> PMID: 25574819
8. Vogel S, Barbic M, Juergeniemk G, Heilmann J. Synthesis, cytotoxicity, anti-oxidative and anti-inflammatory activity of chalcones and influence of A-ring modifications on the pharmacological effect. *Eur J Med Chem*. 2010; 45(6):2206–13. <https://doi.org/10.1016/j.ejmech.2010.01.060> PMID: 20153559

9. Oberbauer E, Urmann C, Steffenhagen C, Bieler L, Brunner D, Furtner T, et al. Chroman-like cyclic prenylflavonoids promote neuronal differentiation and neurite outgrowth and are neuroprotective. *J Nutr Biochem.* 2013; 24(11):1953–62. <https://doi.org/10.1016/j.jnutbio.2013.06.005> PMID: 24070601
10. Aigner L, Oberbauer-Hofmann E, Couillard-Despres S, Rivera FJ, Riepl H, Urmann C, et al., inventors-Chromane-like cyclic prenylflavonoids for the medical intervention in neurological disorders patent US20170128411 A1. 2016.
11. Natarajan P, Katta S, Andrei I, Ambati VBR, Leonida M, Haas G. Positive antibacterial co-action between hop (*Humulus lupulus*) constituents and selected antibiotics. *Phytomedicine.* 2008; 15(3):194–201. <https://doi.org/10.1016/j.phymed.2007.10.008> PMID: 18162387
12. Rozalski M, Micota B, Sadowska B, Stochmal A, Jedrejek D, Wieckowska-Szakiel M, et al. Antiadherent and antibiofilm activity of *Humulus lupulus* L. derived products: new pharmacological properties. *Biomed Res Int.* 2013; 2013:101089. <https://doi.org/10.1155/2013/101089> PMID: 24175280
13. Dixon-Shanies D, Shaikh N. Growth inhibition of human breast cancer cells by herbs and phytoestrogens. *Oncol Rep.* 1999; 6(6):1383–90. <https://doi.org/10.3892/or.6.6.1383> PMID: 10523716
14. Venturelli S, Burkard M, Biendl M, Lauer UM, Frank J, Busch C. Prenylated chalcones and flavonoids for the prevention and treatment of cancer. *Nutrition.* 2016; 32(11):1171–8. <https://doi.org/10.1016/j.nut.2016.03.020> PMID: 27238957
15. Miranda C, Stevens J, Helmrich A, Henderson M, Rodriguez R, Yang Y-H, et al. Antiproliferative and cytotoxic effects of prenylated flavonoids from hops (*Humulus lupulus*) in human cancer cell lines. *Food Chem Toxicol.* 1999; 37(4):271–85. [https://doi.org/10.1016/S0278-6915\(99\)00019-8](https://doi.org/10.1016/S0278-6915(99)00019-8) PMID: 10418944
16. Kang Y, Park M-A, Heo S-W, Park S-Y, Kang KW, Park P-H, et al. The radio-sensitizing effect of xanthohumol is mediated by STAT3 and EGFR suppression in doxorubicin-resistant MCF-7 human breast cancer cells. *BBA-Gen Subjects.* 2013; 1830(3):2638–48. <https://doi.org/10.1016/j.bbagen.2012.12.005> PMID: 23246576
17. Popłoński J, Turlej E, Sordon S, Tronina T, Bartmańska A, Wietrzyk J, et al. Synthesis and Antiproliferative Activity of Minor Hops Prenylflavonoids and New Insights on Prenyl Group Cyclization. *Molecules.* 2018; 23(4):776. <https://doi.org/10.3390/molecules23040776> PMID: 29597299
18. Yang J-Y, Della-Fera MA, Rayalam S, Baile CA. Effect of xanthohumol and isoxanthohumol on 3T3-L1 cell apoptosis and adipogenesis. *Apoptosis.* 2007; 12(11):1953–63. <https://doi.org/10.1007/s10495-007-0130-4> PMID: 17874298
19. Mendes V, Monteiro R, Pestana D, Teixeira D, Calhau C, Azevedo I. Xanthohumol influences preadipocyte differentiation: implication of antiproliferative and apoptotic effects. *J Agric Food Chem.* 2008; 56(24):11631–7. <https://doi.org/10.1021/jf802233q> PMID: 19035642
20. Gerhäuser C, Alt A, Heiss E, Gamal-Eldeen A, Klimo K, Knauff J, et al. Cancer Chemopreventive Activity of Xanthohumol, a Natural Product Derived from Hop 1 Support for this work has been provided by Verein zur Förderung der Krebsforschung in Deutschland e.V. and by Wissenschaftsförderung der Deutschen Brauwirtschaft eV These data were presented, in part, at the 92nd annual meeting of the American Association of Cancer Research, March 24–28, 2001 in New Orleans, LA (64). *Mol Cancer Ther.* 2002:959–69.
21. Gerhäuser C. Broad spectrum anti-infective potential of xanthohumol from hop (*Humulus lupulus* L.) in comparison with activities of other hop constituents and xanthohumol metabolites. *Mol Nutr Food Res.* 2005; 49(9):827–31. <https://doi.org/10.1002/mnfr.200500091> PMID: 16092071
22. Zanolli P, Zavatti M. Pharmacognostic and pharmacological profile of *Humulus lupulus* L. *J Ethnopharmacol.* 2008; 116(3):383–96. <https://doi.org/10.1016/j.jep.2008.01.011> PMID: 18308492
23. Legette L, Karnpracha C, Reed RL, Choi J, Bobe G, Christensen JM, et al. Human pharmacokinetics of xanthohumol, an antihyperglycemic flavonoid from hops. *Mol Nutr Food Res.* 2014; 58(2):248–55. <https://doi.org/10.1002/mnfr.201300333> PMID: 24038952
24. Vogel S, Heilmann Jr. Synthesis, cytotoxicity, and antioxidative activity of minor prenylated chalcones from *Humulus lupulus*. *J Nat Prod.* 2008; 71(7):1237–41. <https://doi.org/10.1021/np800188b> PMID: 18611049
25. Nuti E, Bassani B, Camodeca C, Rosalia L, Cantelmo A, Gallo C, et al. Synthesis and antiangiogenic activity study of new hop chalcone Xanthohumol analogues. *Eur J Med Chem.* 2017; 138:890–9. <https://doi.org/10.1016/j.ejmech.2017.07.024> PMID: 28750311
26. Miranda CL, Stevens JF, Ivanov V, McCall M, Frei B, Deinzer ML, et al. Antioxidant and prooxidant actions of prenylated and nonprenylated chalcones and flavanones in vitro. *J Agric Food Chem.* 2000; 48(9):3876–84. <https://doi.org/10.1021/jf0002995> PMID: 10995285
27. Bertl E, Becker H, Eicher T, Herhaus C, Kapadia G, Bartsch H, et al. Inhibition of endothelial cell functions by novel potential cancer chemopreventive agents. *Biochem Biophys Res Commun.* 2004; 325(1):287–95. <https://doi.org/10.1016/j.bbrc.2004.10.032> PMID: 15522231

28. Mizobuchi S, Sato Y. A new flavanone with antifungal activity isolated from hops. *Agr Biol Chem Tokyo*. 1984; 48(11):2771–5. <https://doi.org/10.1080/00021369.1984.10866564>
29. Forino M, Pace S, Chianese G, Santagostini L, Werner M, Weinigel C, et al. Humulifucol and bioactive prenylated polyphenols from hops (*Humulus lupulus* cv. "Cascade"). *J Nat Prod*. 2016; 79(3):590–7. <https://doi.org/10.1021/acs.jnatprod.5b01052> PMID: 26918635
30. Nikolic D, Van Breemen RB. Analytical methods for quantitation of prenylated flavonoids from hops. *Curr Anal Chem*. 2013:71–85. PMID: 24077106
31. Stevens JF, Ivancic M, Hsu VL, Deinzer ML. Prenylflavonoids from *Humulus lupulus*. *Phytochemistry*. 1997; 44(8):1575–85. [https://doi.org/10.1016/S0031-9422\(96\)00744-3](https://doi.org/10.1016/S0031-9422(96)00744-3)
32. Lee YR, Xia L. Concise total synthesis of biologically interesting pyranochalcone natural products: citronobin, boesenbergin A, boesenbergin B, xanthohumol C, and glabrachromene. *Synthesis*. 2007; 2007(20):3240–6. <https://doi.org/10.1055/s-2007-990796>
33. Roehrer S, Behr J, Stork V, Ramires M, Médard G, Frank O, et al. Xanthohumol C, a minor bioactive hop compound: Production, purification strategies and antimicrobial test. *J Chromatogr B*. 2018; 1095:39–49. <https://doi.org/10.1016/j.jchromb.2018.07.018> PMID: 30053686
34. Aebersold R, Mann M. Mass-spectrometric exploration of proteome structure and function. *Nature*. 2016; 537(7620):347. <https://doi.org/10.1038/nature19949> PMID: 27629641
35. Bantscheff M, Lemeere S, Savitski MM, Kuster B. Quantitative mass spectrometry in proteomics: critical review update from 2007 to the present. *Anal Bioanal Chem*. 2012; 404(4):939–65. <https://doi.org/10.1007/s00216-012-6203-4> PMID: 22772140
36. Bantscheff M, Schirle M, Sweetman G, Rick J, Kuster B. Quantitative mass spectrometry in proteomics: a critical review. *Anal Bioanal Chem*. 2007; 389(4):1017–31. <https://doi.org/10.1007/s00216-007-1486-6> PMID: 17668192
37. Aebersold R, Mann M. Mass spectrometry-based proteomics. *Nature*. 2003; 422(6928):198. <https://doi.org/10.1038/nature01511> PMID: 12634793
38. Lill J. Proteomic tools for quantitation by mass spectrometry. *Mass Spectrom Rev*. 2003; 22(3):182–94. <https://doi.org/10.1002/mas.10048> PMID: 12838544
39. Ong S-E, Mann M. Mass spectrometry-based proteomics turns quantitative. *Nat Chem Biol*. 2005; 1(5):252. <https://doi.org/10.1038/nchembio736> PMID: 16408053
40. Rix U, Superti-Furga G. Target profiling of small molecules by chemical proteomics. *Nat Chem Biol*. 2009; 5(9):616. <https://doi.org/10.1038/nchembio.216> PMID: 19690537
41. Wang J, Gao L, Lee YM, Kalesh KA, Ong YS, Lim J, et al. Target identification of natural and traditional medicines with quantitative chemical proteomics approaches. *Pharmacol Ther*. 2016; 162:10–22. <https://doi.org/10.1016/j.pharmthera.2016.01.010> PMID: 26808165
42. Riss TL, Moravec RA, Niles AL, Duellman S, Benink HA, Worzella TJ, et al. Cell viability assays. Bethesda (MD): Eli Lilly & Company and the National Center for Advancing Translational Sciences; 2016.
43. Rappsilber J, Ishihama Y, Mann M. Stop and go extraction tips for matrix-assisted laser desorption/ionization, nanoelectrospray, and LC/MS sample pretreatment in proteomics. *Anal Chem*. 2003; 75(3):663–70. <https://doi.org/10.1021/ac026117i> PMID: 12585499
44. Cox J, Mann M. MaxQuant enables high peptide identification rates, individualized ppb-range mass accuracies and proteome-wide protein quantification. *Nat Biotechnol*. 2008; 26(12):1367–72. <https://doi.org/10.1038/nbt.1511> PMID: 19029910
45. Cox J, Neuhauser N, Michalski A, Scheltema RA, Olsen JV, Mann M. Andromeda: a peptide search engine integrated into the MaxQuant environment. *J Proteome Res*. 2011; 10(4):1794–805. <https://doi.org/10.1021/pr101065j> PMID: 21254760
46. Cox J, Hein MY, Luber CA, Paron I, Nagaraj N, Mann M. Accurate proteome-wide label-free quantification by delayed normalization and maximal peptide ratio extraction, termed MaxLFQ. *Mol Cell Proteomics*. 2014; 13(9):2513–26. <https://doi.org/10.1074/mcp.M113.031591> PMID: 24942700
47. Bielow C, Mastrobuoni G, Kempa S. Proteomics quality control: quality control software for MaxQuant results. *J Proteome Res*. 2015; 15(3):777–87. <https://doi.org/10.1021/acs.jproteome.5b00780> PMID: 26653327
48. Mi H, Muruganujan A, Casagrande JT, Thomas PD. Large-scale gene function analysis with the PANTHER classification system. *Nat Protoc*. 2013; 8(8):1551–66. <https://doi.org/10.1038/nprot.2013.092> PMID: 23868073
49. Jensen LJ, Kuhn M, Stark M, Chaffron S, Creevey C, Muller J, et al. STRING 8—a global view on proteins and their functional interactions in 630 organisms. *Nucleic Acids Res*. 2008; 37(suppl_1):D412–D6. <https://doi.org/10.1093/nar/gkn760> PMID: 18940858

50. Szklarczyk D, Franceschini A, Wyder S, Forslund K, Heller D, Huerta-Cepas J, et al. STRING v10: protein–protein interaction networks, integrated over the tree of life. *Nucleic Acids Res.* 2014; 43(D1): D447–D52. <https://doi.org/10.1093/nar/gku1003> PMID: 25352553
51. Eden E, Navon R, Steinfeld I, Lipson D, Yakhini Z. GOrrilla: a tool for discovery and visualization of enriched GO terms in ranked gene lists. *BMC bioinformatics.* 2009; 10(1):48. <https://doi.org/10.1186/1471-2105-10-48> PMID: 19192299
52. Stompór M, Zarowska B. Antimicrobial Activity of Xanthohumol and Its Selected Structural Analogues. *Molecules.* 2016; 21(5):608. <https://doi.org/10.3390/molecules21050608> PMID: 27187329
53. Motyl M. The absorption of xanthohumol in in vitro and in vivo studies and the investigation of the biological activity of structurally related chalcones [Doctoral Dissertation]; University of Regensburg, Germany; 2013.
54. Nookandeh A, Frank N, Steiner F, Ellinger R, Schneider B, Gerhäuser C, et al. Xanthohumol metabolites in faeces of rats. *Phytochemistry.* 2004; 65(5):561–70. <https://doi.org/10.1016/j.phytochem.2003.11.016> PMID: 15003419
55. Roy M, Chakraborty S, Siddiqi M, Bhattacharya RK. Induction of apoptosis in tumor cells by natural phenolic compounds. *Asian Pac J Cancer P.* 2002;61–7.
56. Schott A-S, Behr Jr, Geißler AJ, Kuster B, Hahne H, Vogel RF. Quantitative Proteomics for the Comprehensive Analysis of Stress Responses of *Lactobacillus paracasei* subsp. *paracasei* F19. *J Proteome Res.* 2017; 16(10):3816–29. <https://doi.org/10.1021/acs.jproteome.7b00474> PMID: 28862000
57. Suarez RK, Moyes CD. Metabolism in the age of 'omes'. *J Exp Biol.* 2012; 215(14):2351–7. <https://doi.org/10.1242/jeb.059725> PMID: 22723473
58. Champagne A, Boutry M. A comprehensive proteome map of glandular trichomes of hop (*Humulus lupulus* L.) female cones: Identification of biosynthetic pathways of the major terpenoid-related compounds and possible transport proteins. *Proteomics.* 2017; 17(8):1600411. <https://doi.org/10.1002/pmic.201600411> PMID: 28198089
59. Matoušek J, Vrba L, Škopek J, Orctová L, Pešina K, Heyerick A, et al. Sequence Analysis of a “True” Chalcone Synthase (chs_H1) Oligofamily from hop (*Humulus lupulus* L.) and PAP1 Activation of chs_H1 in Heterologous Systems. *J Agric Food Chem.* 2006; 54(20):7606–15. <https://doi.org/10.1021/jf061785g> PMID: 17002429
60. Behr J, Israel L, Gänzle MG, Vogel RF. Proteomic approach for characterization of hop-inducible proteins in *Lactobacillus brevis*. *Appl Environ Microbiol.* 2007; 73(10):3300–6. <https://doi.org/10.1128/AEM.00124-07> PMID: 17369340
61. Shimo A, Tanikawa C, Nishidate T, Lin ML, Matsuda K, Park JH, et al. Involvement of kinesin family member 2C/mitotic centromere-associated kinesin overexpression in mammary carcinogenesis. *Cancer Sci.* 2008; 99(1):62–70. <https://doi.org/10.1111/j.1349-7006.2007.00635.x> PMID: 17944972
62. Alison M, Hunt T, Forbes S. Minichromosome maintenance (MCM) proteins may be pre-cancer markers. *Gut.* 2002; 50(3):290–1. <https://doi.org/10.1136/gut.50.3.290> PMID: 11839701
63. Freeman A, Morris LS, Mills AD, Stoerber K, Laskey RA, Williams GH, et al. Minichromosome maintenance proteins as biological markers of dysplasia and malignancy. *Clin Cancer Res.* 1999. Aug;2121–32. PMID: 10473096
64. Musgrove EA, Sutherland RL. Biological determinants of endocrine resistance in breast cancer. *Nat Rev Cancer.* 2009; 9(9):631–43. <https://doi.org/10.1038/nrc2713> PMID: 19701242
65. Nollen EA, Morimoto RI. Chaperoning signaling pathways: molecular chaperones as stress-sensing shock proteins. *J Cell Sci.* 2002;2809–16. PMID: 12082142
66. Chen S-T, Pan T-L, Tsai Y-C, Huang C-M. Proteomics reveals protein profile changes in doxorubicin-treated MCF-7 human breast cancer cells. *Cancer Lett.* 2002; 181(1):95–107. [https://doi.org/10.1016/S0304-3835\(02\)00025-3](https://doi.org/10.1016/S0304-3835(02)00025-3) PMID: 12430184
67. Oesterreich S, Weng C-N, Qiu M, Hilsenbeck SG, Osborne CK, Fuqua SA. The small heat shock protein hsp27 is correlated with growth and drug resistance in human breast cancer cell lines. *Cancer Res.* 1993. Oct 1;4443–8.
68. Konda JD, Olivero M, Musiani D, Lamba S, Di Renzo MF. Heat-shock protein 27 (HSP27, HSPB1) is synthetic lethal to cells with oncogenic activation of MET, EGFR and BRAF. *Mol Oncol.* 2017; 11(6):599–611. <https://doi.org/10.1002/1878-0261.12042> PMID: 28182330
69. Wu J, Liu T, Rios Z, Mei Q, Lin X, Cao S. Heat shock proteins and cancer. *Trends Pharmacol Sci.* 2017; 38(3):226–56. <https://doi.org/10.1016/j.tips.2016.11.009> PMID: 28012700
70. Katsogiannou M, Andrieu C, Rocchi P. Heat shock protein 27 phosphorylation state is associated with cancer progression. *Frontiers in genetics.* 2014; 5:346. <https://doi.org/10.3389/fgene.2014.00346> PMID: 25339975

71. Rathinasamy K, Jindal B, Asthana J, Singh P, Balaji PV, Panda D. Griseofulvin stabilizes microtubule dynamics, activates p53 and inhibits the proliferation of MCF-7 cells synergistically with vinblastine. *Bmc Cancer*. 2010; 10(1):213. <https://doi.org/10.1186/1471-2407-10-213> PMID: 20482847
72. Banerjee M, Singh P, Panda D. Curcumin suppresses the dynamic instability of microtubules, activates the mitotic checkpoint and induces apoptosis in MCF-7 cells. *The FEBS journal*. 2010; 277(16):3437–48. <https://doi.org/10.1111/j.1742-4658.2010.07750.x> PMID: 20646066
73. Johnson N, Shapiro GI. Cyclin-dependent kinases (cdks) and the DNA damage response: rationale for cdk inhibitor–chemotherapy combinations as an anticancer strategy for solid tumors. *Expert Opin Ther Tar*. 2010; 14(11):1199–212. <https://doi.org/10.1517/14728222.2010.525221> PMID: 20932174
74. Dai Y, Grant S. CDK inhibitor targets—A hit or miss proposition?: Cyclin-dependent kinase inhibitors kill tumor cells by downregulation of antiapoptotic proteins. *Cancer Biol Ther*. 2006:171–3. PMID: 16552171
75. Lapenna S, Giordano A. Cell cycle kinases as therapeutic targets for cancer. *Nat Rev Drug Discovery*. 2009; 8(7):547–66. <https://doi.org/10.1038/nrd2907> PMID: 19568282

4. Discussion and Conclusion

The objective of this thesis was to systematically investigate main factors that influence the separation performance in LLC and to use this knowledge for the development, transfer and scale-up of separation methods for the purification of high value-added natural products. Thus, the focus of the work was on two main topics.

On the one hand, main influencing factors were analyzed to gain a better understanding of their impacts on LLC separations and to improve the development of a separation method for a particular separation task. In this sense, extensive column characterizations of various LLC columns were performed with model systems to analyze and describe the separation performance in dependence of various parameters such as column design, operating conditions (flow rate and rotational speed), the type of new biphasic solvent systems and separation temperature. The so gained insights can be used as important input factors for the exploration of model-based method development and separation method transfer between different columns, which was subsequently investigated in this thesis.

On the other hand, new approaches for the isolation of pure natural minor components with LLC were established. Using the promising bioactive hop compound xanthohumol C as an example, it was shown that LLC can be used to isolate such highly pure natural minor components from complex matrices. In this context, two strategies were established: the selective capture and enrichment from raw extracts with a subsequent separation step, and another two-step production approach involving semi-synthesis and LLC purification.

4.1. Influencing factors in LLC separation method development

Column design

In LLC, the column design is fundamentally different from the one in LC, where cylindrical columns packed with porous stationary phase particles are used. In LLC, both the column design as well as the centrifugal field are used to keep one of the two phases of a liquid biphasic system stationary, while the other one is used as mobile phase. Mainly two different types of columns exist, namely hydrodynamic CCC and hydrostatic CPC columns, but each category itself includes a variety of different designs. In CCC columns, a tube is wound up on a cylinder (bobbin) to form a coil which rotates around its axis and revolves around a second axis of rotation. In CPC columns, usually several discs with circumferentially engraved cells of different size and shape, interconnected by small channels, are mounted together to form the column that rotates around one axis. Independent of the column category, the column efficiency depends on the respective biphasic solvent system, column design, and operating conditions. The probably main driving innovations in CCC and CPC are continuous developments of new column designs and biphasic solvent systems. In recent years, continuous improvements of the columns, especially in terms of CPC cell design, have been made. It is well known that the cell shape and size, but also the number of cells are decisive for the column efficiency. Connecting channels, which are only filled with mobile phase, do not contribute to the separation but to the pressure drop. This limits the applicable flow rate range and therefore, was in focus for the development of the new column investigated in this thesis. In this new column with a special design, the channel volume was significantly reduced and the cell design was optimized towards a spherical cell shape in order to further improve the mass transfer between the phases inside each cell, i.e. to increase the cell efficiency. In

addition, a bigger disk diameter was selected for the new column, which enables a higher g -field at the same rotational speed of the column. In **Paper I**, this new column was characterized and compared to two other columns with the same total column volume. Both columns have twin-cells, which are smaller in one column (CPC) and fewer but bigger in the other column (CPE). In this sense, the cell number and size of the last column is comparable to the new column. The column characteristics were determined with the help of a frequently used aqueous-organic biphasic solvent system as a function of operating conditions, i.e. both flow rate and rotational speed, and compared with columns of conventional twin-cell design. It could be demonstrated that a higher stationary phase retention can be achieved in the column with spherical cell design compared to the two columns with twin-cells. Nevertheless, stationary phase retention, the column efficiency as well as the achievable peak resolution in the new spherical cell column are similar to the column with twin-cells of comparable cell volume. These two column types are especially beneficial for easier separations, i.e. for separation factors $\alpha > 2.5$. Here, a higher productivity can be realized with these columns due to higher flow rates that can be applied. Although the spherical cells show the highest cell efficiency, the column efficiency is similar to the CPE due to the lower number of the cells. It should be kept in mind that a column with a higher number of physical cells is more efficient than a column of the same volume but with a much lower number of cells. Although columns with bigger cells and less connecting channels exhibit a higher stationary phase retention and can be operated at higher flow rates for an improved cell efficiency, this cannot compensate the lower total number of theoretical plates, i.e. column efficiency, for difficult separations with low separation factors. Hence, the CPC columns with large numbers of small cells are essential in case of more difficult separations (small separation factors). The results of **Paper I** are helpful for the user especially when selecting an appropriate column design for the commercial purification of natural products at preparative-scale.

Non-conventional DES-based biphasic solvent systems

The advantages of a liquid nature of the stationary phase are the reason why LLC is widely used for the separation of natural compounds from plant extracts. As part of a biphasic liquid system, the stationary and mobile phase can be tailor-made by the user. In literature, a broad variety of solvent systems already exists for the separation of mainly medium-polar compounds. However, there is only a very limited number of non-aqueous organic solvent-based systems that can be applied for the separation of hydrophobic or nonpolar compounds. A recently upcoming new solvent class is DES. DES are mixtures of compounds, a hydrogen bond donor and a hydrogen bond acceptor, with a melting temperature substantially lower than that of each individual compound. Since many DES are liquid at room temperature, they can be used in mixture as one part of a biphasic liquid solvent system. That opens up new possibilities especially as water-substitutes for creating non-aqueous biphasic liquid solvent systems for the use in LLC. Hence, DES-based biphasic liquid systems might be promising for the separation of hydrophobic and nonpolar compounds. However, DES have a higher density and viscosity than organic solvents and water. Physical properties of the phases are important factors that influence the hydrodynamics in LLC. Therefore, the applicability of non-conventional biphasic liquid DES-based solvent systems has been evaluated for the first time in a CPC column (**Paper II**). In this context, a non-aqueous biphasic system composed of *n*-heptane/ethanol/DES with a DES made of choline chloride and levulinic acid in a molar ratio of 1:2 was tested in a column with large twin-cells (CPE) and bigger connecting channels than

in a conventional CPC column. Despite a higher viscosity of the DES-rich phase compared to phases of aqueous-organic solvent-based systems, a good stationary phase retention could be achieved in ascending and descending mode. With the studied solvent system, a solute polarity range of $-5.1 < \log P_{O/W} < 12$ was evaluated by shake-flask experiments with ten compounds covering the whole range. With these compounds, partition coefficients in or close to the *sweet spot range* were obtained, which enabled a satisfactory separation of β -ionone ($\log P_{O/W} = 3.8$) and α -tocopherol ($\log P_{O/W} = 12$) in the CPE. Hence, DES-based systems were demonstrated to be a promising new class of non-aqueous biphasic solvent systems in LLC, especially of highly hydrophobic compounds. However, an increased pressure drop was observed at the column as a consequence of the physical properties of the phases. This might impede the application of DES-based biphasic systems at very high flow rates and in a broad variety of CPC column designs, especially in columns with small cells and ducts. Choline chloride as one of the individual ingredients of the studied DES in this work is known to be hygroscopic. Since the studied DES were intended to be used for substituting water in liquid biphasic systems to create non-aqueous systems for the separation of hydrophobic compounds, the influence of water absorbance due to air humidity was analyzed. Fortunately, it was shown that the absorbed amounts of water did not significantly affect the studied system. The presence of small portions of water (5-15 wt%) did not influence the partition coefficient of the studied compounds. It must be noted that this is a system specific phenomenon and hence, needs to be investigated for each DES-based biphasic system before its application. Nevertheless, for such systems the addition of small amounts of water could also be intentionally used to slightly adjust the physical properties of the biphasic system for the application in CPC columns with smaller cells and ducts. Furthermore, the system robustness to the presence of water is also advantageous, since it makes an elaborate working under protective atmosphere redundant, especially at preparative scale. Finally and in addition to the evaluation of the general applicability of DES-based systems for the separation in LLC, the solute recovery from the solvent is important for the application in preparative or production scale. In addition, strategies for the solvent recycling are also necessary, which is still an open question in this field. Thus, further research on this topic is needed for a broad application of DES-based systems in LLC.

Temperature fluctuations

In conventional LC, the column temperature is often controlled with the help of a column oven to influence the adsorption and desorption process. In literature, LLC separations are mostly performed at ambient room temperature. While commercial CCC columns are usually placed in a temperature controlled cabinet, commercial CPC columns do not have any temperature control system. They are mostly placed in housing boxes with fans that provide convective cooling with ambient air. However, this does not allow precise temperature control and temperature fluctuations can appear, e.g. due to environmental temperature changes or as a result of heat dissipation in the rotating seals or in the pumps. Up to now, there are no systematic studies of the influence of temperature on the LLC separation. The two liquid phases used in LLC as stationary and mobile phase are equilibrated at a given temperature before using them for the separation. The liquid-liquid equilibrium of the biphasic solvent system and the physical properties of the phases are a function of the temperature. Therefore, temperature fluctuations might influence the separation in LLC, especially when the column is

not temperature-controlled. Especially non-aqueous organic solvent-based systems are likely to be temperature sensitive. In addition to liquid-liquid equilibrium data at different temperatures, the change of the physical properties of the phases with a change in temperature could be an important indicator of temperature susceptibility. In this work, the temperature influence on the LLC separation performance has been compared between frequently used conventional aqueous-organic solvent-based and non-aqueous organic solvent-based biphasic systems (**Paper III**). A stronger temperature effect was observed for the investigated non-aqueous system composed of *n*-hexane/ethyl acetate/acetonitrile compared to the aqueous-organic *n*-heptane/ethyl acetate/methanol/water system (Arizona N). For the non-aqueous system, a decrease in phase density and interfacial tension between the phases was observed, while the viscosity of both phases showed only a small decrease with an increase in temperature. In addition, the phase composition of the non-aqueous system was more affected with an increase in temperature. A decrease in interfacial tension with an increase in temperature leads to a better dispersion of stationary and mobile phase in the column. Consequently, a significantly increased column efficiency N_1 could be observed for the *n*-hexane/ethyl acetate/acetonitrile system and model solutes with a partition coefficient in or close to the *sweet spot range*. At the same time, a significant decrease in stationary phase retention from 65% to 45% occurred, which resulted in a clear decrease in separation resolution of 0.5 difference in R_S . It was furthermore demonstrated that a temperature difference of 10°C between the inlet mobile phase and the column temperature can already lead to a destabilization of the system and can subsequently cause column bleeding. In this sense, a temperature control system would be highly advantageous and in particular necessary for a robust separation method at preparative-scale for all systems. In conclusion and similar to CCC, a temperature controlled housing should be established for CPC columns.

Separation method transferability

LLC separation methods are mostly established at lab-scale. Subsequently, they often need to be transferred to other columns of different design and size. In classical LC, all columns have the same cylindrical shape with the characteristic dimensions column length and column diameter, and are packed with a solid stationary phase, which makes scale-up an easy and straightforward process. Several scale-up rules and methods have been established for the transfer of batch separation methods between columns in LC. A basic rule is the use of same packing material and particle size in both columns. In addition, feed sample concentration and relative sample load are kept constant as well as the column length. The operating conditions and the cross sectional area of the column are then selected so that the same mobile phase velocity is achieved in order to aim a similar number of theoretical stages. This approach has already been studied also for its applicability in CCC and CPC. However, in contrast to LC very different column designs exist especially in CPC, where the cross sectional area of the CPC cells is not constant and changes with cells of different geometries.

Moreover, the generated centrifugal field in combination with the mobile phase flow rate are important factors that influence the flow regime and result in different flow regimes in the columns. Consequently, the columns differ in stationary phase retention and column efficiency as a function of operating conditions. Since these parameters are essential to achieve a certain peak resolution, the same mobile phase velocity does not guarantee similar separation

behavior. The special column design together with the liquid nature of the stationary phase in presence of a centrifugal field makes separation method transfer a major challenge in the field of LLC separations of natural products. The most commonly used separation method transfer approach in LLC is that operating parameters are tuned to keep the same stationary phase retention in both columns. Then, linear scale-up factors are mostly used for calculating the feed sample load. As shown in this work (**Paper IV**), due to differences in column efficiency between the columns, this does not guarantee a satisfactory transferability of the separation methods between two columns. As a result, this can lead to clear differences in separation resolution or even a transfer is not possible at all. To conclude, such attempts of a simple transfer and scale-up are only directly applicable in columns of the same type and design. The objective of this work was to establish a fast and systematic general approach to quickly estimate the separation method transferability between two columns of different design and/or size. For this purpose, a fast column characterization was recommended in order to determine stationary phase retention, column efficiency and resolution in dependence of flow rate. With the solvent system *n*-heptane/ethyl acetate/methanol/water 1/1/1/1 v/v/v/v and a mixture of four parabens, it could be shown that a linear correlation of stationary phase retention and efficiency as a function of flow rate can be obtained in all columns within a certain flow rate range. In order to quickly determine these column, solute, and solvent system specific correlations, a two-point short-cut method was suggested based on two pulse injection experiments at different flow rates, one at a preferably low flow rate and a second one at a high flow rate within the suitable operating range of a particular column. The achievable resolution can then be calculated for different flow rates and used to quickly estimate the separation method transferability between the two different columns. The proposed approach guides the user to achieve a fast transfer and reduces costly and time consuming trial-and-error experiments (**Paper IV**). This is particularly advantageous during scale-up, especially at semi-preparative and preparative scale, where higher solvent and sample amounts are needed per experiment. In addition, the determined column characteristics can then also be used together with models to perform simulations in order to theoretically optimize the operating conditions in the columns.

4.2. Strategies for the recovery of pure minor components from natural extracts and characterization of their bioactivity

The isolation of pure natural compounds from plant extracts or biotechnological products in preparative amounts is often very time consuming and accompanied by several laborious purification steps. In this sense, a typical separation process consists of several extraction steps followed by chromatographic steps. Very often, many of these steps can be replaced by a single LLC step. To obtain the required amount of the target component several repetitive LLC batch injections are performed. However, this is particularly laborious and not practical when the concentrations of the target compounds are very low in the starting extracts. Therefore, new strategies are needed to make such compounds available in preferably high purities.

In recent years, hops has gained increased attention as an interesting natural resource for a huge variety of bioactive substances, like for example xanthohumol. Analogues and especially minor compounds were emphasized to exceed the bioactivity of the related major ingredients such as xanthohumol. One of these promising bioactive minor hop compounds is

xanthohumol C, which is present in a raw hop extract in only very small amounts (0.2-2.2%). Hence, the second part of the thesis focuses on new strategies for obtaining such minor compounds from natural extracts in sufficient amounts for further analysis of their bioactive effects.

The first approach follows a capture and enrichment of xanthohumol C from a hop raw extract. In this context, a biphasic solvent system is selected where the minor component has a preferentially high partition coefficient. In addition, the partition coefficient should be higher than that of the main impurities. The phase that exhibits a higher affinity to the target compound is then used as the stationary phase. High injection volumes of several column volumes of extract are applied and the minor compound xanthohumol C is selectively retained in the stationary phase and enriched in the column, while major ingredients (impurities) like xanthohumol are depleted or completely removed at the same time. In the scope of a preliminary study (Section 3.5.1.) using parabens as model solutes and Arizona N (*n*-heptane/ethyl acetate/methanol/water 1/1/1/1 v/v/v/v) as the solvent system, a systematic methodology for the design of such capture and pre-purification process was established. A five-step model-based procedure for the process design and selection of operating parameters was developed, consisting of solvent system selection, selection of operating mode and conditions, determination of model parameters, model-based determination of injection volume and the duration of the capture and enrichment step, and finally the selection of an extrusion step mode. The elution-extrusion mode was recommended for the recovery of the product. In this sense, the process stability regarding the application of high injection volumes was evaluated by performing breakthrough curve experiments. The model was validated by comparison of experimental and simulated elution profiles. This confirms that basic methodologies from conventional LC are transferable to LLC under conditions of constant stationary phase retention. As a result, there is no need for laborious trial-and-error procedures, since the model-based approach is applicable in this case.

Using the example of a crude hop extract, this concept was transferred to a complex natural mixture (**Paper V**). The promising bioactive minor hop compound xanthohumol C could be enriched from a raw hop extract. The xanthohumol C-enriched extract obtained in the first step, could then be purified with a pulse injection to 95% pure xanthohumol C. Since the amount of natural xanthohumol C in the raw extract is very low, alternative purification and production strategies involving one-step semi-synthesis and LLC as sole purification technique were evaluated for the production of highly pure xanthohumol C at preparative scale. This alternative strategy provided a much higher yield of up to 70 mg xanthohumol C per gram raw extract and a purity >99% could be obtained. Furthermore, such an approach is much more convenient than multistep full-syntheses requiring laborious purification steps in between the single synthesis steps. It could be shown that LLC provides sufficient amounts of pure minor compounds for subsequent bioactivity studies. Furthermore, it was demonstrated that the application of LLC as a preparative separation method in combination with cell-culture and quantitative proteomics experiments is a powerful and fast approach for the evaluation of the bioactivity of minor compounds from natural resources (**Paper VI**).

5. Outlook

As part of a global trend towards a more bio-based economy, the demand for natural bioactive ingredients from natural and sustainable resources is increasing worldwide. Used as additives, these compounds can enhance and support the effect of diverse products, such as dietary supplements or functional foods, as well as pharmaceuticals, cosmetics, or health claim products. Natural sources such as plant extracts or biotechnological products are very complex mixtures containing a huge variety of minor components. This represents an enormous opportunity for new bioactive substances. At the same time, this makes the preparative isolation of highly pure compounds very difficult, because very selective separation methods are required. While conventional chromatographic methods could be employed here, they are expensive and often require extensive sample pre-processing. In contrast, a higher column loading is achievable in LLC due to the presence of a liquid stationary phase. In this sense, LLC has the potential to make a decisive contribution to the selective isolation of natural compounds from crude extracts at preparative and industrial-scale. One column can be used for several applications as the stationary phase can be easily prepared by simply mixing portions of preselected solvents. This eliminates time intensive column packing procedures and the costs of expensive solid resins used as stationary phase in LC. An even greater advantage of the individual stationary and mobile phase preparation is that highly selective tailor-made systems can be prepared for each application and target compound. However, this makes LLC a very complex and therefore not yet fully established standard separation technique.

So far, aqueous-organic biphasic solvent systems are mostly used in CCC and CPC. Especially for food applications and with regard to the general trend towards greener solvents, natural deep eutectic solvents (NADES), which could be prepared using cheap basic chemicals such as sugars, could become increasingly more important. However, this further increases the number of possible solvent combinations. Due to the increasing number of options, solvent system selection would become even more complex, thus requiring more precise model-based and predictive selection methods for users. In addition, this new solvent class has the potential to enable the development of a further variety of new and previously unknown DES-based two-phase systems. Furthermore, a broad testing of such systems regarding their applicability in various LLC column geometries, i.e. CCC and CPC, for corresponding applications might be necessary, due to their potentially different physical properties (density, viscosity, interfacial tension) compared to conventionally used systems. In addition, a better understanding of how external influencing parameters such as temperature fluctuations, changes in the solvent system compositions, and the presence of other solvents or contaminants (e.g. presence of water in actually non-aqueous systems) affect the robustness of LLC separations with a wide variety of biphasic solvent systems is necessary.

Especially for preparative and industrial-scale applications of LLC, efficient solvent recovery solutions will be required. So far, biphasic solvent systems are often freshly prepared before the separation and partly recovered from the product streams after the separation by distillation. At this stage, smarter and less energy intensive alternatives, e.g. membrane processes, preferably with complete recovery of the single solvents are needed in order to guarantee a sustainable and cheap process.

Finally, an efficient and rapid design of robust separation methods, easy transfer, and straightforward scale-up will decide, whether LLC will find its widespread acceptance as a

preparative separation technique for the exploitation of natural bioactive compounds. In the future, the integration of model-based biphasic solvent system selection methods and model-based process design could significantly help make LLC accessible to a broad user base. In this sense, a comprehensive toolbox could guide the user systematically through all steps of method development and optimization, as well as selection of suitable operating parameters. Extensive column characteristics of all common and commercially available CCC and CPC systems with a variety of biphasic solvent systems and model compounds could be incorporated and used as a basis for the model-based separation method design in LLC. Further implementation of models of various operating modes, such as different batch and (quasi-) continuous modes, would allow the user to design and customize the processes individually based on a restricted number of experiments.

6. List of other published manuscripts

Modular biomanufacturing for a sustainable production of terpenoid-based insect deterrents

W. Mischko, M. Hirte, **S. Roehrer**, H. Engelhardt, N. Mehlmer, M. Minceva, & T. Brück, (2018). Modular biomanufacturing for a sustainable production of terpenoid-based insect deterrents. *Green Chemistry*, 20(11), 2637-2650.

<https://doi.org/10.1039/C8GC00434J>

From microbial upcycling to biology-oriented synthesis: combining whole-cell production and chemo-enzymatic functionalization for sustainable taxanoid delivery

M. Hirte, W. Mischko, K. Kemper, **S. Röhrer**, C. Huber, M. Fuchs, W. Eisenreich, M. Minceva, & T.B. Brück (2018). From microbial upcycling to biology-oriented synthesis: combining whole-cell production and chemo-enzymatic functionalization for sustainable taxanoid delivery. *Green Chemistry*, 20(23), 5374-5384.

<https://doi.org/10.1039/C8GC03126F>

Ionic liquids as modifying agents for protein separation in centrifugal partition chromatography

F. Bezold, **S. Roehrer**, M. Minceva, (2019) Ionic Liquids as Modifying Agents for Protein Separation in Centrifugal Partition Chromatography, *Chemical Engineering & Technology*, 42, No. 2, 1-10.

<https://doi.org/10.1002/ceat.201800369>

7. Abbreviations and Symbols

Abbreviations

abbreviations	descriptions
Arizona	<i>n</i> -heptane/ethyl acetate/methanol/water
Asc	ascending mode
ATPS	aqueous two-phase system
BECCC	back-extrusion countercurrent chromatography
BP	butyl paraben
CCC	countercurrent chromatography
ChCl	choline chloride
COSMO-RS	conductor like screening model for realistic solvation
CPC	centrifugal partition chromatography
CPE	centrifugal partition extractor
DES	deep eutectic solvent
DM	dual mode
Dsc	descending mode
EECCC	elution-extrusion countercurrent chromatography
EP	ethyl paraben
F	flow rate
GC – MS	gas chromatography – mass spectrometry
GUESSmix	generally useful estimate of solvent systems
HBA	hydrogen-bond acceptor
HBD	hydrogen-bond donor
HEMWat	<i>n</i> -hexane/ethyl acetate/methanol/water
HPLC	high performance liquid chromatography
IL	ionic liquid
LA	levulinic acid
LC	liquid chromatography
LC – MS	liquid chromatography – mass spectrometry
LLC	liquid-liquid chromatography
LLE	liquid-liquid equilibrium
LP	lower phase
MCF-7	Michigan cancer foundation – 7 (human breast cancer cell line)
MDM	multiple dual mode

abbreviations	descriptions
MP	methyl paraben
NADES	natural deep eutectic solvent
NMR	nuclear magnetic resonance
NRTL	non-random-two-liquid
PC-SAFT	perturbed-chain statistical associating fluid theory
PEG	polyethylene glycol
PP	propyl paraben
ProMISE	probabilistic model for immiscible separations and extractions
PTFE	Polytetrafluoroethylene
ReSS ²	2-dimensional reciprocal shifted symmetry
rpm	revolutions per minute
sCPC	sequential centrifugal partition chromatography
SP	stationary phase
SUF	scale-up factor
TLC	thin layer chromatography
UNIFAC	universal quasichemical functional-group activity coefficients
UNIQUAC	universal quasichemical
UP	upper phase
UV	ultra violet
XN	xanthohumol
XNC	xanthohumol C

Symbols

symbols	descriptions
α	separation factor
a	activity
A	cross-sectional area
BP	butyl paraben
γ	activity coefficient
c	concentration
\overline{CS}	average cross section
Δ	difference
d	inner coil diameter
EP	ethyl paraben
F	Flow rate
F_{SU}	scale-up factor
f_i	fugacity of a phase
f_i^0	standard fugacity
h_{cell}	cell height
IC_{50}	inhibition concentration at 50% cell growth inhibition
K	distribution coefficient (based on molar fractions)
k_{Oa}	overall volumetric mass transfer coefficient
L	coil length
μ_i	chemical potential of compound i
μ_i^0	chemical potential at a reference state
μ_t	first moment of a peak
MP	methyl paraben
N	column efficiency (number of theoretical plates)
P	partition coefficient
PP	propyl paraben
p	pressure
R_S	separation resolution
σ	peak standard deviation
σ^2	second moment of a peak (peak variance)
S_F	stationary phase retention
T	temperature

symbols	descriptions
t	time
t_B	breakthrough time
t_R	retention time
u	average mobile phase velocity
V	volume
V_B	breakthrough volume
V_R	retention volume
v	molar volume
ω	angular velocity
w	peak width
x	molar fraction

Superscripts

symbols	descriptions
α	phase α
β	phase β
π	phase π
E	excess
LP	lower phase
MP	mobile phase
SP	stationary phase
UP	upper phase

Subscripts

symbols	descriptions
0	pure compound/ tracer
Asc	ascending mode
C	column
CCC	countercurrent chromatography
cell	cell
CPC	centrifugal partition chromatography
Dsc	descending mode
Feed	feed
i	compound i
inj	injection
j	compound j
k	cell/stage k
MP	mobile phase
O/W	octanol/water
paraben	paraben
plant	plant (setup)
R	retention
SP	stationary phase

8. List of Figures and Tables

Figure 1: Schematic presentation of a liquid-liquid chromatographic (LLC) setup.	15
Figure 2: Representation of the elution peaks of pulse injection experiments of a tracer and a solute, with and without column connected to the system (modified figure adapted from [28]).	18
Figure 3: Representation of a breakthrough curve and a corresponding pulse injection elution profile	20
Figure 4: Influence of stationary phase retention (SF) on the separation of a multicomponent mixture. Simulated chromatograms for SF between 0.1 and 0.9 in (a) as a function of the retention volume VR and (b) as a function of the partition coefficient P_i : VC = 180 ml, N = 400, $V_{inj} = 1$ ml, $c_{inj} = 1$ mg ml ⁻¹ , F = 12 ml min ⁻¹ , P1 – 8 = 0/0.4/0.8/1/1.3/1.6/2.5/5.....	22
Figure 5: Graphical representation of the dependence of RS on the characteristic parameters SF, N, and P. The resolution RS is shown (a) as a function of P_i at different SF from 0.1 to 0.9. (b) as a function of SF at different P_i from 0.25 to 4. (c) as a function of α at different SF from 0.1 to 0.9. (d) as a function of SF at different α from 1.1 to 5. (e) as a function of N at different SF from 0.1 to 0.9. (f) as a function of N at different α from 1.1 to 5.	23
Figure 6: Schematic representation of a type 1 ternary phase diagram including a miscibility gap at two different temperatures (adapted from [35]).	26
Figure 7: Schematic representation of the <i>sweet spot</i> range in LLC (adapted from [37]).	27
Figure 8: (a) Schematic solid-liquid equilibrium phase diagram for the binary eutectic mixture of choline chloride (ChCl) and levulinic acid (LA). Note: The given melting points of ChCl and LA are estimated melting points. ChCl decomposes before melting. (b) Illustration of the preparation of a binary DES in a crimped flask by mixing LA and ChCl in a molar ratio of 1:2 at room temperature (RT), followed by a heating to 80°C resulting in a clear and homogeneous liquid phase that stays liquid after cooling back to room temperature.	29
Figure 9: Design of a J-type CCC column (a) and illustrated mixing (black) and settling (white) zones inside the coil (b) [41].	32
Figure 10: Schematic illustration of (a) the design of a conventional CPC column with one axis of rotation consisting of several stacked disks and sealing plates in between, (b) an annular disk with cells interconnected by ducts, and (c) an annular plate for sealing (adapted from [86]).	33
Figure 11: Three different flow regimes in CPC cells, namely (a) stuck film, (b) oscillating sheet, and (c) atomization, with white representing the stationary phase, grey representing the two phases in contact, and black representing the mobile phase in descending mode (adapted from [112]).	37
Figure 12: Visualization of the flow regime in different CPC cell designs with black representing the mobile phase and white representing the stationary phase in a (a) modified FCPC cell, (b) Twin-Cell 1, (c) Twin-Cell 2, (d) tailor-made TU-Dortmund cell (adapted from [98]).	38
Figure 13: Schematic illustration of three stacked injections with a complete separation between the compounds (adapted from [28]).	39

Figure 14: Schematic illustration of the dual mode separation in LLC here starting in descending mode and switching to ascending mode with light grey representing the upper phase and dark grey representing the lower phase of the biphasic solvent system (adapted from [9]).....	40
Figure 15: Schematic illustration of (a) the back-extrusion mode and (b) the elution-extrusion mode in LLC indicating the different steps and pumping directions of mobile phase (MP) and stationary phase (SP) (adapted from BECCC [132] und EECCC [137, 138]). (Note: The split of the phases before the extrusion in back-extrusion mode (*) has only be reported for CCC columns.).....	42
Figure 16: Schematic illustration of the cell model with Ni ideally mixed cells (adapted from [150]).....	46
Figure 17: Illustration of the “free-space between the peak” method for scaling-up a sample load maximized separation method to another column of different size and design (adapted from [171]).....	50
Figure 18: Schematic illustration of the process design workflow of a process for the capture and enrichment of minor compounds from complex mixtures using a LLC column.	105
Figure 19: Breakthrough curves of methyl paraben (MP) and butyl paraben (BP) performed on a CPC column in descending mode including UV/Vis signals at 255 nm (UV/Vis signal), experimental elution profiles from HPLC offline analysis (exp.) with corresponding simulation (sim.) using the cell model: descending mode (a) MP (PMP = 0.982, NMP = 797) and (b) BP (PBP = 3.366, NBP = 347) with operating parameters: Arizona N, 1700 rpm, VC = 246.65 ml, SF = 0.5, F = 18 ml min ⁻¹ , t _{inj} = 15 min (V _{inj} = 270 ml);.....	107
Figure 20: Breakthrough curve of methyl paraben (MP) and butyl paraben (BP) performed on a CPC column in descending mode including UV/Vis signal at 255 nm (UV/Vis signal), experimental elution profile from HPLC offline analysis (exp.) with corresponding simulation (sim.) using the cell model, respectively. Operating parameters: descending mode with MP (PMP = 0.982, NMP = 797, cMP = 0.2 mg ml ⁻¹) and BP (PBP = 3.366, NBP = 347, cBP = 0.2 mg ml ⁻¹), Arizona N, 1700 rpm, VC = 246.65 ml, SF = 0.5, F = 18 ml min ⁻¹ , t _{inj} = 40 min (V _{inj} = 720 ml);.....	108
Figure 21: Separation of methyl paraben (MP) and butyl paraben (BP) in back-extrusion mode with a CPC column feed load of V _{inj} = 216 ml (t _{inj} = 12 min) and a switching point (t _{switch}) after 26.8 min, including UV/Vis signal at 255 nm (UV/Vis signal), experimental elution profiles from HPLC offline analysis (exp.), and the corresponding simulated elution profile (sim.) of MP (PMP = 0.982, NMP = 797) using the cell model. Operating parameters: elution mode in descending mode, Arizona N, 1700 rpm, VC = 246.65 ml, SF = 0.5, F = 18 ml min ⁻¹ , c _{Feed} = cMP = cBP = 0.2 mg ml ⁻¹	109
Figure 22: Separation of methyl paraben (MP) and butyl paraben (BP) in elution-extrusion mode with a CPC column feed load of V _{inj} = 216 ml (t _{inj} = 12 min) and a switching point (t _{switch}) after 26.8 min, including UV/Vis signal at 255 nm (UV/Vis signal), experimental elution profiles from HPLC offline analysis (exp.), and the corresponding simulated elution profile (sim.) of MP (PMP = 0.982, NMP = 797) using the cell model. Operating parameters: elution mode in descending mode, Arizona N, 1700 rpm, VC = 246.65 ml, SF = 0.5, F = 18 ml min ⁻¹ , c _{Feed} = cMP = cBP = 0.2 mg ml ⁻¹	110

Table 1: Difference between conventional liquid chromatography (LC), e.g. HPLC, and solid support-free liquid-liquid chromatography (LLC) (partly adapted from [9, 27]).16

Table 2: Overview of different column and cell geometries of available CPC column designs.
.....35

9. References

- [1] Y. Ito, M. Weinstein, I. Aoki, R. Harada, E. Kimura, K. Nunogaki, The Coil Planet Centrifuge, *Nature*, 212 (1966) 985-987.
- [2] Y. Ito, R.L. Bowman, Countercurrent chromatography: Liquid-liquid partition chromatography without solid support, *Science*, 167 (1970) 281-283.
- [3] A. Hazekamp, R. Simons, A. Peltenburg-Looman, M. Sengers, R. van Zweden, R. Verpoorte, Preparative isolation of cannabinoids from *Cannabis sativa* by centrifugal partition chromatography, *Journal of Liquid Chromatography & Related Technologies*, 27 (2004) 2421-2439.
- [4] C.L. Ramirez, M.A. Fanovich, M.S. Churio, Cannabinoids: Extraction Methods, Analysis, and Physicochemical Characterization, *Studies in Natural Products Chemistry* 61 (2018) 143-173.
- [5] A. Rutz, U.S. Patent Application No. 15/552,331., (2018).
- [6] K. Skalicka-Woźniak, I. Garrard, A comprehensive classification of solvent systems used for natural product purifications in countercurrent and centrifugal partition chromatography, *Natural Product Reports*, 32 (2015) 1556-1561.
- [7] M. Bojczuk, D. Żyżelewicz, P. Hodurek, Centrifugal partition chromatography—A review of recent applications and some classic references, *Journal of Separation Science*, 40 (2017) 1597-1609.
- [8] Y. Ito, Origin and Evolution of the Coil Planet Centrifuge: A Personal Reflection of My 40 Years of CCC Research and Development, *Separation & Purification Reviews*, 34 (2005) 131-154.
- [9] A. Berthod, *Countercurrent chromatography*, Elsevier, 2002.
- [10] L. Lorantfy, L. Németh, Z. Kobács, D. Rutterschmidt, Z. Misek, G. Rajsch, Development of industrial scale Centrifugal Partition Chromatography, *Planta Medica*, 81 (2015) 1532-1532.
- [11] A. Foucault, J. Legrand, L. Marchal, C. Elie, P. Agaise, US Patent 2010/0252503 A1, (2010).
- [12] F. Couillard, US Patent 2010/0200488 A1, (2010).
- [13] J. Olšovská, V. Boštíková, M. Dušek, V. Jandovská, K. Bogdanová, P. Čermák, P. Boštík, A. Mikyska, M. Kolář, *Humulus Lupulus L. (Hops) - a Valuable Source of Compounds with Bioactive Effects for Future Therapies*, *Military Medical Science Letters*, 85 (2016) 19-30.
- [14] M. Liu, P. Hansen, G. Wang, L. Qiu, J. Dong, H. Yin, Z. Qian, M. Yang, J. Miao, Pharmacological Profile of Xanthohumol, a Prenylated Flavonoid from Hops (*Humulus lupulus*), *Molecules*, 20 (2015) 754.
- [15] C. Gerhäuser, Broad spectrum anti-infective potential of xanthohumol from hop (*Humulus lupulus L.*) in comparison with activities of other hop constituents and xanthohumol metabolites, *Molecular Nutrition & Food Research*, 49 (2005) 827-831.
- [16] S. Malik, *Biotechnology and Production of Anti-Cancer Compounds*, Springer International Publishing, 2017.
- [17] P. Zanolli, M. Zavatti, Pharmacognostic and pharmacological profile of *Humulus lupulus L.*, *Journal of Ethnopharmacology*, 116 (2008) 383-396.
- [18] M. Forino, S. Pace, G. Chianese, L. Santagostini, M. Werner, C. Weinigel, S. Rummler, G. Fico, O. Werz, O. Tagliatalata-Scafati, Humudifucol and bioactive prenylated polyphenols from hops (*Humulus lupulus* cv. "Cascade"), *Journal of Natural Products*, 79 (2016) 590-597.

- [19] D. Nikolic, R. B Van Breemen, Analytical methods for quantitation of prenylated flavonoids from hops, *Current Analytical Chemistry*, 9 (2013) 71-85.
- [20] C. Miranda, J. Stevens, A. Helmrich, M. Henderson, R. Rodriguez, Y.-H. Yang, M. Deinzer, D. Barnes, D. Buhler, Antiproliferative and cytotoxic effects of prenylated flavonoids from hops (*Humulus lupulus*) in human cancer cell lines, *Food and Chemical Toxicology*, 37 (1999) 271-285.
- [21] E. Oberbauer, C. Urmann, C. Steffenhagen, L. Bieler, D. Brunner, T. Furtner, C. Humpel, B. Bäumer, C. Bandtlow, S. Couillard-Despres, Chroman-like cyclic prenylflavonoids promote neuronal differentiation and neurite outgrowth and are neuroprotective, *Journal of Nutritional Biochemistry*, 24 (2013) 1953-1962.
- [22] S. Vogel, J.r. Heilmann, Synthesis, cytotoxicity, and antioxidative activity of minor prenylated chalcones from *Humulus lupulus*, *Journal of Natural Products*, 71 (2008) 1237-1241.
- [23] S. Vogel, Synthese prenylierter Chalkone aus Hopfen und Bestimmung ihrer cytotoxischen und antioxidativen Aktivität, in: University of Regensburg, Germany, 2008.
- [24] A.P. Foucault, *Centrifugal partition chromatography*, M. Dekker, 1995.
- [25] Y. Ito, High-speed countercurrent chromatography, *Nature*, 326 (1987) 419-420.
- [26] A. Berthod, K. Faure, Separations with a Liquid Stationary Phase: Countercurrent Chromatography or Centrifugal Partition Chromatography, in: *Analytical Separation Science*, 2015.
- [27] I.A. Sutherland, Recent progress on the industrial scale-up of counter-current chromatography, *Journal of Chromatography A*, 1151 (2007) 6-13.
- [28] H. Schmidt-Traub, M. Schulte, A. Seidel-Morgenstern, *Preparative Chromatography*, Second Edition, John Wiley & Sons, 2012.
- [29] J. Ashley, C.N. Reilly, De-tailing and sharpening of response peaks in gas chromatography, *Analytical Chemistry*, 37 (1965) 626-630.
- [30] K. Bielicka-Daszkiwicz, A. Voelkel, Theoretical and experimental methods of determination of the breakthrough volume of SPE sorbents, *Talanta*, 80 (2009) 614-621.
- [31] L. Marchal, J. Legrand, A. Foucault, Mass transport and flow regimes in centrifugal partition chromatography, *AIChE Journal*, 48 (2002) 1692-1704.
- [32] J.M. Prausnitz, R.N. Lichtenthaler, E.G. de Azevedo, *Molecular thermodynamics of fluid-phase equilibria*, Pearson Education, 1998.
- [33] J. Gmehling, B. Kolbe, M. Kleiber, J. Rarey, *Chemical thermodynamics for process simulation*, John Wiley & Sons, 2012.
- [34] D.-B. Ren, Z.-H. Yang, Y.-Z. Liang, Q. Ding, C. Chen, M.-L. Ouyang, Correlation and prediction of partition coefficient using nonrandom two-liquid segment activity coefficient model for solvent system selection in counter-current chromatography separation, *Journal of Chromatography A*, 1301 (2013) 10-18.
- [35] C.H. Schwienheer, *Advances in Centrifugal Purification Techniques for Separating (bio-) Chemical Compounds*, Verlag Dr. Hut, 2016.
- [36] A. Foucault, L. Chevolot, Counter-current chromatography: instrumentation, solvent selection and some recent applications to natural product purification, *Journal of Chromatography A*, 808 (1998) 3-22.
- [37] J. Brent Friesen, G.F. Pauli, GUESS—A generally useful estimate of solvent systems for CCC, *Journal of Liquid Chromatography & Related Technologies*, 28 (2005) 2777-2806.

- [38] F. Oka, H. Oka, Y. Ito, Systematic search for suitable two-phase solvent systems for high-speed counter-current chromatography, *Journal of Chromatography A*, 538 (1991) 99-108.
- [39] I.J. Garrard, L. Janaway, D. Fisher, Minimising Solvent Usage in High Speed, High Loading, and High Resolution Isocratic Dynamic Extraction AU, *Journal of Liquid Chromatography & Related Technologies*, 30 (2007) 151-163.
- [40] J.B. Friesen, G.F. Pauli, Rational development of solvent system families in counter-current chromatography, *Journal of Chromatography A*, 1151 (2007) 51-59.
- [41] Y. Ito, Golden rules and pitfalls in selecting optimum conditions for high-speed counter-current chromatography, *Journal of Chromatography A*, 1065 (2005) 145-168.
- [42] J.B. Friesen, J.B. McAlpine, S.-N. Chen, G.F. Pauli, Countercurrent separation of natural products: an update, *Journal of Natural Products*, 78 (2015) 1765-1796.
- [43] G.F. Pauli, S.M. Pro, J.B. Friesen, Countercurrent separation of natural products, *Journal of Natural Products*, 71 (2008) 1489-1508.
- [44] Y. Ito, M. Knight, T.M. Finn, Spiral countercurrent chromatography, *Journal of Chromatographic Science*, 51 (2013) 726-738.
- [45] F. Bezold, J. Goll, M. Minceva, Study of the applicability of non-conventional aqueous two-phase systems in counter-current and centrifugal partition chromatography, *Journal of Chromatography A*, 1388 (2015) 126-132.
- [46] F. Bouiche, Amélioration instrumentale de la chromatographie de partage centrifuge en vue de la purification de molécules très polaires, in, Université de Lyon, 2018.
- [47] J. Goll, G. Audo, M. Minceva, Comparison of twin-cell centrifugal partition chromatographic columns with different cell volume, *Journal of Chromatography A*, 1406 (2015) 129-135.
- [48] I.A. Sutherland, D. Heywood-Waddington, Y. Ito, Counter-current chromatography: Applications to the separation of biopolymers, organelles and cells using either aqueous—organic or aqueous—aqueous phase systems, *Journal of Chromatography A*, 384 (1987) 197-207.
- [49] I.A. Sutherland, Review of centrifugal liquid-liquid chromatography using aqueous two-phase solvent (ATPS) systems: its scale-up and prospects for the future production of high-value biologics, *BioMed Central*, (2007).
- [50] A. Frey, Systematic Selection and Tailoring of Biphasic Solvent Systems in Liquid-liquid Chromatography, in: University of Erlangen-Nuremberg, 2017.
- [51] W. Zhang, Y. Hu, Y. Wang, J. Han, L. Ni, Y. Wu, Liquid–liquid equilibrium of aqueous two-phase systems containing poly(ethylene glycol) of different molecular weights and several ammonium salts at 298.15K, *Thermochimica Acta*, 560 (2013) 47-54.
- [52] J.G. Huddleston, H.D. Willauer, R.P. Swatoski, A.E. Visser, R.D. Rogers, Room temperature ionic liquids as novel media for 'clean'liquid–liquid extraction, *Chemical Communications*, (1998) 1765-1766.
- [53] S. Shahriari, C.M. Neves, M.G. Freire, J.o.A. Coutinho, Role of the Hofmeister series in the formation of ionic-liquid-based aqueous biphasic systems, *The Journal of Physical Chemistry B*, 116 (2012) 7252-7258.
- [54] S.n.P. Ventura, S.G. Sousa, L.S. Serafim, A.I.S. Lima, M.G. Freire, J.o.A. Coutinho, Ionic-liquid-based aqueous biphasic systems with controlled pH: the ionic liquid anion effect, *Journal of Chemical & Engineering Data*, 57 (2012) 507-512.

- [55] S.P. Ventura, C.M. Neves, M.G. Freire, I.M. Marrucho, J. Oliveira, J.A. Coutinho, Evaluation of anion influence on the formation and extraction capacity of ionic-liquid-based aqueous biphasic systems, *The Journal of Physical Chemistry B*, 113 (2009) 9304-9310.
- [56] S.P. Ventura, S.G. Sousa, L.S. Serafim, Á.S. Lima, M.G. Freire, J.A. Coutinho, Ionic liquid based aqueous biphasic systems with controlled pH: the ionic liquid cation effect, *Journal of Chemical & Engineering Data*, 56 (2011) 4253-4260.
- [57] H. Zhao, S.M. Campbell, L. Jackson, Z. Song, O. Olubajo, Hofmeister series of ionic liquids: kosmotropic effect of ionic liquids on the enzymatic hydrolysis of enantiomeric phenylalanine methyl ester, *Tetrahedron: Asymmetry*, 17 (2006) 377-383.
- [58] A.P. Abbott, G. Capper, D.L. Davies, R.K. Rasheed, V. Tambyrajah, Novel solvent properties of choline chloride/urea mixtures, *Chemical Communications*, (2003) 70-71.
- [59] Q. Zhang, K. De Oliveira Vigier, S. Royer, F. Jérôme, Deep eutectic solvents: syntheses, properties and applications, *Chem. Soc. Rev.*, 41 (2012) 7108-7146.
- [60] Z. Maugeri, P. Domínguez de María, Novel choline-chloride-based deep-eutectic-solvents with renewable hydrogen bond donors: levulinic acid and sugar-based polyols, *RSC Advances*, 2 (2012) 421-425.
- [61] B. Tang, K.H. Row, Recent developments in deep eutectic solvents in chemical sciences, *Monatshefte für Chemie - Chemical Monthly*, 144 (2013) 1427-1454.
- [62] E.L. Smith, A.P. Abbott, K.S. Ryder, Deep Eutectic Solvents (DESs) and Their Applications, *Chemical Reviews*, 114 (2014) 11060-11082.
- [63] B. Tang, H. Zhang, K.H. Row, Application of deep eutectic solvents in the extraction and separation of target compounds from various samples, *Journal of Separation Science*, 38 (2015) 1053-1064.
- [64] Y. Dai, J. van Spronsen, G.-J. Witkamp, R. Verpoorte, Y.H. Choi, Ionic Liquids and Deep Eutectic Solvents in Natural Products Research: Mixtures of Solids as Extraction Solvents, *Journal of Natural Products*, 76 (2013) 2162-2173.
- [65] M. Francisco, A. van den Bruinhorst, M.C. Kroon, New natural and renewable low transition temperature mixtures (LTTMs): screening as solvents for lignocellulosic biomass processing, *Green Chemistry*, 14 (2012) 2153-2157.
- [66] M. Francisco, A. van den Bruinhorst, M.C. Kroon, Low-Transition-Temperature Mixtures (LTTMs): A New Generation of Designer Solvents, *Angewandte Chemie International Edition*, 52 (2013) 3074-3085.
- [67] A.P. Abbott, D. Boothby, G. Capper, D.L. Davies, R.K. Rasheed, Deep Eutectic Solvents Formed between Choline Chloride and Carboxylic Acids: Versatile Alternatives to Ionic Liquids, *Journal of the American Chemical Society*, 126 (2004) 9142-9147.
- [68] R.C. Harris, *Physical Properties of Alcohol Based Deep Eutectic Solvents*, in, University of Leicester, 2009.
- [69] M.A. Kareem, F.S. Mjalli, M.A. Hashim, I.M. AlNashef, Phosphonium-Based Ionic Liquids Analogues and Their Physical Properties, *Journal of Chemical & Engineering Data*, 55 (2010) 4632-4637.
- [70] A. Yadav, S. Trivedi, R. Rai, S. Pandey, Densities and dynamic viscosities of (choline chloride+glycerol) deep eutectic solvent and its aqueous mixtures in the temperature range (283.15–363.15)K, *Fluid Phase Equilibria*, 367 (2014) 135-142.
- [71] A. Pandey, R. Rai, M. Pal, S. Pandey, How polar are choline chloride-based deep eutectic solvents?, *PCCP*, 16 (2014) 1559-1568.

- [72] M.A. Kareem, F.S. Mjalli, M.A. Hashim, I.M. AlNashef, Liquid–liquid equilibria for the ternary system (phosphonium based deep eutectic solvent–benzene–hexane) at different temperatures: A new solvent introduced, *Fluid Phase Equilibria*, 314 (2012) 52-59.
- [73] F.S. Oliveira, A.B. Pereiro, L.P.N. Rebelo, I.M. Marrucho, Deep eutectic solvents as extraction media for azeotropic mixtures, *Green Chemistry*, 15 (2013) 1326-1330.
- [74] A.S.B. Gonzalez, M. Francisco, G. Jimeno, S.L.G. de Dios, M.C. Kroon, Liquid–liquid equilibrium data for the systems {LTTM+benzene+hexane} and {LTTM+ethyl acetate+hexane} at different temperatures and atmospheric pressure, *Fluid Phase Equilibria*, 360 (2013) 54-62.
- [75] F. Bezold, M. Minceva, A water-free solvent system containing an L-menthol-based deep eutectic solvent for centrifugal partition chromatography applications, *Journal of Chromatography A*, 1587 (2019) 166-171.
- [76] F. Bezold, M. Minceva, Liquid-liquid equilibria of n-heptane, methanol and deep eutectic solvents composed of carboxylic acid and monocyclic terpenes, *Fluid Phase Equilibria*, 477 (2018) 98-106.
- [77] Y. Liu, J.B. Friesen, J.B. McAlpine, D.C. Lankin, S.-N. Chen, G.F. Pauli, Natural deep eutectic solvents: Properties, applications, and perspectives, *Journal of Natural Products*, 81 (2018) 679-690.
- [78] W. Bi, M. Tian, K.H. Row, Evaluation of alcohol-based deep eutectic solvent in extraction and determination of flavonoids with response surface methodology optimization, *Journal of Chromatography A*, 1285 (2013) 22-30.
- [79] M.W. Nam, J. Zhao, M.S. Lee, J.H. Jeong, J. Lee, Enhanced extraction of bioactive natural products using tailor-made deep eutectic solvents: application to flavonoid extraction from *Flos sophorae*, *Green Chemistry*, 17 (2015) 1718-1727.
- [80] A. Paiva, R. Craveiro, I. Aroso, M. Martins, R.L. Reis, A.R.C. Duarte, Natural Deep Eutectic Solvents – Solvents for the 21st Century, *ACS Sustainable Chemistry & Engineering*, 2 (2014) 1063-1071.
- [81] J.B. Friesen, S. Ahmed, G.F. Pauli, Qualitative and quantitative evaluation of solvent systems for countercurrent separation, *Journal of Chromatography A*, 1377 (2015) 55-63.
- [82] E. Hopmann, W. Arlt, M. Minceva, Solvent system selection in counter-current chromatography using conductor-like screening model for real solvents, *Journal of Chromatography A*, 1218 (2011) 242-250.
- [83] E. Hopmann, A. Frey, M. Minceva, A priori selection of the mobile and stationary phase in centrifugal partition chromatography and counter-current chromatography, *Journal of Chromatography A*, 1238 (2012) 68-76.
- [84] A. Frey, E. Hopmann, M. Minceva, Selection of Biphasic Liquid Systems in Liquid-Liquid Chromatography Using Predictive Thermodynamic Models, *Chemical Engineering & Technology*, 37 (2014) 1663-1674.
- [85] E.A. Hopmann, *Development of a centrifugal partition chromatographic separation: from molecule to process*, Verlag Dr. Hut, 2013.
- [86] M. Minceva, *Model-based design of preparative liquid-chromatography processes*, in, University of Erlangen-Nuremberg, 2013.
- [87] A. Klamt, Conductor-like screening model for real solvents: a new approach to the quantitative calculation of solvation phenomena, *The Journal of Physical Chemistry*, 99 (1995) 2224-2235.
- [88] A. Fredenslund, J. Gmehling, P. Rasmussen, *Vapor-liquid Equilibria Using UNIFAC: A Group-contribution Methods*, Elsevier Scientific, 1977.

- [89] A. Fredenslund, R.L. Jones, J.M. Prausnitz, Group-contribution estimation of activity coefficients in nonideal liquid mixtures, *AIChE Journal*, 21 (1975) 1086-1099.
- [90] H.K. Hansen, P. Rasmussen, A. Fredenslund, M. Schiller, J. Gmehling, Vapor-liquid equilibria by UNIFAC group contribution. 5. Revision and extension, *Industrial & Engineering Chemistry Research*, 30 (1991) 2352-2355.
- [91] A. Fredenslund, Vapor-liquid equilibria using UNIFAC: a group-contribution method, Elsevier, 2012.
- [92] H. Renon, J.M. Prausnitz, Local compositions in thermodynamic excess functions for liquid mixtures, *AIChE journal*, 14 (1968) 135-144.
- [93] D.S. Abrams, J.M. Prausnitz, Statistical thermodynamics of liquid mixtures: a new expression for the excess Gibbs energy of partly or completely miscible systems, *AIChE Journal*, 21 (1975) 116-128.
- [94] J. Gross, G. Sadowski, Perturbed-chain SAFT: An equation of state based on a perturbation theory for chain molecules, *Industrial & Engineering Chemistry Research*, 40 (2001) 1244-1260.
- [95] I.J. Garrard, Simple approach to the development of a CCC solvent selection protocol suitable for automation, *Journal of Liquid Chromatography & Related Technologies*, 28 (2005) 1923-1935.
- [96] A. Peng, P. Hewitson, I. Sutherland, L. Chen, S. Ignatova, How changes in column geometry and packing ratio can increase sample load and throughput by a factor of fifty in Counter-Current Chromatography, *Journal of Chromatography A*, 1580 (2018) 120-125.
- [97] M. Englert, W. Vetter, Tubing modifications for countercurrent chromatography (CCC): Stationary phase retention and separation efficiency, *Analytica Chimica Acta*, 884 (2015) 114-123.
- [98] C. Schwienheer, J. Merz, G. Schembecker, Investigation, comparison and design of chambers used in centrifugal partition chromatography on the basis of flow pattern and separation experiments, *Journal of Chromatography A*, 1390 (2015) 39-49.
- [99] W. Murayama, T. Kobayashi, Y. Kosuge, H. Yano, Y. Nunogaki, K. Nunogaki, A new centrifugal counter-current chromatograph and its application, *Journal of Chromatography A*, 239 (1982) 643-649.
- [100] Y. Nunogaki, *Centrifugal Counter-Current Distribution Chromatography*, in: S.E. Ltd. (Ed.), 1989.
- [101] F. de La Poype, R. de La Poype, P. Durand, A. Foucault, J. Legrand, G. Patissier, J.M. Rosant, US Patent 2003/6537452 B1, (2003).
- [102] A. Foucault, J. Legrand, L. Marchal, D. Durand, US Patent 2008/0035546 A1, (2008).
- [103] A. Foucault, J. Legrand, L. Marchal, C. Agaise, US 2013/0005556 A1, (2013).
- [104] F. Couillard, WO 2009/066014 A1, (2009).
- [105] L. Lórántfy, L. Németh, WO Patent 2016/055821 A1, (2016).
- [106] L. Lorantfy, L. Németh, WO 2017/037489 A1, (2017).
- [107] Y. Ito, F. Yang, Spiral disk assembly: An improved column design for high-speed countercurrent chromatography (HSCCC), *Encyclopedia of Chromatography 2004 Update Supplement*, 432 (2004) 274.
- [108] P.L. Wood, D. Hawes, L. Janaway, I.A. Sutherland, Stationary phase retention in CCC: modelling the J-type centrifuge as a constant pressure drop pump, *Journal of Liquid Chromatography & Related Technologies*, 26 (2003) 1373-1396.

- [109] P.L. Wood, The hydrodynamics of countercurrent chromatography in J-type centrifuges, in, Brunel University, 2002.
- [110] A. Peng, P. Hewitson, I. Sutherland, L. Chen, S. Ignatova, The effect of increasing centrifugal acceleration/force and flow rate for varying column aspect ratios on separation efficiency in Counter-Current Chromatography, *Journal of Chromatography A*, 1581-1582 (2018) 80-90.
- [111] M. Van Buel, F. Van Halsema, L. Van der Wielen, K. Luyben, Flow regimes in centrifugal partition chromatography, *AIChE Journal*, 44 (1998) 1356-1362.
- [112] S. Adelman, G. Schembecker, Influence of physical properties and operating parameters on hydrodynamics in Centrifugal Partition Chromatography, *Journal of Chromatography A*, 1218 (2011) 5401-5413.
- [113] S. Adelman, C. Schwienheer, G. Schembecker, Multiphase flow modeling in centrifugal partition chromatography, *Journal of Chromatography A*, 1218 (2011) 6092-6101.
- [114] F. Couillard, A. Foucault, A. Durand, WO 2005/011835, (2005).
- [115] A. Peng, H. Ye, J. Shi, S. He, S. Zhong, S. Li, L. Chen, Separation of honokiol and magnolol by intermittent counter-current extraction, *Journal of Chromatography A*, 1217 (2010) 5935-5939.
- [116] E. Hopmann, J. Goll, M. Minceva, Sequential centrifugal partition chromatography: a new continuous chromatographic technology, *Chemical Engineering & Technology*, 35 (2012) 72-82.
- [117] E. Hopmann, M. Minceva, Separation of a binary mixture by sequential centrifugal partition chromatography, *Journal of Chromatography A*, 1229 (2012) 140-147.
- [118] J. Goll, A. Frey, M. Minceva, Study of the separation limits of continuous solid support free liquid-liquid chromatography: Separation of capsaicin and dihydrocapsaicin by centrifugal partition chromatography, *Journal of Chromatography A*, 1284 (2013) 59-68.
- [119] N. Mekaoui, J. Chamieh, V. Dugas, C. Demesmay, A. Berthod, Purification of Coomassie Brilliant Blue G-250 by multiple dual mode countercurrent chromatography, *Journal of Chromatography A*, 1232 (2012) 134-141.
- [120] I. Sutherland, P. Hewitson, S. Ignatova, Scale-up of counter-current chromatography: demonstration of predictable isocratic and quasi-continuous operating modes from the test tube to pilot/process scale, *Journal of Chromatography A*, 1216 (2009) 8787-8792.
- [121] S. Ignatova, P. Hewitson, B. Mathews, I. Sutherland, Evaluation of dual flow counter-current chromatography and intermittent counter-current extraction, *Journal of Chromatography A*, 1218 (2011) 6102-6106.
- [122] P. Hewitson, S. Ignatova, Great Britain Patent. WO2010010366 A1, (2010).
- [123] J. Goll, M. Minceva, Continuous fractionation of multicomponent mixtures with sequential centrifugal partition chromatography, *AIChE Journal*, 63 (2017) 1659-1673.
- [124] J. Goll, R. Morley, M. Minceva, Trapping multiple dual mode centrifugal partition chromatography for the separation of intermediately-eluting components: Operating parameter selection, *Journal of Chromatography A*, 1496 (2017) 68-79.
- [125] R. Morley, M. Minceva, Trapping multiple dual mode centrifugal partition chromatography for the separation of intermediately-eluting components: Throughput maximization strategy, *Journal of Chromatography A*, 1501 (2017) 26-38.
- [126] P. Hewitson, S. Ignatova, H. Ye, L. Chen, I. Sutherland, Intermittent counter-current extraction as an alternative approach to purification of Chinese herbal medicine, *Journal of Chromatography A*, 1216 (2009) 4187-4192.

- [127] Y. Lee, Dual counter-current chromatography—its applications in natural products research, *Journal of Chromatography A*, 538 (1991) 37-44.
- [128] N. Mekaoui, A. Berthod, Using the liquid nature of the stationary phase. VI. Theoretical study of multi-dual mode countercurrent chromatography, *Journal of Chromatography A*, 1218 (2011) 6061-6071.
- [129] E. Delannay, A. Toribio, L. Boudesocque, J.-M. Nuzillard, M. Zeches-Hanrot, E. Dardennes, G. Le Dour, J. Sapi, J.-H. Renault, Multiple dual-mode centrifugal partition chromatography, a semi-continuous development mode for routine laboratory-scale purifications, *Journal of Chromatography A*, 1127 (2006) 45-51.
- [130] R. Morley, M. Minceva, Operating mode selection for the separation of intermediately-eluting components with countercurrent and centrifugal partition chromatography, *Journal of Chromatography A*, (2019).
- [131] A. Berthod, T. Maryutina, B. Spivakov, O. Shpigun, I.A. Sutherland, Countercurrent chromatography in analytical chemistry (IUPAC Technical Report), *Pure and Applied Chemistry*, 81 (2009) 355-387.
- [132] M. Agnely, D. Thiebaut, Dual-mode high-speed counter-current chromatography: retention, resolution and examples, *Journal of Chromatography A*, 790 (1997) 17-30.
- [133] J.-S. Jeon, C.Y. Kim, Preparative separation and purification of flavonoids and stilbenoids from *Parthenocissus tricuspidata* stems by dual-mode centrifugal partition chromatography, *Separation and Purification Technology*, 105 (2013) 1-7.
- [134] H.-B. Li, F. Chen, Separation and purification of epimedin A, B, C, and icariin from the medicinal herb *Epimedium brevicornum* maxim by dual-mode HSCCC, *Journal of Chromatographic Science*, 47 (2009) 337-340.
- [135] Y. Lu, Y. Pan, A. Berthod, Using the liquid nature of the stationary phase in counter-current chromatography: V. The back-extrusion method, *Journal of Chromatography A*, 1189 (2008) 10-18.
- [136] R.A. Menges, T.S. Menges, G.L. Bertrand, D.W. Armstrong, L.A. Spino, Extraction of nonionic surfactants from waste water using centrifugal partition chromatography, *Journal of Liquid Chromatography*, 15 (1992) 2909-2925.
- [137] A. Berthod, M.J. Ruiz-Angel, S. Carda-Broch, Elution– extrusion countercurrent chromatography. Use of the liquid nature of the stationary phase to extend the hydrophobicity window, *Analytical Chemistry*, 75 (2003) 5886-5894.
- [138] A. Berthod, J.B. Friesen, T. Inui, G.F. Pauli, Elution–Extrusion Countercurrent Chromatography: Theory and Concepts in Metabolic Analysis, *Analytical Chemistry*, 79 (2007) 3371-3382.
- [139] G. Guiochon, A. Felinger, D.G. Shirazi, A.M. Katti, *Fundamentals of preparative and nonlinear chromatography*, Elsevier, 2006.
- [140] R.-M. Nicoud, *Chromatographic Processes*, Cambridge University Press, 2015.
- [141] A. Seidel-Morgenstern, *Mathematische Modellierung der präparativen Flüssigchromatographie*, Deutscher Universitätsverlag, 1995.
- [142] G. Guiochon, B. Lin, *Modeling for preparative chromatography*, Academic press, 2003.
- [143] J. Giddings, *Dynamics of Chromatography*, M. Dekker, New York, 1965.
- [144] E. Kučera, Contribution to the theory of chromatography: Linear non-equilibrium elution chromatography, *Journal of Chromatography A*, 19 (1965) 237-248.

- [145] M. Kubin, Beitrag zur theorie der chromatographie II. Einfluss der diffusion ausserhalb und der adsorption innerhalb des sorbens-korns, Collection of Czechoslovak Chemical Communications, 30 (1965) 2900-2907.
- [146] A. Martin, R.M. Synge, A new form of chromatogram employing two liquid phases: A theory of chromatography. 2. Application to the micro-determination of the higher monoamino-acids in proteins, Biochemical Journal, 35 (1941) 1358.
- [147] L.C. Craig, Identification of small amounts of organic compounds by distribution studies II. Separation by counter-current distribution, Journal of Biological Chemistry, 155 (1944) 519-534.
- [148] A. Klinkenberg, F. Sjenitzer, Holding-time distributions of the Gaussian type, Chemical Engineering Science, 5 (1956) 258-270.
- [149] F. Wang, Y. Ito, Y. Wei, Recent progress on countercurrent chromatography modeling, Journal of Liquid Chromatography & Related Technologies, 38 (2015) 415-421.
- [150] A.E. Kostanian, Modelling counter-current chromatography: a chemical engineering perspective, Journal of Chromatography A, 973 (2002) 39-46.
- [151] A.E. Kostanyan, V.V. Belova, A.I. Kholkin, Modelling counter-current and dual counter-current chromatography using longitudinal mixing cell and eluting counter-current distribution models, Journal of Chromatography A, 1151 (2007) 142-147.
- [152] J. Völkl, W. Arlt, M. Minceva, Theoretical study of sequential centrifugal partition chromatography, AIChE Journal, 59 (2013) 241-249.
- [153] Y. Wei, F. Wang, S. Wang, Y. Zhang, Modelling counter-current chromatography using a temperature dependence plate model, Journal of Chromatography B, 933 (2013) 30-36.
- [154] H. Guzlek, I.I. Baptista, P.L. Wood, A. Livingston, A novel approach to modelling counter-current chromatography, Journal of Chromatography A, 1217 (2010) 6230-6240.
- [155] J. Van Deemter, F. Zuiderweg, A.v. Klinkenberg, Longitudinal diffusion and resistance to mass transfer as causes of nonideality in chromatography, Chemical Engineering Science, 5 (1956) 271-289.
- [156] J. Villermaux, Chemical engineering approach to dynamic modelling of linear chromatography: A flexible method for representing complex phenomena from simple concepts, Journal of Chromatography A, 406 (1987) 11-26.
- [157] M. Van Buel, L. Van der Wielen, K.C.A. Luyben, Effluent concentration profiles in centrifugal partition chromatography, AIChE Journal, 43 (1997) 693-702.
- [158] S. Chollet, L. Marchal, M. Jeremy, J.H. Renault, J. Legrand, A. Foucault, Methodology for optimally sized centrifugal partition chromatography columns, Journal of Chromatography A, 1388 (2015) 174-183.
- [159] C. Schwienheer, J. Krause, G. Schembecker, J. Merz, Modelling centrifugal partition chromatography separation behavior to characterize influencing hydrodynamic effects on separation efficiency, Journal of Chromatography A, 1492 (2017) 27-40.
- [160] J. de Folter, I.A. Sutherland, Probabilistic model for immiscible separations and extractions (ProMISE), Journal of Chromatography A, 1218 (2011) 6009-6014.
- [161] I.A. Sutherland, G. Audo, E. Bourton, F. Couillard, D. Fisher, I. Garrard, P. Hewitson, O. Intes, Rapid linear scale-up of a protein separation by centrifugal partition chromatography, Journal of Chromatography A, 1190 (2008) 57-62.
- [162] P. Wood, S. Ignatova, L. Janaway, D. Keay, D. Hawes, I. Garrard, I.A. Sutherland, Counter-current chromatography separation scaled up from an analytical column to a production column, Journal of Chromatography A, 1151 (2007) 25-30.

- [163] F. das Neves Costa, M.N. Vieira, I. Garrard, P. Hewitson, G. Jerz, G.G. Leitão, S. Ignatova, Schinus terebinthifolius countercurrent chromatography (Part II): Intra-apparatus scale-up and inter-apparatus method transfer, *Journal of Chromatography A*, 1466 (2016) 76-83.
- [164] F. das Neves Costa, J. Hubert, N. Borie, A. Kotland, P. Hewitson, S. Ignatova, J.H. Renault, Schinus terebinthifolius countercurrent chromatography (Part III): Method transfer from small countercurrent chromatography column to preparative centrifugal partition chromatography ones as a part of method development, *Journal of Chromatography A*, 1487 (2017) 77-82.
- [165] N. Fumat, A. Berthod, K. Faure, Effect of operating parameters on a centrifugal partition chromatography separation, *Journal of Chromatography A*, 1474 (2016) 47-58.
- [166] A. Peng, P. Hewitson, I. Sutherland, L. Chen, S. Ignatova, The effect of increasing centrifugal acceleration/force and flow rate for varying column aspect ratios on separation efficiency in Counter-Current Chromatography, *Journal of Chromatography A*, 1581 (2018) 80-90.
- [167] S. Roehrer, M. Minceva, Characterization of a centrifugal partition chromatographic column with spherical cell design, *Chemical Engineering Research and Design*, 143 (2019) 180-189.
- [168] L. Marchal, A. Foucault, G. Patissier, J.M. Rosant, J. Legrand, Influence of flow patterns on chromatographic efficiency in centrifugal partition chromatography, *Journal of Chromatography A*, 869 (2000) 339-352.
- [169] S. Adelman, T. Baldhoff, B. Koepcke, G. Schembecker, Selection of operating parameters on the basis of hydrodynamics in centrifugal partition chromatography for the purification of nybomycin derivatives, *Journal of Chromatography A*, 1274 (2013) 54-64.
- [170] A. Foucault, E.C. Frias, C. Bordier, F.L. Goffic, Centrifugal Partition Chromatography: Stability of Various Biphasic Systems and Pertinence of the "Stoke's Model" to Describe the Influence of the Centrifugal Field Upon the Efficiency, *Journal of Liquid Chromatography & Related Technologies*, 17 (1994) 1-17.
- [171] E. Bouju, A. Berthod, K. Faure, Scale-up in centrifugal partition chromatography: The "free-space between peaks" method, *Journal of Chromatography A*, 1409 (2015) 70-78.
- [172] L. Marchal, M. Mojaat-Guemir, A. Foucault, J. Pruvost, Centrifugal partition extraction of β -carotene from *Dunaliella salina* for efficient and biocompatible recovery of metabolites, *Bioresource technology*, 134 (2013) 396-400.
- [173] M. Roy, S. Chakraborty, M. Siddiqi, R.K. Bhattacharya, Induction of apoptosis in tumor cells by natural phenolic compounds, in: *Asian Pacific Journal of Cancer Prevention*, 2002, pp. 61-67.

10. Appendix

10.1. Supplementary information for Paper I

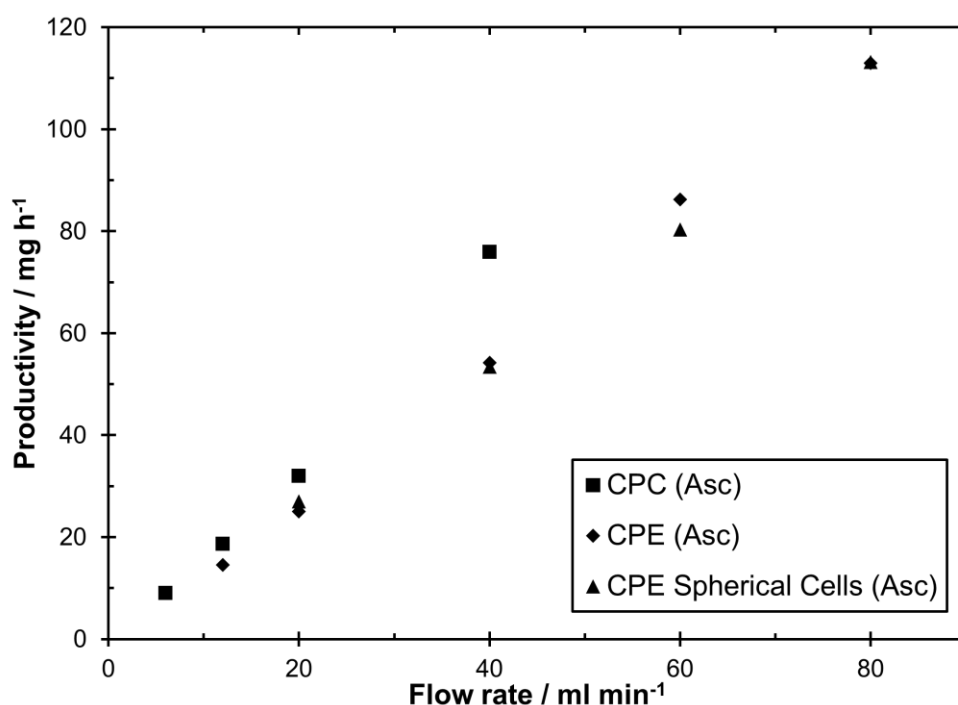
Characterization of a centrifugal partition chromatographic column with spherical cell design

Citation

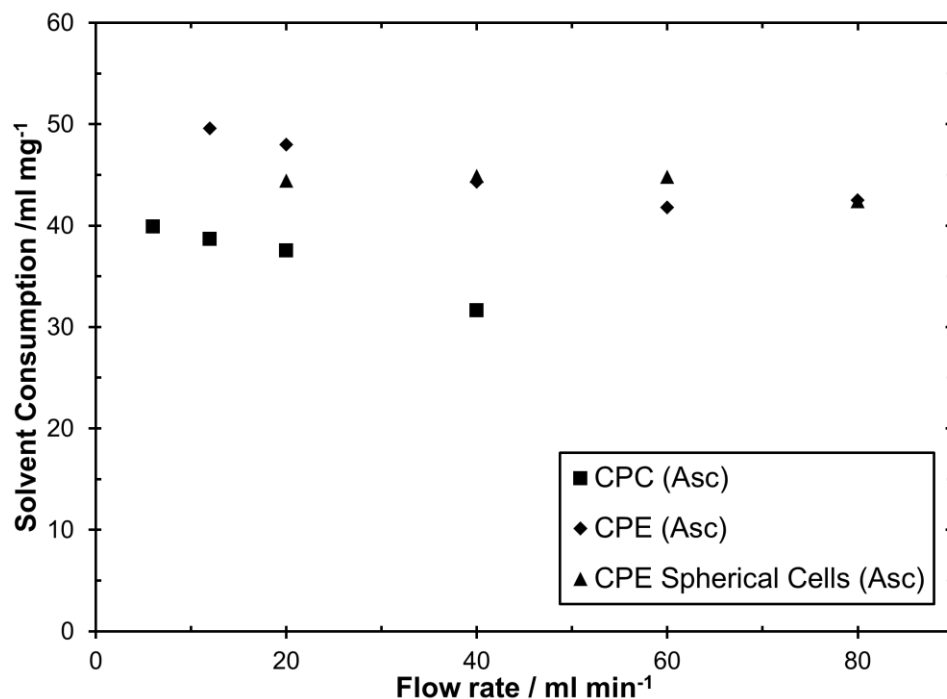
S. Roehrer, M. Minceva, (2019). Characterization of a centrifugal partition chromatographic column with spherical cell design. *Chemical Engineering Research and Design*, 143, 180-189

<https://doi.org/10.1016/j.cherd.2019.01.011>

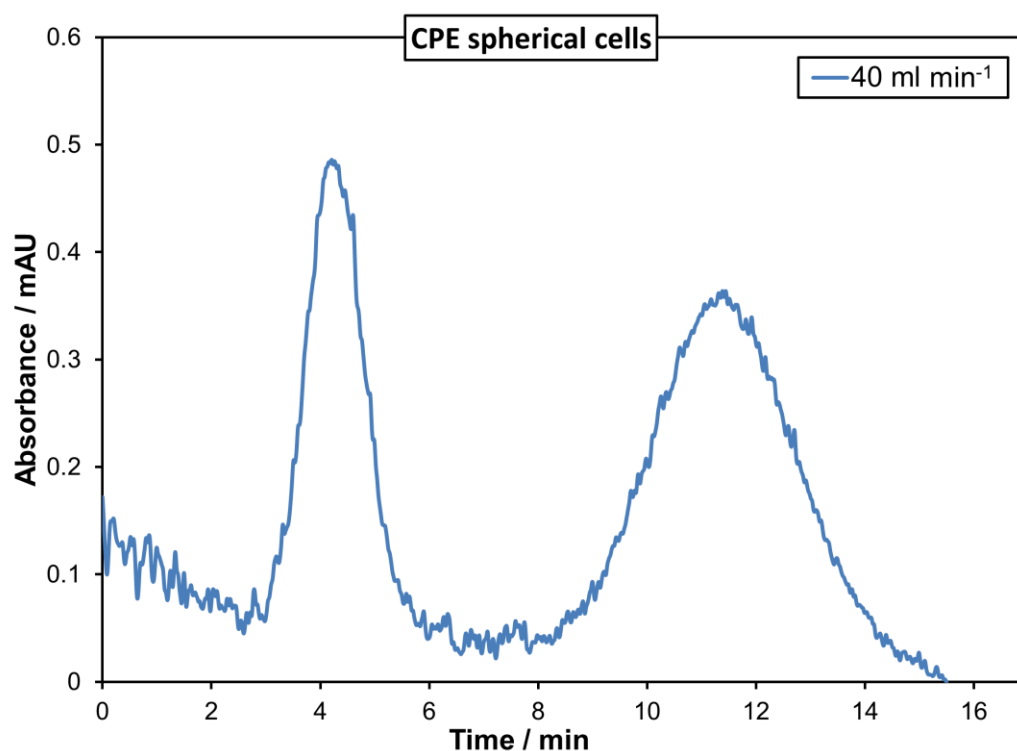
The following are the supplementary data to this article:



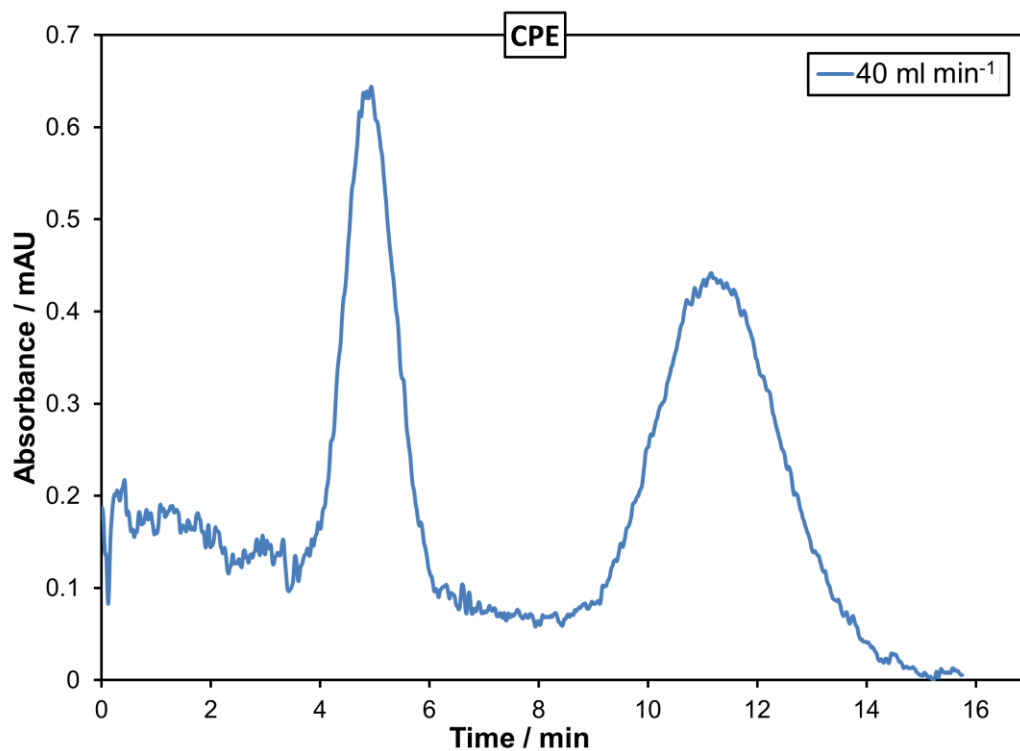
Supplementary Fig. A: Productivity calculated based on the pulse injections (injection volume of 1 ml) and the injected feed mass load in ascending mode of hydroquinone and pyrocatechol in CPC, CPE and CPE spherical cells as a function of flow rate.



Supplementary Fig. B: Solvent consumption calculated based on the pulse injections (injection volume of 1 ml) and the injected feed mass load in ascending mode of hydroquinone and pyrocatechol in CPC, CPE and CPE spherical cells as a function of flow



Supplementary Fig. C: Chromatogram of the CPE spherical cells separation of hydroquinone and pyrocatechol with the solvent system ARIZONA K (heptane/ethyl acetate/methanol/water, 1/2/1/2 v/v/v/v) at the wavelength (DSC mode: 40 ml min⁻¹, $c_{inj} = 5 \text{ mg ml}^{-1}$, $V_{inj} = 1 \text{ ml}$, 2000 rpm, $S_F = 0.80$)



Supplementary Fig. D: Chromatogram of the CPE separation of hydroquinone and pyrocatechol with the solvent system ARIZONA K (heptane/ethyl acetate/methanol/water, 1/2/1/2 v/v/v/v) at the wavelength (DSC mode: 40 ml min⁻¹, $c_{inj} = 5 \text{ mg ml}^{-1}$, $V_{inj} = 1 \text{ ml}$, 1700 rpm, $S_F = 0.67$)

10.2. Supplementary information for Paper III

Influence of temperature on the separation performance in solid support-free liquid-liquid chromatography

Citation

S. Roehrer, M. Minceva, (2019). Influence of temperature on the separation performance in solid support-free liquid-liquid chromatography. *Journal of Chromatography A*, 1594, 129-139.

<https://doi.org/10.1016/j.chroma.2019.02.011>

The following are the supplementary data to this article:

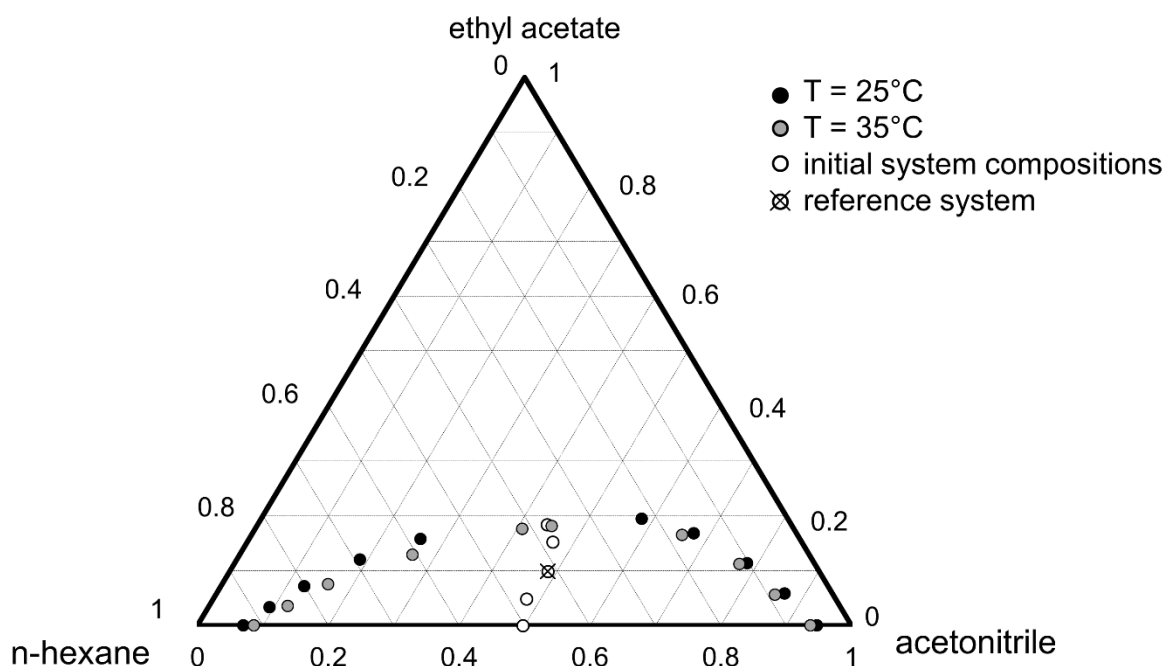


Figure A: Phase diagram of the *n*-hexane/ethyl acetate/acetonitrile system at 25 °C/298.15 K and 35 °C/308.15 K in mole fractions and at atmospheric pressure (1.01 bar).

Table A: Liquid - liquid equilibrium phase composition in mole fractions for *n*-hexane (1)/ ethyl acetate (2)/ acetonitrile (3) at T = (25 °C/298.15 K, 35 °C/308.15 K) under atmospheric pressure (1.01 bar).

Initial system composition			Upper phase composition			Lower phase composition		
X1	X2	X3	X1	X2	X3	X1	X2	X3
25 °C/ 298.15 K								
0.5018	0.0000	0.4982	0.9294	0.0000	0.0706	0.0526	0.0000	0.9474
0.4721	0.0482	0.4797	0.8725	0.0333	0.0942	0.0728	0.0580	0.8692
0.4147	0.0983	0.4870	0.8005	0.0713	0.1283	0.1026	0.1134	0.7840
0.3798	0.1524	0.4677	0.6907	0.1203	0.1890	0.1564	0.1680	0.6756
0.3730	0.1837	0.4433	0.5797	0.1574	0.2629	0.2228	0.1945	0.5828
0.3403	0.2257	0.4340	0.3397	0.2207	0.4395	single phase		
35 °C/ 308.15 K								
0.5024	0.0000	0.4976	0.9130	0.0000	0.0870	0.0621	0.0000	0.9379
0.4723	0.0480	0.4797	0.8436	0.0356	0.1208	0.0884	0.0559	0.8557
0.4146	0.0979	0.4875	0.7620	0.0752	0.1628	0.1151	0.1122	0.7727
0.3796	0.1523	0.4681	0.6065	0.1289	0.2647	0.1760	0.1652	0.6588
0.3695	0.1843	0.4463	0.3676	0.1809	0.4514	0.4146	0.1763	0.4091
0.3396	0.2258	0.4346	0.3385	0.2219	0.4396	single phase		

Mean SD (x) < 0.0045

Table B: Liquid - liquid equilibrium phase composition in mole fractions for the *n*-hexane (1)/ ethyl acetate (2)/ acetonitrile (3) system 41.43/9.92/48.65 mol% (11.2/2.0/5.3 v/v/v at 25 °C, 55.4/13.6/31.0 wt%) at different temperatures under atmospheric pressure (1.01 bar).

T °C	Upper phase composition			Lower phase composition		
	X1	X2	X3	X1	X2	X3
25	0.8005	0.0713	0.1283	0.1026	0.1134	0.7840
30	0.7739	0.0738	0.1523	0.1048	0.1155	0.7796
35	0.7620	0.0752	0.1628	0.1151	0.1122	0.7727
40	0.7100	0.0811	0.2089	0.1381	0.1112	0.7508

Mean SD (x) < 0.0028

Table C: Liquid - liquid equilibrium phase composition in mole fractions for the *n*-heptane (1)/ ethyl acetate (2)/ methanol (3)/ water (4) system Arizona N 7.01/10.5/25.38/57.11 mol% (1/1/1/1 v/v/v/v at 25 °C, 20.2/26.7/23.4/29.7 wt%) at different temperatures under atmospheric pressure (1.01 bar).

T °C	Upper phase composition				Lower phase composition			
	X ₁	X ₂	X ₃	X ₄	X ₁	X ₂	X ₃	X ₄
25	0.6049	0.2878	0.0667	0.0405	0.0005	0.0403	0.2937	0.6655
30	0.6061	0.2834	0.0688	0.0417	0.0007	0.0437	0.2993	0.6564
35	0.6103	0.2755	0.0691	0.0451	0.0006	0.0445	0.3033	0.6516
40	0.5964	0.2744	0.0755	0.0538	0.0008	0.0446	0.2993	0.6554

Mean SD (x) < 0.0019

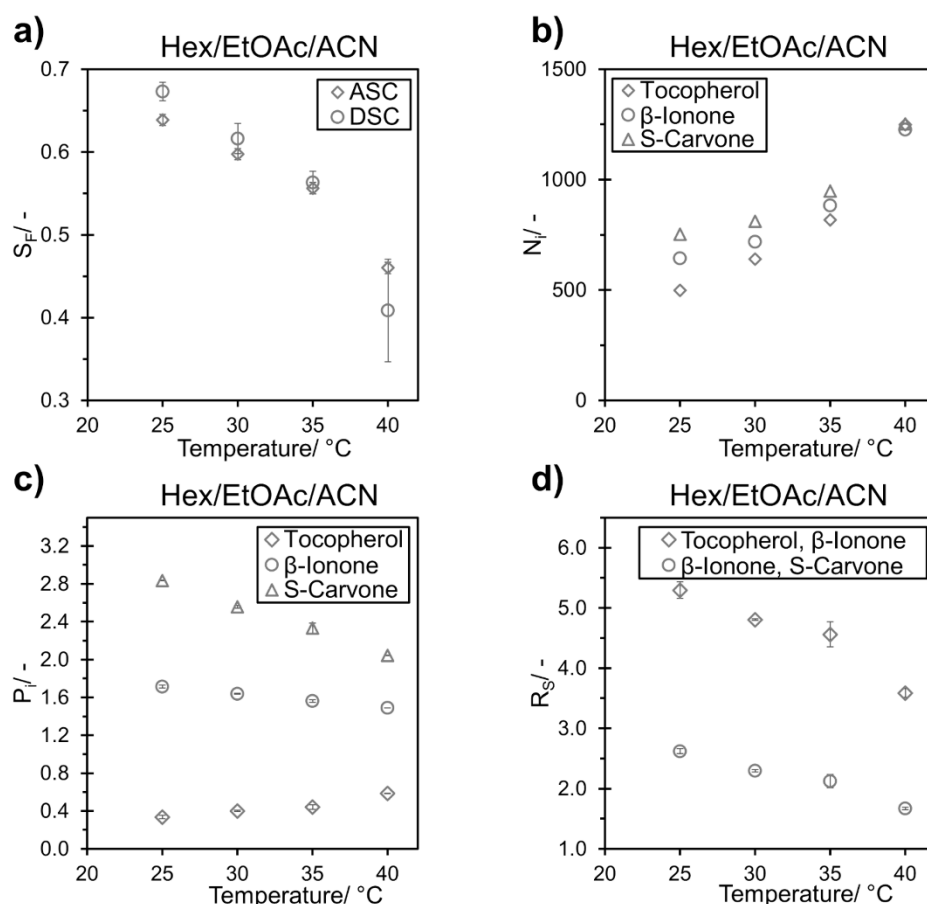


Figure B: Influence of temperature on the separation for the Hex/EtOAc/ACN system in the CCC column on: stationary phase retention (a), column efficiency (b), partition coefficients of selected model compounds (c), and peak resolution in ascending mode (d). Experimental conditions: mobile phase flow rate 1 ml min⁻¹, 1900 rpm, V_{inj} = 72 μ l.

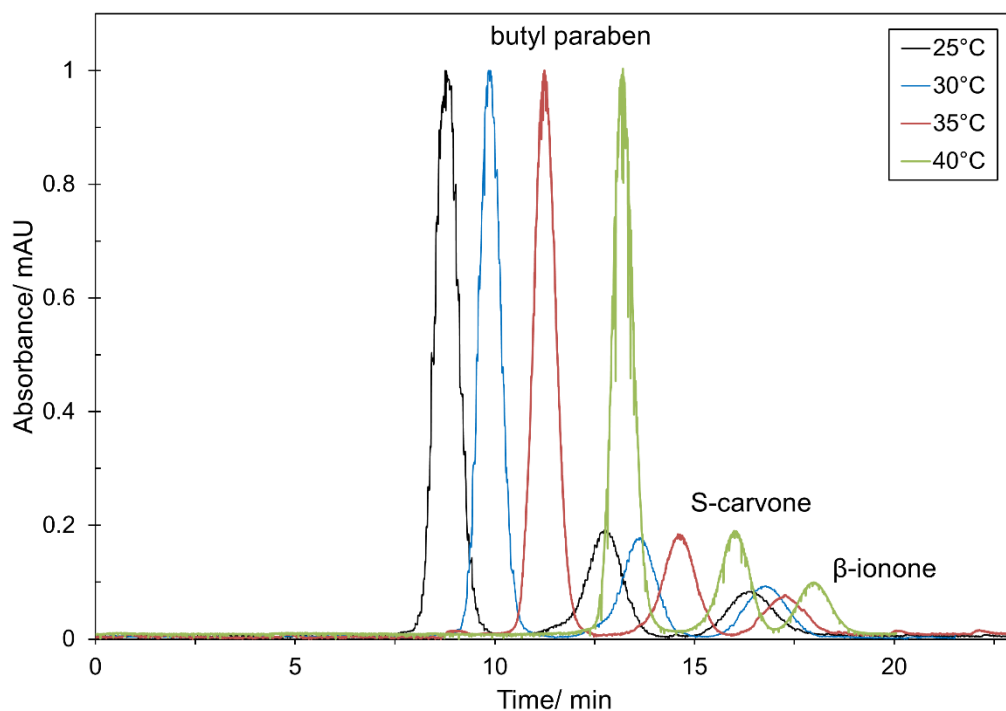


Figure C: CCC pulse injections of butyl paraben, S-carvone, and β -ionone with *n*-hexane/ethyl acetate/acetonitrile system at same column temperatures and mobile phase inlet temperatures between 25 °C and 40 °C (descending mode, 1 ml min⁻¹ mobile phase flow rate, 1900 rpm, $V_{inj} = 72 \mu\text{l}$, detector wavelength 255 nm).

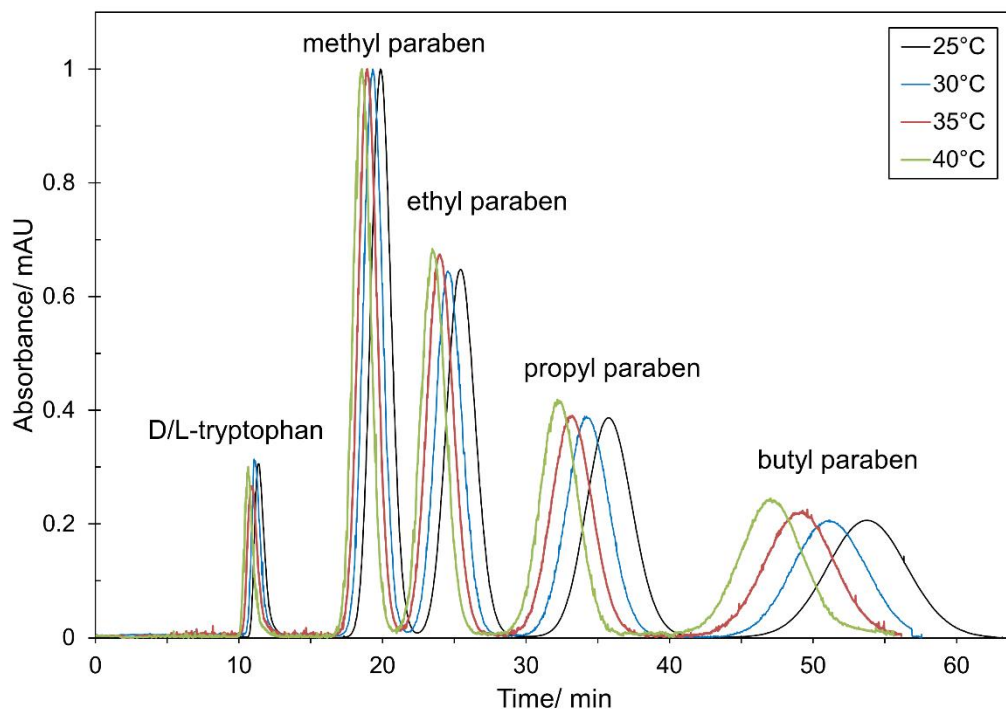


Figure D: CCC pulse injections of D/L-tryptophan, methyl paraben, ethyl paraben, propyl paraben, and butyl paraben with Arizona N system at same column temperatures and mobile phase inlet temperatures between 25 °C and 40 °C (descending mode, 1 ml min⁻¹ mobile phase flow rate, 1900 rpm, $V_{inj} = 72 \mu\text{l}$, detector wavelength 255 nm)

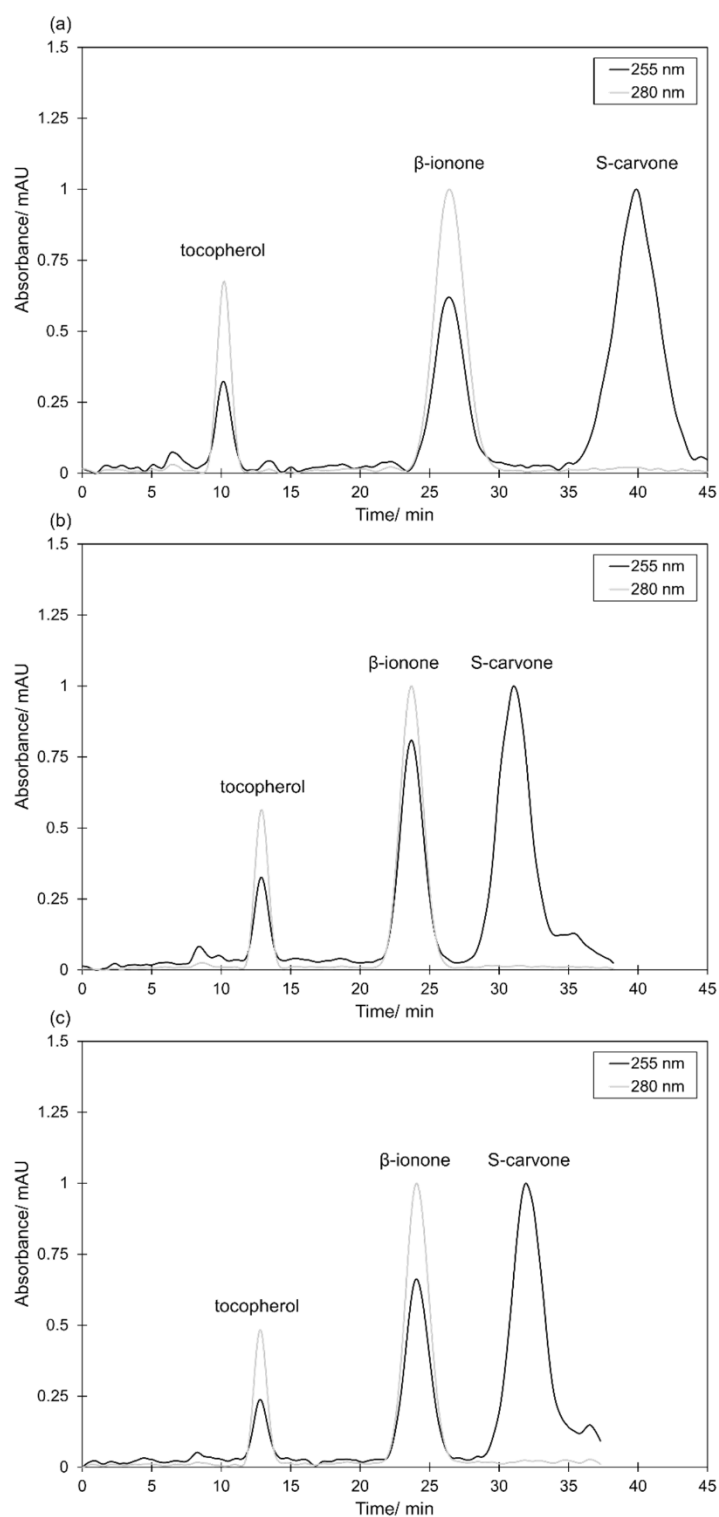


Figure E: CCC pulse injections of tocopherol, β -ionone and S-carvone with the *n*-hexane/ethyl acetate/acetonitrile system at different column temperatures (CT) and mobile phase inlet temperatures (MP) (ascending mode, 1 ml min⁻¹ mobile phase flow rate, 1900 rpm, $V_{inj} = 72 \mu\text{l}$, detector wavelengths 255 nm and 280 nm): (a) 25 °C CT and 25 °C MP; (b) 35 °C CT and 35 °C MP, (c) 35 °C CT and 25 °C MP.

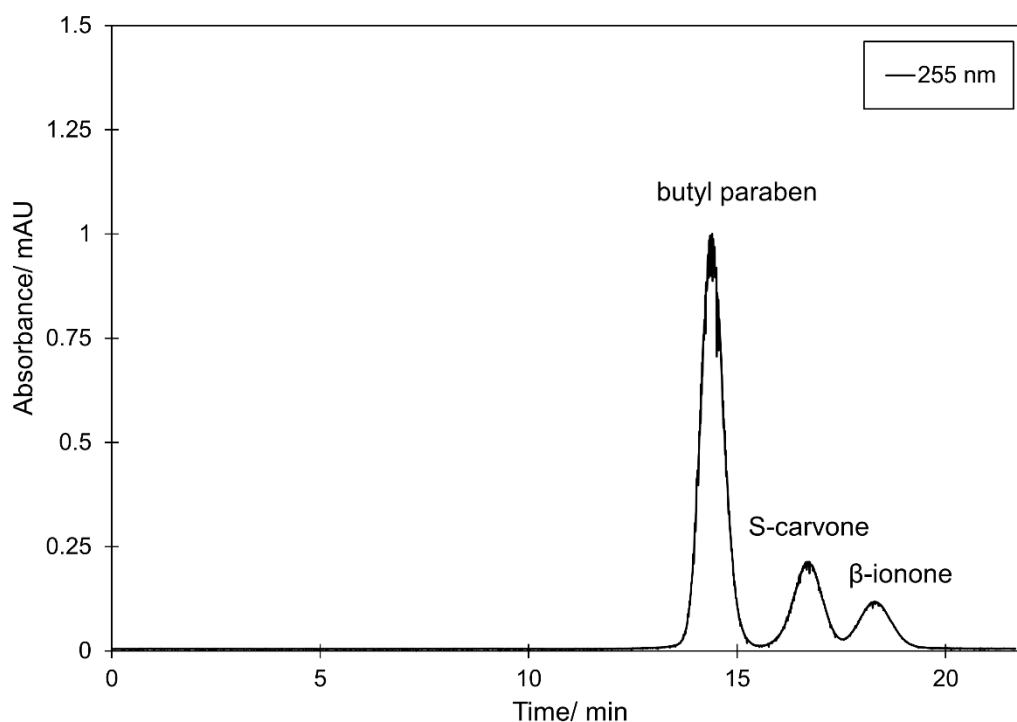


Figure F: CCC pulse injection of butyl paraben, S-carvone and β -ionone with the *n*-hexane/ethyl acetate/acetonitrile system at a column temperature of 40°C and a mobile phase inlet temperature of 25 °C (descending mode, 1 ml min⁻¹ mobile phase flow rate, 1900 rpm, $V_{inj} = 72 \mu\text{l}$, detector wavelengths 255 nm and 280 nm).

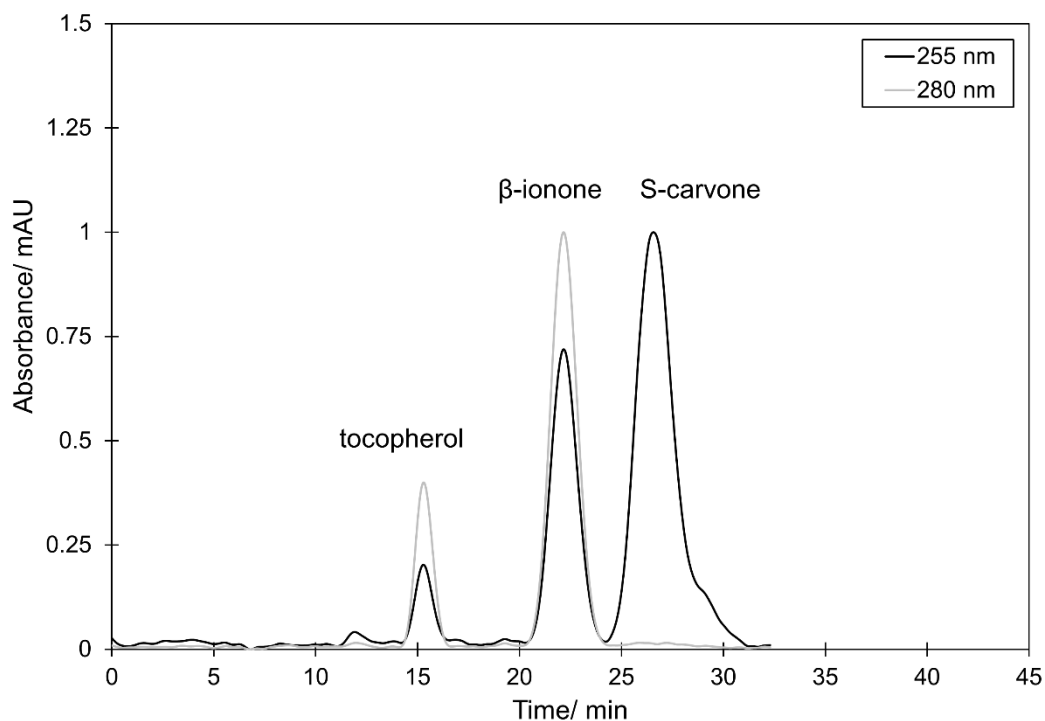


Figure G: CCC pulse injection of tocopherol, β -ionone and S-carvone with the *n*-hexane/ethyl acetate/acetonitrile system at a column temperature of 40°C and a mobile phase inlet temperature of 25 °C (ascending mode, 1 ml min⁻¹ mobile phase flow rate, 1900 rpm, $V_{inj} = 72 \mu\text{l}$, detector wavelengths 255 nm and 280 nm).

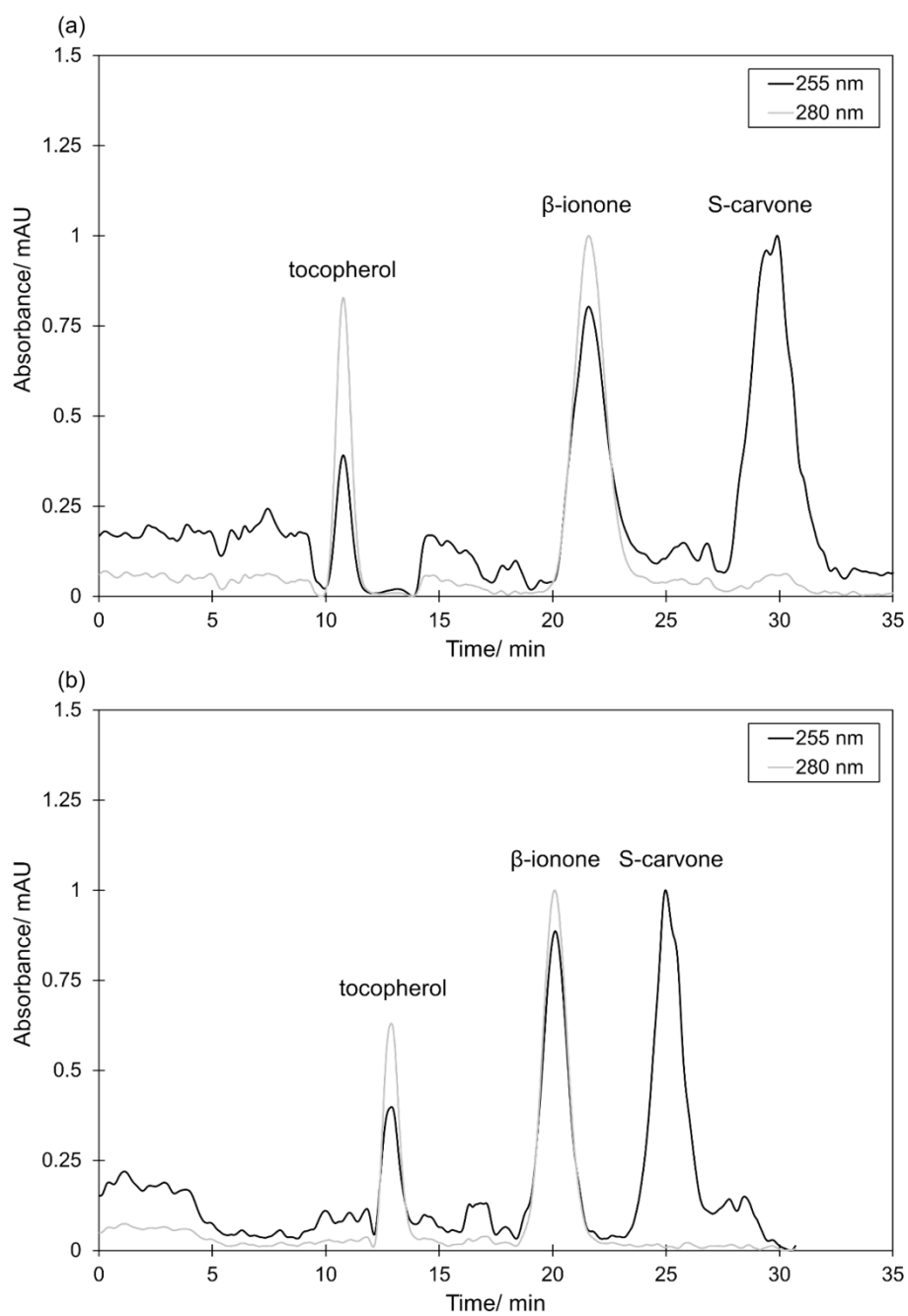


Figure H: CPC pulse injections of tocopherol, β -ionone and S-carvone with the *n*-hexane/ethyl acetate/acetonitrile system, a mobile phase inlet temperature of 25 °C, and (a) a column with and (b) a column without additional cooling (ascending mode, 12 ml min⁻¹ mobile phase flow rate, 1700 rpm, $V_{inj} = 1$ ml, detector wavelengths 255 nm and 280 nm).

10.3. Supplementary information for Paper V

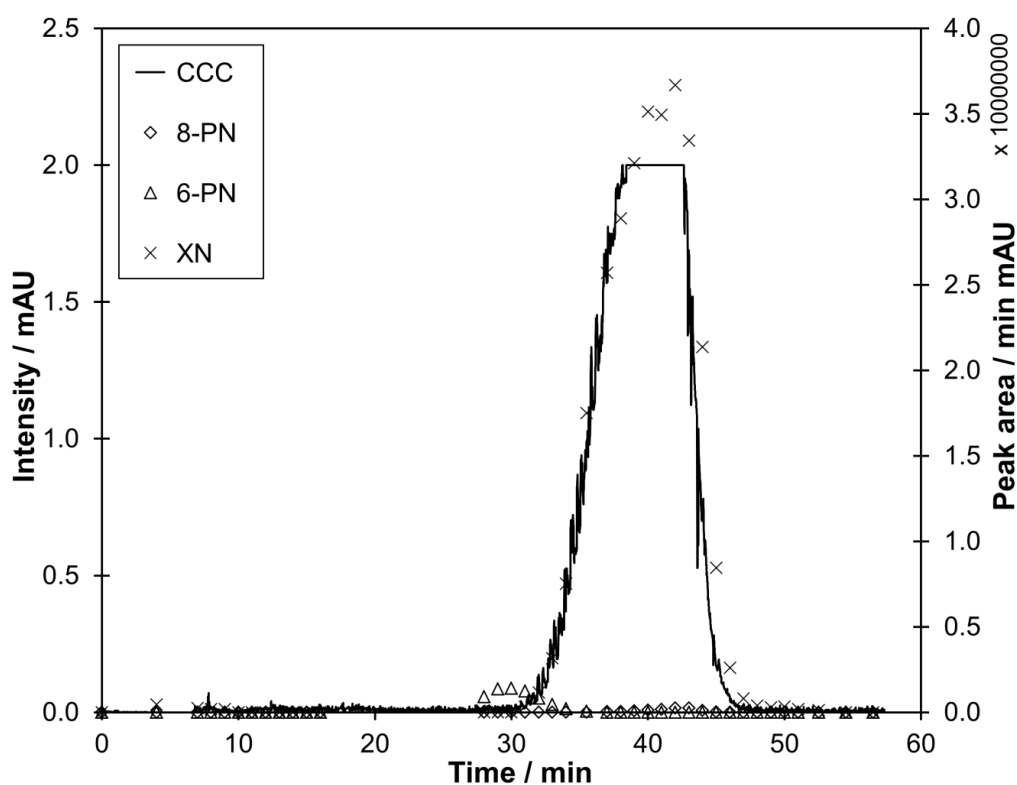
Xanthohumol C, a minor bioactive hop compound: Production, purification strategies and antimicrobial test

Citation

S. Roehrer, J. Behr, V. Stork, M. Ramires, G. Médard, O. Frank, K. Kleigrew, T. Hofmann, M. Minceva, (2018). Xanthohumol C, a minor bioactive hop compound: production, purification strategies and antimicrobial test. *Journal of Chromatography B*, 1095, 39-49

<https://doi.org/10.1016/j.ichromb.2018.07.018>

The following are the supplementary data to this article:

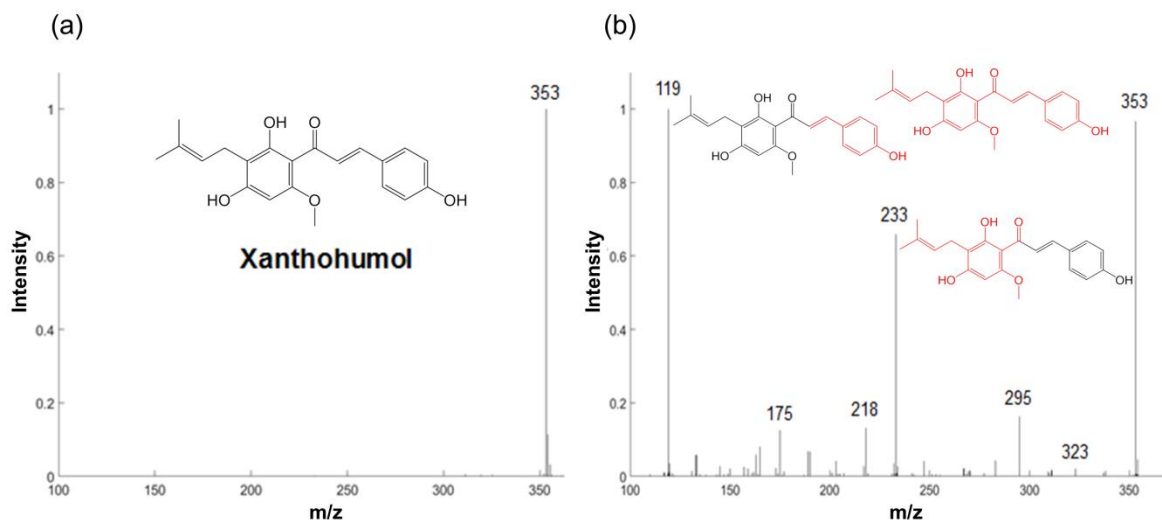


Supplementary Figure A: Chromatogram of CCC separation of xanthohumol (XN) from Xantho-Flav™ with the solvent system HEMWat-3 (hexane/ethyl acetate/methanol/water, 6/4/6/4 v/v/v) at the wavelength 370 nm, including the LC-MS offline analysis of the collected fractions containing xanthohumol and the main impurities 8-prenylnaringenin (8-PN) and 6-prenylnaringenin (6-PN) at 370 nm (ASC mode: 1 ml min⁻¹, c_{inj} = 40 mg ml⁻¹, V_{inj} = 0.5 ml, 1900 rpm, S_F = 0.47).

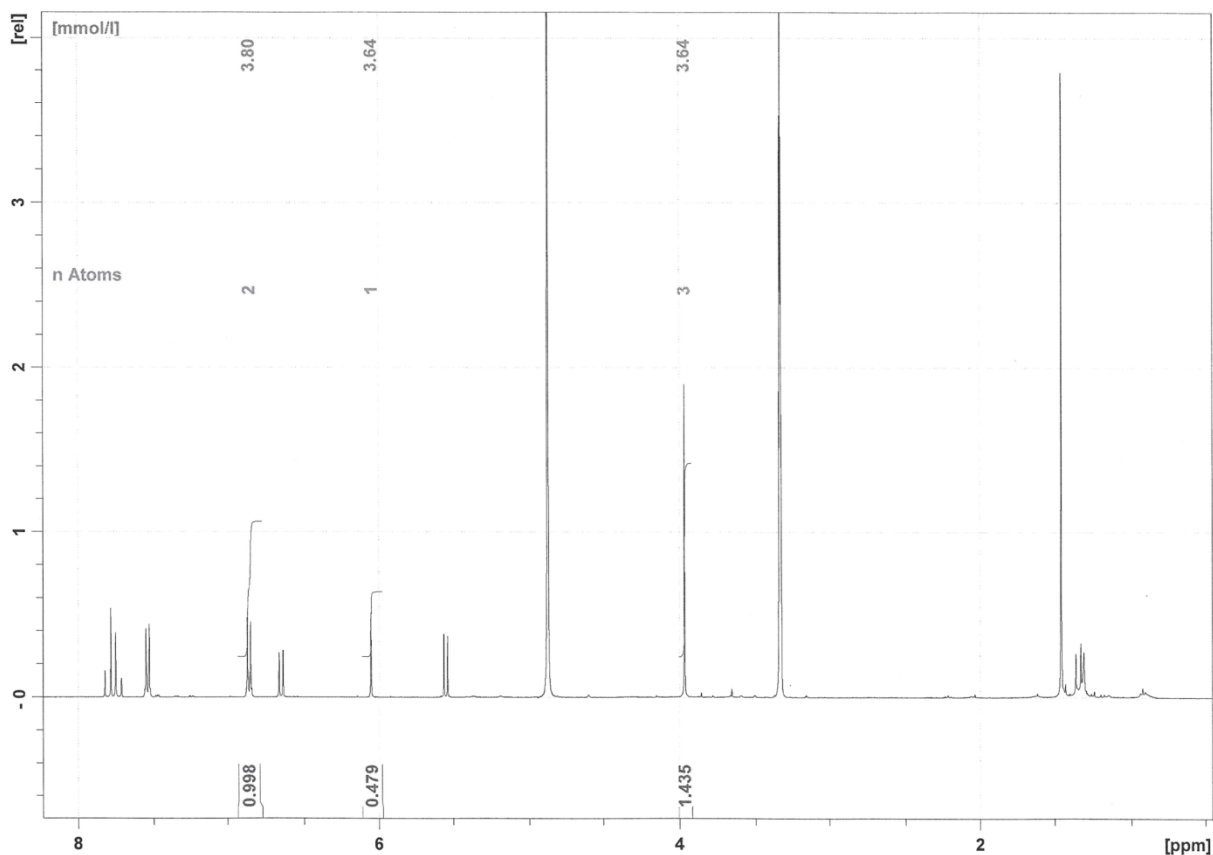
Supplementary Table A: HEMWat (hexane/ethyl acetate/methanol/water) solvent systems: system name, composition in volumetric ratios, stationary phase retention S_F in DSC mode at 1 ml min⁻¹ in a 18.2 ml CCC column at 1900 rpm, partition coefficients of XN, XNC, 6-PN and 8-PN determined by preliminary shake-flask experiments from Xantho-FlavTM, separation factor between XNC and XN, XN and 6-PN as well as XN and 8-PN

HEMWat system	Composition (v/v/v/v)	$S_{F,CCC} / -$	$P_{XN} / -$	$P_{XNC} / -$	$P_{6-PN} / -$	$P_{8-PN} / -$	$\alpha_{XNC-XN} / -$	$\alpha_{XN-6-PN} / -$	$\alpha_{XN-8-PN} / -$
-5	7/3/7/3	0.69	0.09	0.42	-	-	4.67	-	-
-4	7/3/6/4	0.62	0.28	1.13	-	-	4.04	-	-
-3	6/4/6/4	0.63	0.57	1.64	0.23	0.07	2.88	2.48	8.14
-1	6/4/5/5	0.63	1.64	11.96	1.49	0.41	7.29	1.10	4
0	5/5/5/5	0.62	2.48	16.26	2.18	0.41	6.56	1.14	6.05
1	4/6/5/5	0.54	3.08	19.17	3.22	0.58	6.22	0.96	5.31
3	4/6/4/6	-	26.37	153.74	40.90	4.06	5.83	0.64	6.50

Abbreviations: S_F : stationary phase retention, XN: xanthohumol, XNC: Xanthohumol C, 6-PN: 6-prenylnaringenin, 8-PN: 8-prenylnaringenin, α : separation factor



Supplementary Figure B: LC-MS/MS analysis of purified XN from the XN-enriched extract Xantho-Flav™ with (a) the MS spectrum of XN (m/z 353) in negative ionization mode and (b) the corresponding MS/MS fragmentation pattern.



Supplementary Figure C: ^1H qNMR spectrum of a 5 mM xanthohumol C solution purified from synthesis 2 (see Fig. 5b). Conditions: 400 MHz, dissolution in MeOD.

10.4. Supplementary information for Paper VI

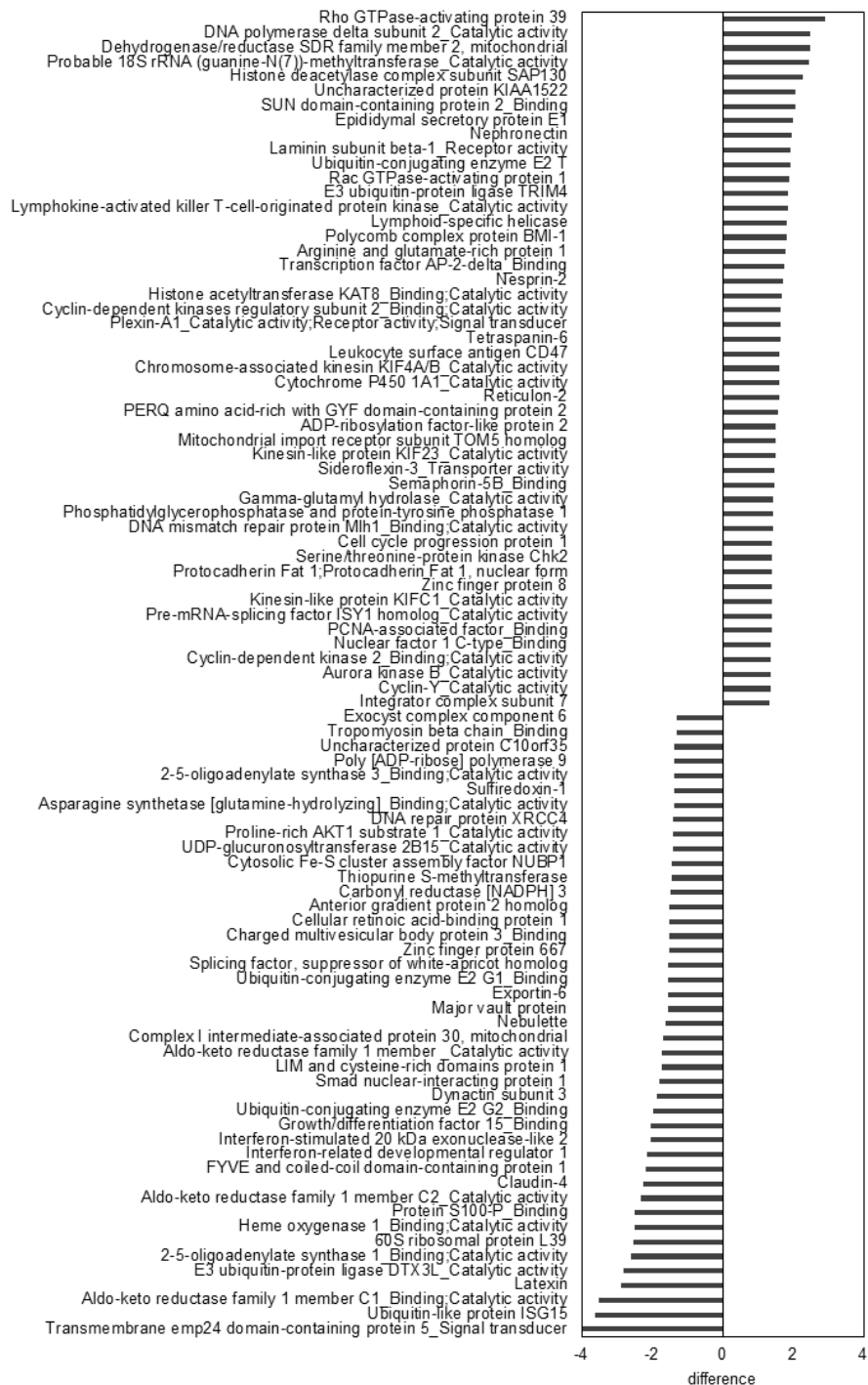
Analyzing Bioactive Effects of the Minor Hop Compound Xanthohumol C on Human Breast Cancer Cells using Quantitative Proteomics

Citation

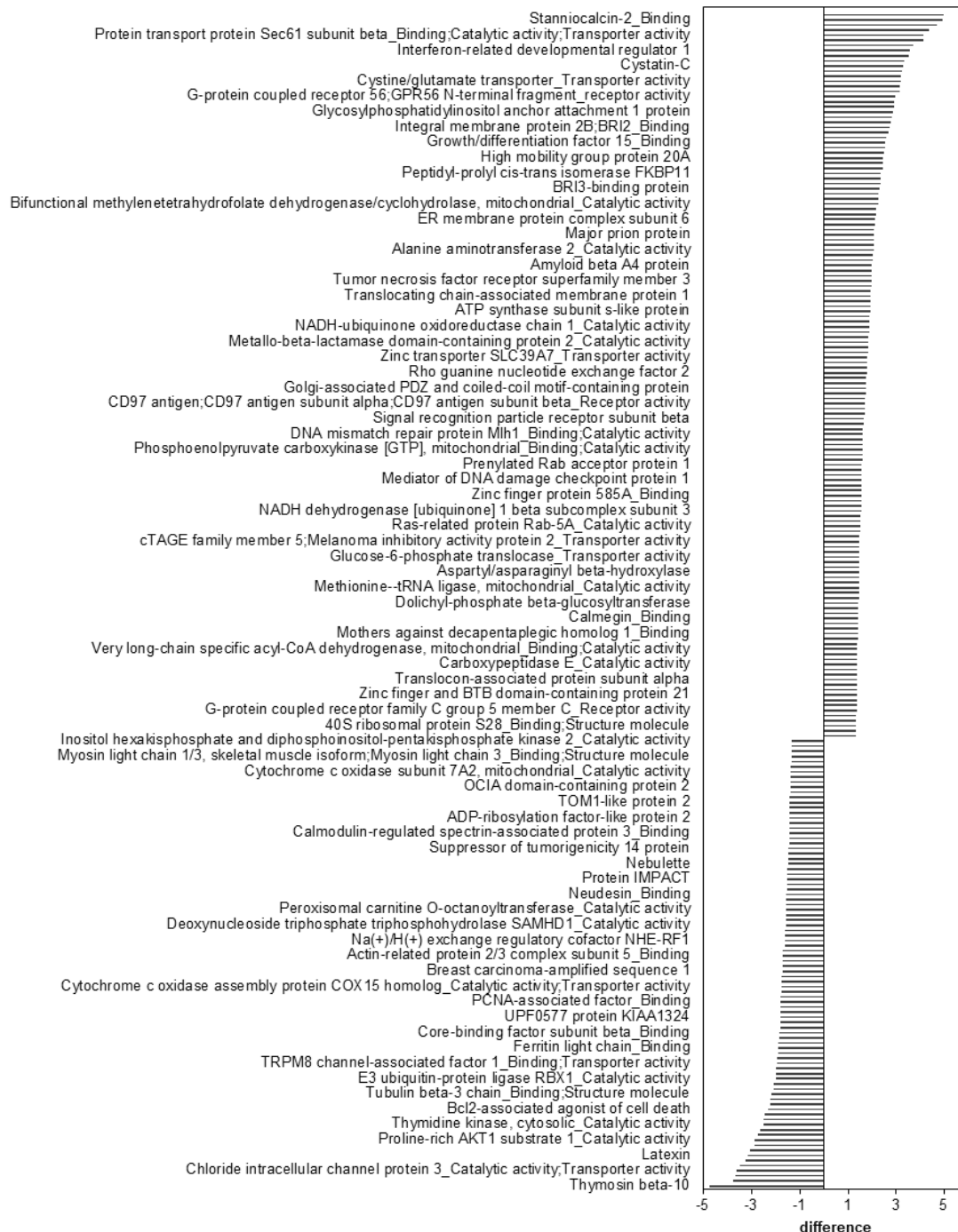
S. Roehrer, V. Stork, C. Ludwig, M. Minceva, J. Behr, (2019). Analyzing Bioactive Effects of the Minor Hop Compound Xanthohumol C on Human Breast Cancer Cells using Quantitative Proteomics. *PLoS ONE*, 14(3), e0213469.

<https://doi.org/10.1371/journal.pone.0213469>

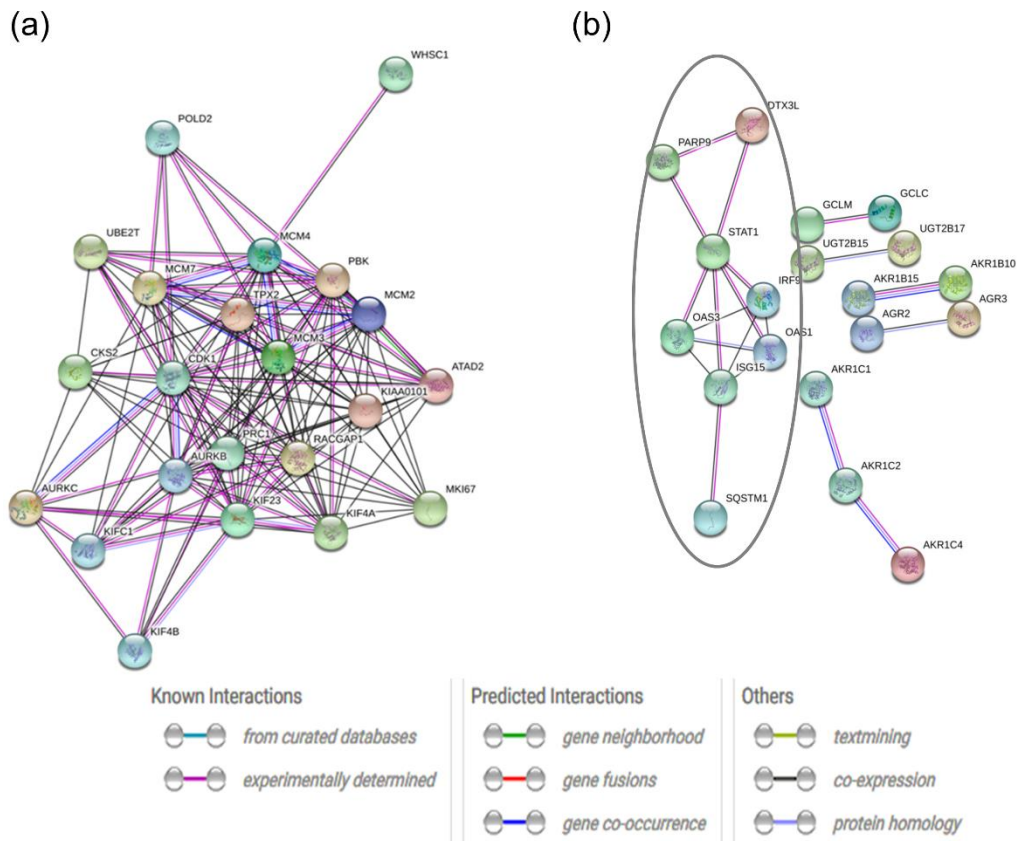
The following are the supporting information to this article:



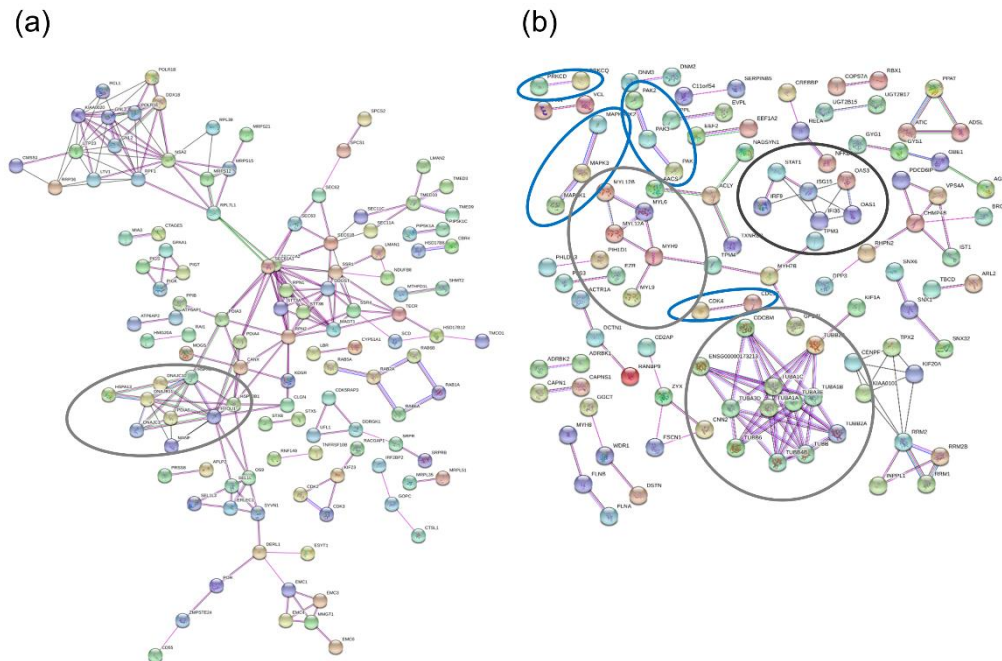
S1 Fig. DE proteins after xanthohumol treatment. Differentially expressed proteins in xanthohumol treated MCF-7 with their respective molecular function. Proteins are sorted by their differences in expression compared to control cells, showing only proteins with 2.5 fold up- or downregulation based on log2 transformed LFQ intensities.



S2 Fig. DE proteins after xanthohumol C treatment. Differentially expressed proteins in xanthohumol C treated MCF-7 with their respective molecular function. Proteins are sorted by their differences in expression compared to control cells, showing only proteins with 2.5 fold up- or downregulation based on log₂ transformed LFQ intensities.



S3 Fig. Functional signal networks after xanthohumol treatment. Functional signal networks of up- (a) and downregulated (b) proteins in xanthohumol treated MCF-7. In (b), proteins were marked that are involved in the type I interferon signaling pathway.



S4 Fig. Functional signal networks after xanthohumol C treatment. Functional signal networks of up- (a) and downregulated (b) DE proteins in xanthohumol C treated MCF-7. (a): Heat shock proteins were marked in grey. (b): In blue kinases were marked, in grey proteins involved in tubulin, and in black proteins implemented in the type I interferon signaling pathway.

S1 Table. Enrichment analysis of upregulated proteins after xanthohumol C treatment. Enrichment analysis of upregulated proteins in xanthohumol C treated MCF-7 implemented in the web tool GOrilla. Gene ontology terms, description of the molecular function in which enriched proteins were involved, p-values, false discovery rates (FDR), and enrichment factors are shown.

GO term	description	p-value	FDR q-value	enrichment (N, B, n, b)
GO:0050896	response to stimulus	6.90E-08	2.54E-04	1.47 (398,124,185,85)
GO:1901700	response to oxygen- containing compound	1.26E-07	2.31E-04	2.55 (398,35,116,26)
GO:0010033	response to organic substance	4.51E-07	5.54E-04	1.91 (398,63,139,42)
GO:0002376	immune system process	6.08E-07	5.61E-04	1.84 (398,51,170,40)
GO:0043562	cellular response to nitrogen levels	2.81E-06	2.07E-03	74.62 (398,4,4,3)
GO:0006995	cellular response to nitrogen starvation	2.81E-06	1.73E-03	74.62 (398,4,4,3)
GO:0071310	cellular response to organic substance	3.45E-06	1.82E-03	3.10 (398,24,91,17)
GO:0009605	response to external stimulus	4.43E-06	2.04E-03	1.82 (398,39,185,33)
GO:0014070	response to organic cyclic compound	6.01E-06	2.46E-03	2.73 (398,23,114,18)
GO:0042221	response to chemical	6.83E-06	2.52E-03	1.73 (398,78,139,47)
GO:0009719	response to endogenous stimulus	7.27E-06	2.44E-03	2.63 (398,25,115,19)
GO:0048518	positive regulation of biological process	9.03E-06	2.77E-03	1.45 (398,105,185,71)
GO:0000422	autophagy of mitochondrion	1.03E-05	2.91E-03	59.70 (398,5,4,3)
GO:0061726	mitochondrion disassembly	1.03E-05	2.71E-03	59.70 (398,5,4,3)

S2 Table. Enrichment analysis of downregulated proteins after xanthohumol C treatment. Enrichment analysis of downregulated proteins in xanthohumol C treated MCF-7 implemented in the web tool GOrilla. Gene ontology terms, description of the molecular function in which enriched proteins were involved, p-values, false discovery rates (FDR), and enrichment factors are shown.

GO term	description	p-value	FDR q-value	enrichment (N, B, n, b)
GO:0042221	response to chemical	1.23E-07	5.95E-04	1.50 (422,91,222,72)
GO:0010033	response to organic substance	1.28E-07	3.10E-04	1.57 (422,74,222,61)
GO:0008285	negative regulation of cell proliferation	2.39E-06	3.85E-03	2.62 (422,25,129,20)
GO:0048856	anatomical structure development	8.03E-06	9.70E-03	1.43 (422,95,220,71)
GO:0098771	inorganic ion homeostasis	9.77E-06	9.45E-03	2.29 (422,16,184,16)
GO:0050801	ion homeostasis	9.77E-06	7.88E-03	2.29 (422,16,184,16)
GO:0006366	transcription from RNA polymerase II promoter	1.15E-05	7.97E-03	1.94 (422,20,217,20)
GO:0042127	regulation of cell proliferation	1.50E-05	9.06E-03	2.13 (422,43,129,28)
GO:0006873	cellular ion homeostasis	2.23E-05	1.20E-02	2.29 (422,15,184,15)
GO:0055080	cation homeostasis	2.23E-05	1.08E-02	2.29 (422,15,184,15)
GO:0009719	response to endogenous stimulus	2.36E-05	1.04E-02	1.76 (422,36,207,31)
GO:0070887	cellular response to chemical stimulus	2.87E-05	1.16E-02	1.54 (422,58,222,47)
GO:0071310	cellular response to organic substance	2.97E-05	1.10E-02	1.59 (422,49,222,41)
GO:0032501	multicellular organismal process	3.03E-05	1.05E-02	1.43 (422,86,223,65)
GO:0007166	cell surface receptor signaling pathway	3.36E-05	1.08E-02	1.48 (422,61,239,51)
GO:0002376	immune system process	4.51E-05	1.36E-02	1.43 (422,83,224,63)
GO:0051239	regulation of multicellular organismal process	4.69E-05	1.33E-02	1.42 (422,86,225,65)
GO:0055082	cellular chemical homeostasis	5.01E-05	1.35E-02	2.17 (422,18,184,17)
GO:0030003	cellular cation homeostasis	5.12E-05	1.30E-02	2.29 (422,14,184,14)

GO term	description	p-value	FDR q-value	enrichment (N, B, n, b)
GO:0071495	cellular response to endogenous stimulus	6.18E-05	1.49E-02	1.82 (422,28,207,25)
GO:0050896	response to stimulus	7.53E-05	1.73E-02	1.32 (422,143,208,93)
GO:0007165	signal transduction	8.05E-05	1.77E-02	1.34 (422,128,212,86)
GO:0019725	cellular homeostasis	1.40E-04	2.95E-02	2.06 (422,20,184,18)
GO:0006937	regulation of muscle contraction	1.64E-04	3.31E-02	4.10 (422,7,103,7)
GO:0001775	cell activation	1.71E-04	3.30E-02	1.62 (422,48,201,37)
GO:0007568	aging	1.74E-04	3.23E-02	2.01 (422,15,210,15)
GO:1901700	response to oxygen-containing compound	2.56E-04	4.58E-02	1.58 (422,49,207,38)
GO:0055065	metal ion homeostasis	2.61E-04	4.51E-02	2.29 (422,12,184,12)
GO:0048878	chemical homeostasis	2.90E-04	4.84E-02	1.82 (422,27,197,23)
GO:0034109	homotypic cell-cell adhesion	3.23E-04	5.20E-02	3.27 (422,10,116,9)

10.5. Curriculum Vitae

Simon Röhrer

Persönliche Angaben

.....

Geburtsdatum: 16.10.1988

Geburtsort: Nürnberg

Staatsangehörigkeit: Deutsch



Akademische Ausbildung

.....

- 10/14 – 05/19 Promotionsstudium, Technische Universität München,
Professur für Biothermodynamik (Prof. Minceva)
Promotionsthema: Advances in Separation Method Development in
Liquid-Liquid Chromatography
- 10/11 – 06/14 Masterstudium: **Life Science Engineering**
Friedrich-Alexander-Universität Erlangen-Nürnberg,
Department Chemie- und Bioingenieurwesen
Masterarbeit: Evaluierung der Kosten- und Energieeffizienz einer
dezentralen anaeroben Abwasseraufbereitungsanlage mittels Referenz-
Petrinetzen und Wirtschaftlichkeitsanalyse
- 10/08 – 05/12 Bachelorstudium: **Life Science Engineering** Friedrich-Alexander-
Universität Erlangen-Nürnberg,
Department Chemie- und Bioingenieurwesen
Bachelorarbeit: Anwendung von auf Ionischen Flüssigkeiten basierenden
wässrigen Zweiphasensystemen in der Flüssig-Flüssig Chromatographie
- 09/99 – 06/08 Gymnasium Eckental
Abschluss: Allgemeine Hochschulreife (Abitur)

Beruflicher Werdegang

.....

- 10/14 – 06/19 **Wissenschaftlicher Mitarbeiter**, Technische Universität München,
Wissenschaftszentrum Weihenstephan, Freising,
Professur für Biothermodynamik (Prof. Minceva)
- 04/13 – 09/13 **Industriepraktikum**, Siemens AG, I IA AS PA VSS Pharma, Karlsruhe
- 12/12 – 03/13 **Studentische Hilfskraft**, Lehrstuhl für Thermische Verfahrenstechnik
(Prof. Arlt), Arbeitsgruppe für Flüssig-Flüssig Chromatographie
- 11/05 – 10/14 **Nebenberufliche Tätigkeit im Rettungsdienst**, staatlich anerkannter
Rettungssanitäter beim Arbeiter Samariter Bund, Regionalverband
Fränkische Schweiz, Gräfenberg